Cover Page

Universiteit Leiden

Leiden University Repository

The handle http://hdl.handle.net/1887/25711 holds various files of this Leiden University dissertation

Author: Ramkisoensing, Arti Anushka
Title: Molecular and environmental cues in cardiac differentiation of mesenchymal stem cells
Issue Date: 2014-05-07

Molecular and environmental cues in cardiac differentiation
of mesenchymal stem cells

MOLECULAR AND ENVIRONMENTAL CUES IN CARDIAC DIFFERENTIATION OF MESENCHYMAL STEM CELLS

Proefschrift

ter verkrijging van
de graad van Doctor aan de Universiteit Leiden,
op gezag van Rector Magnificus prof. mr. C.J.J.M. Stolker,
volgens besluit van het College voor Promoties
te verdedigen op woensdag 7 mei 2014
klokke 16:15 uur

door
Arti Anushka Ramkisoensing

geboren te 's Gravenhage
in 1980

PROMOTIECOMMISSIE

Promotores
Prof. dr. M.J. Schalij
Prof. dr. D.E. Atsma

Co-promotor
Dr. A.A.F. de Vries

Overige leden
Prof. dr. W.E. Fibbe
Prof. dr. R.J.M. Klautz
Prof. dr. P.S. Hiemstra

It matters not how strait the gate,
How charged with punishments the scroll.
I am the master of my fate:
I am the captain of my soul.

(excerpt from Invictus by William Ernest Henley, 1875)

Voor mijn mama en papa
Aan Sterretje

CONTENTS

CHAPTER I

GENERAL INTRODUCTION AND OUTLINE OF THESIS

BACKGROUND

Ischemic heart disease is the leading cause of morbidity and mortality in industrialized countries.[1] A major contributor to ischemic heart disease is myocardial infarction (MI). The erosion or rupture of a coronary atherosclerotic plaque can result in the acute obstruction of myocardial blood supply leading to massive loss of cardiomyocytes. Since mammals are unable to replenish the large number of cardiomyocytes lost as a result of MI, a fibrotic scar with a definitive nature is formed.[2] Although the scar increases the tensile strength of the infarcted myocardium and thereby prevents cardiac rupture, it impairs the contractile capacity of the heart which will eventually culminate in heart failure. Important advances have been made in prevention and treatment of the acute complications of MI and in reducing myocardial infarct size by reperfusion strategies.[3] As a result, the number of patients in developed countries that acutely dies from MI has decreased in recent years. However, patients that do survive are prone to undergo (left) ventricular remodeling and to ultimately develop heart failure. Prognosis of advanced heart failure is only 50% survival after two years. The only therapy for heart failure that addresses the fundamental problem of cardiomyocyte loss and vasculature damage is heart transplantation. Unfortunately, this therapy is restricted since the demand for donor hearts is largely exceeded by donor availability. Furthermore, immune rejection of the transplanted heart remains a major problem. If one could reconstruct the myocardium by replenishing lost cardiomyocytes and blood vessels through cell-based therapy, this would provide a powerful approach to treat cardiovascular disease. The ideal cell population for cardiac cell therapy should be able to generate all major cell types in the heart including endothelial cells, pericytes and smooth muscle cells to form new blood vessels. Newly formed cardiomyocytes must integrate structurally, mechanically, electrically and metabolically with the host myocardium and beat synchronously to be of functional significance and to prevent arrhythmias. The field of cardiac regeneration was fueled by a study of Orlic and colleagues, who reported on the existence of a population of $Lin^-c\text{-}Kit^+$ bone marrow cells that appeared to cause infarct healing and partial restoration of cardiac function after injection into the border zone of freshly infarcted mouse hearts.[4] (As only 44±10% [n=6] of the donor cells were eGFP-positive). Histology analyses revealed the expression by the engrafted donor cells of cardiomyocyte, smooth muscle or endothelial markers and showed that the cells in the regenerated areas were mainly of donor origin. Based on the findings, the authors concluded that the damaged myocardium produces signals causing the donor cells to differentiate into cardiomyocytes, smooth muscle cells or endothelial cells instead of into hematopoietic cells However, in subsequent years, these spectacular results could not be confirmed.[5,6] Nevertheless, the use of bone marrow cells to reduce

the loss of contractile tissue following acute MI was translated to the clinic with an unprecedented speed. The results from placebo-controlled randomized trials at 5-year follow-up show that the administration of bone marrow-derived cells is safe[7] and on average has a very similar small positive effect on cardiac function as existing pharmacotherapies for heart failure. While initially the focus in cardiac cell therapy was on whole bone marrow or hematopoietic/endothelial subfractions of these cells, recently the attention has been largely directed to mesenchymal stem cells (MSCs; see below) and cardiac progenitor cells.

MESENCHYMAL STEM CELLS

CHARACTERIZING MSCS
MSCs are a source of cells that has received a lot of attention with regard to cardiac stem cell therapy due to their abundance and relatively easy isolation and handling. These cells were first characterized by Friendenstein et al., who described fibroblast-like cells derived from adult bone marrow.[8] As no unique marker has been identified yet to distinguish MSCs from other cell types, the International Society for Cell Therapy has put forward a set of criteria for defining human MSCs. These criteria comprise (1) the ability to adhere to tissue culture plastic under standard culture conditions, (2) the presence of a set of surface markers (MSCs have been described to be positive for CD73, CD90 and CD105, but do not express CD79a, CD45, CD34, CD31, CD19, CD14 or CD11b or HLA-DR on their surface as determined by fluorescence-activated cell sorter analysis), and (3) the capacity to differentiate in vitro into osteoblasts, adipocytes and chondroblasts.[9] Additionally, MSCs have been shown to secrete pro-angiogenic and anti-apoptotic cytokines and possess immunomodulatory properties.[10,11] Several studies propose that MSCs have cardiomyogenic properties, together with their pro-angiogenic and anti-apoptotic capacities, these features have made these cells a promising therapeutic tool for cell-based cardiovascular repair.

ORIGIN OF MSCS
Since their first identification, MSCs have been demonstrated in a wide variety of adult, neonatal, fetal, and also embryonic tissues.[12,13] However, differences exist between MSCs derived from various sources, but also from the same source and even from the same tissue isolation, which may have important clinical implications.[14] MSCs were originally isolated from adult bone marrow, but their numbers in this tissue are low.[8] It has been estimated that about 0.001% to 0.01% of cells in a bone marrow aspirate is able to attach and grow as fibroblast-like cells.[10] Recently, cells with similar properties as adult bone marrow MSCs have been found in adult

adipose tissue, albeit in higher numbers.[13,15] The large quantities of MSCs that can be derived from fat aspirates constitute an advantage over bone marrow-derived MSCs.[13,16] MSCs have also been isolated from other adult tissue sources such as lymphoid organs (thymus and spleen)[17], periodontal ligament[18], and peripheral blood[19], but these MSCs have not been used in clinical trials in contrast to adult bone marrow- and adipose tissue-derived MSCs. Recent studies have shown that the number and function of stem cells are depressed in older patients.[20,21] Moreover, regardless of age, stem and progenitor cell number and function are impaired in patients suffering from various cardiovascular risk factors, such as diabetes, hypercholesterolemia and hypertension.[20] Using younger, and likely more healthy sources may circumvent the limitations of adult stem cell therapy. The advantages of MSCs derived from young sources have been extensively described for cells derived from fetal and neonatal tissues, such as umbilical cord[22] and blood[23], amniotic fluid[24] and membrane[25], bone marrow, lung and liver.[26] These "young" MSCs show better intrinsic homing and engraftment, greater multipotentiality, increased ability to self renew and lower immunogenicity.[25,27] The use of young MSCs for cell therapy typically excludes autologous transplantation. Currently the efficacy of allogeneic strategies are being explored in animal models and in clinical trials to overcome this drawback.[28-30] Strategies to modify the immunogenicity of allogeneic MSCs are also being investigated to improve their potential in tissue repair.[31] Recently, MSCs have been derived from human embryonic stem cells (ESCs). These fibroblast-like cells were obtained after co-culture of the human ESCs with the OP9 murine bone marrow stromal cell line or directly from ESCs cultured without feeder cells.[32,33] They resemble MSCs from various other tissue sources with respect to morphology, surface marker profile, immunogenicity and differentiation potential toward osteogenic, adipogenic and chrondrogenic lineages. Moreover, they lack expression of the pluripotency-associated markers and after transplantation they do not form teratomas.[32-35] Although ESC-derived MSCs seem superior to other sources with regard to their differentiation potential, clinical use of embryonic stem cells is still surrounded by ethical issues. This makes it difficult to envision the clinical application of ESC-derived MSCs in the near future.

As MSCs have been shown to differentiate towards a cardiomyocyte-like phenotype, the question arises whether MSCs are involved in cardiac development. The group of Liechty et al. has shown that human MSCs engrafted and underwent site-specific differentiation into various cell types including cardiomyocytes after in utero transplantation in a sheep model.[29] Identical results were obtained by Mackenzie et al., who used a similar ovine model and was also able to identify cardiomyocytes of human origin.[36] These studies suggest that transplanted MSCs could participate in organogenesis during fetal development. Nonetheless, the heterogeneity of MSC populations obtained by plastic adherence and the wide variety of cell

surface markers used to isolate MSCs, make identification of a MSC population in the heart quite difficult.

IN VITRO CARDIAC DIFFERENTIATION OF MSCS

The ability of adult human MSCs to differentiate into functional cardiomyocytes remains a much investigated and debated topic. This may be due to application of different criteria to identify adult MSC-derived cardiomyocytes. While some groups report expression of cardiac sarcomeric protein genes, organization of the encoded proteins into sarcomeres is often absent. Also intrinsic action potentials are rarely detected in these cells indicating that while a cardiomyocyte-like phenotype may be present, a functional cardiomyocyte has not been formed.[37-39] In recent years, several groups have shown that MSCs derived from neonatal tissues can be induced to express cardiac proteins in a sarcomeric pattern while they also could generate an intrinsic action potential which suggests that young MSCs do have the ability to become a functional cardiomyocyte.[25,40] However, these studies do not include the use of species-, strain- or gender-specific markers in combination with cardiomyocyte markers to unambiguously demonstrate that the cardiomyocyte is indeed derived from a stem cell. Without these specific markers heterocellular fusion as a mechanism in the formation of MSC-derived cardiomyocytes can not be excluded. Strikingly, many studies showing both expression of cardiac muscle genes and generation of intrinsic action potentials in MSC-derived cardiomyocytes involve co-cultures of MSCs and native cardiomyocytes to induce cardiomyogenesis. This suggests that interactions with bona fide cardiomyocytes might play an important role in the induction of cardiomyogenic differentiation of human MSCs. With regard to cardiovascular regeneration, the potential of MSCs to differentiate into endothelial and smooth muscle cells is also important. Tamama et al. have shown that bone marrow-derived human MSCs can gain molecular but also functional characteristics of smooth muscle cells after treatment with a small molecular mitogen-activated protein kinase kinase inhibitor.[41] Inducing endothelial differentiation in MSCs has given inconsistent results. After exposing adult bone marrow-derived human MSCs to endothelial cell differentiation-inducing conditions for up to 12 days, the MSCs were able to form capillary-like structures on Matrigel.[42,43] A study by Roobrouck et al. also showed that human MSCs are able to differentiate into endothelial cells in the presence of vascular endothelial growth factor.[44] The aforementioned results are, however, were not in line with those of Au et al. and Delorme et al. who showed that bone marrow-derived human MSCs are not able to differentiate toward the endothelial lineage even after priming the cells under endothelial conditions.[45,46]

IN VIVO CARDIAC DIFFERENTIATION OF MSCS

Multiple in vivo studies have been conducted investigating the regenerative capacity of MSCs in the diseased heart.[25,47-50] Nevertheless, the ability of MSCs to undergo cardiac differentiation in vivo remains a highly controversial topic. While some studies showed expression of cardiomyocyte proteins in a sarcomeric organization after cardiac stem cell transplantation in an animal model, they did not use an additional marker to determine whether these cells were indeed of MSC origin (e.g. species-, strain- or gender-specific markers).[25,50] Also, Toma et al. did not look into the possibility of heterologous cell fusion as an explanation for the expression of cardiomyocyte proteins by the transplanted MSCs.[50] In contrast, Quevedo et al. showed that male MSCs are able to differentiate into cardiomyocytes, smooth muscle cells and endothelial cells after allogeneic stem cell transplantation in the chronically infarcted myocardium of a female swine by co-localization of the Y chromosome with markers of cardiac muscle, vascular muscle and endothelial lineages.[49] Nonetheless, in all the vivo studies mentioned above, the frequency with which MSCs differentiated into cardiac cells was low.[49,50] Furthermore, MSC engraftment rate in these studies is also minimal. Therefore, modest improvements in cardiac function observed in most animal studies have been ascribed to paracrine mechanisms. MSCs secrete cytokines and growth factors that can inhibit apoptosis and fibrosis, suppress the immune system and induce angiogenesis.[48,51-53] In recent animal studies, genetically modified MSCs have been used to increase their therapeutic efficacy. For example, overexpression of chemokine receptors by MSCs have been shown to improve cell viability, migration, engraftment and capillary density in the injured myocardium.[54] Furthermore, paracrine factors that are released by MSCs that overexpress GATA4 increase angiogenesis and cell survival.[55] Also, Akt overexpression led to repair of the infarcted myocardium and improvement of the cardiac function.[56] Therefore, genetic modification of MSCs may be a tool to increase their effectiveness in mediating cardiac repair.

CLINICAL TRIALS OF MSC THERAPY FOR CARDIAC REPAIR

Clinical cardiac stem cell therapy for acute MI and ischemic cardiomyopathy using bone marrow-derived MSCs has been conducted.[28,57,58] In these phase I/II trials different cell delivery routes, such as intravenous and intracoronary infusion and intramyocardial injection were investigated. The main objective of these studies was determining safety of both autologous and allogeneic MSC therapy. Chen et al. investigated the effects of intracoronary autologous MSC infusion in patients with acute MI. Compared to controls, which were infused with saline, cardiac function

was modestly improved in patients who received MSCs. More important, however, was that this study showed intracoronary autologous MSC infusions to be safe with regard to adverse events such as occurrence of arrhythmias after cell administration. Moreover, no deaths were reported during the 6-month follow-up period.[57] Hare et al. investigated the safety and efficacy of intravenous allogeneic human MSC infusion in patients with acute MI. This randomized, double-blind, placebo-controlled dose-escalation study showed that allogeneic intravenous MSC delivery is safe in acute MI patients and also improves cardiac function in these patients compared to that in controls.[28] This study is especially interesting as multiple studies have shown that functional capacities of stem cells decline with age.[59,60] Use of allogeneic stem cells from young donors may help to increase the therapeutic effect of cardiac cell-based therapy.

Cardiac MSC therapy has also been initiated for patients with cardiac injury post-MI. Williams et al. showed that intramyocardial injection of autologous bone marrow-derived MSCs in patients with ischemic cardiomyopathy improved regional contractility of a chronic myocardial scar and led to reverse remodeling. Importantly, the intramyocardial cell injections did not cause sustained ventricular arrhythmias. This clinical trial shows that cardiac stem cell therapy in patients with ischemic cardiomyopathy is safe and has positive effects on cardiac structure and function.[58] The findings of this early-phase clinical trial have led to larger studies in which bone marrow-derived MSCs will be compared to mononuclear cells (TAC-HFT trial)[61], autologous MSC therapy will be compared to allogeneic MSC therapy (POSEIDON study), MSCs will be delivered during coronary artery bypass surgery (PROMETHEUS trial) and MSC therapy will be investigated for treatment of idiopathic dilated cardiomyopathy (POSEIDON-DCM study). In addition, another clinical trial in which MSCs are primed ex vivo with cytokines to improve cardiac differentiation in vivo has been initiated.[62] While the smaller clinical studies have shown that stem cell therapy is safe and feasible and modest improvements in cardiac function were achieved, the outcomes of the larger double-blind, randomized-controlled clinical trials will have to reveal whether MSC-based cardiac therapy is truly beneficial.

The current experience with the use of MSCs to treat cardiac diseases has provided several leads to improve their therapeutic efficacy. First of all, the option of using allogeneic stem cells from young donors in cardiac stem cell therapy should be thoroughly investigated as several studies have exposed that the functional capacity of stem cells declines with age.[59,60] Also, another major issue regarding cell transplantation that deserves examination is the low survival and engraftment rate that have been reported in studies in which MSCs were injected.[25,48,50] Recent studies have focused on improving engraftment rate by using biomaterials.[63-65] The risks of adverse events (e.g. occurrence of arrhythmias) that could occur when the

engraftment rate is improved are largely unknown and future studies should also take these into account. Besides engraftment, alignment with the surrounding myocardial tissue also seems to be of importance as alignment of stem cells could influence the mechanical and electrical activation of the heart. Currently, cardiac patches have been engineered to improve structural and electrical integration in host myocardium after cardiac stem cell transplantation.[66-68] Before MSC-based therapy will find widespread application in the clinic, the issues raised above should be answered in extensive in vitro studies, animal experiments and clinical studies.

AIM AND OUTLINE OF THE THESIS

In recent years stem cell based therapies have shown to give modest improvements in heart function. Most clinical trials have been conducted with autologous and therefore adult stem cells. However, functional capacity of stem cells decline with age. Therefore, **chapter II** of this thesis focuses on the influence of donor age on the in vitro differentiation potential of mesenchymal stem cells (MSCs) towards three cardiac lineages, namely cardiomyocytes, smooth muscle cells and endothelial cells. The exact mechanism behind improvement of cardiac function after stem cell transplantation is unknown, but functional integration with host cardiac tissue is known to be important for therapeutic efficiency and to avoid adverse effects.[69] The myocardium has a typical anisotropic tissue structure, which affects electrical and mechanical activation. Therefore, MSC-derived cardiac cells should align properly with native cardiac cells in order to restore tissue structure and for anisotropic conduction. **Chapter III** discusses the influence of forced alignment of MSCs undergoing cardiomyogenic differentiation on their functional integration with myocardial cells. Besides functional integration, electrical coupling with the surrounding host tissue is fundamental to make MSC-based therapy a safe option. Clinical trials in which skeletal myoblasts were transplanted in the diseased myocardium emphasized the importance of gap junctional coupling with the resident cardiomyocytes. Transplantation of skeletal myoblasts that after differentiation into myotubes do not eletromechanically couple with host myocardium led to an increased incidence of arrhythmias in patients.[70-72] Gap junctional coupling also seems to play an essential role in inducing cardiomyogenic differentiation. Multiple studies show stem cells are able to undergo cardiomyogenesis when they are in close contact with native cardiomyocytes. Therefore, **chapter IV** evaluates the role of gap junctional coupling in the cardiomyogenic differentiation potential of human MSCs. As cardiomyogenic differentiation of stem cells is often investigated after intramyocardial transplantation or in co-cultures with cardiomyocytes, they are commonly labeled through viral transduction with a marker protein to facili-

tate their identification. An often neglected pitfall of these studies is secondary transduction of cardiomyocytes by viral vector-marked stem cells and a second marker to distinguish stem cell-derived cardiomyoctes from native cardiomyocytes is rarely used. In **chapter V**, secondary transduction of neonatal rat cardiomyocytes by adult human cells that had previously been transduced with an enhanced green fluorescent protein-encoding lentiviral vector was studied.

The initial results of cell transplantation studies show improvement in cardiac function, however, therapeutic efficiency is not optimal due to low survival and engraftment rate of the transplanted cells. Biomaterials have been developed to improve survival and engraftment rate and thereby therapeutic efficiency. The possible adverse effects of a higher engraftment rate and of the pattern of distribution of a higher number of transplanted cells are unknown. These aspects are studied in **chapter VI**, which explores the role of engraftment patterns of MSCs on arrhythmicity in controlled *in vitro* models. Not only transplantation of exogenous cells in the diseased myocardium could lead to arrhythmias, proliferation of endogenous myofibroblasts after MI is known to cause conduction disturbances. An alternative way to minimize the negative effects of MI is described in **Chapter VII** of this thesis. In this chapter in a vitro model is used to study whether anti-proliferative treatment of myofibroblasts prevents arrhythmias by limitation of myofibroblast-induced depolarization.

Chapter VIII provides the summary and conclusions of this thesis, as well as future perspectives related to stem cell-based therapies for the treatment of damaged myocardium.

18   # REFERENCES

1. WHO, World Heart Federation, World Stroke Organization. Global Atlas on cardiovascular disease prevention and control. 2011.

2. Bergmann O, Bhardwaj RD, Bernard S et al. Evidence for cardiomyocyte renewal in humans. Science 2009;324:98-102.

3. Gerczuk PZ, Kloner RA. An update on cardioprotection: a review of the latest adjunctive thera-pies to limit myocardial infarction size in clinical trials. J Am Coll Cardiol 2012;59:969-978.

4. Orlic D, Kajstura J, Chimenti S et al. Bone marrow cells regenerate infarcted myocardium. Nature 2001;410:701-705.

5. Balsam LB, Wagers AJ, Christensen JL et al. Haematopoietic stem cells adopt mature haemat-opoietic fates in ischaemic myocardium. Nature 2004;428:668-673.

6. Murry CE, Soonpaa MH, Reinecke H et al. Haematopoietic stem cells do not transdifferentiate into cardiac myocytes in myocardial infarcts. Nature 2004;428:664-668.

7. Lipinski MJ, Biondi-Zoccai GG, Abbate A et al. Impact of intracoronary cell therapy on left ventricular function in the setting of acute myocardial infarction: a collaborative systematic review and meta-analysis of controlled clinical trials. J Am Coll Cardiol 2007;50:1761-1767.

8. Friedenstein AJ, Petrakova KV, Kurolesova AI et al. Heterotopic of bone marrow. Analysis of precursor cells for osteogenic and hematopoietic tissues. Transplantation 1968;6:230-247.

9. Dominici M, Le BK, Mueller I et al. Minimal criteria for defining multipotent mesenchymal stromal cells. The International Society for Cellular Therapy position statement. Cytotherapy 2006;8:315-317.

10. Pittenger MF, Mackay AM, Beck SC et al. Multilineage potential of adult human mesenchymal stem cells. Science 1999;284:143-147.

11. Miyahara Y, Nagaya N, Kataoka M et al. Monolayered mesenchymal stem cells repair scarred myocardium after myocardial infarction. Nat Med 2006;12:459-465.

12. da Silva ML, Chagastelles PC, Nardi NB. Mesenchymal stem cells reside in virtually all post-natal organs and tissues. J Cell Sci 2006;119:2204-2213.

13. Kern S, Eichler H, Stoeve J et al. Comparative analysis of mesenchymal stem cells from bone marrow, umbilical cord blood, or adipose tissue. Stem Cells 2006;24:1294-1301.

14. Pevsner-Fischer M, Levin S, Zipori D. The origins of mesenchymal stromal cell heterogeneity. Stem Cell Rev 2011;7:560-568.

15. Zuk PA, Zhu M, Ashjian P et al. Human adipose tissue is a source of multipotent stem cells. Mol Biol Cell 2002;13:4279-4295.

16. Bunnell BA, Flaat M, Gagliardi C et al. Adipose-derived stem cells: isolation, expansion and differentiation. Methods 2008;45:115-120.

17. Krampera M, Sartoris S, Liotta F et al. Immune regulation by mesenchymal stem cells derived from adult spleen and thymus. Stem Cells Dev 2007;16:797-810.

18. Trubiani O, Orsini G, Caputi S et al. Adult mesenchymal stem cells in dental research: a new approach for tissue engineering. Int J Immunopathol Pharmacol 2006;19:451-460.

19. Roufosse CA, Direkze NC, Otto WR et al. Circulating mesenchymal stem cells. Int J Biochem Cell Biol 2004;36:585-597.

20. Heiss C, Keymel S, Niesler U et al. Impaired progenitor cell activity in age-related endothelial dysfunction. J Am Coll Cardiol 2005;45:1441-1448.

21. Wagner W, Ho AD, Zenke M. Different facets of aging in human mesenchymal stem cells. Tissue Eng Part B Rev 2010;16:445-453.

22. Jo CH, Ahn HJ, Kim HJ et al. Surface characterization and chondrogenic differentiation of mesen-chymal stromal cells derived from synovium. Cytotherapy 2007;9:316-327.

23. Nishiyama N, Miyoshi S, Hida N et al. The significant cardiomyogenic potential of human umbilical cord blood-derived mesenchymal stem cells in vitro. Stem Cells 2007;25:2017-2024.

24. Roubelakis MG, Pappa KI, Bitsika V et al. Molecular and proteomic characterization of human mesenchymal stem cells derived from amniotic fluid: comparison to bone marrow mesenchymal stem cells. Stem Cells Dev 2007;16:931-952.

25. Tsuji H, Miyoshi S, Ikegami Y et al. Xenografted human amniotic membrane-derived mesenchymal stem cells are immunologically tolerated and transdifferentiated into cardiomyocytes. Circ Res 2010;106:1613-1623.

26. Guillot PV, Gotherstrom C, Chan J et al. Human first-trimester fetal MSC express pluripotency markers and grow faster and have longer telomeres than adult MSC. Stem Cells 2007;25:646-654.

27. Roobrouck VD, Ulloa-Montoya F, Verfaillie CM. Self-renewal and differentiation capacity of young and aged stem cells. Exp Cell Res 2008;314:1937-1944.

28. Hare JM, Traverse JH, Henry TD et al. A randomized, double-blind, placebo-controlled, dose-escalation study of intravenous adult human mesenchymal stem cells (prochymal) after acute myocardial infarction. J Am Coll Cardiol 2009;54:2277-2286.

29. Liechty KW, MacKenzie TC, Shaaban AF et al. Human mesenchymal stem cells engraft and demonstrate site-specific differentiation after in utero transplantation in sheep. Nat Med 2000;6:1282-1286.

30. Saito T, Kuang JQ, Bittira B et al. Xenotransplant cardiac chimera: immune tolerance of adult stem cells. Ann Thorac Surg 2002;74:19-24.

31. de la Garza-Rodea AS, Verweij MC, Boersma H et al. Exploitation of herpesvirus immune evasion strategies to modify the immunogenicity of human mesenchymal stem cell transplants. PLoS One 2011;6:e14493.

32. Barberi T, Willis LM, Socci ND et al. Derivation of multipotent mesenchymal precursors from human embryonic stem cells. PLoS Med 2005;2:e161.

33. Trivedi P, Hematti P. Simultaneous generation of CD34+ primitive hematopoietic cells and CD73+ mesenchymal stem cells from human embryonic stem cells cocultured with murine OP9 stromal cells. Exp Hematol 2007;35:146-154.

34. Karlsson C, Emanuelsson K, Wessberg F et al. Human embryonic stem cell-derived mesenchymal progenitors-Potential in regenerative medicine. Stem Cell Res 2009;3:39-50.

35. Hwang NS, Varghese S, Lee HJ et al. In vivo commitment and functional tissue regeneration using human embryonic stem cell-derived mesenchymal cells. Proc Natl Acad Sci U S A 2008;105:20641-20646.

36. MacKenzie TC, Flake AW. Multilineage differentiation of human MSC after in utero transplantation. Cytotherapy 2001;3:403-405.

37. Rose RA, Jiang H, Wang X et al. Bone marrow-derived mesenchymal stromal cells express cardiac-specific markers, retain the stromal phenotype, and do not become functional cardiomyocytes in vitro. Stem Cells 2008;26:2884-2892.

38. Koninckx R, Hensen K, Daniels A et al. Human bone marrow stem cells co-cultured with neonatal rat cardiomyocytes display limited cardiomyogenic plasticity. Cytotherapy 2009;11:778-792.

39. Xu W, Zhang X, Qian H et al. Mesenchymal stem cells from adult human bone marrow differentiate into a cardiomyocyte phenotype in vitro. Exp Biol Med (Maywood) 2004;229:623-631.

40. Nishiyama N, Miyoshi S, Hida N et al. The significant cardiomyogenic potential of human umbilical cord blood-derived mesenchymal stem cells in vitro. Stem Cells 2007;25:2017-2024.

41. Tamama K, Sen CK, Wells A. Differentiation of bone marrow mesenchymal stem cells into the smooth muscle lineage by blocking ERK/MAPK signaling pathway. Stem Cells Dev 2008;17:897-908.

20

42. Oswald J, Boxberger S, Jorgensen B et al. Mesenchymal stem cells can be differentiated into endothelial cells in vitro. Stem Cells 2004;22:377-384.

43. Chen MY, Lie PC, Li ZL et al. Endothelial differentiation of Wharton's jelly-derived mesenchymal stem cells in comparison with bone marrow-derived mesenchymal stem cells. Exp Hematol 2009;37:629-640.

44. Roobrouck VD, Clavel C, Jacobs SA et al. Differentiation potential of human postnatal mesenchymal stem cells, mesoangioblasts, and multipotent adult progenitor cells reflected in their transcriptome and partially influenced by the culture conditions. Stem Cells 2011;29:871-882.

45. Au P, Tam J, Fukumura D et al. Bone marrow-derived mesenchymal stem cells facilitate engineering of long-lasting functional vasculature. Blood 2008;111:4551-4558.

46. Delorme B, Ringe J, Pontikoglou C et al. Specific lineage-priming of bone marrow mesenchymal stem cells provides the molecular framework for their plasticity. Stem Cells 2009;27:1142-1151.

47. Numasawa Y, Kimura T, Miyoshi S et al. Treatment of human mesenchymal stem cells with angiotensin receptor blocker improved efficiency of cardiomyogenic transdifferentiation and improved cardiac function via angiogenesis. Stem Cells 2011;29:1405-1414.

48. Grauss RW, Winter EM, van Tuyn J et al. Mesenchymal stem cells from ischemic heart disease patients improve left ventricular function after acute myocardial infarction. Am J Physiol Heart Circ Physiol 2007;293:H2438-H2447.

49. Quevedo HC, Hatzistergos KE, Oskouei BN et al. Allogeneic mesenchymal stem cells restore cardiac function in chronic ischemic cardiomyopathy via trilineage differentiating capacity. Proc Natl Acad Sci U S A 2009;106:14022-14027.

50. Toma C, Pittenger MF, Cahill KS et al. Human mesenchymal stem cells differentiate to a cardiomyocyte phenotype in the adult murine heart. Circulation 2002;105:93-98.

51. Gnecchi M, Zhang Z, Ni A et al. Paracrine mechanisms in adult stem cell signaling and therapy. Circ Res 2008;103:1204-1219.

52. Kinnaird T, Stabile E, Burnett MS et al. Local delivery of marrow-derived stromal cells augments collateral perfusion through paracrine mechanisms. Circulation 2004;109:1543-1549.

53. Kinnaird T, Stabile E, Burnett MS et al. Marrow-derived stromal cells express genes encoding a broad spectrum of arteriogenic cytokines and promote in vitro and in vivo arteriogenesis through paracrine mechanisms. Circ Res 2004;94:678-685.

54. Huang J, Zhang Z, Guo J et al. Genetic modification of mesenchymal stem cells overexpressing CCR1 increases cell viability, migration, engraftment, and capillary density in the injured myocardium. Circ Res 2010;106:1753-1762.

55. Li H, Zuo S, He Z et al. Paracrine factors released by GATA-4 overexpressed mesenchymal stem cells increase angiogenesis and cell survival. Am J Physiol Heart Circ Physiol 2010;299:H1772-H1781.

56. Noiseux N, Gnecchi M, Lopez-Ilasaca M et al. Mesenchymal stem cells overexpressing Akt dramatically repair infarcted myocardium and improve cardiac function despite infrequent cellular fusion or differentiation. Mol Ther 2006;14:840-850.

57. Chen SL, Fang WW, Ye F et al. Effect on left ventricular function of intracoronary transplantation of autologous bone marrow mesenchymal stem cell in patients with acute myocardial infarction. Am J Cardiol 2004;94:92-95.

58. Williams AR, Trachtenberg B, Velazquez DL et al. Intramyocardial stem cell injection in patients with ischemic cardiomyopathy: functional recovery and reverse remodeling. Circ Res 2011;108:792-796.

59. Bellantuono I, Keith WN. Stem cell ageing: does it happen and can we intervene? Expert Rev Mol Med 2007;9:1-20.

60.   Chambers SM, Goodell MA. Hematopoietic stem cell aging: wrinkles in stem cell potential. Stem Cell Rev 2007;3:201-211.

61.   Trachtenberg B, Velazquez DL, Williams AR et al. Rationale and design of the Transendocardial Injection of Autologous Human Cells (bone marrow or mesenchymal) in Chronic Ischemic Left Ventricular Dysfunction and Heart Failure Secondary to Myocardial Infarction (TAC-HFT) trial: A randomized, double-blind, placebo-controlled study of safety and efficacy. Am Heart J 2011;161:487-493.

62.   Bartunek J, Wijns W, Dolatabadi D et al. C-Cure Multicenter Trial: Lineage Specified Bone Marrow Derived Cardiopoietic Mesenchymal Stem Cells for Treatment of Ischemic Cardiomyopathy. Journal of the American College of Cardiology 2011;57:E200.

63.   Cheng K, Li TS, Malliaras K et al. Magnetic targeting enhances engraftment and functional benefit of iron-labeled cardiosphere-derived cells in myocardial infarction. Circ Res 2010;106:1570-1581.

64.   Segers VF, Lee RT. Biomaterials to enhance stem cell function in the heart. Circ Res 2011;109:910-922.

65.   Zakharova L, Mastroeni D, Mutlu N et al. Transplantation of cardiac progenitor cell sheet onto infarcted heart promotes cardiogenesis and improves function. Cardiovasc Res 2010;87:40-49.

66.   Dvir T, Kedem A, Ruvinov E et al. Prevascularization of cardiac patch on the omentum improves its therapeutic outcome. Proc Natl Acad Sci U S A 2009;106:14990-14995.

67.   Kim DH, Kshitiz, Smith RR et al. Nanopatterned cardiac cell patches promote stem cell niche formation and myocardial regeneration. Integr Biol (Camb) 2012;4:1019-1033.

68.   Simpson D, Liu H, Fan TH et al. A tissue engineering approach to progenitor cell delivery results in significant cell engraftment and improved myocardial remodeling. Stem Cells 2007;25:2350-2357.

69.   Pijnappels DA, Gregoire S, Wu SM. The integrative aspects of cardiac physiology and their implications for cell-based therapy. Ann N Y Acad Sci 2010;1188:7-14.

70.   Menasche P, Hagege AA, Vilquin JT et al. Autologous skeletal myoblast transplantation for severe postinfarction left ventricular dysfunction. J Am Coll Cardiol 2003;41:1078-1083.

71.   Siminiak T, Kalawski R, Fiszer D et al. Autologous skeletal myoblast transplantation for the treatment of postinfarction myocardial injury: phase I clinical study with 12 months of follow-up. Am Heart J 2004;148:531-537.

72.   Makkar RR, Lill M, Chen PS. Stem cell therapy for myocardial repair: is it arrhythmogenic? J Am Coll Cardiol 2003;42:2070-2072.

CHAPTER II

HUMAN EMBRYONIC AND FETAL MESENCHYMAL STEM CELLS DIFFERENTIATE TOWARD THREE DIFFERENT CARDIAC LINEAGES IN CONTRAST TO THEIR ADULT COUNTERPARTS

Arti A. Ramkisoensing[a], Daniël A. Pijnappels[a], Saïd F.A. Askar[a], Robert Passier[b], Jim Swildens[a,c], Marie José Goumans[c], Cindy I. Schutte[a], Antoine A.F. de Vries[a], Sicco Scherjon[d], Christine L. Mummery[b], Martin J. Schalij[a], Douwe E. Atsma[a].

[a]Departments of Cardiology, [b]Embryology and Anatomy, [c]Molecular Cell Biology, [d]Obstetrics and Gynaecology, Leiden University Medical Center, 2300 RC Leiden, The Netherlands.

ABSTRACT

Mesenchymal stem cells (MSCs) show unexplained differences in differentiation potential. In this study, differentiation of human (h) MSCs derived from embryonic, fetal and adult sources toward cardiomyocytes, endothelial and smooth muscle cells was investigated.

Labeled hMSCs derived from embryonic stem cells (hESC-MSCs), fetal umbilical cord, bone marrow, amniotic membrane and adult bone marrow and adipose tissue were co-cultured with neonatal rat cardiomyocytes (nrCMCs) or cardiac fibroblasts (nrCFBs) for 10 days, and also cultured under angiogenic conditions.

Cardiomyogenesis was assessed by human-specific immunocytological analysis, whole-cell current-clamp recordings, human-specific qRT-PCR and optical mapping. After co-culture with nrCMCs, significantly more hESC-MSCs than fetal hMSCs stained positive for α-actinin, whereas adult hMSCs stained negative. Furthermore, functional cardiomyogenic differentiation, based on action potential recordings, was shown to occur, but not in adult hMSCs. Of all sources, hESC-MSCs expressed most cardiac-specific genes. hESC-MSCs and fetal hMSCs contained significantly higher basal levels of connexin43 than adult hMSCs and co-culture with nrCMCs increased expression. After co-culture with nrCFBs, hESC-MSCs and fetal hMSCs did not express α-actinin and connexin43 expression was decreased. Conduction velocity (CV) in co-cultures of nrCMCs and hESC-MSCs was significantly higher than in co-cultures with fetal or adult hMSCs. In angiogenesis bioassays, only hESC-MSCs and fetal hMSCs were able to form capillary-like structures, which stained for smooth muscle and endothelial cell markers.

Human embryonic and fetal MSCs differentiate toward three different cardiac lineages, in contrast to adult MSCs. Cardiomyogenesis is determined by stimuli from the cellular microenvironment, where connexin43 may play an important role.

INTRODUCTION

Despite significant advances in the management of cardiovascular disease, it remains the predominant cause of morbidity and mortality in Western countries [1]. The risk of developing cardiovascular disease increases with age and is associated with progressive impairment of cardiovascular repair mechanisms, including the capacity of the heart to replace damaged cells [2].

In recent years, cell therapy has been studied intensively as novel therapeutic option for cardiac diseases. After transplantation and engraftment of cells in the host myocardium, different mechanisms are thought to be responsible for the improvement in cardiac function, including angiogenesis and cardiomyogenesis [3]. Mesenchymal stem cells (MSCs) are one of the cell types studied in clinical trials for treatment of ischemic heart disease. However, MSCs themselves are prone to the effects of aging and disease and if autologous MSCs are used, may suffer from decreased ability to proliferate, differentiate, home, engraft and exert immunosuppressive effects [4,5]. Moreover, the developmental stage of tissues and different states of disease alter the microenvironmental regulation of stem cell behaviour [6]. Whether the developmental stage of MSC donor tissue also affects the cardiac differentiation potential of MSCs is not completely understood. While the role of MSCs in cardiac development is largely unknown, several studies indicate that MSCs derived from young cell sources, like umbilical cord blood, appear to retain their primitive characteristics [7,8]. Also, some of these MSCs seem to possess cardiovascular differentiation potential *in vitro* and *in vivo* [9,10]. More recently, cells with MSC-like characteristics have been derived from human embryonic stem cells (ESCs) [11–15]. These cells resemble hMSCs derived from various tissue sources with respect to morphology, surface marker profile, immunogenicity and differentiation potential toward osteogenic, adipogenic and chrondrogenic lineages [12,14]. More important, they lack expression of pluripotency-associated markers, and after transplantation, no teratoma formation has been reported [12,16]. MSCs derived from human ESCs may therefore be mesoderm progenitors like primitive MSCs and may constitute the most primitive committed mesodermal cell type.

In this study, it was investigated whether the developmental stage of the tissue, from which hMSCs were derived, had an effect on the cardiac differentiation potential of these cells. To this end, the ability of hMSCs derived from ESCs, fetal (amniotic membrane, umbilical cord and bone marrow) and adult (adipose tissue and bone marrow) tissue sources to differentiate towards cardiomyocytes, smooth muscle cells and endothelial cells was studied.

MATERIALS AND METHODS

ISOLATION AND CULTURE OF NEONATAL RAT CARDIOMYOCYTES AND FIBROBLASTS

All animal experiments were approved by the Animal Experiments Committee of the Leiden University Medical Center (LUMC) and conform to the Guide for the Care and Use of Laboratory Animals, as stated by the US National Institutes of Health (permit numbers: 09012 and 10236). Neonatal rat ventricular cardiomyocytes (nrCMCs) and fibroblasts (nrCFBs) were isolated and cultured as described previously [10].

ISOLATION, CULTURE AND CHARACTERIZATION OF HMSCS

All human-derived tissues were collected based on individual written (parental) informed consent, after approval by the Medical Ethics committee of the LUMC, where all investigations were performed. The investigation conforms with the principles outlined in the Declaration of Helsinki. Human mesenchymal stem cells (hMSCs) were derived from embryonic stem cells (hESC-MSCs), fetal amniotic membrane (amniotic), umbilical cord (UC), bone marrow (BM), adult BM and adipose tissue (adipose). Furthermore, fetal human skin fibroblasts (hSFBs) were also isolated and used as control cells (see Online Supplement for extensive description of cell isolation and culture procedures). All hMSCs were characterized by flow cytometry, adipogenic and osteogenic differentiation ability, immunocytological analyses, growth kinetics and telomere length. After characterization, cells were labeled with enhanced green fluorescent protein (eGFP) and put in co-culture with nrCMCs or nrCFBs for 10 days to study their cardiomyogenic differentiation potential. Differentiation was assessed by human-specific immunocytological analyses, whole-cell current-clamp recordings, human-specific quantitative reverse transcription-polymerase chain reaction (qRT-PCR) analysis and optical mapping of action potential propagation. In addition, Western Blot analysis was used to study the expression of connexin43 (Cx43) in relation to differentiation of hMSCs. All experiments described below were conducted using hMSCs from passage 3-6.

FLOW CYTOMETRY

Analysis of surface marker expression was carried out by flow cytometry using fluorescein isothiocyanate-, phycoerythrin- or allophycocyanin-conjugated antibodies directed against human CD105 (Ancell, Bayport, MN, USA), CD90, CD73, CD45, CD34, CD31, CD24 and stage-specific embryonic antigen-4 (SSEA-4) (all from Becton Dickinson, Franklin Lakes, NJ, USA).

ADIPOGENIC AND OSTEOGENIC DIFFERENTIATION

Adipogenesis and osteogenesis of hMSCs were induced by incubating hMSCs in appropriate differentiation media. Lipid accumulation was assessed by Oil Red O

(Sigma-Aldrich, St. Louis, MO, USA), while calcium deposits were visualized by staining the cells with 2% Alizarine Red S (Sigma-Aldrich).

GROWTH KINETICS

Growth kinetics of the hMSCs was analyzed by calculating population doublings (PDs). hMSCs were plated in triplicate and trypsinized every 5 days and subjected to Trypan Blue staining to determine the viable cell concentration using a hemocytometer.

RELATIVE TELOMERE LENGTH

Genomic DNA from experimental and reference samples was obtained using DNA-zol (Invitrogen, Breda, The Netherlands). Relative telomere lengths were measured by SYBR Green-based (Qiagen, Valencia, CA, USA) qRT-PCR amplification of telomere repeats (T) and single-copy gene 36B4 (S) in a LightCycler 480 Real-Time PCR System (Roche, Foster City, CA, USA).

IMMUNOCYTOCHEMICAL ANALYSES

Co-cultures or monocultures were fixed in 4% paraformaldehyde, permeabilized with 0.1% Triton X-100, and stained with primary antibodies. Primary antibodies specific for human lamin A/C (Vector laboratories, Burlingame, CA, USA), SSEA-4, Oct3/4 (both Santa Cruz Biotechnologies, Santa Cruz, CA, USA), Nanog (R&D Systems, Minneapolis, MN, USA), CD90, CD73, and CD105 were used to characterize hESC-MSCs. Co-cultures were stained with α-actinin, Cx43 (both Sigma-Aldrich) and human lamin A/C. Primary antibodies were visualized with Alexa fluor-conjugated antibodies (Invitrogen). Nuclei were stained using Hoechst 33342 (Invitrogen). A fluorescence microscope equipped with a digital camera (Nikon Eclipse, Nikon Europe, Badhoevedorp, The Netherlands) and dedicated software (Image-Pro Plus, Version 4.1.0.0, Media Cybernetics, Silver Spring, MD, USA) were used to analyze data. All cultures were treated equally using the same antibody dilutions and exposure times.

ELECTROPHYSIOLOGICAL MEASUREMENTS IN PHARMACOLOGICALLY UNCOUPLED HMSCS IN CO-CULTURE WITH NRCMCS

In order to study functional cardiomyogenic differentiation in hMSCs, either eGFP-labeled fetal or adult hMSCs were put in co-culture with nrCMCs and studied as described previously [10]. In brief, at day 10 of co-culture, 180 μmol/L of 2-aminoethoxydiphenyl borate (2-APB) (Tocris, Ballwin, MO, USA) was added to the extracellular solution, resulting in gap junction uncoupling [17,18], which allowed for single-cell studies within the co-culture. Next, whole-cell current-clamp recordings were performed in eGFP-labeled hMSCs.

HUMAN-SPECIFIC QUANTITATIVE REVERSE TRANSCRIPTION PCR

Total cellular RNA was extracted from monocultures of hMSCs and from co-cultures consisting of hMSCs and nrCMCs using the RNeasy Mini kit (Qiagen). Oligo (dT)-primed reverse transcription was performed on 2 μg of total cellular RNA and the resultant cDNA was used for PCR amplification using SYBR Green. To detect changes in cardiac and pluripotency gene expression levels, only human-specific primers were used. The expression of the genes of interest was normalized to that of the housekeeping gene *glyceraldehyde-3-phosphate dehydrogenase* (GAPDH). Specific primer information and annealing temperatures are provided in the Online Supplement. Data were analyzed using the ΔCt method.

OPTICAL MAPPING TO DETERMINE CONDUCTION VELOCITY IN CO-CULTURES OF NRCMCS AND DIFFERENT TYPES OF HMSCS

Action potential conduction velocity (CV) was investigated on a whole-culture scale in wells of a 24-well plate by optically mapping using the voltage-sensitive dye di-4-ANEPPS (Invitrogen). The measurements were performed 10 days after seeding of either $8x10^5$ nrCMCs (nrCMC monoculture) or $8x10^5$ nrCMCs plus $8x10^4$ nrCFBs or $8x10^4$ hMSCs (nrCMC/nrCFB or nrCMC/hMCS co-cultures) per well. The co-cultures were mapped using the Ultima-L optical mapping setup (SciMedia, Costa Mesa, CA, USA). Optical signal recordings were analyzed using Brain Vision Analyze 0909 (Brainvision Inc, Tokyo, Japan). The CV of all (co-)cultures was determined in a blinded manner.

ASSESSMENT OF ANGIOGENESIS

All types of hMSCs were were plated on Matrigel (Becton Dickinson) and cultured in Endothelial Growth Medium-2 (Cambrex IEP, Wiesbaden, Germany) containing 100 ng/mL recombinant human VEGF-A$_{165}$ (R&D Systems) up to 24 h to determine their ability to form capillary-like structures. Following culture under angiogenic conditions, cells were fixed and stained with antibodies specific for smooth muscle myosin heavy chain (smMHC; Sigma-Aldrich) and platelet/endothelial cell adhesion molecule-1 (PECAM-1; Santa Cruz).

WESTERN BLOT ANALYSIS

Homogenates were made from at least 5 different isolations of hMSCs per source. Equal amounts of protein were size-fractionated in a 12% NuPage Tris-Acetate gel (Invitrogen) and transferred to a Hybond-P PVDF membrane (GE Healthcare, Waukesha, WI, USA). This membrane was incubated for 1 h with an antibody against Cx43 followed by incubation with horse radish peroxidase conjugated goat anti-rabbit secondary antibody (Santa Cruz). To check for equal protein loading, the housekeeping protein GAPDH (Chemicon International, Temecula, CA, USA) was used.

STATISTICS

Experimental results were expressed as mean±standard deviation (SD) for a given number (n) of observations. Data was analyzed by Student's t-test for direct comparisons. Analysis of variance followed by the appropriate post-hoc analysis was performed for multiple comparisons. Statistical analysis was performed using SPSS 16.0 for Windows (SPSS Inc, Chicago, IL, USA). Differences were considered statistically significant at $P<0.05$.

A detailed description of the materials and methods can be found in the Supplemental Materials and Methods S1.

RESULTS

ISOLATION AND CHARACTERIZATION OF HMSCS

All types of hMSCs displayed a spindle-shaped morphology (Supplemental Figure S1A1-F1). To evaluate MSC properties, their surface phenotype and adipogenic and osteogenic differentiation capacity were studied. All types of hMSCs were negative for CD31 (endothelial cell marker), CD34, CD45 (hematopoietic cell markers), and SSEA-4 (embryonic stem cell marker), whereas they were positive for CD90, CD73 and CD105 (mesenchymal cell markers). Furthermore, hESC-MSCs were negative for CD24, indicating absence of hESCs in our cultures (Supplemental Table S1). *In vitro* differentiation assays confirmed that all types of hMSCs were able to differentiate into adipocytes and osteoblasts thus confirming their multipotent differentiation potential (Supplemental Figure S1A2-F2 and S1A3-F3, respectively).

GROWTH KINETICS

Comparison of the growth kinetics of hESC-MSCs with those of fetal or adult hMSCs showed that hESC-MSCs had a significantly larger replication capacity during 20 days in culture (35.1 PDs) than any of the fetal hMSCs types (22.3-31.6 PDs) and both types of adult MSCs (6.4-12.8 PDs) ($P<0.001$). Fetal hMSCs also proliferated more rapidly and grew to higher densities than both types of adult hMSCs ($P<0.001$) (Supplemental Figure S1G).

TELOMERE LENGTH

Replicative stability of hMSCs was determined by estimating their relative telomere lengths (i.e. telomere repeat copy number to single gene copy number [T/S] ratio). Relative telomere length was significantly longer in hESC-MSCs (4.87±0.7) and in fetal hMSCs (2.48±0.4) than in adult hMSCs (0.89±0.2) ($P<0.05$; n=10 samples from different isolations for each hMSC group). Relative telomere length was also
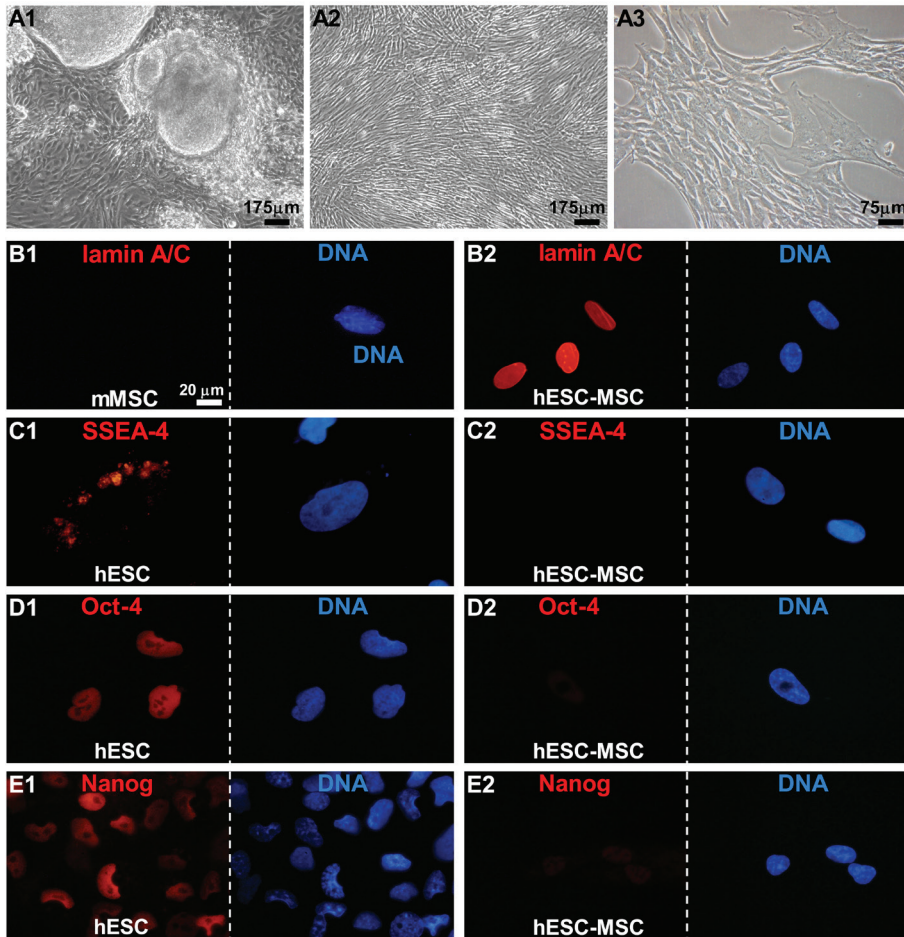
Figure 1. Characterization of hESC-MSCs: (A1) Bright field image of a hESC colony in which the cells at the periphery are differentiating toward spindle-shaped fibroblast-like cells and (A2-A3) pure cultures of hESC-MSC. (B1-B2) Confirmation of the human origin of the hMSCs derived from hESC colonies with the aid of a human-specific lamin A/C antibody. Incubation of murine MSCs (mMSCs; negative control cells) with this antibody (B1) did not produce signal corroborating its species specificity. (C1-E2) Immunostaining of hESC colonies and hMSCs derived from these colonies for the embryonic stem cell marker SSEA-4 and the pluripotency markers Oct-4 and Nanog. Nuclei were detected with Hoechst.

significantly longer in hESC-MSCs than in fetal hMSCs ($P<0.05$; n=10 samples from different isolations for each hMSC group) (Supplemental Figure S1H).

IMMUNOCYTOLOGICAL CHARACTERIZATION OF HESC-MSCS

All fibroblast-like cells derived from the hESC colonies (Figure 1A1-A3) were recognized by a monoclonal antibody specific for human lamin A/C confirming the human origin of these cells (Figure 1B2). Murine MSCs (mMSCs), which served as a negative control, were negative for this marker (Figure 1B1). In addition, hESC-MSCs were negative for the undifferentiated hESC marker SSEA-4 and the pluripotency markers Oct-4 and Nanog (Figure 1C2-E2) in contrast to the hESC colonies from which the fibroblast-like cells were derived (Figure 1C1-E1). However, hESC-MSCs were positive for the mesenchymal cell markers CD90, CD73 and CD105 (Supplemental Figure S2A1-A3).

ASSESSMENT OF CARDIOMYOGENIC DIFFERENTIATION

Human-specific immunocytological evaluation
At day 10 of co-culture with nrCMCs, 7.17±0.4% eGFP-labeled hESC-MSCs (n=1,500 cells analyzed from 5 different isolations) were positive for the sarcomeric protein α-actinin (Figure 2A1 and 2E), which was a significantly higher fraction than the percentage of fetal hMSCs staining for α-actinin (fetal amniotic MSCs 2.15±0.2%, fetal BM MSCs 1.8±0.3% and fetal UC MSCs 2.56±0.7%, n=1,200 cells analyzed from 4 different isolations per type of fetal hMSC) ($P<0.001$) (Figure 2B and 2E). Furthermore, in some of the hESC-MSCs (30.8%), fetal amniotic MSCs (25.8%) and fetal BM MSCs (5.89%) α-actinin was distributed in a cross-striated pattern typical for CMCs. After 10 days of co-culture with nrCMCs, adult BM and adipose MSCs did not stain for α-actinin (n=1,200 cells analyzed from 4 different isolations per type of adult hMSC) (Figure 2C and 2E). eGFP-labeled fetal hSFBs in co-culture with nrCMCs were not positive for α-actinin (n=1,200 cells analyzed from 4 different isolations) (Figure 2D and 2E) indicating that not all fibroblastic human cell types acquire cardiomyocyte properties in co-culture with nrCMCs. To exclude fusion of nrCMCs with hMSCs or secondary transduction of nrCMCs with eGFP, all co-cultures were also stained for human-specific lamin A/C. None of the eGFP positive cells were negative for human-specific lamin A/C or contained multiple nuclei (n≥8,500 eGFP-positive cells analyzed) confirming the validity of the assay system.

To assess the influence of the cellular microenvironment on cardiomyogenic differentiation of hESC-MSCs and fetal hMSCs the presence of α-actinin in these cells after 10 days of co-culture with nrCFBs rather than nrCMCs was determined. Alpha-actinin was not expressed by hESC-MSCs (Figure 3A1) or any of the fetal hMSC types (Figure 3A2) after co-culture with nrCFBs (n=1,200 cells analyzed from 3 different isolation of each hMSC type) (Figure 3B).
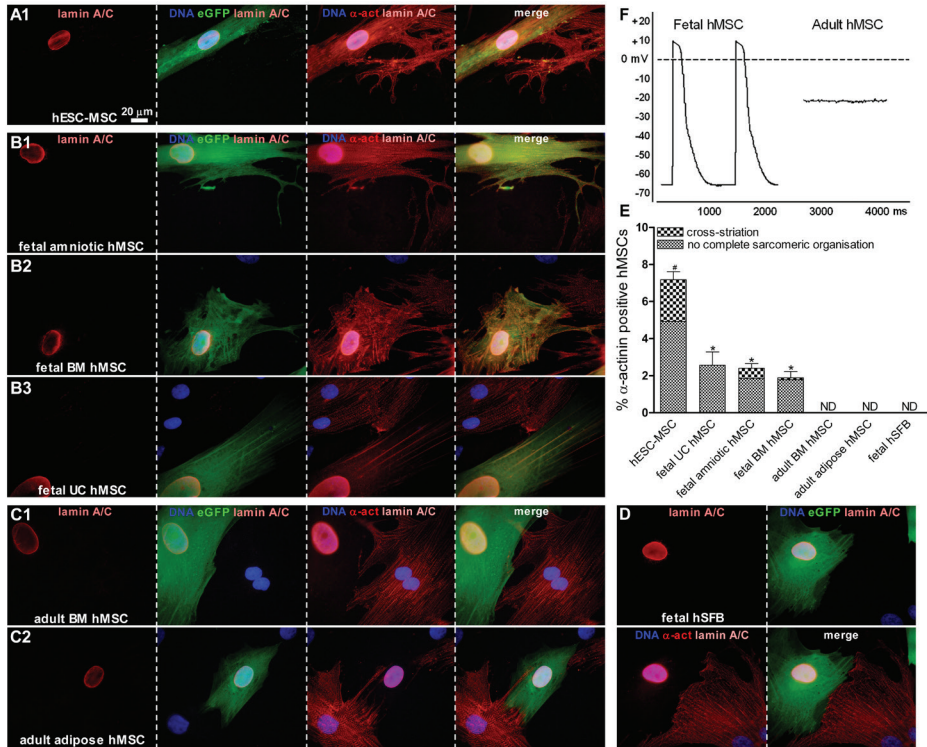
Figure 2. Immunocytological assessment of cardiomyogenic differentiation of different types of hMSCs after 10 days of co-culture with nrCMCs. (A1-B3) A fraction of eGFP-labeled, human-specific lamin A/C positive hESC-MSCs and fetal amniotic, BM and UC hMSCs expressed α-actinin (indicated as α-act), while (C1-C2) adult BM and adipose hMSCs did not. (D) eGFP-labeled human fetal skin fibroblasts (hSFBs; negative control cells) in co-culture with nrCMCs did not stain positive for α-actinin. (E) Quantitative analysis of the cardiomyogenic differentiation of different types of hMSCs. The graph is based on a minimum of 1,200 cells analyzed from 4 separate isolations per hMSC type. [#]$P<0.001$ vs all fetal and adult hMSC types; [*]$P<0.05$ vs adult hMSCs; ND is not detected. (F) Intracellular electrophysiological measurements in fetal (amniotic) and adult (adipose) hMSCs at day 10 of co-culture with nrCMCs and after pharmacological uncoupling of gap junctions. Intrinsic action potentials could be recorded from eGFP-labeled fetal cells, while adult hMSCs showed only steady membrane potentials.
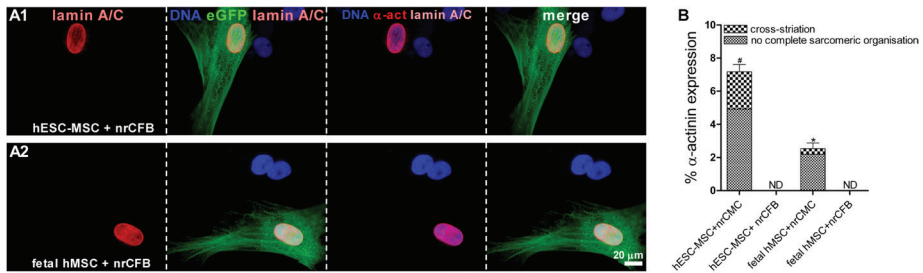
Figure 3. Study of cardiomyogenic differentiation in hESC-MSCs and fetal hMSCs after co-culture with nrCFBs for 10 days assessed by immunocytological analysis. (A1-A2) No α-actinin expression, indicated as α-act, was detected in eGFP-labeled, human-specific lamin A/C positive hESC-MSCs or fetal hMSCs after co-incubation with nrCFBs. Nuclei were detected with Hoechst. (B) Quantitative analysis of cardiomyogenic differentiation of hESC-MSCs and all of the fetal hMSC types co-cultured with nrCFBs or nrCMCs. The graph is based on a minimum of 1,200 cells analyzed from 3 separate isolations per hMSC type. #$P<0.001$ vs hESC-MSCs and fetal hMSCs co-cultured with nrCFBs and fetal hMSCs in co-culture with nrCMCs; *$P<0.01$ vs fetal hESC-MSCs and fetal hMSCs co-cultured with nrCFBs; ND is not detected.

Intracellular electrophysiological measurements in pharmacologically uncoupled hMSCs in co-culture with nrCMCs.
Patch-clamp recordings were obtained from eGFP-labeled fetal and adult hMSCs at day 10 of co-culture with nrCMCs after electrical isolation through incubation with the gap junction uncoupler 2-APB. Action potentials could only be measured in fetal hMSCs (n=5, amniotic), this in contrast to adult hMSCs (n=8, adipose), which only showed steady membrane potentials (Figure 2F). Selection of cells was based on eGFP-labeling and the presence of 2-4 nrCMCs adjacent to the cells of interest.

Human-specific qRT-PCR analysis to detect pluripotency and cardiac differentiation
qRT-PCR showed that at the mRNA level, hESC-MSCs expressed the following cardiac markers: *Nkx2.5*, *GATA-4*, *ANP*, *MLC2v* and *Cx43*. These mRNAs were upregulated after co-culture with nrCMCs ($P<0.001$ for both *ANP* and *MLC2v*; $P<0.01$ for *Nkx2.5*; $P<0.05$ for both *GATA-4* and *Cx43*). However, *Islet-1* and *c-kit* mRNA levels were lower in co-cultured hESC-MSCs compared to hESC-MSC monocultures ($P<0.01$ and $P<0.05$, respectively). No significant difference in gene expression of *VEGF* was detected in hESC-MSCs before or after co-incubation with nrCMCs (Figure 4A). Fetal amniotic hMSCs showed an increase in *Nkx2.5* ($P<0.05$), *ANP*, *Cx43* and *VEGF* (all $P<0.01$) gene expression after co-culture with nrCMCs, while *Islet-1* mRNA levels were decreased under these circumstances ($P<0.05$). No

difference in *c-kit* gene expression was detected in these fetal hMSCs before or after co-incubation with nrCMCs (Figure 4B). In fetal UC hMSCs, mRNA levels of *GATA-4*, *Cx43* (both *P*<0.05) and *VEGF* (*P*<0.001) were significantly upregulated after their co-culture with nrCMCs, while *Islet-1* and *c-kit* gene expression were downregulated (*P*<0.001 and *P*<0.01, respectively). No change in the expression of *ANP* was detected in fetal UC hMSCs following co-incubation with nrCMCs (Figure 4C). Fetal BM hMSCs showed an increase in *ANP* (*P*<0.001), *Cx43* and *c-kit* (both *P*<0.05) gene expression co-incubation with nrCMCs, while no difference in *Islet-1* and *VEGF* mRNA levels were detected under these circumstances (Figure 4D). At the mRNA level, *ANP*, *Cx43*, *VEGF* and *c-kit* were detected in adult BM and adipose hMSCs. However, after co-culture with nrCMCs, only the expression of *ANP* (*P*<0.05) and *VEGF* (*P*<0.01) increased in both types of adult hMSCs. In adult adipose hMSCs *c-kit* mRNA levels were also upregulated in the presence of nrCMCs (*P*<0.05) (Figure 4E-4F). *Oct-4*, *Nanog*, *cTnI* and β-*MHC* gene expression was not detected in any of the hMSC types. qRT-PCR analysis of RNA from appropriate human control samples confirmed the functionality of all human-specific primer pairs. The same primer pairs did not give rise to amplification products using nrCMC RNA as starting material. Expression of the qRT-PCR target genes in nrCMCs was confirmed using rat-specific primers. Quantitative differences in gene expression between hMSCs cultured alone or with nrCMCs are given in supplemental table S2.

Optical mapping analysis to determine action potential CV in co-cultures of nrCMCs with different types of hMSCs
CV in nrCMC co-cultures with hESC-MSCs (25.9±0.9 cm/s) was similar to the CV in nrCMC cultures alone (24.8±1.2 cm/s) (Figure 5B1-B2 and 5C). However, it was significantly higher than in co-cultures of nrCMCs with fetal amniotic hMSCs (22.0±1.8 cm/s), adult adipose hMSCs (18.2±1.1 cm/s) and nrCFBs (17.0±1.2 cm/s) (*P*<0.001; n≥15 co-cultures with each cell type) (Figure 5B3-B5 and C). CV was also higher in co-cultures of nrCMCs with fetal amniotic hMSCs than in co-cultures with adult adipose hMSCs or with nrCFBs (*P*<0.001) (Figure 5B3-B5 and C).
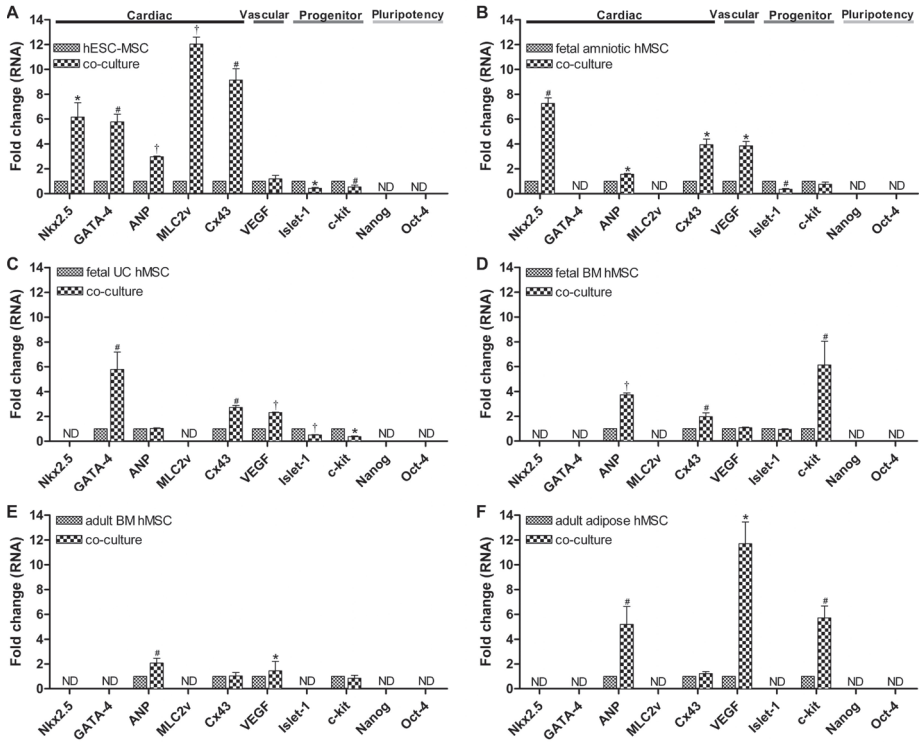
Figure 4. Analysis by qRT-PCR of expression of pluripotency and cardiac genes in hMSCs alone or after co-incubation with nrCMCs. (A) hESC-MSCs expressed most cardiac-specific genes, which were significantly upregulated after co-incubation with nrCMCs. Expression of the cardiac progenitor genes, *Islet-1* and *c-kit*, was downregulated in the presence of nrCMCs. (B-D) The fetal hMSC types expressed a variety of cardiac-specific genes, which were upregulated after co-culture with nrCMCs. *Islet-1* and *c-kit* mRNA levels decreased in the presence of nrCMCs with the exception of the upregulation of *c-kit* gene expression in fetal BM MSCs following their co-culture with nrCMCs. (E-F) *ANP*, *Cx43*, *VEGF* and *c-kit* gene expression was detected in adult hMSCs before and after co-incubation with nrCMCs. (A-F) hMSCs did not express the pluripotency genes Oct-4 and Nanog. #$P<0.05$ vs specific hMSC monoculture; *$P<0.01$ vs specific hMSC monoculture; †$P<0.001$ vs specific hMSC monoculture.
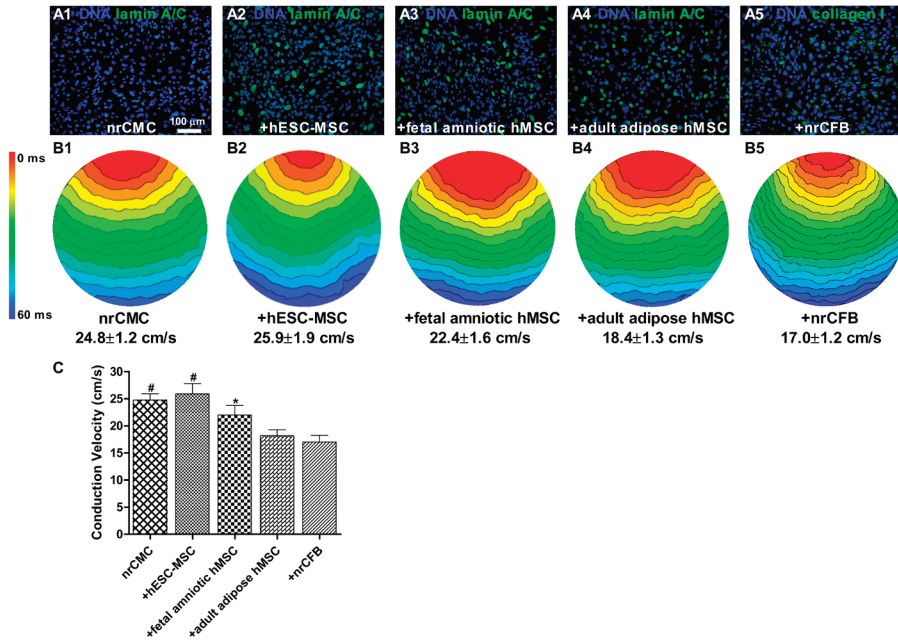
Figure 5. Assessment of CV by optical mapping in co-cultures of nrCMCs and different types of hMSCs. (A) The presence of hMSCs and nrCFBs after optical mapping was confirmed by immunostaining for human-specific lamin A/C and collagen type I, respectively. Nuclei were detected with Hoechst. (B) Activation maps of the different (co-)cultures reveal significantly higher CVs in nrCMCs monocultures and in hESC-MSCs/nrCMC and fetal amniotic hMSCs/nrCMC co-cultures than in co-cultures of nrCMCs with adult adipose hMSCs or with nrCFBs. CVs were also significantly higher in nrCMC monocultures and in hESC-MSCs/nrCMC co-cultures than in co-cultures between nrCMCs and fetal amniotic hMSCs. Spacing of isochronal lines in activation maps is 4 ms, and colors indicate temporal sequence of activation, starting from the red area. (C) Bar graph of the CVs in nrCMC monocultures and in co-cultures (+) between nrCMCs and nrCFBs or different types of hMSCs as indicated. #$P<0.001$ vs fetal amniotic hMSCs, adult adipose hMSCs and nrCFBs co-incubated with nrCMCs; *$P<0.01$ vs adult adipose hMSCs and nrCFBs co-incubated with nrCMCs.

IN VITRO ANGIOGENESIS ASSAYS

hESC-MSCs and all types of fetal hMSCs were able to form capillary-like structures on Matrigel (n≥5 isolations of each hMSC type incubated in triplicate) (Figure 6A1-D1). These networks stained positively for the smooth muscle marker smMHC and the endothelial cell marker PECAM-1 (Figure 6A2-D2). Formation of cellular networks was established by hESC-MSCs 12 h after incubation on Matrigel. For hMSCs derived from the fetal sources it took 18 h to establish capillary-like networks. Adult BM and adipose tissue hMSCs failed to form capillary-like structures (n≥5 isolations of each hMSC type incubated in triplicate) (Figure 6E-F). Formation of vessel-like networks was checked every hour for a total period of 24 h.

EVALUATION OF CX43 EXPRESSION LEVELS

To further analyze mechanisms underlying differences in cardiomyogenic potential, Cx43 expression levels were evaluated. Immunocytological analysis showed that Cx43 protein expression was more abundant in hESC-MSCs and fetal amniotic MSCs than in adult adipose MSCs and nrCFBs (n=5 isolations of each hMSC type were assessed) (Figure 7A). These results were confirmed by Western blot analysis (n=5 different isolations for each cell type) (Figure 7C). Cx43 expression was also detected at the interfaces between nrCMCs and hESC-MSCs or fetal MSCs, while under equivalent staining conditions it was not present at contact-areas between nrCMCs and adult hMSCs or nrCFBs (Figure 7A). Moreover, Cx43 did not line borders between nrCFBs and any of the types of hMSCs (n≥1,500 cells analyzed from 5 isolations of each cell type under each condition) (Figure 7A). qRT-PCR showed a significant increase in *Cx43* expression following the incubation of hESC-MSCs or fetal amniotic hMSCs with nrCMCs (9.14±0.9 ($P<0.01$) and 3.94±0.5 fold ($P<0.001$), respectively), while no (hESC-MSCs) or 19.4±0.1 fold less (fetal amniotic hMSCs) *Cx43* mRNA was detected in co-cultures with nrCFBs ($P<0.05$) (Figure 7B1-B2). No significant difference in *Cx43* mRNA levels was detected between adult adipose tissue hMSCs cultured alone or together with nrCMCs or nrCFBs (Figure 7B3).
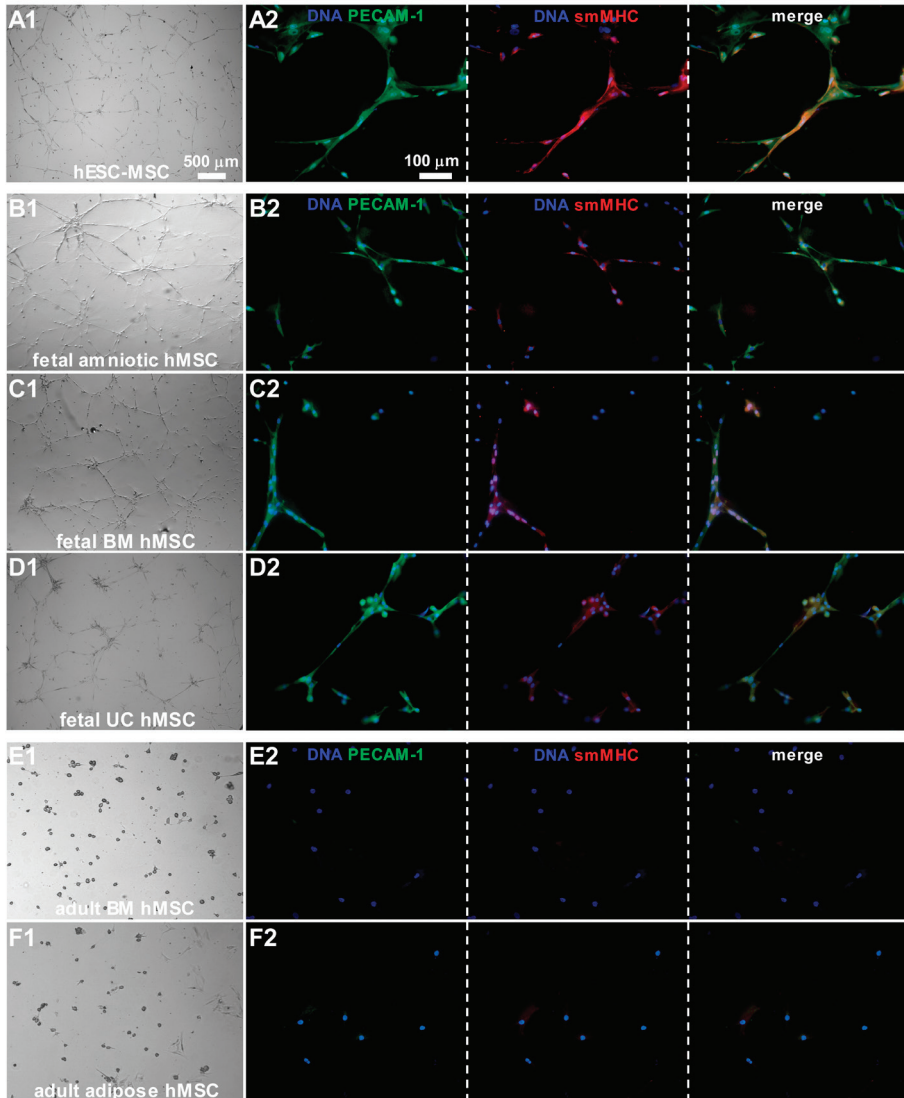
Figure 6. Angiogenic differentiation capacity of different types of hMSCs assessed by formation of capillary-like structures and expression of angiogenic markers following their culture on Matrigel. (A1-D1) Bright field images show that hESC-MSCs and fetal hMSCs were able to form stable cellular networks on a basement membrane matrix, while (E1-F1) adult hMSCs could not. (A2-D2) hESC-MSCs and all fetal hMSC types stained positive for the endothelial cell protein, PECAM-1, and the smooth muscle cell protein, smMHC, while (E2-F2) the adult hMSCs were negative for these markers. Nuclei were stained with Hoechst.
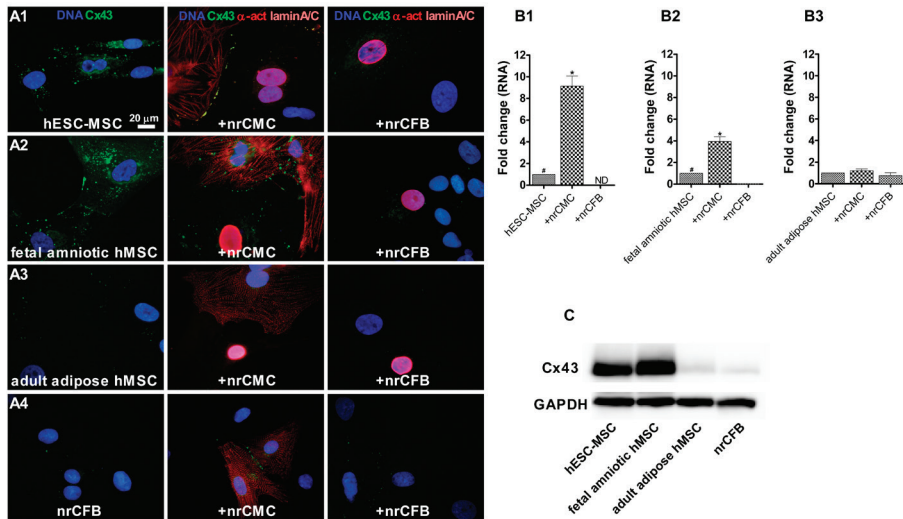
Figure 7. Analysis by immunofluorescence microscopy, qRT-PCR and Western blotting of *Cx43* expression in hMSC monocultures and in co-cultures of nrCMCs or nrCFBs with different types of hMSCs. (A1-A2) Immunocytological analysis shows high Cx43 levels in monocultures of hESC-MSCs and fetal amniotic hMSCs. Cx43 was also detected at the interfaces of these young hMSCs with nrCMCs but not with nrCFBs. nrCMCs were visualized by staining with α-actinin (indicated as α-act), while an antibody against human-specific lamin A/C was used to detect hMSCs. Nuclei were detected with Hoechst. (A3-A4) Adult adipose hMSCs contain very low amounts of Cx43 in both monocultures and co-cultures with nrCMCs or nrCFBs. Also in nrCFB monocultures and nrCFB/nrCMC co-cultures Cx43 is barely detectable. (B1-B3) Bar graphs of the assessment by qRT-PCR of *Cx43* mRNA levels in hESC-MSC, fetal amniotic hMSC and adult adipose hMSC monocultures and co-cultures (+) of these cells with either nrCMCs or nrCFBs as indicated. (C) Picture of representative part of a Western blot showing that hESC-MSCs and fetal amniotic hMSCs contain large amounts of Cx43 in contrast to adult adipose hMSCs and nrCFBs. The housekeeping protein glyceraldehyde-3-phosphate dehydrogenase (GAPDH) was used to check for equal protein loading. [#]$P<0.05$ vs hMSCs in co-culture with nrCFBs; [*]$P<0.01$ vs hMSC monocultures and hMSCs in co-culture with nrCFBs.

DISCUSSION

Key findings of the present study are: 1) Differentiation potential of hMSCs toward three cardiac cell lineages depends on the developmental stage of donor tissue; 2) Cardiomyogenesis of hMSCs is influenced by stimuli from the cellular microenvironment; and 3) The propensity of different types of hMSCs to acquire properties of heart muscle cells correlates with Cx43 expression levels.

DEVELOPMENT AND STEMNESS

During embryonic development, stem cells contribute to organ formation, while later in life these cells or their derivatives are involved in repair and regeneration of organs [6]. However, with increasing age, the potential of stem cells declines [19,20]. This decrease in the regenerative ability is associated with cumulative organ dysfunction, which may lead to increased morbidity and mortality. Consistent with this developmental stage-dependent decline in function of stem cells, this study showed that MSCs derived from hESCs have significantly greater proliferative capacity and longer telomeres than MSCs derived from human fetal tissue, or adult hMSCs. The intrinsic age-associated decrease in telomere length is one of the mechanisms that contributes to the loss of stem cell properties with age [21]. The results of this first-time direct comparison of the proliferative capacity of hESC-MSCs, fetal hMSCs and adult hMSCs are in line with previous studies [12,13,22–24]. All together, these findings show that MSCs derived from human ESCs are more immature and display greater stemness than those derived from fetal tissues.

MSCS AND CARDIAC DIFFERENTIATION

In the present study, it was also shown that hMSCs derived from either embryonic or fetal sources have the capacity to undergo cardiac differentiation, while those derived from adult sources do not. Our results revealed that developmental stage of the donor tissue not only influences the ability of hMSCs to differentiate into CMCs but also their capacity to undergo smooth muscle and endothelial differentiation. This information may be of value in extending the repertoire of cells considered suitable for studies of cardiac repair. We showed that after co-culture with nrCMCs the sarcomeric protein α-actinin is expressed by a significantly higher percentage of hESC-MSCs than of fetal hMSCs, while it was not expressed by adult hMSCs. Although the cardiomyogenic potential of MSCs derived from neonatal sources has been described before, a direct comparison of hMSCs derived from embryonic, fetal and adult sources was not conducted [9,10]. Controversy still exists on whether MSCs actually differentiate into CMCs or whether this apparent cardiomyogenesis is due to fusion of MSCs with CMCs [25]. Therefore, in all our co-culture experiments eGFP-transduced hMSCs were stained for human-specific

lamin A/C. Neither multinucleated eGFP positive cells nor eGFP positive cells negative for human-specific lamin A/C were detected. In addition, only human-specific primers were used in the qRT-PCR experiments to exclude detection of rat cardiac-specific genes expressed by nrCMCs. Accordingly, the cardiomyogenic differentiation of hMSCs observed in our experiments does not result from cell fusion. Importantly, the records of intrinsic action potentials in eGFP positive cells at day 10 of co-culture provides direct evidence for functional cardiomyogenic differentiation.

With respect to smooth muscle and endothelial differentiation, only hESC-MSCs and fetal hMSCs were able to form capillary-like structures on Matrigel. These networks stained positive for the smooth muscle marker smMHC and the endothelial marker PECAM-1. Previous studies showed that adult BM-derived MSCs were able to form capillary-like structures after priming the cells in endothelial differentiation medium. However, after priming, UC hMSCs had higher endothelial potential than adult BM hMSCs [26,27].

Concerning the underlying mechanisms why adult hMSCs do not form CMCs, Cx43 expression may be of importance. In this study, hMSCs are co-cultured with nrCMCs, resulting in physical contact between these two cell types, and allowing the possibility for gap junction formation. Gap junctions, which in the ventricles are mainly formed by Cx43, allow a low-resistant spread of chemical and electrical signals between adjacent cells [28]. Interestingly, hMSCs derived from adult human sources express very low levels of Cx43, both at mRNA and protein level, as compared to hMSCs derived from embryonic and fetal sources. In addition, hMSCs, which underwent functional cardiomyogenic differentiation, were always adjacent to native CMCs, naturally containing high levels of Cx43. As hMSCs are able to form functional gap junctions with adjacent CMCs [29], electrical and chemical interaction can occur between both cell types and this was shown to play a role in cardiomyogenic differentiation [30]. Interestingly, co-culture of MSCs with cardiac fibroblasts, expressing very low levels of Cx43, did not result in cardiomyogenic differentiation. In fact, using human-specific primers, *Cx43* expression levels in hMSCs were shown to decrease significantly in this microenvironment.

As Cx43 plays an essential role in myocardial electrical conduction across the ventricular muscle, and cardiomyogenic differentiation would make non-excitable MSCs become excitable, we also studied the CV across co-cultures of hMSCs with nrCMCs. It was shown that co-cultures with hESC-MSCs showed a significantly higher CV than those with fetal hMSCs and adult hMSCs, while the CV in co-cultures with fetal hMSCs was also significantly higher than that in those with adult hMSCs. Of note, embryonic MSCs did not only show high expression of Cx43, but had the greatest cardiomyogenic differentiation potential. The type of MSC that

contributes to the highest CV may be preferable to accomplish functional integration with host myocardium after transplantation.

MSC TRANSPLANTATION FOR CARDIAC DISEASES

Besides providing new insights into the factors that stimulate cardiac differentiation, the findings of this study may also have implications for the use of MSCs in patients. Currently, in myocardial cell therapy studies mainly autologous cells from aged patients suffering from chronic diseases are used. Based on our results, it may be expected that the therapeutic effects of MSC transplantation, to improve cardiac function, are affected by intrinsic properties of the transplanted cells. Furthermore, the beneficial effects of stem cell therapy in the damaged heart seems to be largely mediated by paracrine factors promoting neo-angiogenesis and CMC survival with little evidence of the differentiation of transplanted cells into CMCs [3]. As these effects will be of limited help in case of extensive loss of myocardial tissue there is still a great demand for stem cells that can differentiate in vivo into new CMCs. In this study, we have shown that hMSCs of prenatal origin can differentiate into functional CMCs and that this process is dependent on instructive cues provided by neighboring CMCs. Therefore selection of MSCs from donor sources, such as the umbilical cord or amniotic membrane/fluid, may be an attractive source of immature or young cells for autologous cell transplantation. Even allogeneic transplantation may be considered as MSCs are reported to have immunomodulatory properties [31–33]. However, many aspects related to transplantation of cardiomyogenic stem cells need to be studied in more detail before optimal therapeutic efficacy and minimal hazardous potential can be achieved.

CONCLUSIONS

Human MSCs of embryonic stem cell or fetal but not adult origin can differentiate into three cardiac lineages: cardiomyocytes, endothelial cells and smooth muscle cells. The ability to undergo functional cardiomyogenic differentiation is amongst others determined by the microenvironment of the cells, in particular their communication with adjacent cell types. The gap junction protein Cx43 may play an important role in this differentiation process.

STUDY LIMITATIONS

It would have been more clinically relevant to co-culture the different hMSC subtypes with adult human hCMCs, but obtaining these cells in the numbers needed to conduct these experiments seems not feasible. Furthermore, adult hCMCs cannot be cultured long enough to perform some of the key experiments described in this paper.

ACKNOWLEDGEMENTS

REFERENCES

1.   Lloyd-Jones D, Adams R, Carnethon M, De SG, Ferguson TB et al. (2009) Heart disease and stroke statistics--2009 update: a report from the American Heart Association Statistics Committee and Stroke Statistics Subcommittee. Circulation 119: 480-486.

2.   Ballard VL, Edelberg JM (2007) Stem cells and the regeneration of the aging cardiovascular system. Circ Res 100: 1116-1127.

3.   Passier R, van Laake LW, Mummery CL (2008) Stem-cell-based therapy and lessons from the heart. Nature 453: 322-329.

4.   O'Donoghue K, Fisk NM (2004) Fetal stem cells. Best Pract Res Clin Obstet Gynaecol 18: 853-875.

5.   Roobrouck VD, Ulloa-Montoya F, Verfaillie CM (2008) Self-renewal and differentiation capacity of young and aged stem cells. Exp Cell Res 314: 1937-1944.

6.   Ballard VL (2010) Stem cells for heart failure in the aging heart. Heart Fail Rev 15: 447-56.

7.   Semenov OV, Koestenbauer S, Riegel M, Zech N, Zimmermann R et al. (2010) Multipotent mesenchymal stem cells from human placenta: critical parameters for isolation and maintenance of stemness after isolation. Am J Obstet Gynecol 202: 193.

8.   Jo CH, Kim OS, Park EY, Kim BJ, Lee JH et al. (2008) Fetal mesenchymal stem cells derived from human umbilical cord sustain primitive characteristics during extensive expansion. Cell Tissue Res 334: 423-433.

9.   Nishiyama N, Miyoshi S, Hida N, Uyama T, Okamoto K et al. (2007) The significant cardiomyogenic potential of human umbilical cord blood-derived mesenchymal stem cells in vitro. Stem Cells 25: 2017-2024.

10.   Pijnappels DA, Schalij MJ, Ramkisoensing AA, van Tuyn J, de Vries AA et al. (2008) Forced alignment of mesenchymal stem cells undergoing cardiomyogenic differentiation affects functional integration with cardiomyocyte cultures. Circ Res 103: 167-176.

11.   Hwang NS, Varghese S, Lee HJ, Zhang Z, Ye Z et al. (2008) In vivo commitment and functional tissue regeneration using human embryonic stem cell-derived mesenchymal cells. Proc Natl Acad Sci U S A 105: 20641-20646.

12.   Lian Q, Lye E, Suan YK, Khia Way TE, Salto-Tellez M et al. (2007) Derivation of clinically compliant MSCs from CD105+. Stem Cells 25: 425-436.

13.   Olivier EN, Rybicki AC, Bouhassira EE (2006) Differentiation of human embryonic stem cells into bipotent mesenchymal stem cells. Stem Cells 24: 1914-1922.

14.   Trivedi P, Hematti P (2008) Derivation and immunological characterization of mesenchymal stromal cells from human embryonic stem cells. Exp Hematol 36: 350-359.

15.   Barberi T, Willis LM, Socci ND, Studer L (2005) Derivation of multipotent mesenchymal precursors from human embryonic stem cells. PLoS Med 2: e161.

16.   Karlsson C, Emanuelsson K, Wessberg F, Kajic K, Axell MZ et al. (2009) Human embryonic stem cell-derived mesenchymal progenitors-Potential in regenerative medicine. Stem Cell Res 3:39-50.

44

17. Bai D, del CC, Srinivas M, Spray DC (2006) Block of specific gap junction channel subtypes by 2-aminoethoxydiphenyl borate (2-APB). J Pharmacol Exp Ther 319: 1452-1458.

18. Harks EG, Camina JP, Peters PH, Ypey DL, Scheenen WJ et al. (2003) Besides affecting intracellular calcium signaling, 2-APB reversibly blocks gap junctional coupling in confluent monolayers, thereby allowing measurement of single-cell membrane currents in undissociated cells. FASEB J 17: 941-943.

19. Bellantuono I, Keith WN (2007) Stem cell ageing: does it happen and can we intervene? Expert Rev Mol Med 9: 1-20.

20. Chambers SM, Goodell MA (2007) Hematopoietic stem cell aging: wrinkles in stem cell potential. Stem Cell Rev 3: 201-211.

21. Torella D, Rota M, Nurzynska D, Musso E, Monsen A et al. (2004) Cardiac stem cell and myocyte aging, heart failure, and insulin-like growth factor-1 overexpression. Circ Res 94: 514-524.

22. In 't Anker PS, Scherjon SA, Kleijburg-van der KC, de Groot-Swings GM, Claas FH et al. (2004) Isolation of mesenchymal stem cells of fetal or maternal origin from human placenta. Stem Cells 22: 1338-1345.

23. Roubelakis MG, Pappa KI, Bitsika V, Zagoura D, Vlahou A et al. (2007) Molecular and proteomic characterization of human mesenchymal stem cells derived from amniotic fluid: comparison to bone marrow mesenchymal stem cells. Stem Cells Dev 16: 931-952.

24. Miao Z, Jin J, Chen L, Zhu J, Huang W et al. (2006) Isolation of mesenchymal stem cells from human placenta: comparison with human bone marrow mesenchymal stem cells. Cell Biol Int 30: 681-687.

25. Alvarez-Dolado M (2007) Cell fusion: biological perspectives and potential for regenerative medicine. Front Biosci 12: 1-12.

26. Oswald J, Boxberger S, Jorgensen B, Feldmann S, Ehninger G et al. (2004) Mesenchymal stem cells can be differentiated into endothelial cells in vitro. Stem Cells 22: 377-384.

27. Chen MY, Lie PC, Li ZL, Wei X (2009) Endothelial differentiation of Wharton's jelly-derived mesenchymal stem cells in comparison with bone marrow-derived mesenchymal stem cells. Exp Hematol 37: 629-640.

28. Kleber AG, Rudy Y (2004) Basic mechanisms of cardiac impulse propagation and associated arrhythmias. Physiol Rev 84: 431-488.

29. Pijnappels DA, Schalij MJ, van Tuyn J, Ypey DL, de Vries AA et al. (2006) Progressive increase in conduction velocity across human mesenchymal stem cells is mediated by enhanced electrical coupling. Cardiovasc Res 72: 282-291.

30. van Vliet P, de Boer TP, van der Heyden MA, El Tamer MK, Sluijter JP et al. (2010) Hyperpolarization Induces Differentiation in Human Cardiomyocyte Progenitor Cells. Stem Cell Rev 6:178-85.

31. Yoo KH, Jang IK, Lee MW, Kim HE, Yang MS et al. (2009) Comparison of immunomodulatory properties of mesenchymal stem cells derived from adult human tissues. Cell Immunol 259: 150-156.

32. Liechty KW, MacKenzie TC, Shaaban AF, Radu A, Moseley AM et al. (2000) Human mesenchymal stem cells engraft and demonstrate site-specific differentiation after in utero transplantation in sheep. Nat Med 6: 1282-1286.

33. Hare JM, Traverse JH, Henry TD, Dib N, Strumpf RK et al. (2009) A randomized, double-blind, placebo-controlled, dose-escalation study of intravenous adult human mesenchymal stem cells (prochymal) after acute myocardial infarction. J Am Coll Cardiol 54: 2277-2286.

SUPPLEMENTAL MATERIALS AND METHODS S1

EXPANDED MATERIALS & METHODS

ISOLATION AND CULTURE OF HUMAN MESENCHYMAL STEM CELLS (HMSCS)

All human-derived tissues were collected based on individual written (parental) informed consent, after approval by the Medical Ethics committee of the Leiden University Medical Center (LUMC), where all investigations were performed. The investigation conforms with the principles outlined in the Declaration of Helsinki.

Derivation of MSCs from human embryonic stem cells (hESCs)

MSCs were derived from undifferentiated hESC colonies (hES3 subclones) as previously described [1,2]. Briefly, the undifferentiated hESC colonies were removed from their mouse embryonic fibroblast (mEF) feeder layer and propagated in gelatin-coated culture dishes in standard MSC culture medium (Dulbecco's modified Eagle's medium [Invitrogen, Breda, The Netherlands] containing 10% fetal bovine serum [FBS; Invitrogen], penicillin [100 U/mL] and streptomycin [100 μg/mL]; hereinafter referred to as MSC-CM) at 37°C in a humidified 5% CO_2 incubator. After 2-3 days of culture, a portion of the cells at the periphery of the hESC colonies differentiated toward spindle-shaped fibroblast-like cells. Next, the undifferentiated portions of the hESC colonies were removed by physical scraping and suctioning. Consecutive enzymatic passaging as single cell suspensions led to a reproducible derivation of morphologically homogeneous fibroblast-like cells from cultures of pluripotent undifferentiated hESCs within 2-3 passages (n=5 different isolations). Medium was replaced twice a week until the primary cultures were 60-80% confluent, after which the so-called hESC-MSCs were amplified by serial passage using a buffered 0.05% trypsin-0.02% ethylenediaminetetraacetic acid/EDTA solution (TE; BioWhittaker, Vervier, Belgium) for cell detachment.

Fetal hMSC isolation and culture

Human fetal tissues (gestational age between 17-22 weeks) were collected through legal interventions by the Department of Obstetrics. Fetal umbilical cords (UCs) and amniotic membranes were washed twice with phosphate-buffered saline (PBS) and were finely minced into 1-2 mm fragments using scissors and scalpels. Cells were released by treatment with 0.1% collagenase type I (Worthington, Lakewood, NJ, USA) for 3 h. Thereafter, 10 mL MSC-CM was added. The cell suspension was transferred to a 25-cm^2 culture flask (Becton Dickinson, Franklin Lakes, NJ, USA) and incubated for 3-4 days at 37°C in a humidified 5% CO_2 atmosphere to allow the cells to adhere. Fetal UC and amniotic membrane (amniotic) hMSCs were subcultured as described in the previous section. Single cell suspensions of fetal bone

marrow (BM) were obtained by punching fetal *femora* and *tibiae* with a 23-gauge needle and flushing them with culture medium. The cell suspension was centrifuged at 330 g for 10 min after which the same culture methods were applied as for the other fetal hMSCs. To obtain human fibroblasts, sections of human fetal skin (5×5 mm) were transferred to 25-cm² culture flasks containing 5 ml MSC-CM and maintained in a humidified 5% CO_2 incubator at 37°C. Fetal human skin fibroblasts (hSFBs) were allowed to migrate from the skin sections for 7 days. Thereafter, the skin sections were removed and the remaining hSFBs were cultured using standard procedures.

Adult MSC isolation and culture

Adult hMSCs were purified from leftover BM samples derived from adult donors undergoing orthopedic surgery (n=8 donors, mean donor age 72±2.4 yrs). Briefly, the mononuclear cell fraction of the BM was isolated by Ficoll density gradient centrifugation. Twenty-four hours after seeding of the BM mononuclear cell fraction in 75-cm² culture flasks (Becton Dickinson), the non-adherent cells were removed and the remaining hMSCs were expanded by serial passage using standard methods.

Adult adipose tissue (adipose) hMSCs were derived from subcutaneous adbdominal fat tissue (n= 10 donors, mean donor age 39.6±1.1 yrs). Tissue samples were washed twice with PBS containing penicillin (100 U/mL) and streptomycin (100 µg/mL). For tissue disruption 0.1% collagenase type I solution was added and tissue samples were finely minced. Next, samples were incubated at 37°C in a humidified 5% CO_2 incubator for 1 h. Collagenase type I activity was quenched by adding excess MSC-CM. Samples were then centrifuged at 330 g for 10 min. After centrifugation the layer of primary adipocytes could be removed and the collagenase type I-containing solution was aspirated. The cell pellet was resuspended in MSC-CM, filtered through a 70 mm cell strainer (Becton Dickinson) and the cells were once again collected by centrifugation. This step was repeated twice, after which the cell pellet was resuspended in 5 ml culture medium. The resulting cell suspension was transferred to a 25-cm² culture flask and these adult adipose tissue (adipose) hMSCs were propagated as all the other hMSCs.

ISOLATION AND CULTURE OF NEONATAL RAT (NR) CARDIOMYOCYTES (CMCS) AND CARDIAC FIBROBLASTS (CFBS)

All animal experiments were approved by the Animal Experiments Committee of the LUMC and conform to the Guide for the Care and Use of Laboratory Animals, as stated by the US National Institutes of Health (permit numbers: 09012 and 10236) [3].

nrCMCs and nrCFBs were dissociated from ventricles of 2-day old male Wistar rats, separated from each other by differential plating and maintained in nrCMC

culture medium containing 5% horse serum (Invitrogen), penicillin (100 U/mL; Bio-Whittaker) and streptomycin (100 μg/mL; BioWhittaker), as previously described [4]. nrCFBs were cultured in MSC-CM and passaged at least three times before they were used in co-culture experiments.

Five hundred thousand or one million nrCMCs were plated on collagen type I -coated (Sigma-Aldrich) glass coverslips in 6-well culture dishes and incubated in a humidified incubator at 37 C and 5% CO_2. Proliferation of residual nrCFBs in nrCMC cultures was inhibited by incubation of the cells with 100 mmol/L 5-bromo-2-deoxyuridine (Sigma-Aldrich) during the first 24 h after culture initiation.

For optical mapping experiments, 8×10^4 nrCMCs were plated on fibronectin -coated (Sigma-Aldrich) glass coverslips in 24-well culture dishes. As the conduction velocity (CV) through monolayers of nrCMCs is inversely related to their CFB content, prior to their use in co-incubation experiments with hMSCs, the nrCMC cultures were treated for 2 h with 10 mg/mL mitomycin-C (Sigma-Aldrich) to stop proliferation of residual nrCFBs present in these cultures [12].

CHARACTERIZATION OF HMSCS

Flow cytometry
Analysis of surface marker expression was carried out by flow cytometry. hMSCs (passage³3) were detached using TE, resuspended in PBS containing 1% bovine serum albumin fraction V (BSA; Sigma-Aldrich) and divided in aliquots of 2×10^5 cells. Cells were then incubated for 30 min at 4°C with fluorescein isothiocyanate-, phycoerythrin- or allophycocyanin-conjugated antibodies directed against human CD105 (Ancell, Bayport, MN, USA), CD90, CD73, CD45, CD34, CD31, CD24 and stage-specific embryonic antigen-4 (SSEA-4) (all from Becton Dickinson). Labeled cells were washed three times with PBS containing 1% BSA and analyzed using an LSR II three-laser, 12-color, flow cytometer (Becton Dickinson). Isotype-matched control antibodies (Becton Dickinson) were used to determine background fluorescence. At least 10^4 cells per sample were acquired and data were processed using FACSDiva software (Becton Dickinson).

Adipogenic and osteogenic differentiation of hMSCs
The hMSCs were characterized by established differentiation assays [5]. Briefly, 5×10^3 hMSCs per well were plated in a 12-well culture plate and exposed to adipogenic or osteogenic differentiation medium. Adipogenic differentiation medium consisted of MEM-plus (i.e. α-minimum essential medium [Invitrogen] containing 15% FBS, 100 U/L penicillin and 100 μg/mL streptomycin) supplemented with insulin, dexamethason, indomethacin and 3-isobutyl-1-methylxanthine (all from Sigma-Aldrich) to final concentrations of 5 μg/mL, 1 μM, 50 μM and 0.5 μM, respectively,

and was refreshed every 3-4 days for a period of 3 weeks. Lipid accumulation was assessed by Oil Red O (Sigma-Aldrich) staining of the cultures (15 mg of Oil Red O/mL of 60% isopropanol) and light microscopy. Osteogenic differentiation medium consisted of MEM-plus containing 10 mM b-glycerophosphate, 50 µg/mL ascorbic acid and 10 nM dexamethason (all from Sigma-Aldrich) and was refreshed every 3-4 days for a period of 3 weeks. Afterwards, the cells were washed with PBS and calcium deposits were visualized by staining of the cells for 5 min with 2% Alizarine Red S (Sigma-Aldrich) in 0.5% NH_4OH (pH 5.5).

Immunocytological characterization of hESC-MSCs
hESC colonies were originally grown on a feeder layer of mEFs. To verify the human origin of the fibroblast-like cells derived from the hESC colonies, the cells were incubated with a monoclonal antibody (MAb) specific for human lamin A/C (clone 636; Vector laboratories, Burlingame, CA, USA) at a dilution of 1:200, as previously described [6]. Binding of the primary antibody to its target antigen was visualized using Alexa 568-linked donkey anti-mouse IgG secondary antibodies (Invitrogen; dilution 1:200). Murine MSCs (mMSCs) were not labeled with the human lamin A/C-binding MAb, confirming its species specificity.

In addition, hESC-MSCs were stained with antibodies directed against the hESC marker SSEA-4 (MAb MC813; Santa Cruz Biotechnologies, Santa Cruz, CA, USA) or against the pluripotency-associated transcription factors Oct-3/4 (MAb N-19; Santa Cruz) and Nanog (goat polyclonal antibody [PAb]; R&D Systems, Minneapolis, MN, USA). Each of these primary antibodies was applied at a dilution of 1:100. As secondary antibodies we used Alexa 568-conjugated donkey anti-mouse IgG or donkey anti-goat IgG (both from Invitrogen) at a dilution of 1:200. hESC colonies from which the hESC-MSCs were derived, were used as a positive control in these stainings. Lastly, hESC-MSCs were stained with fluorescein isothiocyanate- and phycoerythrin- conjugated antibodies directed against the mesenchymal stem cell markers CD90, CD73 and CD105 at a dilution of 1:200.

Growth kinetics
Growth kinetics of the hMSCs was analyzed by calculating population doublings (PDs). Each type of hMSC was plated in triplicate at a concentration of $2x10^3$ hMSCs per cm^2 in $25-cm^2$ culture flasks (n=3 isolations for each type of hMSC). After every 5 days of culture at 37°C in 95% humidified air-5% CO_2, the cells were trypsinized and resuspended in 5 mL. Subsequently, a part of each cell suspension was subjected to Trypan Blue staining to determine the viable cell concentration using a hemocytometer. This information was used to initiate the next cell passage in a new culture flask and to determine the number of PDs during the previous culture period.

Relative telomere length using quantitative real-time polymerase chain reaction (qRT-PCR)

Genomic DNA from experimental (n³6 samples of ESC-derived, fetal or adult MSCs cultured for the same period of time) and reference samples was obtained using DNAzol (Invitrogen) according to the recommendations of the manufacturer. Relative telomere lengths were measured by SYBR Green-based (QuantiTect SYBR Green PCR kit; Qiagen, Valencia, CA, USA) qRT-PCR amplification of telomere repeats (T) and single-copy gene *36B4* (S) in a LightCycler 480 Real-Time PCR System (Roche, Foster City, CA, USA). The *36B4* gene was analyzed to normalize for differences in DNA amount between samples. The primers, primer concentrations and thermal cycling profiles were identical to those of Cawthon *et al* [7]. T and S standard curves were generated using serial dilutions (100 to 20 ng) of the DNA from the reference sample. The telomere- and *36B4*-specific qPCRs were carried out in separate plates and a standard curve was produced in each run to allow relative quantification between samples (50 ng per sample). The T/S ratio of one sample relative to that of another corresponds to the relative telomere lengths of their DNA. Since the amount of PCR product approximately doubles during each amplification cycle, the T/S ratio is approximately $[2^{Ct(telomeres)}/ 2^{Ct(36B4)}]^{-1} = 2^{-\Delta Ct}$. The relative T/S ratio is $2^{-(\Delta Ct1 - \Delta Ct2)} = 2^{-\Delta\Delta Ct}$.

CARDIAC DIFFERENTIATION POTENTIAL OF HMSCS DERIVED FROM DIFFERENT SOURCES

To facilitate the identification of hMSCs in co-cultures with nrCMCs or nrCFBs, these cells were transduced with *enhanced green fluorescent protein* (eGFP) using the vesicular stomatitis virus G protein-pseudotyped self-inactivating human immunodeficiency virus type 1 (HIV-1) vector CMVPRES [8], essentially as described by van Tuyn *et al* [9]. Before being used in co-culture experiments, the *eGFP*-transduced hMSCs were subcultured for several passages to avoid undesired secondary transductions of nrCMCs or nrCFBs by infectious HIV-1 particles carried over by the hMSCs. Cardiomyogenic differentiation was studied in co-cultures of 5×10^4 eGFP-labeled hMSCs and 5×10^5 nrCMCs or 5×10^5 nrCFBs. As a control group, 5×10^4 eGFP-labeled fetal hSFBs were co-incubated with 5×10^5 nrCMCs. The eGFP-labeled hMSCs and fetal hSFBs were added to the nrCMCs two days after they had been isolated and put into culture. All experiments described below were conducted using hMSCs from passage 3-6.

Human-specific immunocytochemical analysis of cardiomyogenic differentiation potential

Co-cultures of 5×10^5 nrCMCs and 5×10^4 eGFP-labeled hMSCs or eGFP-labeled fetal hSFBs and co-cultures of 5×10^5 nrCFBs with 5×10^4 eGFP-labeled hMSCs were stained

with a MAb recognizing the sarcomeric protein α-actinin (clone EA53; Sigma-Aldrich; dilution 1:400) on day 10 after culture initiation, as previously described [6]. The primary antibody was visualized using Alexa 568-coupled donkey anti-mouse IgG secondary antibodies at a dilution of 1:200. The human lamin A/C-specific MAb mentioned above was used to detect hMSCs in the co-cultures. Lamin A/C staining was visualized with Qdot 655-streptavidin conjugates (Invitrogen) after incubation of the cells with biotinylated goat anti-mouse IgG2b secondary antibodies (Santa Cruz). Nuclei were stained using a 10 μg/mL solution of Hoechst 33342 (Invitrogen) in PBS containing 1% FBS. The percentage of eGFP-labeled cells showing positive staining for α-actinin was determined by analyzing at least 3 cultures (100 cells per culture, at 100x magnification) of at least 4 hMSC isolations per type of hMSC). The presence of well-organized sarcomeres in eGFP-labeled hMSCs was assessed by comparing the α-actinin staining pattern in these cells with that of the native nrCMCs in each culture.

A fluorescence microscope equipped with a digital camera (Nikon Eclipse, Nikon Europe, Badhoevedorp, The Netherlands) and dedicated software (Image-Pro Plus, Version 4.1.0.0, Media Cybernetics, Silver Spring, MD, USA) were used to analyze data. All co-cultures were treated equally using the same antibody dilutions and exposure times.

Electrophysiological measurements in pharmacologically uncoupled hMSCs in co-culture with nrCMCs

Whole-cell patch-clamp measurements were performed in co-cultures of 5×10^4 eGFP-labeled fetal (amniotic) or adult (adipose) hMSCs and 5×10^5 nrCMCs, plated on collagen-coated glass coverslips, at day 10 of culture. To perform single-cell measurements from eGFP-labeled cells in a field of beating nrCMCs, cells were pharmacologically uncoupled by incubation with 180 μmol/L of 2-aminoethoxy-diphenyl borate (2-APB) (Tocris, Ballwin, MO, USA) for 15 min [6]. This agent blocks gap junctional intercellular coupling by Cx40, Cx43, and Cx45 [10,11]. Whole-cell current-clamp recordings were performed at 25°C using a L/M-PC patch-clamp amplifier (3 kHz filtering) (List-Medical, Darmstadt, Germany). Pipette solution contained (in mmol/L) 10 Na_2ATP, 115 KCl, 1 $MgCl_2$, 5 EGTA, 10 HEPES/KOH (pH 7.4). Tip resistance was 2.0 - 2.5 MW, and seal resistance >1 GW. The bath solution contained (in mmol/L) 137 NaCl, 4 KCl, 1.8 $CaCl_2$, 1 $MgCl_2$, 10 HEPES (pH 7.4). For data acquisition and analysis pClamp/Clampex8 software (Axon Instruments, Molecular Devices, Sunnyvale, CA, USA) was used. Current-clamp recording were performed in eGFP-labeled cells which were adjacent to 2-4 nrCMCs, and from these cells the data were analyzed and compared between the two different groups.

Human-specific quantitative reverse transcription-PCR (qRT-PCR) to detect mRNAs associated with pluripotency and cardiac differentiation

Total cellular RNA was extracted from monocultures of hMSCs (n³4 samples from each type of hMSC) and from co-cultures consisting of 10^5 hMSCs and 10^6 nrCMCs using the RNeasy Mini kit (Qiagen). Oligo (dT)-primed reverse transcription was performed on 2 μg of total cellular RNA and the resultant cDNA was used for PCR amplification using SYBR Green. To detect changes in cardiac and pluripotency gene expression levels, the following human-specific primers: gap junction protein, alpha 1 (Cx43/GJA1; QT00012684), vascular endothelial growth factor A (VEGF/ VEGFA; QT01682072), GATA-binding protein 4 (GATA-4/GATA4; QT00031997), Nanog homeobox (Nanog/NANOG; QT01844808), octamer-binding protein 3/4 (Oct-3/4/POU5F1; QT00210840), NK2 transcription factor related, locus 5 (Drosophila) (Nkx2.5/NKX2-5; QT00010619), v-kit Hardy-Zuckerman 4 feline sarcoma viral oncogene homolog (c-kit/KIT; QT01844549), natriuretic peptide precursor A (ANP/NPPA; QT00203322), myosin, light chain 2, regulatory, cardiac, slow (MLC2v/MYL2; QT00012999), ISL LIM homeobox 1 (Islet-1/ISL1; QT00000294), troponin I type 3 (cardiac) (cTnI/TNNI3; QT00084917) (all with an annealing temperature of 55°C; all from Qiagen) and myosin heavy chain 7, cardiac muscle, beta (b-MCH/MYH7; forward primer: 5'-TGTGTCACCGTCAACCCTTA-3', reverse primer: 5'-TGGCTGCAATAACAGCAAAG-3'; annealing temperature 63°C; Invitrogen). The expression of the genes of interest was normalized to that of the housekeeping gene *glyceraldehyde-3-phosphate dehydrogenase* (GAPDH, forward primer: 5′-GAAGGTGAAGGTCGGAGTC-3′, reverse primer: 5′-GAAGATGGTGATGGGATTTC-3′; annealing temperature 60°C; Invitrogen). Agarose gel electrophoresis was used to ensure that each primer pair yielded a single PCR product of the expected size. PCR primers were checked for human specificity with the aid of appropriate positive human right atrium and hESC control and negative nrCMC control samples, while rat-specific primers were used to detect expression of the cardiac genes in the nrCMC control samples. Data were analyzed using the ΔCt method.

Optical mapping to determine CV in co-cultures between nrCMCs and different types of hMSCs

Action potential propagation was investigated on a whole-culture scale in wells of a 24-well plate by optically mapping using the voltage-sensitive dye di-4-ANEPPS (Invitrogen). The measurements were performed 10 days after seeding of either 8×10^5 nrCMCs (nrCMC monoculture) or 8×10^5 nrCMCs plus 8×10^4 nrCFBs or 8×10^4 hMSCs (nrCMC/nrCFB or nrCMC/hMCS co-cultures) per well (n³15 cultures per cell type or combination of cell types). Co-cultures were loaded with 16 μmol/L di-4-ANEPPS for 30 minutes. After which medium was refreshed and the co-cultures were mapped using the Ultima-L optical mapping setup (SciMedia, Costa

Mesa, CA, USA). Throughout mapping experiments, cultures were kept at 37°C. Optical signal recordings were analyzed using Brain Vision Analyze 0909 (Brainvision Inc, Tokyo, Japan). For more details regarding the optical mapping protocol see Askar *et al* [12]. The CV of all (co-)cultures was determined in a blinded manner.

IN VITRO ANGIOGENESIS ASSAYS

hMSCs of different origin ($n \geq 5$ isolations for each type of hMSC) were plated on Matrigel (Becton Dickinson) to determine their ability to form capillary-like structures. Ninety microliters of gel matrix solution was applied to each well of a 24-well plate on top of a glass coverslip and the plate was incubated for 1 h at 37°C. After trypsinization, 1.5×10^4 cells were suspended in 1 mL of Endothelial Growth Medium-2 (Cambrex IEP, Wiesbaden, Germany) containing 100 ng/mL recombinant human VEGF-A$_{165}$ (R&D Systems), plated onto the basement membrane matrix and incubated for up to 24 h at 37°C in 95% humidified air-5% CO_2. Formation of capillary-like structures was checked every hour. Maximum time of incubation was determined for each type of hMSC. Following culture on the basement membrane matrix, cells were fixed and stained with antibodies specific for smooth muscle myosin heavy chain (smMHC; MAb hSM-V; Sigma-Aldrich, dilution 1:100) and platelet/endothelial cell adhesion molecule-1 (PECAM-1; rabbit PAb M20; Santa Cruz, dilution 1:200). The primary antibodies were visualized with Alexa 568-coupled donkey anti-mouse IgG and Alexa 488-conjugated donkey anti-rabbit IgG (Invitrogen), respectively. All cultures were treated equally using the same antibody dilutions and exposure times, which were based on titration of the antibodies using appropriate positive and negative controls.

DETERMINATION OF CX43 EXPRESSION

Cx43 protein levels and gene expression were detected in monocultures of hESC-MSCs, fetal amniotic hMSCs and adult adipose hMSCs, but also in co-cultures of these cells with nrCMCs or nrCFBs using immunocytology and qRT-PCR, as described earlier. The Cx43-specific rabbit PAb (C6219; Sigma Aldrich, dilution 1:200) was visualized with Alexa 488-conjugated donkey anti-rabbit IgG. Cx43 expression was determined for at least 5 different isolations of each type of hMSCs under the different conditions (100 cells per culture and at least 3 cultures per isolation were analyzed). All cultures were treated equally using the same antibody dilutions and exposure times, which were based on titration of the antibodies using appropriate positive and negative controls.

Western blot analysis was used to quantify Cx43 levels in cultures of hMSCs. Homogenates were made from at least 5 different isolations of hMSCs per source. After determining the protein concentration in each sample using the BCA Protein Assay Reagent (Pierce Biotechnology, Rockford, IL, USA), equal amounts of

protein were size-fractionated in a 12% NuPage Tris-Acetate gel (Invitrogen) and transferred to a Hybond-P PVDF membrane (GE Healthcare, Waukesha, WI, USA). This membrane was incubated for 1 h with the PAb directed against Cx43 followed by incubation with horse radish peroxidase (HRP)-conjugated goat anti-rabbit secondary antibody (Santa Cruz). To check for equal protein loading, a mouse MAb recognizing the housekeeping protein GAPDH (Chemicon International, Temecula, CA, USA) was used, which was detected by an HRP-conjugated goat anti-mouse secondary antibody (Santa Cruz). Chemiluminescence was induced with the aid of the ECL Advance Western Blotting Detection Kit and caught on Hyperfilm ECL (both from GE Healthcare).

REFERENCES

1. Trivedi P, Hematti P (2008) Derivation and immunological characterization of mesenchymal stromal cells from human embryonic stem cells. Exp Hematol 36: 350-359.
2. Karlsson C, Emanuelsson K, Wessberg F, Kajic K, Axell MZ et al. (2009) Human embryonic stem cell-derived mesenchymal progenitors-Potential in regenerative medicine. Stem Cell Res.
3. National Institutes of Health (2002) Guide for the Care and Use of Laboratory Animals.
4. Pijnappels DA, Schalij MJ, van Tuyn J, Ypey DL, de Vries AA et al. (2006) Progressive increase in conduction velocity across human mesenchymal stem cells is mediated by enhanced electrical coupling. Cardiovasc Res 72: 282-291.
5. Pittenger MF, Mackay AM, Beck SC, Jaiswal RK, Douglas R et al. (1999) Multilineage potential of adult human mesenchymal stem cells. Science 284: 143-147.
6. Pijnappels DA, Schalij MJ, Ramkisoensing AA, van Tuyn J, de Vries AA et al. (2008) Forced alignment of mesenchymal stem cells undergoing cardiomyogenic differentiation affects functional integration with cardiomyocyte cultures. Circ Res 103: 167-176.
7. Cawthon RM (2002) Telomere measurement by quantitative PCR. Nucleic Acids Res 30: e47.
8. Seppen J, Rijnberg M, Cooreman MP, Oude Elferink RP (2002) Lentiviral vectors for efficient transduction of isolated primary quiescent hepatocytes. J Hepatol 36: 459-465.
9. van Tuyn J, Pijnappels DA, de Vries AA, de V, I, van der Velde-van Dijke et al. (2007) Fibroblasts from human postmyocardial infarction scars acquire properties of cardiomyocytes after transduction with a recombinant myocardin gene. FASEB J 21: 3369-3379.
10. Bai D, del CC, Srinivas M, Spray DC (2006) Block of specific gap junction channel subtypes by 2-aminoethoxydiphenyl borate (2-APB). J Pharmacol Exp Ther 319: 1452-1458.
11. Harks EG, Camina JP, Peters PH, Ypey DL, Scheenen WJ et al. (2003) Besides affecting intracellular calcium signaling, 2-APB reversibly blocks gap junctional coupling in confluent monolayers, thereby allowing measurement of single-cell membrane currents in undissociated cells. FASEB J 17: 941-943.
12. Askar SFA, Ramkisoensing AA, Schalij MJ, Bingen BO, van der Laarse A, Atsma DE, Ypey DL, Pijnappels DA (2011) Antiproliferative Treatment of Endogenous Myofibroblasts Prevents the Occurrence of Spontaneous Reentrant Tachyarrhythmias in Rat Myocardial Cultures. Cardiovasc Res 90: 295-304.

SUPPORTING INFORMATION LEGENDS

Supplemental Materials and Methods S1. A detailed description of the materials and methods can be found in this supporting information file.
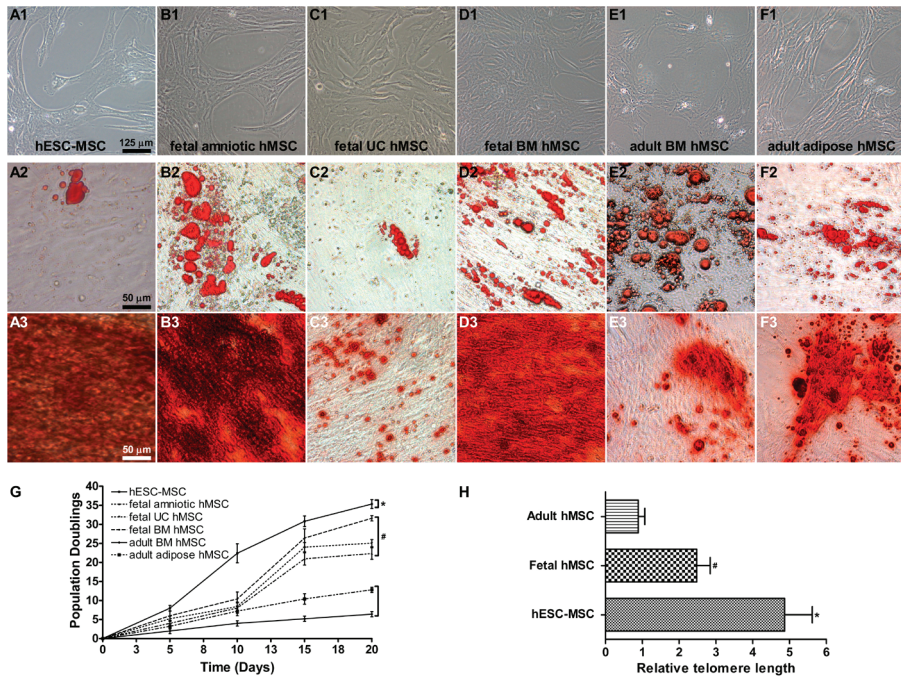
Supplemental figure S1. Cellular characteristics of hMSCs. (A1-F1) Bright field images of cultured hMSCs displaying a spindle-shaped morphology. (A2-F2) Presence of oil red O-stained fat vacuoles after adipogenic differentiation. (A3-F3) Calcium depositions after osteogenic differentiation was visualized by alizarine red S staining. (A) hESC-MSC; (B) fetal amniotic hMSC; (C) fetal UC hMSC; (D) fetal BM hMSC; (E) adult BM hMSC; (F) adult adipose hMSC. (G) Growth kinetics of the different types of hMSCs estimated by cumulative population doublings over 20 days (*$P<0.001$ vs fetal hMSCs and adult hMSCs, #$P<0.001$ vs adult hMSCs). (H) Mean relative telomere lengths of hESC-MSCs, all fetal hMSC types and both adult hMSC types (*$P<0.05$ vs fetal hMSCs and adult hMSCs, #$P<0.05$ vs adult hMSCs).

	hESC-MSC	Fetal amniotic hMSC	Fetal BM hMSC	Fetal UC hMSC	Adult BM hMSC	Adult adipose hMSC
CD24	0.30±0.7	NT	NT	NT	NT	NT
CD31	0.0±0.0	0.0±0.0	0.0±0.0	0.0±0.0	0.0±0.0	0.0±0.0
CD34	0.13±0.1	0.0±0.0	0.13±0.1	0.0±0.0	0.17±0.1	0.06±0.0
CD45	0.20±0.4	0.07±0.0	0.10±0.1	0.18±0.1	0.20±0.1	0.6±0.5
CD73	97.6±1.9	95.4±0.8	97.3±1.3	97.7±1.1	96.6±1.4	96.4±0.3
CD90	96.0±1.7	98.2±1.3	96.3±1.5	96.3±3.1	98.2±0.9	94.6±1.8
CD105	94.0±0.9	95±0.9	96.6±0.2	97.4±0.6	96.0±2.8	96.0±0.2
SSEA-4	0.0±0.0	0.0±0.0	0.0±0.0	0.0±0.0	0.0±0.0	0.0±0.0

Supplemental table S1. Analysis of surface marker expression. All hMSC types were positive for the established MSC surface markers CD105, CD90 and CD73. They were negative for the hematopoietic, endothelial and embryonic stem cell markers CD45 and CD34, CD31 and SSEA-4, respectively. The hESC-MSCs were also negative for CD24, a protein present on the surface of hESCs. Mean percentages ± standard deviations are given; n=6 for each group. NT is not tested.
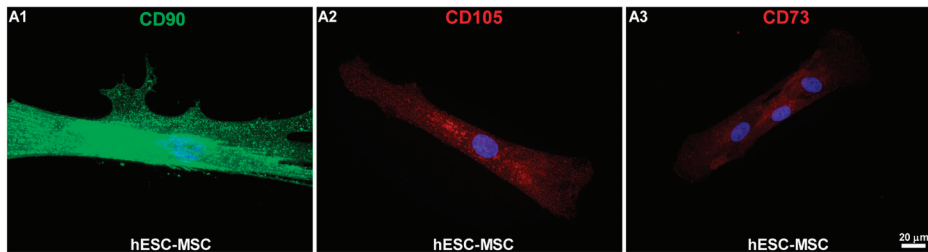
Supplemental figure S2. Immunocytological characterization of hESC-MSCs for MSC surface markers. Immunostaining of hESC-MSCs for CD90, CD105 and CD73 (A1-A3) showed that these cells were positive for these established MSC surface markers.

	Nkx2.5	GATA-4	ANP	MLC2v	Cx43	VEGF	Islet-1	c-kit
hESC-MSC	6.15±1.2*	5.77±0.6#	2.97±0.1†	12.0±0.6†	9.13±0.9#	1.18±0.3	0.43±0.1*	0.53±0.2#
Fetal amniotic hMSC	7.26±0.4#	ND	1.56±0.1*	ND	3.94±0.5*	3.85±0.3*	0.35±0.1#	0.75±0.2
Fetal UC hMSC	ND	5.79±1.4#	1.04±0.1	ND	2.72±0.2#	2.32±0.1†	0.50±0.1†	0.36±0.1*
Fetal BM hMSC	ND	ND	3.73±0.1†	ND	1.97±0.3#	0.93±0.1	6.13±1.9	6.13±1.9†
Adult BM hMSC	ND	ND	2.07±0.4#	ND	1.03±0.3	1.44±0.8*	ND	0.84±0.3
Adult adipose hMSC	ND	ND	5.18±1.5#	ND	1.22±0.2	11.7±1.8*	ND	5.71±1.0#

Supplemental table S2. qRT-PCR analysis to detect mRNAs associated with cardiac differentiation. Indicated is the fold change in the expression of cardiac genes in hMSCs cultured alone or together with nrCMCs. #$P<0.05$ vs hMSC monoculture; *$P<0.01$ vs hMSC monoculture; †$P<0.001$ vs hMSC monoculture; ND is not detected.

CHAPTER III

FORCED ALIGNMENT OF MESENCHYMAL STEM CELLS UNDERGOING CARDIOMYOGENIC DIFFERENTIATION AFFECTS FUNCTIONAL INTEGRATION WITH CARDIOMYOCYTE CULTURES

Daniël A. Pijnappels[1], Martin J. Schalij[1], Arti A. Ramkisoensing[1], John van Tuyn[1,2], Antoine A. F. de Vries[2], Arnoud van der Laarse[1], Dirk L. Ypey[1], Douwe E. Atsma[1].

Departments of Cardiology[1], and Molecular Cell Biology[2], Leiden University Medical Center, Leiden, The Netherlands.

58

ABSTRACT

Alignment of cardiomyocytes (CMCs) contributes to the anisotropic (direction-related) tissue structure of the heart, thereby facilitating efficient electrical and mechanical activation of the ventricles. This study aimed to investigate the effects of forced alignment of stem cells during cardiomyogenic differentiation on their functional integration with CMC cultures.

Labeled neonatal rat (nr) mesenchymal stem cells (MSCs) were allowed to differentiate into functional heart muscle cells in different cell-alignment patterns during 10 days of co-culture with nrCMCs. Development of functional cellular properties was assessed by measuring impulse transmission across these stem cells between two adjacent nrCMC fields, cultured onto micro-electrode arrays and previously separated by a laser-dissected channel (230 ± 10 mm) for nrMSC transplantation. Coatings in these channels were micro-abraded in a direction (1) parallel, or (2) perpendicular to the channel, or (3) left unabraded, to establish different cell patterns.

Application of cells onto micro-abraded coatings resulted in anisotropic cell alignment within the channel. Application on unabraded coatings resulted in isotropic (random) alignment. Upon co-culture, conduction across seeded nrMSCs occurred from day 1 (perpendicular and isotropic) or day 6 (parallel) onward. Conduction velocity (CV) across nrMSCs at day 10 was highest in the perpendicular (11 ± 0.9 cm/s,n=12), intermediate in the isotropic (7.1 ± 1 cm/s,n=11), and lowest in the parallel configuration (4.9 ± 1 cm/s,n=11) ($p<0.01$). nrCMCs and fibroblasts served as positive and negative control, respectively. Also, immunocytochemical analysis showed alignment-dependent increases in Cx43 expression.

In conclusion, forced alignment of nrMSCs undergoing cardiomyogenic differentiation affects the time course and degree of functional integration with surrounding cardiac tissue.

INTRODUCTION

The developing heart is characterized by increases in the number and size of cells resulting from hyperplasia and hypertrophy.[1,2] During this process, the initially round-shaped cardiomyocytes (CMCs) become elongated through unidirectional growth and align in a specific direction, thereby defining a long and short cellular axis.[3] Later in development, intercalated disc components (including gap junction proteins), initially distributed more or less uniformly over the surface of the cells, cluster at the polar ends of the cells.[4,5] Consequently, the elongated terrace-shaped cells are coupled end-to-end to surrounding cells and organized in unit bundles. This anisotropic tissue architecture has implications for the electrical activation of the cardiac muscle. Conduction of the electrical impulse parallel to the myocardial fiber axis is about 3 times faster than perpendicular to the fiber axis, indicating anisotropic conduction.[6] In the intact heart, the resulting inhomogeneity in conduction is circumvented by a ~120 degrees rotation of the fiber axis from epi- to endocardium. As a consequence the spread of activation through the ventricular muscle is more or less homogeneous, coordinated and fast.[7,8] Any disruption of this architecture, for example after myocardial infarction, may cause conduction abnormalities, associated with diminished pump function and increased risk of arrhythmias.[9]

Recently, stem cell therapy has been introduced as a treatment option to improve left ventricular function after myocardial infarction.[10] Ideally, to be successful, stem cells should not only differentiate into CMCs but also engraft and align with the surrounding anisotropic tissue. This latter process can be referred to as spatial integration. As a result, these *de novo* CMCs will be an integral part of the 3-dimentional myocardial architecture, thereby contributing to cardiac impulse conduction. Until now it is unknown how transplanted stem cells integrate with the surrounding myocardial cells, and to which extent alignment of these cells may influence electrical conduction. In other words, spatial integration of stem cell-derived CMCs may contribute to restoration of tissue structure and conduction or, in contrast, result in increased structural and electrical inhomogeneity. In theory, each cell type that is coupled electrically, excitable, and aligned can acquire anisotropic properties as in this situation the resistance in the transverse direction is higher than in the longitudinal direction. In case of stem cells this is of special interest as they may acquire anisotropic properties during cardiomyogenic differentiation after they have been transplanted into the anisotropic myocardium, thereby potentially improving their functional integration with the surrounding myocardium. Of note, functional integration of such transplanted cells is essential for cell therapy to be safe and effective.[11]

In the present study, we used a standardized 2-dimensional *in vitro* co-incubation model with a growth-directing substrate,[12,13] to investigate the effects of cell alignment on functional integration and electrical conduction across neonatal rat (nr) mesenchymal stem cells (MSCs) undergoing cardiomyogenic differentiation. The process of differentiation occurred in a cardiac syncytium of neonatal rat cardiomyocytes (nrCMCs) thereby allowing the study of functional integration.

MATERIALS AND METHODS

Animal experiments were approved by the Animal Experiments Committee of the Leiden University Medical Center and conformed to the Guide for the Care and Use of Laboratory Animals as stated by the US National Institutes of Health.

A detailed description of harvesting and culturing of nrCMCs, nrMSCs, and cardiac fibroblasts (nrCFBs), as well as the characterization of the nrMSCs can be found in the online Data Supplement.

ASSESSMENT OF FUNCTIONAL CARDIOMYOGENESIS

Differentiation of nrMSCs was assessed by a combination of immunofluorescence microscopy and electrophysiological measurements in isotropic co-cultures of nrCMCs and eGFP-labeled nrMSCs grown on glass coverslips during the course of 10 days. The assessment of cardiomyogenesis by immunofluorescence and intracellular measurements is described in the online Data Supplement.

MICRO-ELECTRODE HIGH-DENSITY MAPPING

Simultaneous micro-electrode high density mapping of cultured nrCMCs and nrMSCs was performed using micro-electrode arrays (MEA, number of titanium nitride electrodes: 60; inter-electrode distance: 200 mm; electrode diameter: 30 mm) and associated data acquisition system (sampling rate 5 kHz/channel, Multi Channel Systems, Reutlingen, Germany). Further descriptions can be found in the online Data Supplement.

INDUCTION OF CONDUCTION BLOCK AND ANISOTROPIC CELL ALIGNMENT

Activation maps of nrCMCs were generated 2 days after culture to confirm the presence of a synchronously beating monolayer. Conduction block was generated using a P.A.L.M. microlaser system (Microlaser Technologies GmbH, Bernried, Germany).[14] Briefly, two pre-programmed linear laser dissections were made, separated by 225 µm, crossing the entire diameter of the monolayer in the coated MEA culture dish. This resulted in a detached strip of monolayer between the two laser dissection lines, which was removed from the culture, creating a clean a-cellular

channel electrically separating the two nrCMC fields. Subsequently, the uncovered coatings in the a-cellular channels were given a micro-groove pattern by micro-abrasion[15] with a soft micro-brush (bristle diameter: 30 mm diameter) using a micro-manipulator (Seizz, Göttingen, Germany) and light-microscope (40x magnification), either in a direction (1) parallel or (2) perpendicular to the a-cellular channel. Another group (3) consisted of MEA culture dishes with an a-cellular channel that was not micro-abraded.

After confirming the presence of a conduction block between the two nrCMC fields, either (a) $5x10^4$ CM-Dil-labeled nrCMCs, (b) $5x10^4$ eGFP-labeled nrMSCs or (c) $5x10^4$ eGFP-labeled nrCFBs were applied in a channel-crossing pattern in each of the three groups. This was achieved by gently adding the cells onto the coating in-between the CMC fields, using a pipette fixed to a micro-manipulator in combination with a light-microscope (20x magnification). After 24 h, the culture medium was refreshed to remove non-attached cells, as well as 1 h before and after measurements. During the following 10 days the electrical conduction (impulse transmission) across seeded cells was assessed daily.

The two separated and asynchronously beating nrCMC fields were considered electrically coupled upon application of cells, if the timing of the electrograms of the two nrCMC fields correlated consistently with each other for 30 consecutive LATs recorded at both fields, while stimulating one nrCMC field.

In an additional series of experiments, a mixture of $5x10^4$ nrCMCs and nrCFBs (20%:80%) was applied to the channel and subjected to electrophysiological measurements 24 h after seeding and served as positive control for the results obtained in the nrMSC group at day 10.

STATISTICS

Statistical analysis was performed using SPSS 11.0 for Windows (SPSS Inc., Chicago, IL, USA). Data were compared with Student's t-test or ANOVA test with Bonferroni correction for multiple comparisons, and expressed as mean±SD for a given number (n) of observations. P-values <0.05 were considered statistically significant.

RESULTS

CHARACTERIZATION OF BONE MARROW-DERIVED NEONATAL RAT MESENCHYMAL STEM CELLS

Analysis of in vitro adipogenic and osteogenic differentiation potential
The nrMSCs (Fig 1, A1) were assessed for their multipotency by investigating their adipogenic and osteogenic differentiation potential. After incubation in appropriate differentiation media, nrMSCs readily differentiated into adipocytes and osteoblasts, as determined by formation of lipid vacuoles and calcium deposits, respectively (Fig 1, A2-3).

Analysis of surface marker and connexin expression
A very large fraction of the nrMSCs (p2) expressed the mesenchymal markers CD29 (97.3%), and CD90 (96.2%) at their surface, while almost none of them stained positive for the hematopoietic marker CD34 (1.5%). CD44 (32.8%), CD45 (10.2%), and CD106 (10.3%) were expressed in a small to medium sized fraction of nrMSCs (Fig 1, B).[16]

    After 3 days of culture, nrMSCs showed positive staining for Cx43 ($220\pm26\times10^3$ intensity units (iu) in 1024 pixel x 768 pixel image) and Cx45 ($149\pm9\times10^3$ iu) inside the cell and at cell-cell contacts, whereas Cx40 staining was hardly detectable ($15\pm7\times10^3$ iu) (Fig 2, A1-3). At day 10, positive staining for Cx43, Cx40, and Cx45 had increased significantly ($p<0.01$, Fig 2, E), without a noticeable change in their distribution patterns (Fig 2, C1-3).

    In co-cultures of nrCMCs and eGFP-labeled nrMSCs, the latter cells stained positive for Cx43 ($291\pm15\times10^3$ iu) and Cx45 ($204\pm9\times10^3$ iu) in a dense punctuated pattern at day 3 of culture, with Cx40 being hardly detectable ($19\pm9\times10^3$ iu) (Fig 2, B1-3). At day 10 after cell seeding, only Cx43 and Cx45 staining had significantly increased ($p<0.01$) as compared to day 3 of culture, but distribution patterns did not changed over time. In contrast, no increase in Cx40 staining was observed in or between cells at day 10 of culture (Fig 2, D1-3).
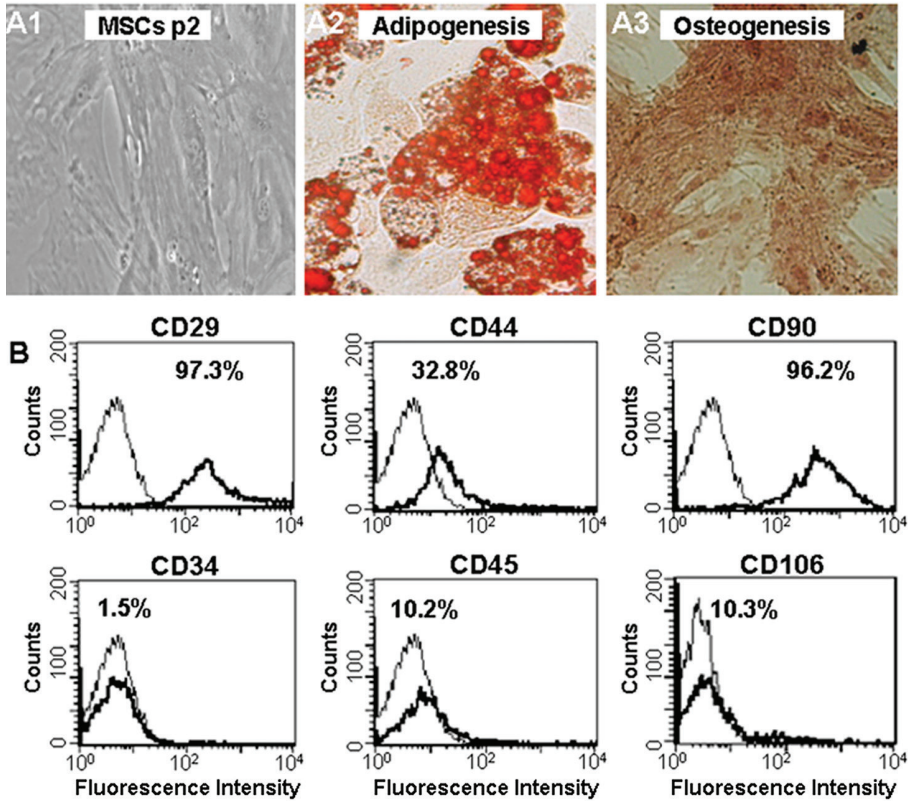
Figure 1. Characterization of neonatal rat mesenchymal stem cells (nrMSCs). A1, Brightfield image of cultured nrMSCs. A2, presence of Oil Red O-stained fat vacuoles after adipogenic differentiation. A3, calcium accumulation was visualized by Alizarine Red S staining after osteogenic differentiation. B, Flow cytometric analysis of nrMSCs showed abundant surface expression of CD29 and CD90, but hardly any expression of the hematopoietic marker CD34. Furthermore, CD44, CD45 and CD106 were expressed at low or medium levels. Flow cytometric analyses with isotype-matched control antibodies are included to determine background fluorescence levels (thin black line).
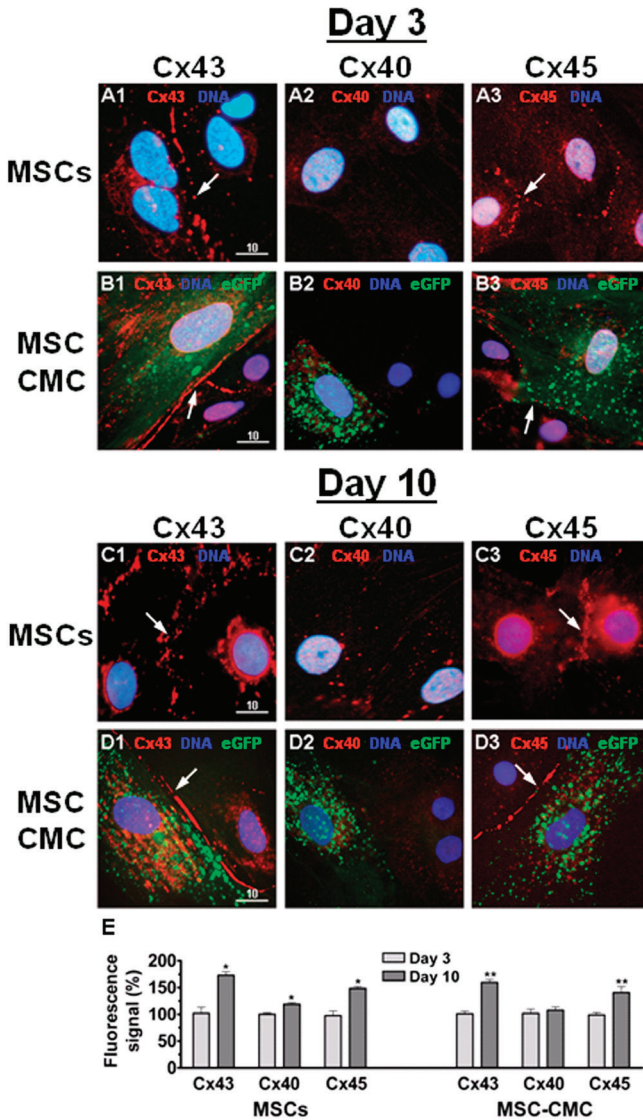
Figure 2. Immunocytochemical analysis of connexin (Cx) staining in isotropic co-cultures of neonatal rat mesenchymal stem cells (nrMSCs) and nrCMCs at day 3 and day 10 of culture. Staining for Cx43 and Cx45 increased significantly over time in nrMSCs (A1, A3, C1 and C3) as well as in nrMSCs adjacent to nrCMCs (B1, B3, D1 and D3). Positive staining for Cx40 increased only in MSCs during follow-up (A2 and C2). Quantitative analysis (E) was based on 36 random samples taken from 12 adjacent nrMSC-nrMSC and nrCMC-nrMSC cell pairs on 3 different coverslips at each time point. White arrows pinpoint the presence of Cxs at the site of gap junctions. *$p<0.01$ vs. nrMSCs at day 3, **$p<0.01$ vs. nrMSC-nrCMC pairs at day 3.

ASSESSMENT OF CARDIOMYOGENIC DIFFERENTIATION

Immunocytochemistry

At day 3 of co-culture, a fraction of the eGFP-labeled nrMSCs stained positive for sarcomeric α-actinin and cardiac troponin-I in a diffuse and speckled staining pattern (Fig 3, A2 and A4).

However, a larger fraction of nrMSCs stained negative for both markers (Fig 3, A1 and A3). Cross-striation in nrMSCs was first observed at day 6, while at day 10, ~17% of the eGFP-labeled nrMSCs showed typical cardiac cross-striated patterns of sarcomeric α-actinin (Fig 3, D1-3) and cardiac troponin-I (Fig 3, D4-6). Most of the nrMSCs displaying cross-striation were adjacent to native CMCs. Importantly, none of the nrMSCs having cross-striation of contractile proteins (>60 cells analyzed per sarcomeric protein type) were heterokaryomeric, making cell fusion of eGFP-labeled cells with nrCMCs unlikely. Total positive staining for sarcomeric α-actinin and cardiac troponin-I in eGFP-labeled cells increased significantly from 34±5% and 30±6% at day 3, to 63±3% and 60±4% at day 10 (now including 17.1±3% and 16.3±4% of cells that show positive staining with cross-striation), respectively (p<0.001) (Fig 3, B). Furthermore, sarcomere length (i.e. distance between two Z-lines) in differentiated nrMSCs at day 10 was comparable to that in native nrCMCs (Fig 3, C1-2). Samples having irregularities in sarcomere structures (less than 10% of samples) were excluded.

Electrophysiological measurements after uncoupling

Patch-clamp recordings were obtained from nrCMCs and eGFP-labeled nrMSCs at day 3 and day 10 of co-culture after electrical isolation with the gap junction uncoupler 2-aminoethoxydiphenyl borate (2-APB). Upon 2-APB treatment, the synchronously beating monolayer disintegrated into asynchronously beating cells, and input resistance increased from 20-120 MW (n=15) to 0.9-1.2 GW (18 other cells). These increases in input resistances were considered to reflect electrical uncoupling of the patched cell from the surrounding cells, thereby reaching the approximate seal resistance.[17] After electrical uncoupling at day 3, eGFP-labeled nrMSCs (n=9) had maximal diastolic potentials of -16±5 mV and showed no spontaneous action potentials (APs). In contrast, uncoupled nrCMCs (n=12) had maximal diastolic potentials of -69±8 mV in the presence of spontaneous APs.

Interestingly, after 10 days of co-culture and incubation with 2-APB, a considerable fraction of nrMSC-derived nrCMCs (~16%, n=9) was found to be beating independently from surrounding nrCMCs (as judged by timing and frequency of beating), while showing AP characteristics (maximal diastolic potential: -63±4 mV) comparable to native nrCMCs (n=10) (Fig 4, A1-2, B1-4). The remaining nrMSCs (n=47) were non-beating and had a maximal diastolic potential of -19±4 mV, in the absence of APs (Fig 4, A2).
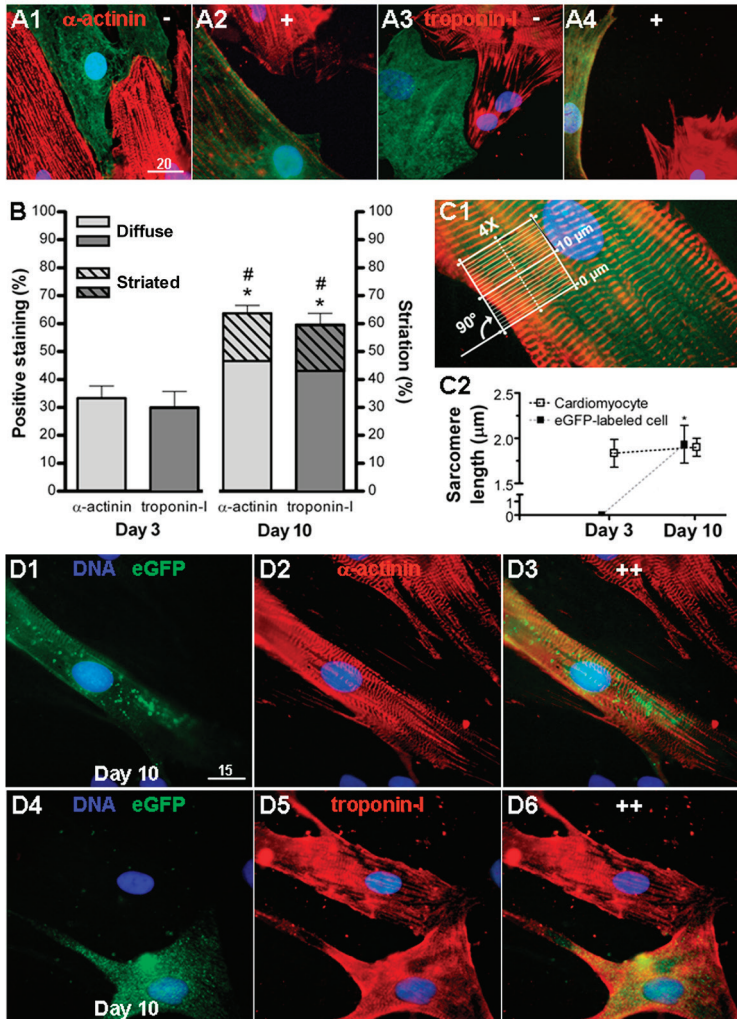
Figure 3. Cardiomyogenic differentiation of neonatal rat mesenchymal stem cells (nrMSCs) co-cultured with nrCMCs assessed by immunocytochemistry. A fraction of eGFP-labeled nrMSCs stained negative for (A1) sarcomeric α-actinin and (A3) cardiac troponin-I at day 3 of culture. However, other nrMSCs stained positive for (A2) sarcomeric α-actinin and (A4) cardiac troponin-I, which percentage increased significantly over time (B). At day 10 of co-culture, positive staining in typical cardiac cross-striated pattern was observed for both (D1-6) sarcomeric α-actinin and cardiac troponin-I in 17.1±3% and 16.3±4% of the nrMSCs, respectively (B). (C1-2) Estimation of sarcomere lengths in native nrCMCs and eGFP-labeled cells showed no significant difference. Quantitative analysis was based on 360 cells per sarcomeric protein at each time point. *P<0.01, vs. percentage positive staining at day 3. #P<0.01, vs. percentage cross-striation at day 3.
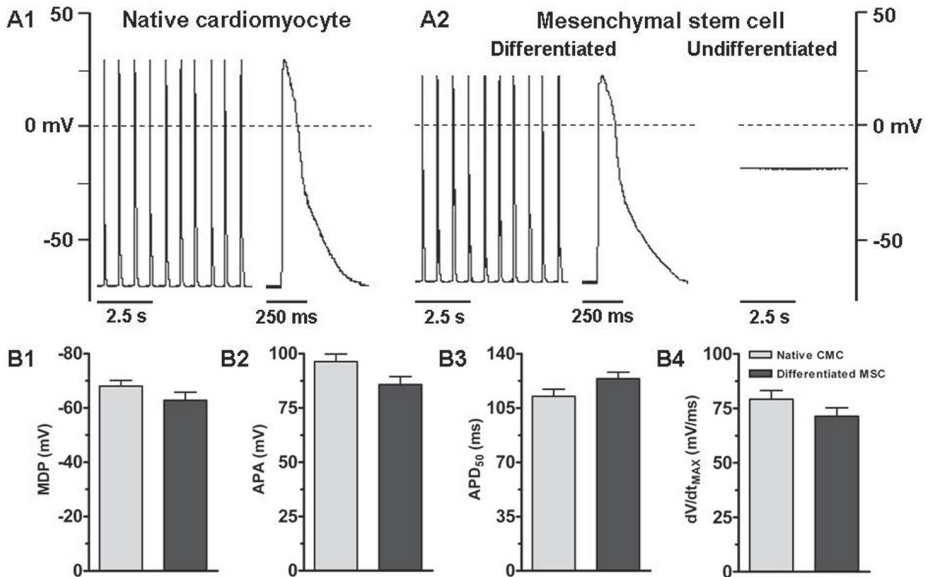
Figure 4. Whole-cell patch-clamp recordings from nrCMCs and eGFP-labeled neonatal rat mesenchymal stem cells (nrMSCs) after 10 days of co-culture and gap junction uncoupling. Stable and spontaneous action potentials were recorded in (A1) nrCMCs (n=10), as well as in (A2, left panel) differentiated eGFP-labeled cells (n=9). In contrast, undifferentiated, non-beating nrMSCs had resting membrane potentials of -19±4 mV, in the absence of action potentials (A2, right panel; n=47). Action potential characteristics were comparable to each other, as shown by maximum diastolic potential (MDP, B1); action potential amplitude (APA, B2); action potential duration till 50% repolarization (APD$_{50}$, B3) and maximal rate of depolarization (dV/dt$_{MAX}$, B4).

CELL ALIGNMENT AFTER MICRO-ABRASION

Only confluent monolayers with a high degree of structural and functional homogeneity were included in this study as determined by light-microscopy and electrophysiological mapping. Furthermore, damaged and/or detached nrCMC fields, due to laser dissection or micro-abrasion, were excluded from the study. As a consequence only 40% of the cultures were included for further experiments.

Application of nrCMCs, nrMSCs or nrCFBs onto the uncovered fibronectin-gelatin coating in the a-cellular channel resulted in a confluent, isotropic cell layer (Fig 5, A1). Micro-abrasion of the coating, either parallel or perpendicular to the channel, resulted in alignment of each cell type according to the direction of abrasion (Fig 5, B1 and C1). nrMSCs, as other applied cells, appeared elongated with an average length-width ratio of 4:1 and maintained their shape throughout follow-up

(Fig 5, D1-2). In contrast, cells applied onto unabraded coatings had a variable length-width ratio (Fig 5, D3), but never reaching 4:1 of anisotropically aligned cells.

EFFECT OF CELL ALIGNMENT ON CONDUCTION VELOCITY AND FUNCTIONAL INTEGRATION

After creating an a-cellular channel (230±10 μm) in the MEA culture dish, two asynchronously beating nrCMC fields were present, proving the presence of a conduction block. CV across the two isotropic nrCMC fields was 21.3±2.3 cm/s at day 1, and increased slightly to 22.7±2.6 cm/s at day 10.

Isotropic cell alignment
Application of nrCMCs onto unabraded coatings in the channels resulted in conduction between the two nrCMC fields within 1 day. CV across nrCMCs in the channel was 19.7±0.7 cm/s at day 1 and 20.7±1 cm/s at day 10 (n=12, NS) (Fig 5, A2), which was comparable to the CV values measured across neighboring nrCMC fields (Fig 6, A1).

    Application of nrMSCs in the channel also restored conduction between both nrCMC fields, but CV was significantly lower: 1.7±0.7 cm/s (p<0.01). CV across these isotropically aligned nrMSCs increased to 7.1±1 cm/s at day 10 (n=11, p<0.01) (Fig 5, A2 and Fig 6, A1). Electrical conduction between the nrCMC fields was also restored after application of nrCFBs, however, CV across these cells was 1.8±0.8 cm/s at day 1 and remained stable till day 10 (n=12, NS and Fig 6, A1), being significantly lower than the CV across nrMSCs at day 10 (p<0.01) (Fig 5, A2).

Anisotropic cell alignment: parallel versus perpendicular cell alignment
Application of nrCMCs onto coatings abraded in a direction parallel to the channel resulted, after 1 day, in electrical recoupling of the two nrCMC fields, which was associated with a CV of 13.5±0.9 cm/s across the nrCMC-filled channel and persisted during follow-up (CV: 14.1±1 cm/s, n=10, NS) (Fig 5, B2 and Fig 6, B1). Application of nrCMCs onto coatings abraded in a direction perpendicular to the channel, however, resulted in a CV of 26.0±1.1 cm/s (p<0.01) across the channel, which also persisted during the follow-up till day 10 (CV: 26.8±0.9 cm/s, n=11, NS) (Fig 5, C2 and Fig 6, C1).

    In contrast, application of nrMSCs onto coatings abraded in a direction parallel to the channel failed to restore electrical conduction between the two nrCMC fields up to day 7. However, at day 7, restoration had occurred and was associated with a CV of 4.9±1 cm/s at day 10 (n=11, p<0.01) (Fig 5, B2 and Fig 6, B1). Application of nrMSCs onto perpendicularly abraded coatings restored electrical conduction between the two nrCMC fields from day 1 onward. CV increased from 4.3±1 cm/s at day 1 to 11±0.9 cm/s at day 10 (n=12, p<0.01) (Fig 5, C2 and Fig 6, C1), thereby
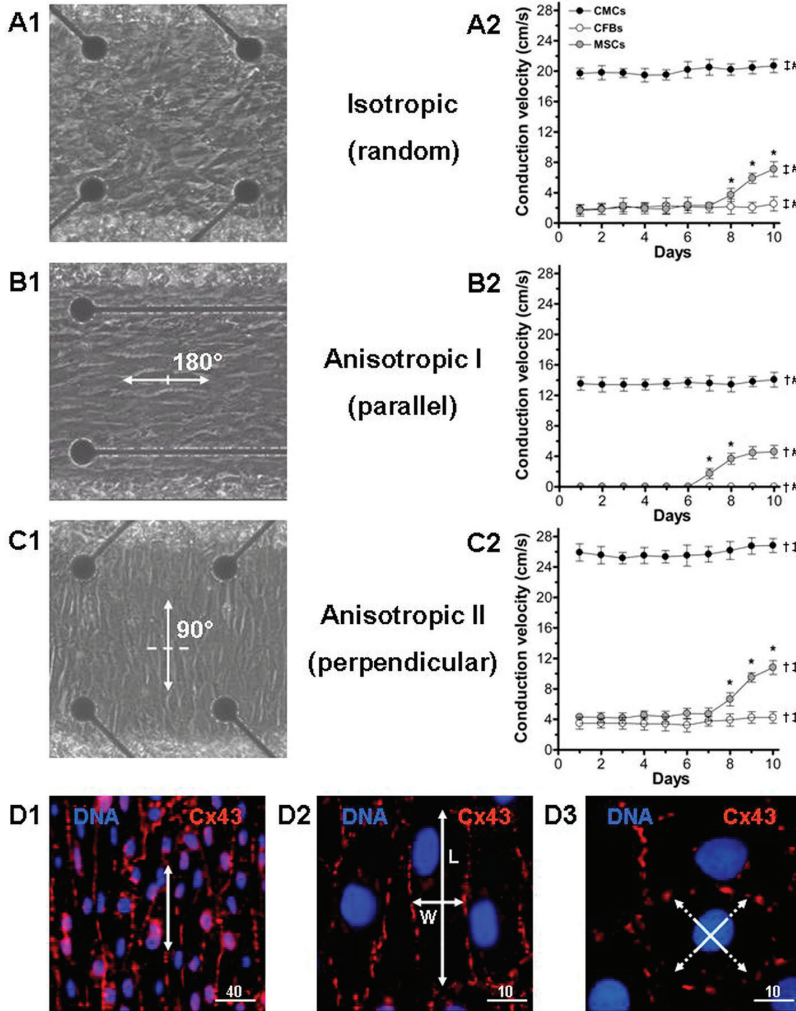
Figure 5. The effect of cell alignment on the development of conduction across the cell strip displaying a random, parallel or perpendicular configuration. (D1) Cells applied on micro-abraded coatings showed typical alignment throughout follow-up. (D2) After alignment, neonatal rat mesenchymal stem cells (nrMSCs) appeared elongated with oval shaped nuclei (average length-width ratio of 4:1, L=length, W=width), and displayed Cx43 staining uniformly distributed along cell-cell contacts. (D3) In contrast, application of cells onto una-braded coatings resulted in random cell alignment, with a variable length-width ratio (but always lower than the 4:1), which was maintained till day 10. Two-factor mixed ANOVA test (Bonferroni-corrected); †$p < 0.01$ vs. CV at day 10 in random configuration, ‡$p < 0.01$ vs. CV at day 10 in parallel configuration, #$p < 0.01$ vs. CV at day 10 in perpendicular configuration. One-way repeated-measures ANOVA (Bonferroni-corrected); *$p < 0.05$.

reaching the highest CV in the nrMSC group in the different configurations (isotropic: 7.1±1 cm/s and parallel: 4.9±1 cm/s at day 10). This indicates that alignment of nrMSCs undergoing cardiomyogenic differentiation influences the degree of functional integration with respect to CV across adjacent cardiac tissue.

Application of nrCFBs onto the parallel abraded coatings did not result in electrical conduction between the two nrCMC fields during 10 days of culture (n=10, p<0.0001) (Fig 5, B2 and Fig 6, B1). However, after application of nrCFBs in perpendicular abraded coatings, electrical conduction was restored at day 1, associated with a CV across these cells of 3.5±0.8 cm/s at day 1 and 4.3±1 cm/s at day 10 (n=10, NS) (Fig 5, C2 and Fig 6, C1).

Interestingly, quantitative analysis of Cx43 in different cells, configurations, and locations at day 10 of culture showed significant differences, revealing that the highest Cx43 expression was found in the group of parallel alignment (Fig 6, corresponding panels A2, B2, and C2).

The degree of cell alignment and confluence did not change significantly over time, as was shown by quantification and spatial measurements using (immuno) fluorescence microscopy (data not shown).

Conduction velocity across control cultures of cardiomyocyte/fibroblast mixtures
In order to mimic the composition of the cell population in the channel at day 10, which consisted of nrMSCs-derived CMCs and undifferentiated nrMSCs (~18% and ~82%, respectively), mixtures of native nrCMCs and nrCFBs (20% and 80%) were applied in all three different configurations (n=8, 8 and 9). After application of these mixtures onto the coatings, CVs determined at day 1 were comparable to CVs across eGFP-labeled nrMSCs at day 10 of culture (n=11, 10 and 10) (Fig 7). This suggests that the increase in CV across eGFP-labeled MSCs that was observed depends on the functional cardiomyogenic differentiation of nrMSCs.
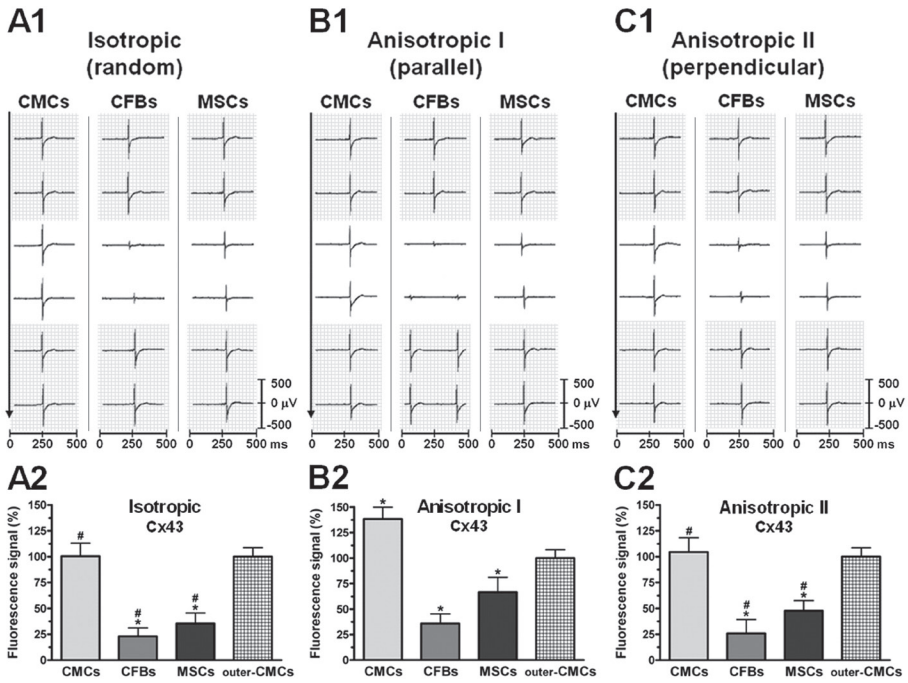
Figure 6. (A1-C1) Extracellular electrograms derived from 10-day old cultures of neonatal rat cardiomyocytes (nrCMCs), cardiac fibroblasts (nrCFBs), or mesenchymal stem cells (nrM-SCs) cultured in different configurations and from different locations (white background). In grey, electrograms of adjacent cardiomyocyte fields are shown, and referred to as outer-CMCs. (A2-C2) Cx43 expression was quantified in all three cell types and compared to expression in adjacent cardiomyocyte fields (gritted bars for outer-CMCs, set to 100%). Cx43 expression was also quantified and compared between all three cell types in each configuration. *$p<0.05$ vs Cx43 expression of outer-CMCs, #$p<0.05$ vs Cx43 expression in corresponding cells aligned parallel to the channel.
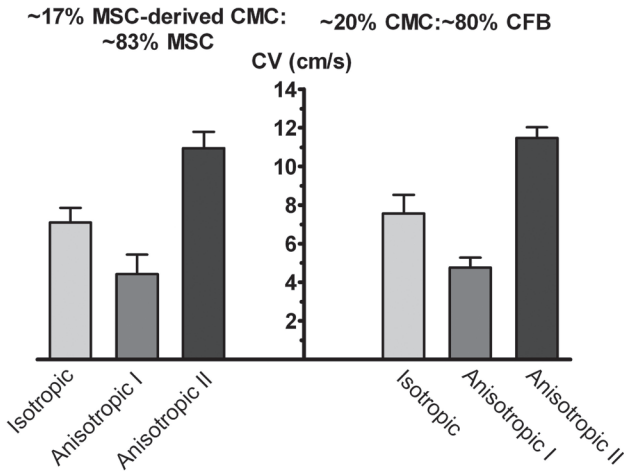
Figure 7. Positive control for cardiomyogenesis-related increase in CV across neonatal rat mesenchymal stem cells (nrMSCs). CVs across nrMSCs at day 10, cultured in one of the three configurations (n=11, 10 and 10), were compared to CVs across a mixture of 20% nrC-MCs and 80% neonatal rat cardiac fibroblasts at day 1 (n=8, 8 and 9).

DISCUSSION

The present study shows that alignment of transplanted neonatal rat mesenchymal stem cells (nrMSCs) undergoing cardiomyogenic differentiation affects the time course and degree of functional integration with cultured neonatal rat cardiomyocyte tissue.

Functional differentiation of neonatal rat mesenchymal stem cells
In this study, a significant fraction of nrMSCs differentiated into functional cardiomyocytes upon co-culture with nrCMCs. In additional co-culture experiments, differentiation percentages of nrMSCs were assessed at day 14, showing ~18% differentiation (compared to ~17% differentiation at day 10), which may indicate that maximal differentiation percentages were reached under our culture conditions. Previously, Nishiyama *et al.* also showed the cardiomyogenic differentiation potential of premature MSCs upon co-culture with CMCs.[18] The results of our study confirm these results using nrMSCs and nrCMCs. In addition, Jiang *et al.* demonstrated that MSCs from young rats differentiated into cardiac-like cells after transplantation in the infarcted rat myocardium, whereas MSCs from old rats did not.[19]

In the present study, differentiation of nrMSCs into functional cardiomyocytes was also demonstrated by intracellular (patch-clamp) membrane potential recordings after uncoupling. One might argue that the 2-APB-induced uncoupling in the patch-clamp experiments may be incomplete and that 180 mmol/L 2-APB may have affected plasma membrane ion channels, thereby affecting excitability of the nrCMCs and differentiated nrMSCs. However, the observed desynchronized beating and high whole-cell input resistance (~1 GW) in the presence of 2-APB indicated preserved single-cell excitability and strong uncoupling. These findings, together with the presence of cardiomyocyte-like action potentials in the uncoupled differentiated nrMSCs but not in uncoupled undifferentiated nrMSCs are indicative for functional differentiation of at least a fraction of the nrMSCs.

Alignment of stem cell-derived cardiomyocytes and electrical conduction
Several studies have shown anisotropic conduction across aligned CMCs *in vitro*. The longitudinal and transverse CVs measured across nrCMCs in this study are in line with the results of previous studies using the same source,[13] although some studies have reported higher CVs.[15,20] These differences in CV might have been caused by the presence of different numbers of cardiac fibroblasts in the CMC culture, or by the methods used to produce anisotropic cell cultures.[13] However, in our study, we also applied other cells than CMCs to the micro-abraded coatings and these also appeared elongated with oval shaped nuclei and a certain level of Cx43 uniformly distributed along cell-cell contacts. Anisotropic alignment of cells in our model most likely created a low-resistance conduction pathway in longitudinal direction, where fewer (high resistance) cell borders have to be crossed, thereby favoring conduction in this direction. These phenomena were not restricted to a specific cell type. However, after culture and cardiomyogenic differentiation of nrMSCs the anisotropic electrical properties further developed and functional integration with adjacent cardiomyocyte fields improved. The anisotropic ratio (perpendicular CV vs parallel CV) was comparable between nrCMCs and nrMSCs at day 10 of culture, however only CV across nrMSCs increased over time.

Distribution patterns of Cx43 did not appear to be of major influence on conduction, which has been confirmed by other studies.[15,21] The uniform distribution of Cx43 in nrCMCs, reported in the present and other studies, is typical for neonatal CMCs. Importantly, cells aligned parallel to the channel, thereby having adjacent, beating cardiac tissue perpendicular to their cell axis, were associated with the highest increase in Cx43 expression levels. A previous study reporting on neonatal CMCs subjected to anisotropic stretch showed a higher increase in Cx43 expression in CMCs stretched perpendicular to their cell axis than when CMCs

were stretched in a parallel direction.[22] In our model, the cells in the channel seem to be influenced by stretch originating from the adjacent cardiomyocyte fields, thereby indicating that alignment per se is not only affecting functional integration but that it also has an effect on gap junction regulation. In fact, our model could allow the study of stretch-related protein expression levels, as alternative to mechanically induced pulsatile stretch, which also was shown to significantly increase Cx43 expression in nrCMCs.[23] In addition, cardiomyogenic differentiation of nrMSCs may lead to increased Cx expression. Also, long-term culturing of MSCs itself leads to upregulation of Cx expression.[24] However, the relative contributions of each of these phenomena to the improvement of AP transmission by increased gap junctional coupling warrants further study.

In the present study, nrMSCs in all three cell orientation groups showed a time-dependent increase in CV which correlated with differentiation of nrMSCs, although the maximum CV differed among the groups. Comparison of the CV values of the transplanted nrMSCs with CV values of nrCMCs at different time points revealed the effect of stem cell alignment on functional integration with cardiac tissue. This is best illustrated by the finding that non-excitable nrMSCs aligned parallel to the channel were unable to conduct the electrical current across the channel for up to 6 days. However, after cardiomyogenic differentiation of these cells, electrical conduction across the channel was established. Most likely, in this situation passive conduction across non-differentiated nrMSCs is supported by active propagation across nrMSC-derived CMCs, resulting in AP transmission across the channel and subsequent activation of the distal CMC field. Thus, the alignment of stem cells not only influences the degree of functional integration, as reflected by CV values, but also the time course of functional integration. Whether alignment also influenced the degree of cardiomyogenic differentiation in itself is intriguing. The minor differences between CVs across mixtures of native nrCMCs and nrCFBs and CVs across differentiated nrMSCs indicate that alignment per se is a major determinant of functional integration. However, the increased expression of Cx43 in the nrMSCs aligned to the channel could suggest that alignment has some effect on cardiomyogenic differentiation, but this increase may also be due to the factors mentioned above. Future studies will be necessary to investigate the role of cell alignment in cardiomyogenic differentiation and subsequent effects on structural and electrical integration.

Possible therapeutic implications
To our knowledge, no study of stem cell transplantation has yet reported on the effects of cell alignment on electrical conduction, functional integration and the therapeutic implications. Furuta *et al.* have used transplanted sheets of nrCMCs onto the epicardial surface of the heart to improve cardiac function and showed

anisotropic electrical conduction across the cell sheets.[25] Interestingly, these cells appeared to orientate themselves spontaneously in line with the fiber axis of native cells. However, it is unknown whether and how stem cells align after transplantation into the myocardium of the infarcted heart, and to which extent alignment of these cells is influencing conduction and contraction. Of note, alignment of resident ventricular CMCs has major influence on electrical and mechanical activation of the heart,[26] but the cellular assessment *in vivo* is technically challenging. The present study introduces alignment of transplanted stem cells as a novel determinant of functional integration, and although conducted *ex vivo*, the study may have important implications for future cardiac cell therapy. Presumably, cell alignment will become even more important in the near future, as higher engraftment rates of transplanted cells will be achieved using novel application techniques. For example, misalignment of transplanted cells with respect to the native cardiac architecture might result in increased electrical heterogeneity potentially leading to arrhythmias as well as dyssynchronous contraction leading to decreases in cardiac output.[9] On the other hand, enforcing transplanted cells to adapt to the native tissue architecture might contribute to improved therapeutic efficiency and safety. In this view, an important and promising role is reserved for tissue engineering, in which the transplanted cells can be aligned with the use of scaffolds.[27,28]

Study limitations
Ideally, the nrCMC fields adjacent to the channel should be made anisotropic to mimic cardiac tissue architecture. This was however not possible with the techniques described in the study. Although the spatial resolution of the extracellular mapping experiments is acceptable to allow standardized measurements, the relatively low spatial resolution may have resulted in an underestimation of actual CVs. In the present study, a growth-directing substrate was created by micro-abrasion and although effective and reproducible, this procedure is time-consuming and yields only a limited number of cultures suitable for further study. Nevertheless, our study provides the first evidence that alignment of stem cells undergoing cardiomyogenic differentiation has significant impact on functional integration of these cells with cardiac tissue.

CONCLUSIONS

Forced alignment of nrMSCs undergoing cardiomyogenic differentiation affects the time course and degree of functional integration with surrounding host cardiac tissue. This study introduces cell alignment as an important determinant of functional integration of transplanted cells, which may contribute to the improvement

of therapeutic outcome and reduction of potential hazards. Further study is needed to determine the full biological, biophysical, and therapeutic relevance of cell alignment in functional integration of transplanted cells with host myocardium.

REFERENCES

1.   Li F, Wang X, Capasso JM, Gerdes AM. Rapid transition of cardiac myocytes from hyperplasia to hypertrophy during postnatal development. *J Mol Cell Cardiol*. 1996;28:1737-1746.
2.   Oparil S, Bishop SP, Clubb FJ, Jr. Myocardial cell hypertrophy or hyperplasia. *Hypertension*. 1984;6:III38-III43.
3.   Hirschy A, Schatzmann F, Ehler E, Perriard JC. Establishment of cardiac cytoarchitecture in the developing mouse heart. *Dev Biol*. 2006;289:430-441.
4.   Angst BD, Khan LU, Severs NJ, Whitely K, Rothery S, Thompson RP, Magee AI, Gourdie RG. Dissociated spatial patterning of gap junctions and cell adhesion junctions during postnatal differentiation of ventricular myocardium. *Circ Res*. 1997;80:88-94.
5.   Gourdie RG, Green CR, Severs NJ, Thompson RP. Immunolabelling patterns of gap junction connexins in the developing and mature rat heart. *Anat Embryol (Berl)*. 1992;185:363-378.
6.   Saffitz JE, Kanter HL, Green KG, Tolley TK, Beyer EC. Tissue-specific determinants of anisotropic conduction velocity in canine atrial and ventricular myocardium. *Circ Res*. 1994;74:1065-1070.
7.   Streeter DD, Jr., Spotnitz HM, Patel DP, Ross J, Jr., Sonnenblick EH. Fiber orientation in the canine left ventricle during diastole and systole. *Circ Res*. 1969;24:339-347.
8.   Wiegner AW, Bing OH, Borg TK, Caulfield JB. Mechanical and structural correlates of canine pericardium. *Circ Res*. 1981;49:807-814.
9.   Peters NS, Wit AL. Myocardial architecture and ventricular arrhythmogenesis. *Circulation*. 1998;97:1746-1754.
10. Orlic D, Hill JM, Arai AE. Stem cells for myocardial regeneration. *Circ Res*. 2002;91:1092-1102.
11. Leobon B, Garcin I, Menasche P, Vilquin JT, Audinat E, Charpak S. Myoblasts transplanted into rat infarcted myocardium are functionally isolated from their host. *Proc Natl Acad Sci U S A*. 2003;100:7808-7811.
12. Fast VG, Kleber AG. Microscopic conduction in cultured strands of neonatal rat heart cells measured with voltage-sensitive dyes. *Circ Res*. 1993;73:914-925.
13. Bursac N, Parker KK, Iravanian S, Tung L. Cardiomyocyte cultures with controlled macroscopic anisotropy: a model for functional electrophysiological studies of cardiac muscle. *Circ Res*. 2002;91:e45-e54.
14. Pijnappels DA, van Tuyn J, de Vries AA, Grauss RW, van der Laarse A, Ypey DL, Atsma DE, Schalij MJ. Resynchronization of separated rat cardiomyocyte fields with genetically modified human ventricular scar fibroblasts. *Circulation*. 2007;116:2018-2028.
15. Fast VG, Kleber AG. Anisotropic conduction in monolayers of neonatal rat heart cells cultured on collagen substrate. *Circ Res*. 1994;75:591-595.
16. Pittenger MF, Martin BJ. Mesenchymal stem cells and their potential as cardiac therapeutics. *Circ Res*. 2004;95:9-20.
17. Harks EG, Camina JP, Peters PH, Ypey DL, Scheenen WJ, van Zoelen EJ, Theuvenet AP. Besides affecting intracellular calcium signaling, 2-APB reversibly blocks gap junctional coupling in confluent monolayers, thereby allowing measurement of single-cell membrane currents in undissociated cells. *FASEB J*. 2003;17:941-943.

18. Nishiyama N, Miyoshi S, Hida N, Uyama T, Okamoto K, Ikegami Y, Miyado K, Segawa K, Terai M, Sakamoto M, Ogawa S, Umezawa A. The significant cardiomyogenic potential of human umbilical cord blood-derived mesenchymal stem cells in vitro. *Stem Cells.* 2007;25:2017-2024.

19. Jiang S, Kh HH, Ahmed RP, Idris NM, Salim A, Ashraf M. Transcriptional profiling of young and old mesenchymal stem cells in response to oxygen deprivation and reparability of the infarcted myocardium. *J Mol Cell Cardiol.* 2008;44:582-596.

20. Fast VG, Darrow BJ, Saffitz JE, Kleber AG. Anisotropic activation spread in heart cell monolayers assessed by high-resolution optical mapping. Role of tissue discontinuities. *Circ Res.* 1996;79:115-127.

21. Spach MS, Heidlage JF, Barr RC, Dolber PC. Cell size and communication: role in structural and electrical development and remodeling of the heart. *Heart Rhythm.* 2004;1:500-515.

22. Gopalan SM, Flaim C, Bhatia SN, Hoshijima M, Knoell R, Chien KR, Omens JH, McCulloch AD. Anisotropic stretch-induced hypertrophy in neonatal ventricular myocytes micropatterned on deformable elastomers. *Biotechnol Bioeng.* 2003;81:578-587.

23. Zhuang J, Yamada KA, Saffitz JE, Kleber AG. Pulsatile stretch remodels cell-to-cell communication in cultured myocytes. *Circ Res.* 2000;87:316-322.

24. Pijnappels DA, Schalij MJ, van Tuyn J, Ypey DL, de Vries AA, van der Wall EE, van der Laarse A, Atsma DE. Progressive increase in conduction velocity across human mesenchymal stem cells is mediated by enhanced electrical coupling. *Cardiovasc Res.* 2006;72:282-291.

25. Furuta A, Miyoshi S, Itabashi Y, Shimizu T, Kira S, Hayakawa K, Nishiyama N, Tanimoto K, Hagiwara Y, Satoh T, Fukuda K, Okano T, Ogawa S. Pulsatile cardiac tissue grafts using a novel three-dimensional cell sheet manipulation technique functionally integrates with the host heart, in vivo. *Circ Res.* 2006;98:705-712.

26. Hooks DA, Tomlinson KA, Marsden SG, LeGrice IJ, Smaill BH, Pullan AJ, Hunter PJ. Cardiac microstructure: implications for electrical propagation and defibrillation in the heart. *Circ Res.* 2002;91:331-338.

27. Radisic M, Park H, Shing H, Consi T, Schoen FJ, Langer R, Freed LE, Vunjak-Novakovic G. Functional assembly of engineered myocardium by electrical stimulation of cardiac myocytes cultured on scaffolds. *Proc Natl Acad Sci U S A.* 2004;101:18129-18134.

28. Feinberg AW, Feigel A, Shevkoplyas SS, Sheehy S, Whitesides GM, Parker KK. Muscular thin films for building actuators and powering devices. *Science.* 2007;317:1366-1370.

EXPANDED MATERIALS AND METHODS

ISOLATION AND CULTURE OF NEONATAL RAT CARDIOMYOCYTES AND CARDIAC FIBROBLASTS.

All animal experiments were approved by the Animal Experiments Committee of the Leiden University Medical Center and conformed to the Guide for the Care and Use of Laboratory Animals as stated by the US National Institutes of Health.

Cardiomyocytes (CMCs) were dissociated from ventricles of 2-day old male neonatal (nr) Wistar rats and grown in culture medium supplemented with 5% horse serum (HS, Invitrogen, Carlsbad, CA, USA), penicillin (100 U/mL) and streptomycin (100 μg/mL; P/S; Bio-Whittaker, Verviers, Belgium), as previously described [1].

Before their use in cell pattern experiments, nrCMCs were collected in culture flasks and labeled with the viable fluorescent dye chloromethylbenzamido (CM-DiI) (CellTrackerä, Molecular Probes, Eugene, OR, USA) according to the recommendations of the manufacturer.

Micro-electrode array culture dishes (MEA, Multi Channel Systems, Reutlingen, Germany) and glass coverslips were pre-coated for 4 h with fibronectin-gelatin (8:2,$^v/_v$, 0.1% fibronectin and gelatin in PBS), and dried using pressurized nitrogen. nrCMCs were plated ($1.5x10^6$ cells) on MEAs or on glass coverslips in 6-well culture dishes ($2x10^6$ cells/well) and incubated in a humidified incubator at 37° C and 5% CO_2 to obtain confluent spontaneously beating monolayer of nrCMCs.

In addition, adherent neonatal rat cardiac fibroblasts (nrCFBs) were collected, purified (by re-plating), enhanced green fluorescent protein (eGFP)-labeled and cultured in a 1:1 ($^v/_v$) mixture of Dulbecco's modified Eagle's medium (DMEM, Invitrogen) and Ham's F10 medium (ICN Biomedicals, Irvine, CA, USA) supplemented with 10% fetal bovine serum (FBS, Invitrogen), penicillin (100 U/mL) and streptomycin (100 μg/mL). CFBs were labeled with eGFP using the vesicular stomatitis virus G protein-pseudotyped self-inactivating lentivirus vector CMVPRES [2] essentially as described by van Tuyn et al [3].

Proliferation of residual nrCFBs in nrCMC cultures was inhibited by incubation with 100 mmol/L 5-bromo-2-deoxyuridine (BrdU, Sigma-Aldrich, Saint Louis, MO, USA) in culture medium during the first 24 after culture initiation.

HARVESTING AND CHARACTERIZATION OF BONE MARROW-DERIVED NEONATAL RAT MESENCHYMAL STEM CELLS AND CARDIOMYOGENIC DIFFERENTIATION.

Harvesting

Bone marrow was isolated from *femora* and *tibiae* of the same 2-day-old male Wistar rats used for nrCMC harvesting. Marrow was extruded from the bones by centrifugation at 13,000 rpm for 30 s (rotor diameter: 15 cm), suspended in 10 mL

of stem cell medium [human mesenchymal stem cell growth medium (MSCGM) consisting of 440 ml basal medium, 50 ml of mesenchymal growth supplements, 15% FBS (Invitrogen), 4 mmol/L of L-glutamine, penicillin (50 U/L) and streptomycin (50 mg/L), amphothericin B solution (1 mL/mL, Sigma-Aldrich) (Cambrex Bio Science, Walkersville, MD, USA)], and 6% heparin (400 IE/ml). This suspension was centrifuged again at 1000 rpm for 10 min. Next, the pellet was resuspended in 7 ml of this medium supplemented with 5.75 μg/mL deoxyribonuclease I (DNase, Sigma-Aldrich). The cells were then plated in 25-cm^2 culture flasks (Becton Dickinson, Franklin Lakes, NJ, USA) and incubated at 37° C and 5% CO_2 for 2 days after which non-adherent cells were removed. Stem cell medium was refreshed twice a week until the primary cultures of nrMSCs were confluent, after which they were expanded by serial passage. In this study passages 2 to 4 were used. To ensure identification, nrMSCs were transduced with CMVPRES as described earlier in this section.

CHARACTERIZATION OF NRMSCS

Adipogenic and osteogenic differentiation of mesenchymal stem cells
The nrMSCs were characterized by established differentiation assays[4]. Briefly, 5x10^3 nrMSCs per well were plated in a 12-well culture plate, and exposed to adipogenic or osteogenic induction medium. Adipogenic differentiation medium consisted of a regular culture medium (DMEM supplemented with 15% FBS, 100 U/L penicillin and 100 μg/mL streptomycin, 1 μg/mL amphothericin B solution) supplemented with 5 μg/mL insulin, 1 μmol/L dexamethason, 50 μmol/L indomethacin and 0.5 μmol/L 3-isobutyl-1-methylxanthine (IBMX) (all from Sigma-Aldrich), and was refreshed every 3-4 days for a period of 3 weeks. Lipid accumulation was assessed by Oil Red O staining of the cultures (15 mg Oil Red O/mL 60% isopropanol) and light microscopy. Osteogenic differentiation medium consisted of culture medium supplemented with 10 mmol/L b-glycerophosphate, 50 μg/mL ascorbic acid and 10 nmol/L dexamethason (all from Sigma-Aldrich), and was refreshed every 3-4 days for a period of 2 weeks. Afterwards, the cells were washed with phosphate-buffered saline (PBS), and calcium deposits were visualized by staining of the cells for 2-5 min with 2% Alizarine Red S in 0.5% NH_4OH (pH 5.5).

Flow cytometry
Analysis of surface marker expression was carried out by flow cytometry. The nrMSCs were detached using trypsin/EDTA (Bio-Whittaker) and resuspended in PBS containing 0.5% bovine serum albumine (BSA, Sigma-Aldrich), and divided in aliquots of 5x10^4 cells. Cells were then incubated for 30 min at 4°C with fluorescein isothiocyanate (FITC)- or phycoerythrin (PE)-conjugated antibodies against

80   rat CD34 (Santa Cruz Biotechnology, Santa Cruz, CA, USA), CD29, CD44, CD45, CD90, CD106 (Becton Dickinson). Labeled cells were washed and analyzed using a FACSort flow cytometer (Becton Dickinson), equipped with a 488-nm argon ion laser and a 635-nm red diode laser. Isotype-matched control antibodies (Becton Dickinson) were used to determine background fluorescence. At least 5×10^3 cells per sample were acquired and data were processed using CellQuest software (Becton Dickinson).

IMMUNOCYTOLOGICAL ANALYSIS OF GAP JUNCTION CONTENT AND CARDIOMYOGENIC DIFFERENTIATION POTENTIAL

Isotropic co-cultures of 2×10^6 nrCMCs and 5×10^4 eGFP-labeled nrMSCs were stained for cardiac connexins and sarcomeric proteins on day 3 or day 10 after culture initiation. To detect sarcomeric proteins, we used mouse monoclonal antibodies specific for sarcomeric α-actinin (Sigma-Aldrich) or mouse anti-cardiac troponin I (HyTest Ltd., Turku, Finland), both at a dilution of 1:400. Rabbit polyclonal anti-connexin 40 (Cx40), anti-Cx43 and anti-Cx45 antibodies were used to stain gap junctional proteins, and examined as previously described.[1] In addition, anisotropic co-cultures were stained for Cx43 to show the effects of anisotropic cell alignment on Cx distribution in nrMSCs. In these cultures, cellular distribution and quantity of Cx43 were studied by the use of fixed Areas of Interest (AOI) which were placed on both longitudinal and transversal sides of the cells (n=32 for each cell type in each configuration). In each AOI the fluorescent spots were quantified using dedicated software (Image-Pro Plus, Version 4.1.0.0, Media Cybernetics, Silver Spring, MD, USA), this allowed us the estimate global distribution of Cx staining. An AOI covering the whole cell-area was used in cultures of isotropic cell alignment. The primary antibodies were visualized with rabbit anti-mouse IgG or goat anti-rabbit IgG Alexa antibodies (Invitrogen). Unless stated otherwise, antibodies were used at a dilution of 1:200.

The percentage of eGFP-labeled cells showing positive staining for sarcomeric proteins was calculated by quantification of 6 cultures (60 cells per culture per sarcomeric protein, at 40x magnification) at each time point, using a threshold value of 50 on the 0-255 intensity scale. To assess structural integrity, sarcomere lengths in native nrCMCs and eGFP-labeled cells were estimated from 64 standardized individual measurements (4 areas of 20µmx20µm per cell). The area of measurement covered the cell-surface aspect of in total 8 native nrCMCs and 8 eGFP-labeled cells that exhibited typical sarcomeric α-actinin cross-striation without any observable inhomogeneities. A fluorescence microscope equipped with a digital camera (Nikon Eclipse, Nikon Europe, Badhoevedorp, The Netherlands) and dedicated software (Image-Pro Plus, Version 4.1.0.0, Media Cybernetics, Silver Spring, MD, USA) were used to analyze data. All co-cultures of nrCMCs and eGFP-labeled

nrMSCs were stained using the same solutions, and equal exposure times. Quantifications were performed by an independent investigator.

ELECTROPHYSIOLOGICAL MEASUREMENTS IN PHARMACOLOGICALLY UNCOUPLED CELL MONOLAYERS

Whole-cell patch-clamp measurements were performed in co-cultures of $5x10^4$ eGFP-labeled nrMSCs and $2x10^6$ nrCMCs. To perform single-cell measurements from eGFP-labeled nrMSCs in a syncytium of beating nrCMCs, cells were pharmacologically uncoupled by incubation with 180 µmol/L of 2-aminoethoxydiphenyl borate (2-APB) (Tocris, Ballwin, MO, USA) for 15 min. This agent largely,[5] or fully[6] blocks gap junctional intercellular coupling by Cx40, Cx43, and Cx45. Whole-cell current-clamp recordings were performed at 25°C using a L/M-PC patch-clamp amplifier (3 kHz filtering) (List-Medical, Darmstadt, Germany) 3 and 10 days after culture initiation. Pipette solution contained (in mmol/L) 10 Na_2ATP, 115 KCl, 1 $MgCl_2$, 5 EGTA, 10 HEPES/KOH (pH 7.4). Tip resistance was 2.0 - 2.5 MW, and seal resistance >1 GW. The bath solution contained (in mmol/L) 137 NaCl, 4 KCl, 1.8 $CaCl_2$, 1 $MgCl_2$, 10 HEPES (pH 7.4). For data acquisition and analysis pClamp/Clampex8 software (Axon Instruments, Molecular Devices, Sunnyvale, CA, USA) was used. Action potentials were analyzed and compared between nrCMCs and eGFP-labeled nrMSCs. We did not correct for an existing tip potential during the membrane potential measurements, because this tip potential is assumed to be relatively small (~3 mV) for our bath and pipette solutions.[7] Input resistance of whole-cells coupled to their surrounding cells was measured in voltage-clamp by dividing the applied voltage steps by the stationary membrane current change.[6]

Micro-electrode high-density mapping
Electrograms were analyzed off-line using MC-Rack software (version 3.5.6, Multi Channel Systems). Electrical stimulation of cell cultures was performed via an external pipette electrode producing bipolar rectangular pulses (1.5x threshold, pulse width 10 ms), placed ~1 mm above the cell culture and >5 mm away from the measurement sites. Cultures were stimulated for at least 30 s, before recordings were started.

The maximal negative intrinsic deflection was taken as local activation time (LAT) and used to construct 2-dimensional color-coded activation maps (S-plus, version 6.2, Insightful Corporation, Seattle, WA, USA). Conduction velocities were calculated from averaged LATs recorded at 8 fixed measuring points, distributed equally over the two lines of electrodes adjacent to the channel.[1,8]

REFERENCES

1. Pijnappels DA, Schalij MJ, van Tuyn J, Ypey DL, de Vries AA, van der Wall EE, van der Laarse A, Atsma DE. Progressive increase in conduction velocity across human mesenchymal stem cells is mediated by enhanced electrical coupling. *Cardiovasc Res.* 2006;72:282-291.

2. Seppen J, Rijnberg M, Cooreman MP, Oude Elferink RP. Lentiviral vectors for efficient transduction of isolated primary quiescent hepatocytes. *J Hepatol.* 2002;36:459-465.

3. van Tuyn J, Pijnappels DA, de Vries AA, de V, I, van der Velde-van Dijke, Knaan-Shanzer S, van der Laarse A, Schalij MJ, Atsma DE. Fibroblasts from human postmyocardial infarction scars acquire properties of cardiomyocytes after transduction with a recombinant myocardin gene. *FASEB J.* 2007;21:3369-3379.

4. Pittenger MF, Mackay AM, Beck SC, Jaiswal RK, Douglas R, Mosca JD, Moorman MA, Simonetti DW, Craig S, Marshak DR. Multilineage potential of adult human mesenchymal stem cells. *Science.* 1999;284:143-147.

5. Bai D, del Corsso C, Srinivas M, Spray DC. Block of specific gap junction channel subtypes by 2-aminoethoxydiphenyl borate (2-APB). *J Pharmacol Exp Ther.* 2006;319:1452-1458.

6. Harks EG, Camina JP, Peters PH, Ypey DL, Scheenen WJ, van Zoelen EJ, Theuvenet AP. Besides affecting intracellular calcium signaling, 2-APB reversibly blocks gap junctional coupling in confluent monolayers, thereby allowing measurement of single-cell membrane currents in undissociated cells. *FASEB J.* 2003;17:941-943.

7. E. Neher. Correction for Liquid Junction Potentials in Patch Clamp Experiments. In: Rudy B and Iverson LE, eds. *Methods in Enzymology, volume 207, Ion Channels,* eds. New York, London: Academic Press; 1992.

8. Pijnappels DA, van Tuyn J, de Vries AA, Grauss RW, van der Laarse A, Ypey DL, Atsma DE, Schalij MJ. Resynchronization of separated rat cardiomyocyte fields with genetically modified human ventricular scar fibroblasts. *Circulation.* 2007;116:2018-2028.

CHAPTER IV

GAP JUNCTIONAL COUPLING WITH CARDIOMYOCYTES IS ESSENTIAL FOR CARDIOMYOGENIC DIFFERENTIATION OF FETAL HUMAN MESENCHYMAL STEM CELLS

Arti A. Ramkisoensing[a], Daniël A. Pijnappels[a], Jim Swildens[a,b], Marie José Goumans[b], Willem E. Fibbe[c], Martin J. Schalij[a], Antoine A.F. de Vries[a,b]*, Douwe E. Atsma[a]*
*Equal contribution

[a]Departments of Cardiology, [b]Molecular Cell Biology, [c]Hematology, Laboratory of Experimental Cardiology, Leiden University Medical Center, 2300 RC Leiden, The Netherlands.

ABSTRACT

Rationale: Gap junctional coupling is important for functional integration of transplanted cells with host myocardium. However, the role of gap junctions in cardiomyogenic differentiation of transplanted cells has not been directly investigated.

Objective: To study the role of connexin43 (Cx43) in cardiomyogenic differentiation of human mesenchymal stem cells (hMSCs).

Methods: Knockdown of Cx43 gene expression was established in naturally Cx43-rich fetal amniotic membrane hMSCs (Cx43↓ fetal AM hMSCs), while Cx43 was overexpressed in inherently Cx43-poor adult adipose tissue hMSCs (Cx43↑ adult AT hMSCs). The hMSCs were exposed to cardiomyogenic stimuli by co-incubation with neonatal rat cardiomyocytes (nrCMCs) for 10 days. Differentiation was assessed by immunostaining and whole-cell current-clamping. To establish whether the effects of Cx43 knockdown could be rescued Cx45 was overexpressed in Cx43↓ fetal AM hMSCs.

Results: Ten days after co-incubation not a single Cx43↓ fetal AM hMSC or adult AT MSC expressed α-actinin, while control fetal AM hMSCs did (2.18±0.4%, n=5,000). Moreover, functional cardiomyogenic differentiation, based on action potential recordings, occurred only in control fetal AM hMSCs. Of interest, Cx45 overexpression in Cx43↓ fetal AM hMSCs restored their ability to undergo cardiomyogenesis (1.57±0.4%, n=2,500) in co-culture with nrCMCs.

Conclusion: Gap junctional coupling is required for differentiation of fetal AM hMSCs into functional cardiomyocytes after co-incubation with nrCMCs. Heterocellular gap junctional coupling thus plays an important role in the transfer of cardiomyogenic signals from nrCMCs to fetal hMSCs but is not sufficient to induce cardiomyogenic differentiation in adult AT hMSCs.

INTRODUCTION

Gap junctional coupling is essential in establishing electrochemical communication between cardiomyocytes (CMCs).[1] Such coupling of cytoplasmic compartments is mediated by gap junctions, consisting of two hexameric assemblies of connexin (Cx) proteins embedded in the plasma membranes of neighboring cells thereby forming so-called hemichannels or connexons. Gap junctions permit the bidirectional passage of small molecules and ions between cells and play an important role in the regulation of both physiological and pathophysiological processes.

During embryonic development, spreading of signals across tissues through gap junctions contribute to the migration and specialization of cells.[2] In the developing heart, connexin40 (Cx40), connexin43 (Cx43) and/or connexin45 (Cx45) deficiency results in serious cardiac malformation.[3-7] Besides cardiac development, gap junctional communication also affects the therapeutic and hazardous potential of cardiac cell therapy.[8-10] However, the role of gap junctional coupling in cardiomyogenic differentiation of stem cells remains unclear, although gap junction-mediated processes, such as spread of micro RNAs (miRs) and hyperpolarization, have been implicated in the induction of cardiomyogenesis.[11,12]

Mesenchymal stem cells (MSCs) are a population of mononuclear stromal cells that can be harvested from a wide variety of tissues, are easily expandable *in vitro*, have immunomodulatory properties, secrete paracrine factors that stimulate tissue regeneration and can differentiate into various types of mesodermal and non-mesodermal cells.[13,14] In addition, these cells were shown to improve cardiac function upon transplantation in diseased rodent, pig and human hearts.[15] However, to what extent MSCs can undergo cardiac differentiation and which factors are involved in this process is still unclear.[16-18] Although donor age and heterocellular interactions were found to affect the cardiomyogenic differentiation potential of MSCs[19], more research is needed into their biological properties and the modification thereof to improve the therapeutic potential of MSC-based cardiac cell therapy.

Accordingly, in this study, we specifically investigated the role of Cx43, the major gap junction protein of the working myocardium, in cardiomyogenic differentiation of naturally Cx43-rich fetal and Cx43-poor adult human MSCs (hMSCs)[19] in co-cultures with neonatal rat ventricular CMCs (nrCMCs). To this end, Cx43 expression levels in hMSCs were either downregulated by short hairpin RNA (shRNA)-mediated RNA interference (RNAi) or upregulated by recombinant human Cx43 (hCx43) gene delivery. To control for possible off-target effects of hCx43-specific shRNAs, an RNAi rescue experiment based on the forced expression of human Cx45 (hCx45) in Cx43 knockdown cells was included. The consequences of these genetic interventions on the cardiomyogenic differentiation capacity of the hMSCs were assessed using immunocytological and patch-clamp analyses.

The present study shows that gap junctions are directly involved in the transfer of cardiomyogenic signals from nrCMCs to fetal hMSCs. Downregulation of Cx43 gene expression in these hMSCs prevented their cardiomyogenic differentiation in co-cultures with nrCMCs. Overexpression of hCx45 in the Cx43 knockdown cells, on the other hand, restored their ability to respond to cardiomyogenic stimuli provided by neighboring nrCMCs.

MATERIALS AND METHODS

The role of gap junctional coupling in the transfer of cardiomyogenic signals from nrCMCs to hMSCs was investigated by suppressing Cx43 expression in naturally Cx43-rich fetal amniotic membrane (AM) hMSCs using two lentiviral vectors (LVs) encoding different hCx43-specific shRNAs (Cx43↓(1) fetal AM hMSCs and (Cx43↓(2) fetal AM hMSCs) and by LV-mediated overexpression of hCx43 in intrinsically Cx43-poor adult adipose tissue (AT) hMSCs (Cx43↑ adult AT hMSCs). To facilitate the identification of genetically modified cells, the LVs also directed the synthesis of the green fluorescent protein (GFP) of *Renilla reniformis* (hrGFP). Fetal AM hMSCs transduced with an LV encoding an shRNA directed against the *Aequorea victoria* enhanced green fluorescent protein (eGFP) gene and adult AT hMSCs transduced with an LV coding for hrGFP alone served as control cells (control fetal AM hMSCs and control adult AT hMSCs, respectively). For an optimized analysis of the adult AT hMSCs these cells were also transduced with an LV encoding Cx43 and a puromycin resistence gene. Control cells were transduced with an LV coding for the puromycin-resistence gene alone. Immunocytological analysis, quantitative reverse transcriptase-polymerase chain reaction (qRT-PCR) and western blot analysis were applied to determine Cx43 expression levels, while dye transfer assays and whole-cell current-clamp recordings were used to assess the level of functional coupling. To induce cardiomyogenic differentiation, hMSCs were co-incubated with nrCMCs for 10 days. Differentiation was assessed by immunocytological staining and whole-cell current-clamping. LV-encoded hCx45 was overexpressed in Cx43↓(1) fetal AM hMSCs (Cx43↓(1)+Cx45↑ fetal AM hMSCs) to establish whether the effects of Cx43 knockdown could be reversed using the techniques described above. Cx43↓(1) fetal AM hMSCs transduced with an LV encoding eGFP were used as control cells (Cx43↓(1)+eGFP fetal AM hMSCs) in these experiments. For a detailed description of the materials and methods the reader is referred to the Supplement Material and previous papers of our research group.[19-21]

RESULTS

CHARACTERIZATION OF FETAL AM HMSCS AND ADULT AT HMSCS

Both fetal AM hMSCs and adult AT hMSCs were characterized according to established criteria. To this purpose, their cell surface marker profile and adipogenic and osteogenic differentiation capacity were studied. Both types of hMSCs were negative for CD31 (endothelial cell marker), CD34 and CD45 (both hematopoietic cell markers), whereas they were positive for CD73, CD90 and CD105 (mesenchymal stem cell markers) (Figure 1A-C). *In vitro* differentiation assays showed that the two types of hMSCs were able to differentiate into adipocytes (Figure 1D1-D2) and osteoblasts (Figure 1E1-E2) confirming their multipotency.

EVALUATION OF CX43 EXPRESSION LEVELS

The impact of the different genetic interventions on the Cx43 expression levels in fetal AM hMSCs and adult AT hMSCs was investigated by three different methods. Immunocytological analysis showed that Cx43↑ adult AT hMSCs (Figure 2A2) contained higher levels of Cx43 than control adult AT hMSCs (Figure 2A1), while the protein was also more abundant in control fetal AM hMSCs (Figure 2B1) than in Cx43↓(1) fetal AM hMSCs (Figure 2B2) or in Cx43↓(2) fetal AM hMSCs (Figure 2B3) (for each genetic modification n=4 isolates of each hMSC type were assessed). These results were validated by western blot analysis (n=4 hMSC isolates per experimental group), which showed that Cx43↑ adult AT hMSCs contained 1,798±146% more Cx43 protein than control adult AT hMSCs ($P<0.001$) (Figure 2C1 and C3). Western blot analysis also confirmed the presence of significantly less Cx43 in Cx43↓(1) fetal AM hMSCs (79.4±3.0% reduction) and in Cx43↓(2) fetal AM hMSCs (77.4±2.6% reduction) than in control fetal AM hMSCs ($P<0.001$) (Figure 2C2 and C4). In agreement with these results, qRT-PCR revealed that Cx43↑ adult AT hMSCs contained 9.77±0.63-fold ($P<0.001$) (Figure 2D1) more Cx43 transcripts than control adult AT hMSCs while the amount of Cx43 RNA in Cx43↓(1) fetal AM hMSCs and in Cx43↓(2) fetal AM hMSCs was, respectively, 3.67±0.14- and 3.94±0.25-fold ($P<0.001$) lower than in control fetal AM hMSCs (Figure 2D2).
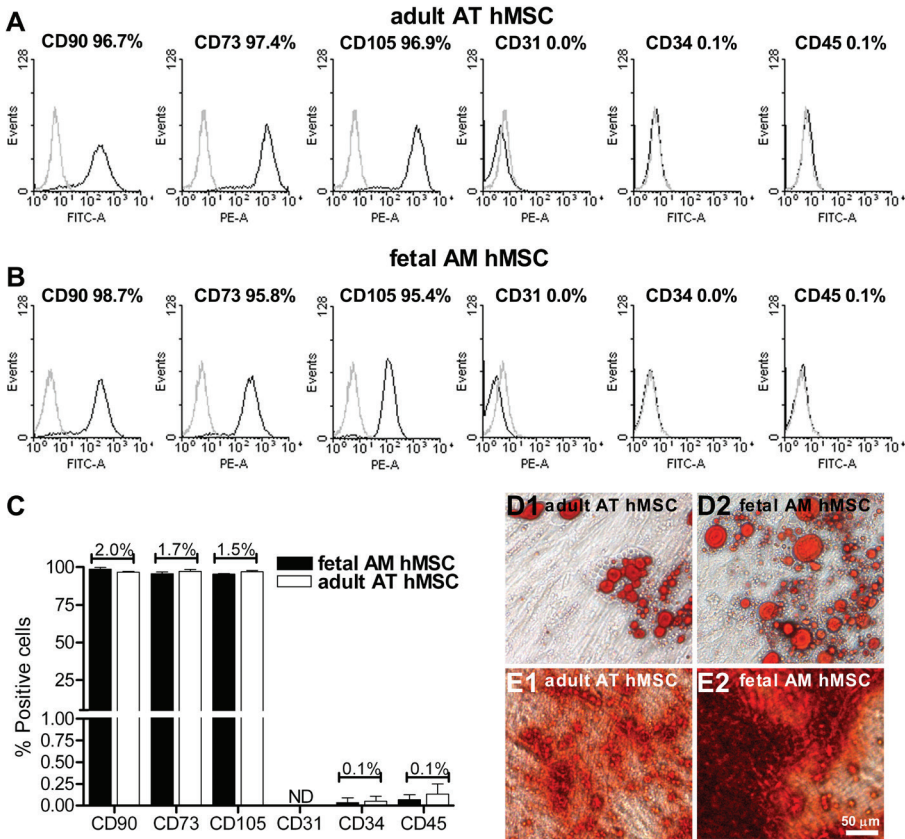
Figure 1. Characterization of fetal AM hMSCs and adult AT hMSCs. (A-B) Flow cytometric analyses showed for both types of hMSCs abundant surface expression of the MSC markers, CD90, CD105 and CD73 and hardly any surface expression of the hematopoietic cell markers CD34 and CD45 or the endothelial cell marker CD31 (black lines). Isotype-matched control antibodies were included to determine background fluorescence levels (gray lines). Percentages are means of ≥4 measurements. (C) Only minor differences in the expression levels of the surface marker proteins were present between fetal AM hMSCs and adult AT hMSCs. ND is not detected. (D1-D2) Adipogenic differentiation was visualized by the presence of Oil Red O-stained fat vacuoles. (E1-E2) Calcium depositions after osteogenic differentiation were visualized by Alizarin Red S staining.
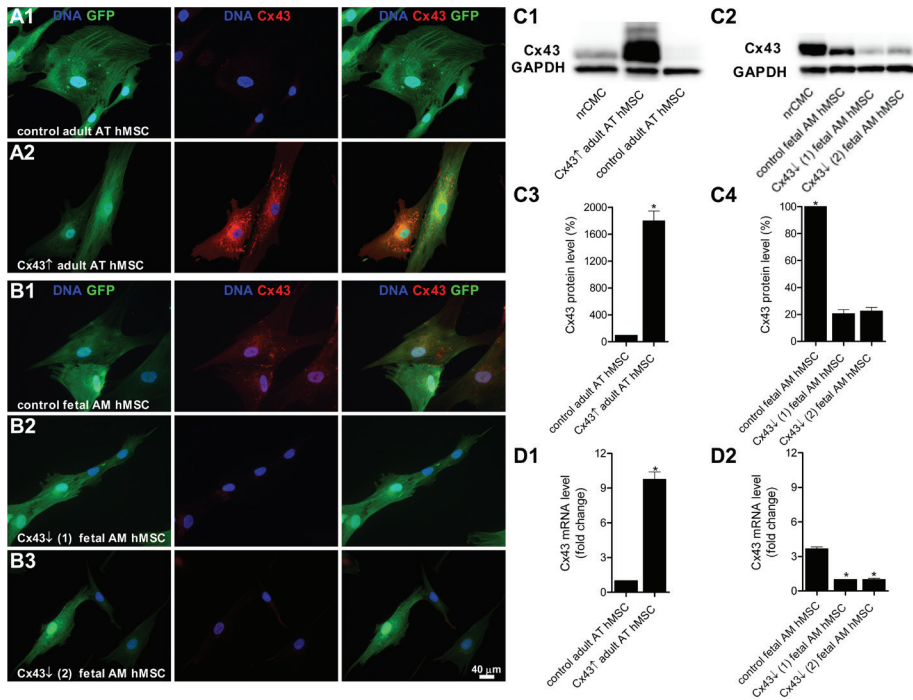
Figure 2. Analysis by immunofluorescence microscopy, western blotting and qRT-PCR of Cx43 expression in monocultures of genetically modified fetal AM hMSCs and adult AT hMSCs. (A1-A2) Immunocytological analyses revealed low Cx43 levels in control adult AT hMSCs, while high levels of Cx43 were detected in Cx43↑ adult AT hMSCs. (B1) High Cx43 levels were present in control fetal AM hMSCs. (B2-B3) After knockdown of Cx43 gene expression, low Cx43 levels were detected in Cx43↓(1) fetal AM hMSCs and in Cx43↓(2) fetal AM hMSCs. Nuclei were stained with the DNA-binding fluorochrome Hoechst 33342. (C1-C2) Pictures of representative western blots showing that Cx43↑ adult AT hMSCs have large amounts of Cx43 in contrast to control adult AT hMSCs and that control fetal AM hMSCs contain large amounts of Cx43 in contrast to Cx43↓(1) fetal AM hMSCs and Cx43↓(2) fetal AM hMSCs. The GAPDH-specific immunostaining was included for normalization purposes. (C3-C4) Bar graphs of the quantification by western blotting of Cx43 levels in the different populations of hMSCs corrected for differences in GAPDH expression. *$P<0.001$ vs. Cx43↑ adult AT hMSCs or vs. Cx43↓(1) fetal AM hMSCs and Cx43↓(2) fetal AM hMSCs. (D1-D2) Bar graphs of the assessment by qRT-PCR of Cx43 mRNA levels in control adult AT hMSCs, Cx43↑ adult AT hMSCs and in control fetal AM hMSCs, Cx43↓(1) fetal AM hMSCs and Cx43↓(2) fetal AM hMSCs. *$P<0.001$ vs. control adult AT hMSCs or vs. Cx43↓(1) fetal AM hMSCs and Cx43↓(2) fetal AM hMSCs.

ASSESSMENT OF FUNCTIONAL HETEROCELLULAR GAP JUNCTIONAL COUPLING VIA CX43

The effects of modulating Cx43 expression levels in fetal AM hMSCs and in adult AT hMSCs on their functional heterocellular coupling with nrCMCs were investigated by dye transfer experiments using the gap junction-permeable fluorochrome calcein red-orange AM (calcein). Cx43↑ adult AT hMSCs showed a significantly higher dye intensity than control adult AT hMSCs (67.6±4.7% vs. 8.43±1.6% of that in adjacent nrCMCs) ($P<0.001$) (Figure 3A1-A2 and C1). Furthermore, the fraction of hMSCs that took up calcein from neighboring nrCMCs was much higher for the Cx43↑ adult AT hMSCs than for the control adult AT hMSCs (71.6±7.6% vs. 28.3±4.6% of cells) ($P<0.001$) (Figure 3C3). The relative dye intensity in control fetal AM hMSCs (63.2±3.8%) was higher than in Cx43↓(1) fetal AM hMSCs (5.94±1.4%) and in Cx43↓(2) fetal AM hMSCs (6.00±1.9%) ($P<0.001$) (Figure 3B1-B3 and C2). Moreover, significantly more of the control fetal AM hMSCs (75.9±9.2%) had taken up calcein than of the Cx43↓(1) fetal AM hMSCs (13.2±2.4%) or of the Cx43↓(2) fetal AM hMSCs (13.0±2.1%) ($P<0.001$) (Figure 3C4).

To further assess functional coupling between hMSCs and nrCMCs, maximal diastolic membrane potentials (MDPs) were measured in each group of hMSCs in the absence and presence of adjacent nrCMCs. Similar average MDPs were found in hMSC monocultures (n=6) (Figure 3D, black bars). However, MDPs, on average, became more negative when nrCMCs were adjoining the hMSCs, although the degree of hyperpolarization differed between the various groups (n=8) (Figure 3D, white bars). Cx43↑ adult AT hMSCs and control fetal AM hMSCs showed the most negative MDPs (-38±4 mV and -43±5 mV, respectively). On the other hand, control adult AT hMSCs, Cx43↓(1) fetal AM hMSCs and Cx43↓(2) fetal AM hMSCs, which all contain low levels of Cx43, showed less negative MDPs.
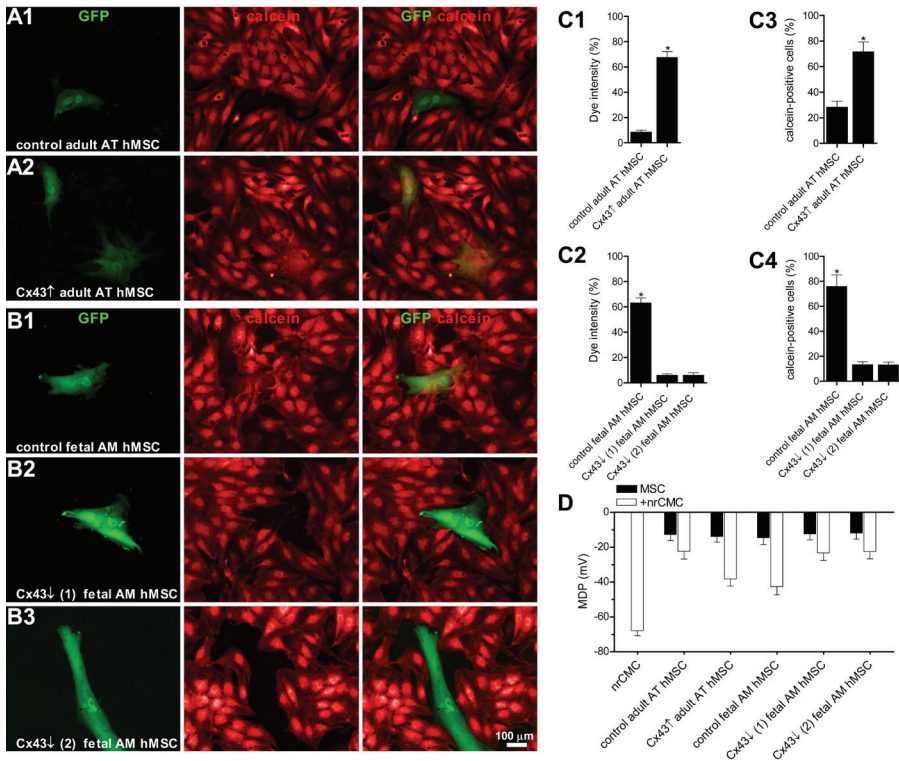
Figure 3. Study of the influence of Cx43 levels in hMSCs on their functional coupling with nrCMCs. (A1-A2) Calcein transfer from nrCMCs to Cx43↑ adult AT hMSCs was much more efficient than to control adult AT hMSCs. (B1-B3) Dye transfer from nrCMCs to fetal AM hMSCs was strongly inhibited by shRNA-mediated downregulation of Cx43 gene expression in the hMSCs. (C1-C2) Bar graphs of the quantification of dye intensity in GFP-positive hMSCs. Dye intensity in the GFP-positive hMSCs was expressed as percentage of the dye intensity in the surrounding nrCMCs. (C3-C4) Bar graphs of the assessment of the percentage of GFP-positive hMSCs that had taken up calcein from neighboring nrCMCs. *$P<0.001$ vs. control adult AT hMSC or vs. Cx43↓(1) fetal AM hMSCs and Cx43↓(2) fetal AM hMSCs. (D) Average MDPs in hMSC monocultures (indicated as MSC) as measured by whole-cell current-clamping were similar for the different experimental groups. However, the average MDP in hMSCs became more negative in the presence of adjoining nrCMCs (indicated as MSC-CMC), with Cx43↑ adult AT hMSCs and control fetal AM hMSCs reaching the most negative values.

ASSESSMENT OF CARDIOMYOGENIC DIFFERENTIATION ABILITY OF HMSCS WITH GENETICALLY ALTERED CX43 LEVELS

Human-specific immunocytological evaluation
At day 10 of co-culture with nrCMCs, 2.27±0.4% GFP/human lamin A/C-double-positive control fetal AM hMSCs were positive for the sarcomeric protein α-actinin with a cross-striated staining pattern like that of the nrCMCs (Figure 4A1-A2 and C). However, GFP/human lamin A/C-double-positive Cx43↓(1) fetal AM hMSCs and Cx43↓(2) fetal AM hMSCs did not contain detectable amounts α-actinin (Figure 4A3-A4 and C). Furthermore, neither Cx43↑ adult AT hMSCs nor control adult AT hMSCs stained positive for α-actinin (Figure 4B1-B3 and C). These results were confirmed with Cx43↑ adult AT hMSCs and control adult AT hMSCs that were transduced with LVs that encoded the puromycin-resistence gene instead of GFP (Supplemental figure 1A – B). Also, only in co-cultures of control fetal AM hMSCs with nrCMCs, some GFP-positive cells were detected to be positive for the cardiac transcription factors Nkx2.5 and GATA4 (Supplemental figure 2A1 and 3A1). In the other hMSC groups, all GFP-positive cells were negative for these cardiac transcription factors (Supplemental figure 2A2-B2 and 3A2-B2).

hMSC-specific intracellular electrophysiological measurements
To assess cardiomyogenic differentiation at a functional level, the ability of GFP-positive hMSCs to generate spontaneous action potentials was studied after gap junction uncoupling (Figure 5A-B). A fraction of the control fetal AM hMSCs showed spontaneous action potentials (n=6), with MDPs similar to those of native CMCs (n=9) (Figure 5B-C). In contrast, both Cx43↑ adult AT hMSCs and control adult AT hMSCs (n=7) showed more depolarized MDPs of -15.0±4 mV and -14.8±3 mV, respectively. Also, Cx43↑ adult AT hMSCs stayed inexcitable (n=5). Importantly, knockdown of Cx43 in fetal AM hMSCs rendered these cells incapable of generating spontaneous action potentials after 10 days of co-culture with nrCMCs (n=9 for both shRNAs) and left them with an MDP comparable to those of adult AT hMSCs (-15 mV vs. -12 and -14 mV for Cx43↓(1) fetal AM hMSCs and for Cx43↓(2) fetal AM hMSCs, respectively).
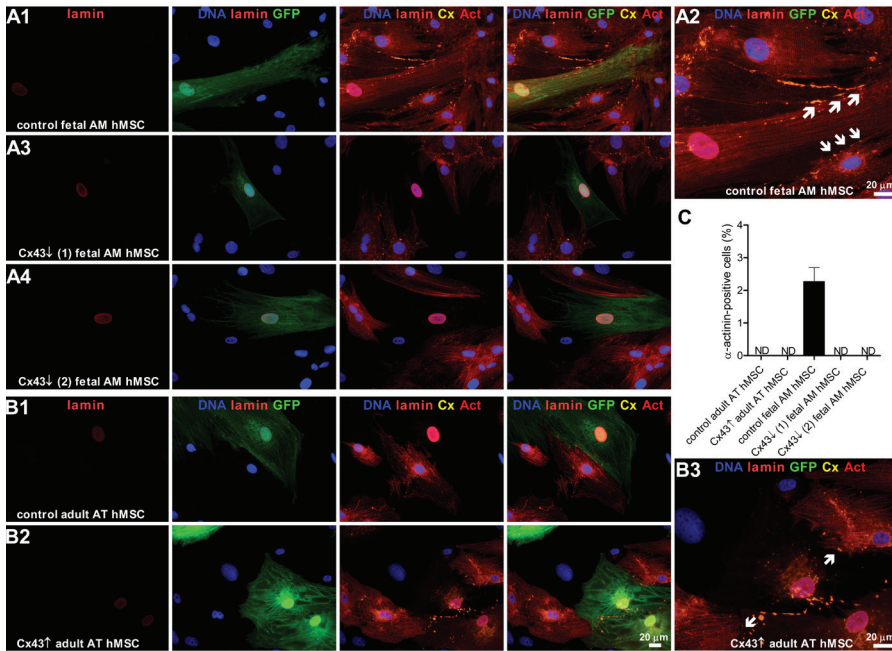
Figure 4. Immunocytological assessment of cardiomyogenic differentiation of genetically modified adult AT hMSCs and fetal AM hMSCs after 10 days of co-culture with nrCMCs. (A1) Upon co-culture with nrCMCs, a fraction of the GFP- and human lamin A/C-double-positive control fetal AM hMSCs became positive for sarcomeric α-actinin (indicated as Act). (A2) Intense punctate Cx43 (indicated as Cx) immunostaining of the interfaces between a control fetal AM hMSC and two adjacent nrCMCs (white arrows). (A3-A4, B1-B2) GFP-labeled Cx43↓(1) fetal AM hMSCs, Cx43↓(2) fetal AM hMSCs, Cx43↑ adult AT hMSCs and control adult AT hMSCs in co-culture with nrCMCs did not stain positive for α-actinin. (B3) Presence of Cx43 plaques at the interfaces between Cx43↑ adult AT hMSCs and two bordering nrCMCs (white arrows). (C) Quantitative analysis of the cardiomyogenic differentiation ability of the genetically modified hMSCs using immunopositivity for sarcomeric α-actinin as read-out. The graph is based on a minimum of 5,000 cells analyzed from 4 separate hMSC isolates per experimental group. ND is not detected.
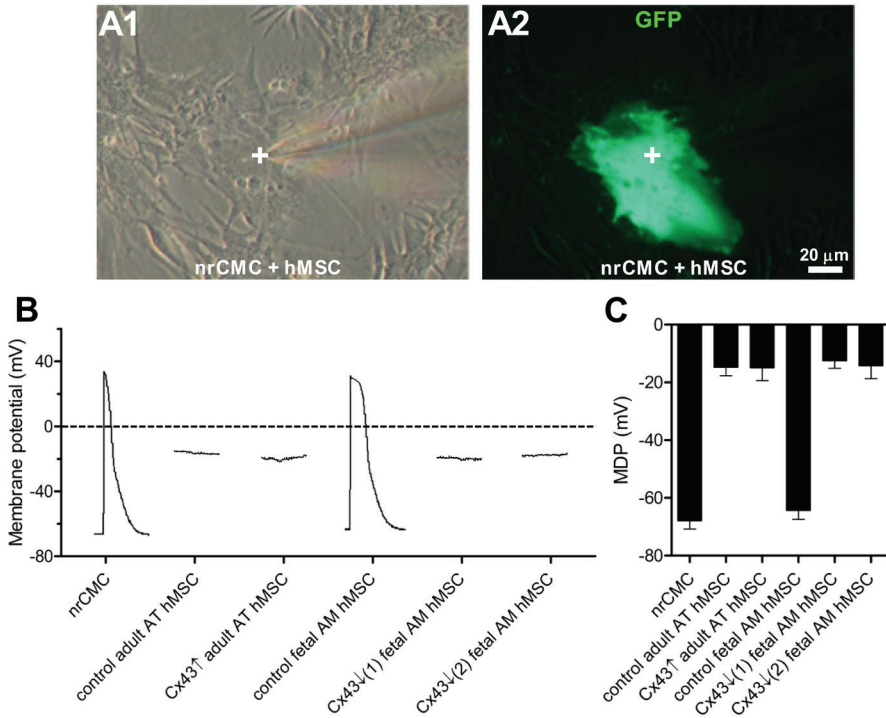
Figure 5. Electrophysiological assessment, after gap junctional uncoupling, of cardiomyogenic differentiation of hMSCs. (A1-A2) Bright field (A1) and fluorescence (A2) image of a GFP-positive hMSC with adjacent nrCMCs and patch-clamp electrode. (B) Current-clamp recordings in nrCMCs and in GFP-positive hMSCs from the different experimental groups. Action potentials were measured in nrCMCs and in some control fetal AM hMSCs, while the other cells displayed stable membrane potentials. (C) Average MDPs of nrCMCs and in the different groups of GFP-positive hMSCs. For the control fetal AM hMSCs, only the average MDP of cells showing action potentials is presented.

EVALUATION OF CX45 EXPRESSION LEVELS

To check whether the inability of Cx43↓ fetal AM hMSCs to undergo cardiomyogenic differentiation in co-cultures with nrCMCs was not caused by some off-target effect(s) of the hCx43-specific shRNAs, a rescue experiment was carried out. To this end, the Cx43↓(1) fetal AM hMSCs were transduced with an LV encoding hCx45 or with a control LV directing the synthesis of eGFP. Immunocytological analysis of the resulting cell populations showed that Cx45 was much more abundant in Cx43↓(1)+Cx45↑ fetal AM hMSCs than in Cx43↓(1)+eGFP fetal AM hMSCs (Figure 6A1-A2). Western blot analysis confirmed these results by showing 1,163±57% higher levels of Cx45 in Cx43↓(1)+Cx45↑ fetal AM hMSCs than in Cx43↓(1)+eGFP fetal AM hMSCs (n=4 for both sample types) ($P<0.001$) (Figure 6B1-B2). Consistently, qRT-PCR showed that Cx45 transcript levels were 12.5±1.9 fold higher in Cx43↓(1)+Cx45↑ fetal AM hMSCs than in Cx43↓(1)+eGFP fetal AM hMSCs ($P<0.01$) (Figure 6C).

ASSESSMENT OF FUNCTIONAL HETEROCELLULAR GAP JUNCTIONAL COUPLING VIA CX45

The extent of functional heterocellular coupling between nrCMCs and Cx43↓(1)+Cx45↑ fetal AM hMSCs or Cx43↓(1)+eGFP fetal AM hMSCs was determined in dye transfer assays. The dye intensity relative to that in neighboring nrCMCs was much higher in Cx43↓(1)+Cx45↑ fetal AM hMSCs (92.3±3.2%) than in Cx43↓(1)+eGFP fetal AM hMSCs (5.96±0.8%) ($P<0.001$) (Figure 6D1-D2 and E1). Also, the proportion of hMSCs that took up calcein from adjacent nrCMCs was ~4-fold higher for the Cx43↓(1)+Cx45↑ fetal AM hMSCs than for the Cx43↓(1)+eGFP fetal AM hMSCs (66.7±7.6% vs. 16.0±2.3%) ($P<0.001$) (Figure 6E2).

To study the impact of Cx45 overexpression on the electrophysiological properties of Cx43↓ fetal AM hMSCs, whole-cell current-clamp measurements were performed. Cx45 overexpression did not significantly alter the average MDP of Cx43↓(1) fetal AM hMSCs in monoculture (n=6) (Figure 6F). However, in co-culture with nrCMCs, Cx43↓(1)+Cx45↑ fetal AM hMSCs (n=6) showed more negative MDPs as compared to Cx43↓(1)+eGFP fetal AM hMSCs (-24.8±5 mV and -43±5 mV, respectively) (Figure 6F), indicating that electrical coupling of Cx43↓ fetal AM hMSCs with neighboring nrCMCs was enhanced by Cx45 overexpression.
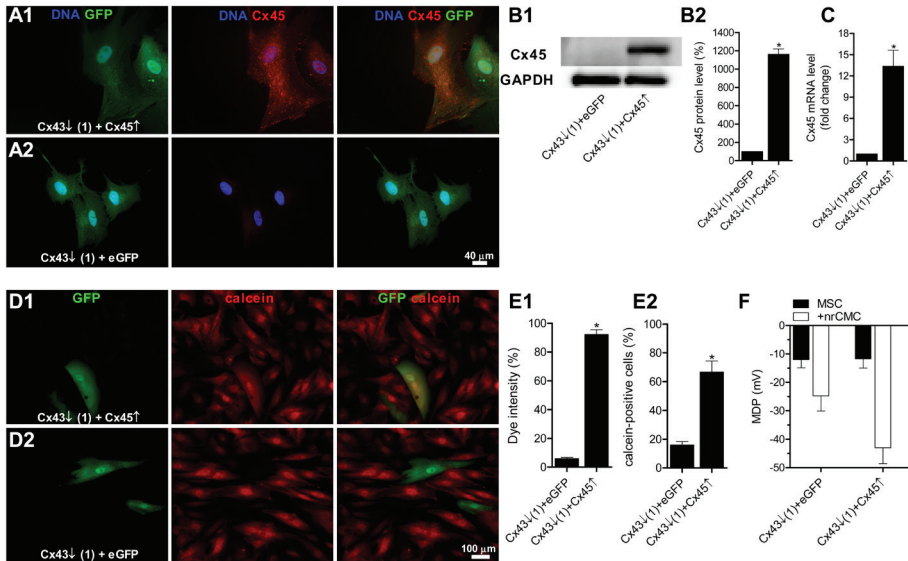
Figure 6. Assessment of Cx45 expression and functionality. (A1-A2) Immunocytological analyses showed abundant Cx45 expression in monocultures of Cx43↓(1)+Cx45↑ fetal AM hMSCs but not of Cx43↓(1)+eGFP fetal AM hMSCs. A part of the Cx45 signal was detected at the interfaces between Cx43↓(1)+Cx45↑ fetal AM hMSCs. Nuclei were stained with Hoechst 33342. (B1) Representative picture of a western blot confirming high-level expression of Cx45 in Cx43↓(1)+Cx45↑ fetal AM hMSCs and the presence of very low amounts of Cx45 in Cx43↓(1)+eGFP fetal AM hMSCs. The GAPDH-specific immunostaining was included for normalization purposes. (B2) Bar graph of the assessment by western blotting of Cx45 levels in Cx43↓(1)+Cx45↑ fetal AM hMSCs and in Cx43↓(1)+eGFP fetal AM hMSCs corrected for differences in GAPDH expression. *$P<0.001$ vs. Cx43↓(1)+eGFP fetal AM hMSCs. (C) Bar graph of the quantification by qRT-PCR of Cx45 mRNA levels in Cx43↓(1)+Cx45↑ fetal AM hMSCs and in Cx43↓(1)+eGFP fetal AM hMSCs. *$P<0.01$ vs. Cx43↓(1)+eGFP fetal AM hMSCs. (D1-D2) Cx43↓(1)+Cx45↑ fetal AM hMSCs much more readily take up calcein from adjacent nrCMCs than Cx43↓(1)+eGFP fetal AM hMSCs. (E1) Quantitative analysis of the dye intensity in Cx43↓(1)+Cx45↑ fetal AM hMSCs and in Cx43↓(1)+eGFP fetal AM hMSCs. Dye intensity in GFP-positive hMSCs was expressed as percentage of the dye intensity in the surrounding nrCMCs. (E2) Bar graph of the assessment of the percentage GFP-positive hMSCs that had taken up calcein from neighboring nrCMCs. *$P<0.001$ vs. Cx43↓(1)+eGFP fetal AM hMSCs. (F) The average MDPs of Cx43↓(1)+Cx45↑ fetal AM hMSCs and of Cx43↓(1)+eGFP fetal AM hMSCs in monocultures are less negative than in co-cultures with nrCMCs. The effect of adjacent nrCMCs on the average MDP was bigger for fetal AM hMSCs in which the knockdown of Cx43 expression was compensated by Cx45 overexpression than for Cx43↓(1)+eGFP fetal AM hMSCs.
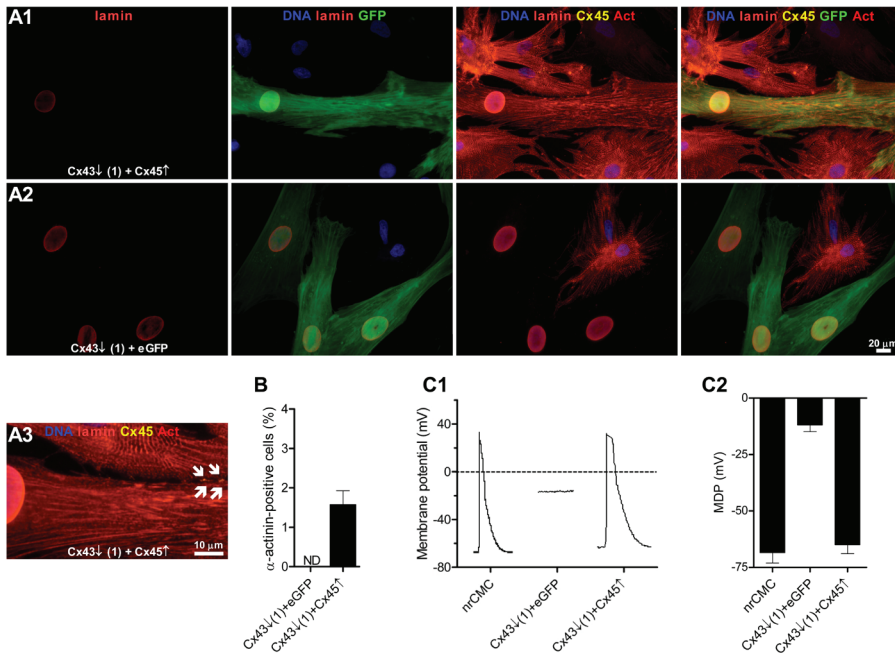
Figure 7. Investigation by immunocytological and patch-clamp analysis of cardiomyogenic differentiation of fetal AM hMSCs in co-culture with nrCMCs after rescue of Cx43 knockdown by Cx45 overexpression. In the presence of nrCMCs, a fraction of the GFP- and human lamin A/C-double-positive Cx43↓(1)+Cx45↑ fetal AM hMSCs (A1) expressed α-actinin (indicated as Act) in a striated pattern typical of sarcomeric proteins, while Cx43↓(1)+eGFP fetal AM hMSCs (A2) did not. (A3) Punctate Cx45 immunostaining of the interface between a Cx43↓(1)+Cx45↑ fetal AM hMSC and an adjacent nrCMC (white arrows). (B) Quantitative analysis of the cardiomyogenic differentiation capacity of Cx43↓(1)+Cx45↑ fetal AM hMSCs and of Cx43↓(1)+eGFP fetal AM hMSCs using immunopositivity for sarcomeric α-actinin as read-out. The graph is based on a minimum of 5,000 cells analyzed from 4 separate hMSC isolates per experimental group. ND is not detected. (C1) Current-clamp recordings in pharmacologically uncoupled co-cultures of nrCMCs and Cx43↓(1)+eGFP fetal AM hMSCs or Cx43↓(1)+Cx45↑ fetal AM hMSCs. Fetal AM hMSCs that had lost the capacity to produce action potentials due to knockdown of Cx43 expression regained this ability following forced Cx45 expression but not after eGFP overexpression. (C2) Average MDPs of nrCMCs, Cx43↓(1)+eGFP fetal AM hMSCs and Cx43↓(1)+Cx45↑ fetal AM hMSCs. For the Cx43↓(1)+Cx45↑ fetal AM hMSCs, only the average MDP of cells showing action potentials is presented.

ASSESSMENT OF CARDIOMYOGENIC DIFFERENTIATION ABILITY OF FETAL AM HMSCS AFTER RESCUE OF CX43 KNOCKDOWN BY CX45 OVEREXPRESSION

Human-specific immunocytological evaluation
Ten days after co-incubation with nrCMCs, Cx43↓(1)+Cx45↑ fetal AM hMSCs and Cx43↓(1)+eGFP fetal AM hMSCs were analyzed for α-actinin positivity. While Cx43↓(1)+eGFP fetal AM hMSCs did not contain detectable amounts of α-actinin, 1.57±0.4% (n=2,500) GFP/human lamin A/C-double-positive Cx43↓(1)+Cx45↑ fetal AM hMSCs stained positive for this sarcomeric protein indicating that these human cells had differentiated into CMCs (Figure 7A1-A2 and B). Furthermore, only in co-cultures of Cx43↓(1)+Cx45↑ fetal AM hMSCs with nrCMCs, GFP-positive cells were detected that were positive for the cardiac transcription factors Nkx2.5 and GATA4 (Supplemental figure 4A1-B1). Cx43↓(1)+eGFP fetal AM hMSCs in co-culture with nrCMCs did not stain positive for these transcription factors (Supplemental figure 4A2-4B2).

hMSC-specific intracellular electrophysiological measurements
To further study the cardiomyogenic differentiation capacity of Cx43↓(1)+Cx45↑ fetal AM hMSCs, these cells were subjected to whole-cell current-clamp measurements following pharmacological uncoupling. Cx43↓(1)+eGFP fetal AM hMSCs (n=5) showed steady membrane potentials, while some of the Cx43↓(1)+Cx45↑ fetal AM hMSCs (n=5) produced spontaneous action potentials with MDPs comparable to those of nrCMCs (n=7) (-65±4 mV and -69±5 mV, respectively) (Figure 7C1-C2). Thus, the loss of excitability in Cx43↓(1) fetal AM hMSCs could be overcome by Cx45 overexpression, at least in a subpopulation of cells.

DISCUSSION

The key findings of this study are 1) Fetal hMSCs, which intrinsically express Cx43 at high levels, efficiently communicate with adjacent nrCMCs via gap junctions and can differentiate into functional heart muscle cells when co-cultured with nrCMCs. 2) Adult hMSCs that contain low amounts of Cx43 by nature do not undergo cardiomyogenic differentiation in co-culture with nrCMCs. 3) Overexpression of Cx43 in adult hMSCs does not lead to their cardiomyogenic differentiation upon co-culture with nrCMCs. 4) Cardiomyogenic differentiation of fetal hMSCs in co-culture with nrCMCs is inhibited by Cx43 knockdown, but is rescued by concurrent overexpression of Cx45.

GAP JUNCTIONS AND HMSCS

The expression of the three major cardiac Cx (i.e. Cx40, Cx43 and Cx45) genes by hMSCs has previously been demonstrated.[22,23] Also, the formation of functional gap junctions, important for integration of donor cells with the surrounding myocardium after cardiac stem cell therapy, has been shown to occur.[9,22,23] Recently, our group showed that hMSCs derived from fetal tissues contain much higher levels of Cx43 than those derived from adult tissues.[19] In addition, evidence was provided that hMSCs of embryonic or fetal origin can undergo cardiomyogenesis when co-cultured with nrCMCs while hMSCs derived from adult sources fail to do so. To directly investigate the role of gap junctional coupling in cardiomyogenic differentiation of hMSCs, in the present study, Cx43 expression was downregulated in fetal AM hMSCs and upregulated in adult AT hMSCs through LV gene transfer. These genetic interventions resulted in a strong reduction in gap junctional communication between fetal AM hMSCs and nrCMCs and led to a substantial increase in the gap junctional coupling between adult AT hMSCs and nrCMCs. In addition, it was investigated whether the effects of Cx43 knockdown could be reversed by Cx45 overexpression. The reason to choose Cx45 for this purpose was that it can be engaged in the formation of functional homotypic as well as heterotypic gap junctions composed of homomeric or heteromeric connexins.[24-27] In the current study, it was indeed established that after transduction with a Cx45-encoding LV, Cx43↓(1) fetal AM hMSCs express high levels of Cx45 mRNA leading to rescue of their efficient gap junctional communication with nrCMCs.

ROLE OF GAP JUNCTIONAL COMMUNICATION IN CARDIOMYOGENIC DIFFERENTIATION

Connexins have been reported to be involved in differentiation processes such as osteogenesis, neural differentiation and hematopoiesis.[28-32] However, little is known about the role of gap junctional communication in cardiomyogenic differentiation. As already stated above, our group recently found that fetal AM hMSCs express Cx43 at high levels in contrast to adult AT hMSCs. Interestingly, these fetal AM hMSCs were able to differentiate, in co-culture with nrCMCs, into functional CMCs while adult AT hMSCs were not.[19] Other investigators using co-cultures with CMCs to induce cardiomyogenic differentiation in stem cells have also proposed that intercellular communication through gap junctions might be essential in this differentiation process.[33,34] However, the role of gap junctional communication in the transfer of cardiomyogenic signals from CMCs to other cell types has not yet been investigated. In the current study, the role of Cx43 in cardiomyogenic differentiation of hMSCs in the presence of neighboring CMCs was further elucidated. Fetal AM hMSCs lost their ability to differentiate into functional CMCs after knockdown of Cx43 gene expression. However, not only did overexpression of Cx45 restore the ability of these hMSCs to form functional gap junctions with nrCMCs but it also

rescued the cardiomyogenic differentiation capacity of these fetal hMSCs upon co-incubation with nrCMCs. In contrast to these findings, adult AT hMSCs did not gain the ability to differentiate into functional CMCs after overexpression of Cx43. The inability of adult AT hMSCs to undergo cardiomyogenesis following co-culture with nrCMCs could have an epigenetic explanation.[35-37] According to this hypothesis, genes important for cardiomyogenic differentiation could, in adult AT hMSCs, exist in a transcriptionally repressive state imposed by specific DNA methylation patterns and/or chromatin signatures. Also, qualitative and/or quantitative differences in the repertoire of transcription factors and miRs expressed by fetal AM hMSCs and by adult AT hMSCs might contribute to their differential responsiveness to cardiomyogenic signals produced by neighboring nrCMCs.[38,39]

Since gap junctions enable intercellular communication, induction of cardiomyogenesis after co-incubation with nrCMCs may be caused by exchange of signals between nrCMCs and fetal hMSCs. Stimulation of cardiomyogenic differentiation by miRs-499, as previously described, has been inferred to be a gap junction-mediated process.[11] Moreover, intercellular communication makes $[Ca^{2+}]$ oscillations possible, which has been shown to increase the regenerative potential of human cardiac progenitor cells in a mouse myocardial infarction model.[40] In line with these findings are the observations by Muller-Borer et al. who found that in co-culture with nrCMCs rat liver stem cells obtain CMC-like properties and display $[Ca^{2+}]$ oscillations synchronous with those of adjoining CMCs. The $[Ca^{2+}]$ oscillations in the liver stem cells were dependent on gap junctional communication with neighboring CMCs and their inhibition led to a decrease in the expression of CMC-specific genes by the liver stem cells.[34] The recent observation that hyperpolarization is sufficient to induce cardiomyogenic differentiation of human CMC progenitor cells underlines the importance of gap junctional coupling in this process.[12] In the current study, fetal AM hMSCs in co-culture with nrCMCs were hyperpolarized in contrast to those that were transduced with hCx43-specific shRNAs. More importantly, Cx43↓(1) fetal AM hMSCs were also hyperpolarized in co-culture with nrCMCs after overexpression of Cx45. As a matter of fact, the average MDPs of control fetal AM hMSCs and Cx43↓(1)+Cx45↑ fetal AM hMSCs in contact with nrCMCs were identical. This could explain why knockdown of Cx43 leads to an inability of fetal AM hMSCs to differentiate towards functional CMCs, while after subsequent Cx45 overexpression their cardiomyogenic differentiation potential was restored. So while the precise composition of the gap junctions involved in the restoration of the cardiomyogenic differentiation capacity in Cx43↓(1) fetal hMSCs following Cx45 overexpression remains elusive, the factor(s) that exert their cardiomyogenic effects on fetal AM hMSCs via gap junctions can pass Cx45-containing channels in high enough amounts to set off the cardiomyogenic differentiation of these cells.

CONCLUSIONS

The results of this study indicate that efficient gap junctional coupling with adjacent CMCs is essential to induce cardiomyogenic differentiation of naturally Cx43-rich fetal hMSCs in co-culture with nrCMCs. However, adult AT hMSCs that contain relatively low intrinsic levels of Cx43 and do not undergo cardiomyogenesis in the presence of nrCMCs, cannot be endowed with cardiomyogenic differentiation ability by overexpression of Cx43.

LIMITATION

It would have been of interest to conduct Cx43 knockdown experiments using a cell type with a higher propensity to differentiate into functional CMCs than fetal hMSCs. However, such a cell type was not available to us. Furthermore, it would have been clinically more relevant to co-culture different hMSC subtypes with adult human CMCs, but obtaining these cells in the numbers needed to conduct these experiments was impossible. Also, adult human CMCs cannot be maintained ex vivo long enough in a differentiated state to perform some of the key experiments described in this paper.

FUNDING

102

REFERENCES

1.   Maeda S, Tsukihara T. Structure of the gap junction channel and its implications for its biological functions. Cell Mol Life Sci 2011;68:1115-1129.

2.   Levin M. Gap junctional communication in morphogenesis. Prog Biophys Mol Biol 2007;94:186-206.

3.   Kumai M, Nishii K, Nakamura K et al. Loss of connexin45 causes a cushion defect in early cardiogenesis. Development 2000;127:3501-3512.

4.   Reaume AG, de Sousa PA, Kulkarni S et al. Cardiac malformation in neonatal mice lacking connexin43. Science 1995;267:1831-1834.

5.   Kirchhoff S, Kim JS, Hagendorff A et al. Abnormal cardiac conduction and morphogenesis in connexin40 and connexin43 double-deficient mice. Circ Res 2000;87:399-405.

6.   Gu H, Smith FC, Taffet SM et al. High incidence of cardiac malformations in connexin40-deficient mice. Circ Res 2003;93:201-206.

7.   Chi NC, Bussen M, Brand-Arzamendi K et al. Cardiac conduction is required to preserve cardiac chamber morphology. Proc Natl Acad Sci U S A 2010;107:14662-14667.

8.   Abraham MR, Henrikson CA, Tung L et al. Antiarrhythmic engineering of skeletal myoblasts for cardiac transplantation. Circ Res 2005;97:159-167.

9.   Roell W, Lewalter T, Sasse P et al. Engraftment of connexin 43-expressing cells prevents post-infarct arrhythmia. Nature 2007;450:819-824.

10.   Coppen SR, Fukushima S, Shintani Y et al. A factor underlying late-phase arrhythmogenicity after cell therapy to the heart: global downregulation of connexin43 in the host myocardium after skeletal myoblast transplantation. Circulation 2008;118:S138-S144.

11.   Hosoda T, Zheng H, Cabral-da-Silva M et al. Human cardiac stem cell differentiation is regulated by a mircrine mechanism. Circulation 2011;123:1287-1296.

12.   van Vliet P, de Boer TP, van der Heyden MA et al. Hyperpolarization induces differentiation in human cardiomyocyte progenitor cells. Stem Cell Rev 2010;6:178-185.

13.   Gerson SL. Mesenchymal stem cells: no longer second class marrow citizens. Nat Med 1999;5:262-264.

14.   Prockop DJ. Marrow stromal cells as stem cells for nonhematopoietic tissues. Science 1997;276:71-74.

15.   Choi YH, Kurtz A, Stamm C. Mesenchymal stem cells for cardiac cell therapy. Hum Gene Ther 2011;22:3-17.

16.   Pijnappels DA, Schalij MJ, Atsma DE. Response to the letter by Rose et al. Circ Res 2009;104:e8.

17.   Quevedo HC, Hatzistergos KE, Oskouei BN et al. Allogeneic mesenchymal stem cells restore cardiac function in chronic ischemic cardiomyopathy via trilineage differentiating capacity. Proc Natl Acad Sci U S A 2009;106:14022-14027.

18.   Rose RA, Jiang H, Wang X et al. Bone marrow-derived mesenchymal stromal cells express cardiac-specific markers, retain the stromal phenotype, and do not become functional cardiomyocytes in vitro. Stem Cells 2008;26:2884-2892.

19.   Ramkisoensing AA, Pijnappels DA, Askar SF et al. Human Embryonic and Fetal Mesenchymal Stem Cells Differentiate toward Three Different Cardiac Lineages in Contrast to Their Adult Counterparts. PLoS One 2011;6:e24164.

20.   Pijnappels DA, Schalij MJ, Ramkisoensing AA et al. Forced alignment of mesenchymal stem cells undergoing cardiomyogenic differentiation affects functional integration with cardiomyocyte cultures. Circ Res 2008;103:167-176.

21.   Swildens J, de Vries AA, Li Z et al. Integrin stimulation favors uptake of macromolecules by cardiomyocytes in vitro. Cell Physiol Biochem 2010;26:999-1010.

22. Valiunas V, Doronin S, Valiuniene L et al. Human mesenchymal stem cells make cardiac connexins and form functional gap junctions. J Physiol 2004;555:617-626.

23. Pijnappels DA, Schalij MJ, van Tuyn J et al. Progressive increase in conduction velocity across human mesenchymal stem cells is mediated by enhanced electrical coupling. Cardiovasc Res 2006;72:282-291.

24. Rackauskas M, Kreuzberg MM, Pranevicius M et al. Gating properties of heterotypic gap junction channels formed of connexins 40, 43, and 45. Biophys J 2007;92:1952-1965.

25. Schulte JS, Scheffler A, Rojas-Gomez D et al. Neonatal rat cardiomyocytes show characteristics of nonhomotypic gap junction channels. Cell Commun Adhes 2008;15:13-25.

26. Darrow BJ, Laing JG, Lampe PD et al. Expression of multiple connexins in cultured neonatal rat ventricular myocytes. Circ Res 1995;76:381-387.

27. Kwak BR, van Kempen MJ, Theveniau-Ruissy M et al. Connexin expression in cultured neonatal rat myocytes reflects the pattern of the intact ventricle. Cardiovasc Res 1999;44:370-380.

28. Yang SR, Cho SD, Ahn NS et al. Role of gap junctional intercellular communication (GJIC) through p38 and ERK1/2 pathway in the differentiation of rat neuronal stem cells. J Vet Med Sci 2005;67:291-294.

29. Montecino-Rodriguez E, Leathers H, Dorshkind K. Expression of connexin 43 (Cx43) is critical for normal hematopoiesis. Blood 2000;96:917-924.

30. Villars F, Guillotin B, Amedee T et al. Effect of HUVEC on human osteoprogenitor cell differentiation needs heterotypic gap junction communication. Am J Physiol Cell Physiol 2002;282:C775-C785.

31. Wong RC, Pera MF, Pebay A. Role of gap junctions in embryonic and somatic stem cells. Stem Cell Rev 2008;4:283-292.

32. Rossello RA, Wang Z, Kizana E et al. Connexin 43 as a signaling platform for increasing the volume and spatial distribution of regenerated tissue. Proc Natl Acad Sci U S A 2009;106:13219-13224.

33. Xu M, Wani M, Dai YS et al. Differentiation of bone marrow stromal cells into the cardiac phenotype requires intercellular communication with myocytes. Circulation 2004;110:2658-2665.

34. Muller-Borer BJ, Cascio WE, Esch GL et al. Mechanisms controlling the acquisition of a cardiac phenotype by liver stem cells. Proc Natl Acad Sci U S A 2007;104:3877-3882.

35. De Carvalho DD, You JS, Jones PA. DNA methylation and cellular reprogramming. Trends Cell Biol 2010;20:609-617.

36. Fisher CL, Fisher AG. Chromatin states in pluripotent, differentiated, and reprogrammed cells. Curr Opin Genet Dev 2011;21:140-146.

37. Goldberg AD, Allis CD, Bernstein E. Epigenetics: a landscape takes shape. Cell 2007;128:635-638.

38. Aranda P, Agirre X, Ballestar E et al. Epigenetic signatures associated with different levels of differentiation potential in human stem cells. PLoS One 2009;4:e7809.

39. Jansen BJ, Gilissen C, Roelofs H et al. Functional differences between mesenchymal stem cell populations are reflected by their transcriptome. Stem Cells Dev 2010;19:481-490.

40. Ferreira-Martins J, Rondon-Clavo C, Tugal D et al. Spontaneous calcium oscillations regulate human cardiac progenitor cell growth. Circ Res 2009;105:764-774.

SUPPLEMENTAL MATERIALS AND METHODS

ISOLATION, CULTURE AND CHARACTERIZATION OF HUMAN MESENCHYMAL STEM CELLS (HMSCS)

All investigations with human-derived tissues conformed to the Declaration of Helsinki and were approved by the Medical Ethics Committee of the Leiden University Medical Centre (LUMC). Written informed consent was obtained from all subjects or, in case of the fetal material, from the parents of the fetuses.

Human fetal amniotic membranes were collected from placentas at gestational weeks 17-22 through legal interventions by the Department of Obstetrics. The membranes were washed twice with phosphate-buffered saline (PBS) and finely minced into 1-2 mm fragments using scissors and scalpels. Cells were dissociated by treatment with 0.1% collagenase type I (Worthington, Lakewood, NJ) for 3 h at 37°C in a humidified 95% air/5% CO_2 atmosphere. Thereafter, 10 mL of Dulbecco's modified Eagle's medium (DMEM) containing 10% fetal bovine serum (FBS), 100 U/mL penicillin and 100 µg/mL streptomycin (all from Invitrogen, Breda, the Netherlands; hereinafter referred to as MSC medium) was added. The cell suspension was transferred to a 25-cm² culture flask (Becton Dickinson, Franklin Lakes, NJ) and incubated for 3-4 days at 37°C in a humidified atmosphere of 95% air/5% CO_2 to allow the cells to adhere. The MSC medium was replaced twice a week until the primary cultures had reached ±80% confluency, after which the fetal amniotic membrane (AM) hMSCs were amplified by serial passage using a buffered 0.05% trypsin-0.02% EDTA solution (TE; Lonza Vervier, Vervier, Belgium) for cell detachment.

Adult adipose tissue (AT) hMSCs were derived from subcutaneous abdominal fat tissue (n=4 donors, mean donor age 42.5±5.4 yrs). Tissue samples were washed twice with PBS containing 100 U/mL penicillin and 100 µg/mL streptomycin and finely minced with a scissor. For tissue disruption 0.1% collagenase type I solution was added and the samples were incubated for 1 h at 37°C in a humidified incubator containing 95% air and 5% CO_2. Collagenase type I activity was quenched by adding MSC medium. Samples were then centrifuged at 330×g for 10 min. After centrifugation the top layer of primary adipocytes was removed and the collagenase type I-containing solution was aspirated. The cell pellet was suspended in MSC medium, passed through a nylon cell strainer with a mesh pore size of 70 µm (Becton Dickinson) and the cells were once again collected by centrifugation. The latter procedure was repeated twice, after which the cell pellet was resuspended in 8 ml MSC medium. The resulting cell suspension was transferred to a 75-cm² culture flask (Becton Dickinson) and the adult AT hMSCs were expanded by serial passage using standard methods.

The isolated cells were characterized according to generally accepted criteria using flow cytometry for the detection of surface antigens and adipogenic and osteogenic differentiation assays to establish multipotency. Surface marker expression was examined after culturing the cells for at least 3 passages. Thereafter, the hMSCs were detached using TE, suspended in PBS containing 1% bovine serum albumin fraction V (BSA; Sigma-Aldrich Chemie, Zwijndrecht, the Netherlands) and divided in aliquots of 10^5 cells. Cells were then incubated for 30 min at 4°C with fluorescein isothiocyanate- or phycoerythrin-conjugated monoclonal antibodies (MAbs) directed against human CD105 (Ancell, Bayport, MN), CD90, CD73, CD45, CD34 or CD31 (all from Becton Dickinson). Labeled cells were washed three times with PBS containing 1% BSA and analyzed using a BD LSR II flow cytometer (Becton Dickinson). Isotype-matched control MAbs (Becton Dickinson) were used to determine background fluorescence. At least 10^4 cells per sample were acquired and data were processed using FACSDiva software (Becton Dickinson).

Established differentiation assays were used to determine the adipogenic and osteogenic differentiation ability of the cells.[1] Briefly, 5×10^3 hMSCs per well were plated in a 12-well culture plate (Corning Life Sciences, Amsterdam, the Netherlands) and exposed to adipogenic or osteogenic differentiation medium. Adipogenic differentiation medium consisted of MEM-plus (i.e. α-minimum essential medium [Invitrogen] containing 10% FBS, 100 U/mL penicillin and 100 μg/mL streptomycin) supplemented with insulin, dexamethason, indomethacin and 3-isobutyl-1-methylxanthine (all from Sigma-Aldrich Chemie) to final concentrations of 5 μg/mL, 1 μM, 50 μmol/L and 0.5 μmol/L, respectively, and was refreshed every 3-4 days for a period of 3 weeks. Lipid accumulation was assessed by Oil Red O (Sigma-Aldrich Chemie) staining of the cultures (15 mg of Oil Red O per mL of 60% 2-propanol). Osteogenic differentiation medium consisted of MEM-plus containing 10 mmol/L b-glycerophosphate, 50 μg/mL ascorbic acid and 10 nmol/L dexamethason (all from Sigma-Aldrich Chemie) and was refreshed every 3-4 days for a period of 3 weeks. Afterwards, the cells were washed with PBS and calcium deposits were visualized by staining of the cells for 5 min with 2% Alizarin Red S (Sigma-Aldrich Chemie) in 0.5% NH_4OH (pH 5.5).

ISOLATION AND CULTURE OF NEONATAL RAT CARDIOMYOCYTES AND CARDIAC FIBROBLASTS

All animal experiments were approved by the Animal Ethics Committee of the LUMC and conformed to the Guide for the Care and Use of Laboratory Animals, as stated by the US National Institutes of Health (permit number: 10236).[2]

Primary myocardial cells were dissociated from ventricles of 2-day-old male Wistar rats. Neonatal rat cardiomyocytes (nrCMCs) and cardiac fibroblasts (nrCFBs) were separated from each other by differential plating and maintained

in a 1:1 (v/v) mixture of DMEM and Ham's F-10 medium (MP Biomedicals, Solon, OH) containing 5% horse serum (Invitrogen), 100 U/mL penicillin and 100 µg/mL streptomycin as previously described.[3]

Myocardial cells were plated on fibronectin (Sigma-Aldrich Chemie)-coated coverslips (15 mm Ø) at a density of 2×10^5 cells per well in 12-well plates and incubated at 37°C in a humidified incubator containing 95% air and 5% CO_2. Proliferation of residual nrCFBs in nrCMC cultures was inhibited by incubating the cells with 10 mg/mL mitomycin-C (Sigma-Aldrich Chemie) in PBS for 1 h.[4]

Production of lentiviral vectors

Two self-inactivating (SIN) lentiviral vector (LV) shuttle plasmids encoding short hairpin (sh) RNAs targeting the human connexin 43 (hCx43) gene (i.e. TRCN0000059773 and TRCN0000059775) were selected from the Mission Library (Sigma-Aldrich Chemie). The shRNAs encoded by these constructs efficiently inhibit hCx43 expression in hMSCs as assessed by western blotting and contain sense strands that differ at 3 positions from the coding sequence of the rat Cx43 gene. As negative control, a SIN-LV shuttle plasmid directing the synthesis of an enhanced green fluorescent protein (eGFP) gene-specific shRNA (SHC005; Sigma-Aldrich Chemie) was used. To allow for the easy assessment of transduction efficiencies, the puromycin N-acetyl transferase-coding sequence in each of these constructs was replaced by that of version I of the green fluorescent protein of *Renilla reniformis* (hrGFPI) as previously described.[5] The resulting SIN-LV shuttle plasmids were designated pLV.shRNA-hCx43.1.hPGK1.hrGFPI, pLV.shRNA-hCx43.2.hPGK1.hrGFPI and pLV.shRNA-eGFP.hPGK1.hrGFPI, respectively.

Overexpression of hCx43 or hCx45 in hMSCs was accomplished using bicistronic SIN-LVs. The shuttle plasmids for generating these SIN-LVs were made as follows. First, pIRES.hrGFPII (Stratagene/Agilent Technologies, Santa Clara, CA) was digested with HincII and XbaI and the 2.1-kb fragment containing the human cytomegalovirus immediate-early gene promoter, the internal ribosome entry site of encephalomyocarditis virus and the hrGFP version II open reading frame was combined with the 6.1-kb SmaI×XbaI fragment of pLV.MCS.WHVPRE (GenBank accession number: JN622008) to create pLV.hCMV-IE.IRES.hrGFPII.WHVPRE. Next, the hCx43- and hCx45-coding sequences were released from Mammalian Gene Collection clones IRATp970C0822D and IRAMp995E152Q (Source BioScience, LifeSciences, Nottingham, United Kingdom) by restriction enzyme digestion using EcoRI (hCx45) or CfrI and MunI (hCx43). After treatment with the Klenow fragment of DNA polymerase I, the resulting hCx43- and hCx45-coding fragments of 1.3 and 1.2 kb, respectively, were combined with the 8.3-kb Eco32I fragment of pLV.hCMV.IRES.hrGFPII.WHVPRE using T4 DNA ligase to create pLV.hCMV-IE.hCx43.IRES.hrGFPII.WHVPRE and pLV.hCMV-IE.hCx45.IRES.hrGFPII.WHVPRE.

As negative control the original SIN-LV shuttle plasmid pLV.hCMV-IE.IRES.hrGFPII. WHVPRE was used. All restriction and DNA modifying enzymes were obtained from Fermentas (St. Leon-Rot, Germany).

Ligation mixtures were introduced in chemocompetent GeneHogs cells (Invitrogen) and large stocks of the correct plasmids were prepared with the aid of the JETSTAR 2.0. Plasmid Maxiprep Kit (Genomed, Löhne, Germany).

Vesicular stomatitis virus G-protein-pseudotyped SIN human immunodeficiency virus type I vectors were produced in 175-cm^2 culture flasks (Greiner Bio-One, Alphen a/d Rijn, the Netherlands) seeded with 10^5 293T cells per cm^2 in DMEM supplemented with 10% FBS and 0.01 mmol/L cholesterol. The next day, the producer cells in each flask were transfected with a total of 35 µg of DNA at a 2:1:1 molar ratio of 1) one of the SIN-LV shuttle plasmids, 2) psPAX2 (Addgene, Cambridge, MA) and 3) pLP/VSVG (Invitrogen) using 3 µg of polyethyleneimine (Polysciences Europe, Eppelheim, Germany) per µg of DNA as transfection agent. Sixteen hours later, the transfection medium in each flask was replaced by 15 ml of DMEM containing 5% FBS, 10 mmol/L HEPES-NaOH (pH 7.4) and 0.01 mmol/L cholesterol. At 64 h post-transfection, the culture fluid was collected and freed of cellular debris by centrifugation at room temperature for 10 min at 825×g and filtration through a 0.45-µm pore-size cellulose acetate filter (Pall Corporation, East Hills, NY). To concentrate the SIN-LV particles, 5 ml of 20% (w/v) sucrose in PBS was carefully layered under 30 ml of the cleared culture medium, which was then centrifuged for 2 h at 15,000 rounds per min and 10°C in an SW28 rotor (Beckman Coulter, Fullerton, CA). Next, the supernatant was discarded and the pellet containing the SIN-LV particles was suspended in 500 µl of PBS-1% BSA by gentle rocking overnight at 4°C.

The gene transfer activity of the SIN-LV stocks was determined by end-point titration on HeLa indicator cells using flow cytometric analysis of hrGFPI or hrGFPII expression as read-out. The titers of the SIN-LV preparations are thus expressed in HeLa cell-transducing units (HTUs) per ml.

Overexpression of hCx43 was also established by a SIN-LV shuttle plasmid pLV. hCMV-IE.hCx43.IRES.PurR.hHBVPRE. This SIN-LV shuttle plasmid was constructed using a PCR-based cloning procedure. The hCx43-coding sequence was amplified by high-fidelity PCR from pLV.hCMV-IE.hCx43.IRES.hrGFPII.WHVPRE in 30 cycles using the primers 5' atacgcgttaacatgggtgactggagc 3' and 5' cgtgtacagttaacttagatctccaggtcatcagg 3' (Eurofins MWG Operon, Ebersberg, Germany), Bioline's VELOCITY DNA polymerase (GC biotech, Alphen aan den Rijn, the Netherlands) and the standard reaction conditions, including an annealing temperature of 55°C, recommended by the supplier. The 1175-bp PCR product was purified using Sure-Clean (Bioline), incubated with the restriction enzymes MluI and Bsp1407I (both from Fermentas) and the 1.2-kb digestion product was extracted from agarose gel

using JetSorb Gel Extraction Kit (GENOMED). Finally, the hCx43-coding DNA fragment was combined with the 8.2-kb MluI× Bsp1407I fragment of pLV.CMV.IRES.PURO[6] to generate pLV.hCMV-IE.hCx43.IRES.PurR.hHBVPRE. This SIN-LV shuttle plasmid was subsequently used for the production of SIN-LV vector particles as described above.

TRANSDUCTION OF HMSCS

hMSCs were seeded at a density of 2×10^4 cells per well in 6-well plates (Corning) and incubated overnight in a humidified 95% air/5% CO_2 atmosphere. Next, the culture fluid was replaced by 1 ml per well of fresh MSC medium supplemented with 10 μg/ml diethylaminoethyl-dextran sulfate (GE Healthcare, Leiderdorp, the Netherlands) and 20 HTUs per cell of SIN-LV. After an incubation period of 4 h at 37°C in a humidified atmosphere of 5% CO_2 in air, the cells were washed with PBS, cultured in MSC medium and passaged ≥2 times before being used in any of the co-culture experiments. AT hMSCs were transduced with LV.hCMV-IE.hCx43.IRES.hrGFPII.WHVPRE or pLV.hCMV-IE.hCx43.IRES.PurR.hHBVPRE to overexpress Cx43 (Cx43↑ adult AT hMSCs), while cells exposed to LV.hCMV-IE.IRES.hrGFPII.WHVPRE or pLV.CMV.IRES.PURO served as control (control adult AT hMSCs). Adult AT hMSCs transduced with LVs encoding for the puromycin-resistence gene, were cultured in MSC medium supplemented with 5 ug/mL puromycin (Sigma-Aldrich) for at least three weeks before any of the following experiments were conducted. To suppress hCx43 gene expression, fetal AM hMSCs were transduced with LV.shRNA-hCx43.1.hPGK1.hrGFPI (Cx43↓[1] fetal AM hMSCs) or with LV.shRNA-hCx43.2.hPGK1.hrGFPI (Cx43↓[2] fetal AM hMSCs). Fetal AM hMSCs used as control cells (control fetal AM hMSCs) were incubated with LV.shRNA-eGFP.hPGK1.hrGFPI. Cx43↓(1) fetal AM hMSCs were transduced with LV.hCMV-IE.hCx45.IRES.hrGFPII.WHVPRE to overexpress Cx45 (Cx43↓(1)+Cx45↑ fetal AM hMSCs) in these cells. Cx43↓(1) fetal AM hMSCs transduced with the eGFP-encoding SIN-LV LV.hCMV-IE.IRES.eGFP.HBVPRE (previously designated LV-CMV-IRES-eGFP[7]) were used as control cells (Cx43↓(1)+eGFP fetal AM hMSCs).

ANALYSIS OF CX43 AND CX45 EXPRESSION

The distribution of Cx43 and Cx45 was studied by immunocytological stainings as described previously.[8] In short, cells were fixed on ice with 4% paraformaldehyde in PBS for 30 min, washed with PBS, permeabilized with 0.1% Triton X-100 in PBS for 5 min at 4°C and rinsed again with PBS. To decrease non-specific binding of the primary antibodies the cells were incubated with 1% donkey serum (Sigma Aldrich Chemie) in PBS for 30 min. Thereafter, cells were incubated overnight at 4°C with Cx43-specific rabbit polyclonal antibodies (PAbs; C6219; Sigma Aldrich Chemie) or with Cx45-specific goat PAbs (C-19; Santa Cruz Biotechnology, Santa Cruz, CA)

diluted 1:200 and 1:100, respectively, in PBS containing 0.1% donkey serum. Binding of these primary antibodies to their target antigen was visualized using Alexa 568-conjugated donkey anti-rabbit IgG or anti-goat IgG (both from Invitrogen) at dilutions of 1:200. Nuclei were stained by incubating the cells for 10 min at room temperature with 10 µg/mL Hoechst 33342 (Invitrogen) in PBS. Cells that went through the entire staining procedure but were not exposed to primary antibodies served as negative controls. A fluorescence microscope equipped with a digital color camera (Nikon Eclipse 80i; Nikon Europe, Badhoevedorp, the Netherlands) and dedicated software (NIS Elements, Nikon) were used to analyze the data.

Quantification of Cx43 and Cx45 protein levels was done by western blot analysis. Lysates were made from $\geq$4 different isolates of hMSCs per experimental group. After determining the protein concentration in each sample using the BCA Protein Assay Reagent (Thermo Fisher Scientific, Etten-Leur, the Netherlands), equal amounts of protein per slot was size-fractionated in a 12% NuPage Bis-Tris gel (Invitrogen) and transferred to a Hybond-P polyvinylidene difluoride membrane (GE Healthcare) using a wet blotting system. This membrane was blocked for 1 h at room temperature with 2% blocking buffer (ECL Advance blocking agent; GE Healthcare) in Tris-buffered saline wit Tween-20 (TBST) solution composed of 10 mmol/L Tris-HCl (pH7.6), 0.05% Tween-20 and 150 mmol/L NaCl. Thereafter, the membrane was incubated for 1 h at room temperature with the PAbs directed against Cx43 or Cx45 diluted 1:15,000 and 1:2,000 in blocking buffer, respectively. After multiple washing steps in TBST, the membrane was incubated with horseradish peroxidase (HRP)-conjugated goat anti-rabbit or donkey anti-goat secondary antibodies (both from Santa Cruz Biotechnology) diluted 1:15,000. For normalization purposes, a mouse MAb recognizing the housekeeping protein glyceraldehyde-3-phosphate dehydrogenase (GAPDH; Chemicon International, Temecula, CA; clone 6C5) was used, which was detected by HRP-conjugated goat anti-mouse secondary antibodies (Santa Cruz Biotechnology; 1:15,000). Chemiluminescence was induced with the aid of the ECL Advance Western Blotting Detection Kit and was captured on Hyperfilm ECL (both from GE Healthcare). The intensity of the Cx43-, Cx45- and GAPDH-specific signals was quantified using Image J software (version 1.43; National Institutes of Health, Bethesda, MD). For each sample, the ratios between the GAPDH signal intensity and that of the Cx43 or Cx45 protein were taken as measure of the absolute amounts of both these gap junction proteins in the different hMSC cultures. The Cx43 or Cx45 levels in the experimental samples were expressed as percentage of those of the corresponding control samples, which were set to 100%.

hCx43 and hCx45 transcript levels were determined by quantitative reverse transcription-polymerase chain reaction (qRT-PCR). To this purpose, total cellular RNA was extracted from $\geq$4 samples for each group of hMSCs using the RNeasy Mini

Kit (QIAGEN Benelux, Venlo, the Netherlands). cDNA was synthesized in 20-µl volumes using 2 µg of RNA, 0.25 µg of random hexanucleotides, 25 nmol of dNTPs and 500 U of Superscript III RNase H⁻ reverse transcriptase (all from Invitrogen). The resultant cDNA was amplified by PCR using the primer pairs QT00012684 and QT00239659 (both from QIAGEN), which are specific for the hCx43 (official name: human gap junction protein, alpha 1 [GJA1]) and hCx45 (official name: human gap junction protein, gamma 1 [GJC1]) gene, respectively. The annealing temperature for these primer combinations was 55°C. The expression of the genes of interest was normalized to that of the housekeeping gene GAPDH using primer set QT01192646 (QIAGEN) also at an annealing temperature of 55°C. The resultant cDNA was PCR amplified using the QuantiTect SYBR Green PCR kit (QIAGEN) following the recommendations of the supplier. Agarose gel electrophoresis and melting curve analysis were carried out to verify that each primer pair yielded a single PCR product of the expected size. PCR amplifications carried out with human right atrium-specific cDNA or without cDNA served as positive and negative controls, respectively. Data were analyzed using the ΔCt method.[9]

ASSESSMENT OF FUNCTIONAL HETEROCELLULAR GAP JUNCTIONAL

Dye transfer
Dye transfer assays were used to directly determine functional heterocellular coupling between nrCMCs and the GFP-positive hMSCs. Four days after cell isolation, nrCMC cultures with a density of 2×10^5 cells per 3.8-cm² well were loaded with dye by incubation for 15 min with 4 mmol/L calcein red-orange AM (calcein; Invitrogen) in Hank's balanced salt solution (Invitrogen). Thereafter, the cells were rinsed three times with PBS and were kept in the incubator in nrCMC culture medium supplemented with 2.5 mmol/L probenecid (Invitrogen) for [3]30 min before 2×10^4 GFP-positive hMSCs were added. Fluorescent images ([3]30 per group) were captured after 10 h and evaluated in a blinded manner. In all experimental groups, GFP-positive hMSCs surrounded by the same number of nrCMCs were analyzed. ImageJ software was used to determine the intensity of the calcein-associated fluorescence in several randomly-chosen, equally-sized subcellular regions for both the GFP-positive hMSCs and the adjoining nrCMCs. To correct for possible variations in calcein loading efficiency, the dye intensity in the GFP-positive hMSCs was expressed as a percentage of that in the surrounding nrCMCs. The percentage of calcein-positive cells among the GFP-labeled hMSCs was also determined by counting these cells in [3]60 fields of view per group.

Intracellular measurements

Whole-cell patch-clamp measurements were performed in co-cultures of 2×10^6 nrCMCs and 5×10^4 GFP-positive hMSCs. Typically, 4-6 nrCMCs were adjacent to a single hMSC. Four days after culture initiation, current-clamp recordings were performed at 25°C using an L/M-PC patch-clamp amplifier (List-Medical, Darmstadt, Germany; 3 kHz filtering).[8] Tip and seal resistance were 2.0-2.5 MW and >1 GW, respectively. The pipette solution contained (in mmol/L) 10 Na_2ATP, 115 KCl, 1 $MgCl_2$, 5 EGTA and 10 HEPES/KOH (pH 7.4) and the bath solution consisted of (in mmol/L) 137 NaCl, 4 KCl, 1.8 $CaCl_2$, 1 $MgCl_2$ and 10 HEPES (pH 7.4) in water. pClamp/Clampex8 software (Axon Instruments, Molecular Devices, Sunnyvale, CA) was used for data acquisition and analysis. All patch-clamp measurements were conducted in a blinded manner.

ASSESSMENT OF CARDIOMYOGENIC DIFFERENTIATION

To investigate their cardiomyogenic differentiation ability, 2×10^4 hMSCs from each experimental group were co-incubated for 10 days with 2×10^5 nrCMCs. The GFP-positive hMSCs were added to the nrCMC cultures 2 days after isolation of the nrCMCs.

Human-specific immunocytological analysis of cardiomyogenic differentiation potential

Immunocytological stainings were conducted as previously described.[3] On day 10 after culture initiation, the co-cultures of nrCMCs and GFP-positive hMSCs were fixed and stained with a mouse MAb recognizing the sarcomeric protein α-actinin (clone EA53; Sigma-Aldrich Chemie; dilution 1:400) and with the Cx43-specific PAb described above or in case of nrCMC co-cultures with Cx43↓(1)+Cx45↑ fetal AM hMSCs with a Cx45-specific PAb (clone H-85; Santa Cruz Biotechnology, dilution 1:200). The primary antibodies were visualized using Alexa 568-coupled donkey anti-mouse IgG and Alexa 532-linked goat anti-rabbit IgG secondary antibodies at dilutions of 1:200. Besides through their green fluorescence, the hMSCs in the co-cultures were identified by labeling with a human lamin A/C-specific murine MAb (clone 636; Vector Laboratories, Burlingame, CA; dilution 1:200). Lamin A/C staining was visualized with Qdot 655-streptavidin conjugates (Invitrogen; dilution 1:200) after incubation of the cells with biotinylated goat anti-mouse IgG2b secondary antibodies (Santa Cruz Biotechnology; dilution 1:200). Nuclei were stained using a 10 µg/mL solution of Hoechst 33342 in PBS. Co-cultures of nrCMCs with adult AT hMSCs transduced with LVs encoding for the puromycin-resistence gene instead of GFP were stained with primary Abs recognizing α-actinin, Cx43 and human-specific lamin A/C. The Cx43 PAb was visualized using an Alexa 488-coupled donkey anti-rabbit IgG, while α-actinin and human-specific lamin A/C

were visualized as described above. The percentage of GFP/lamin A/C-double-positive cells expressing α-actinin was determined by the microscopic analysis, at 40× magnification, of 25 cultures (200 cells per culture) of a total of 4 hMSC isolates per experimental group. Furthermore, the co-cultures were also stained with a goat PAb recognizing the cardiac transcription factor GATA4 (clone C-20; Santa Cruz Biotechnology, dilution 1:100) or with an Nkx2.5-specific rabbit PAb (clone H-114; Santa Cruz Biotechnology, dilution 1:200). These primary antibodies were visualized using Alexa 568-coupled donkey anti-goat or anti-rabbit IgG secondary antibodies (dilutions of 1:200). A fluorescence microscope equipped with a digital color camera (Nikon Eclipse 80i, Nikon Europe, Badhoevedorp, the Netherlands) and dedicated software (NIS Elements, Nikon) were used to analyze the data. All co-cultures were treated equally using the same antibody dilutions and exposure times.

Electrophysiological measurements in co-cultures of hMSCs and nrCMCs after pharmacological uncoupling

Cells were plated, cultured and studied under the same conditions as described above. Whole-cell current-clamp recordings were performed 10 days after culture initiation. Prior to the start of the measurements, the cells were treated for 15 min with 180 µmol/L of the pharmacological gap junctional uncoupler 2-aminoethoxy-diphenyl borate (Tocris, Ballwin, MO) as previously described.[8] All measurements were conducted in a blinded manner.

STATISTICS

Experimental results were expressed as mean±standard deviation for a given number (n) of observations. Data was analyzed by Student's t-test for direct comparisons. Analysis of variance followed by appropriate *post-hoc* analysis was performed for multiple comparisons. Statistical analysis was carried out using SPSS 16.0 for Windows (SPSS, Chicago, IL). Differences were considered statistically significant at $P<0.05$.

REFERENCES

1. Pittenger MF, Mackay AM, Beck SC et al. Multilineage potential of adult human mesenchymal stem cells. Science 1999;284:143-147.
2. National Institutes of Health. Guide for the Care and Use of Laboratory Animals. 1-1-2002.
3. Pijnappels DA, Schalij MJ, van Tuyn J et al. Progressive increase in conduction velocity across human mesenchymal stem cells is mediated by enhanced electrical coupling. Cardiovasc Res 2006;72:282-291.
4. Askar SF, Ramkisoensing AA, Schalij MJ et al. Antiproliferative treatment of myofibroblasts prevents arrhythmias in vitro by limiting myofibroblast-induced depolarization. Cardiovasc Res 2011;90:295-304.
5. Swildens J, de Vries AA, Li Z et al. Integrin stimulation favors uptake of macromolecules by cardiomyocytes in vitro. Cell Physiol Biochem 2010;26:999-1010.
6. Uil TG, de VJ, Vellinga J et al. A lentiviral vector-based adenovirus fiber-pseudotyping approach for expedited functional assessment of candidate retargeted fibers. J Gene Med 2009;11:990-1004.
7. van Tuyn J, Pijnappels DA, de Vries AA et al. Fibroblasts from human postmyocardial infarction scars acquire properties of cardiomyocytes after transduction with a recombinant myocardin gene. FASEB J 2007;21:3369-3379.
8. Pijnappels DA, Schalij MJ, Ramkisoensing AA et al. Forced alignment of mesenchymal stem cells undergoing cardiomyogenic differentiation affects functional integration with cardiomyocyte cultures. Circ Res 2008;103:167-176.
9. Schefe JH, Lehmann KE, Buschmann IR et al. Quantitative real-time RT-PCR data analysis: current concepts and the novel "gene expression's CT difference" formula. J Mol Med (Berl) 2006;84:901-910.
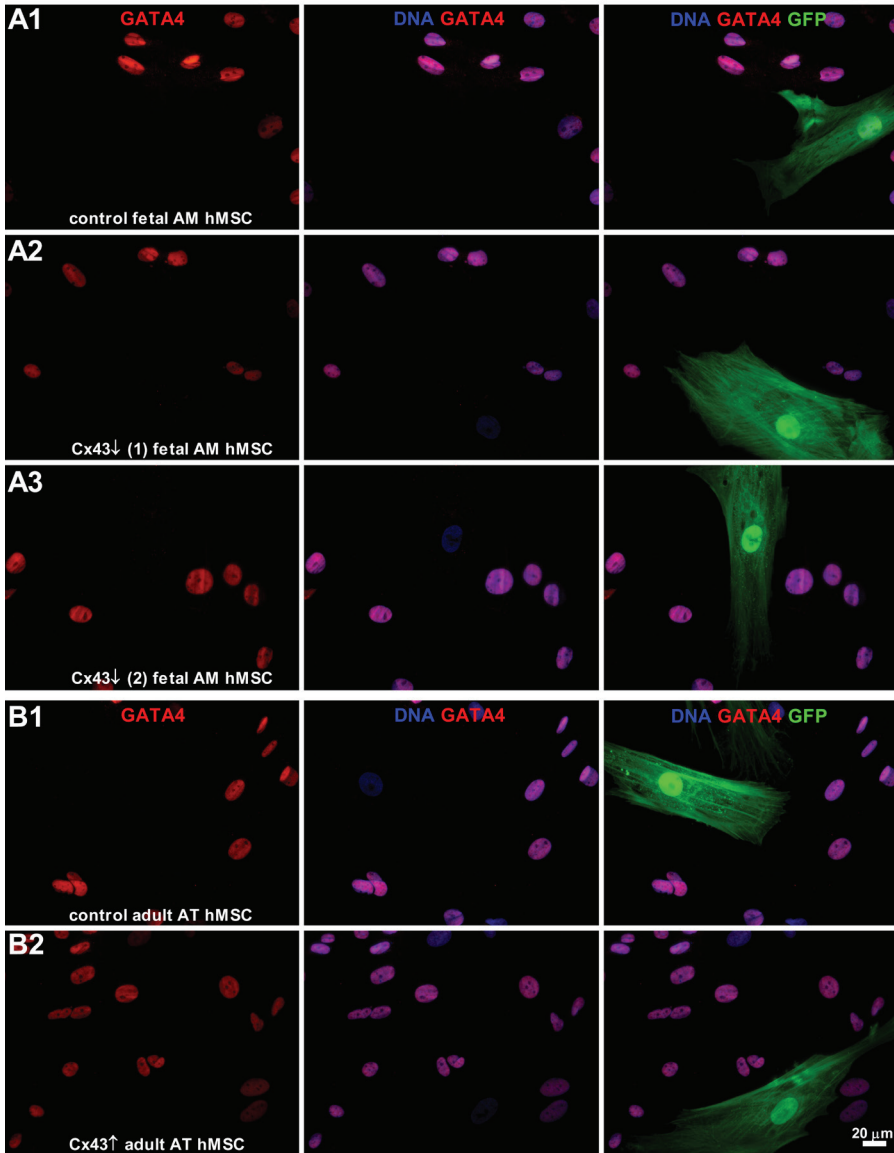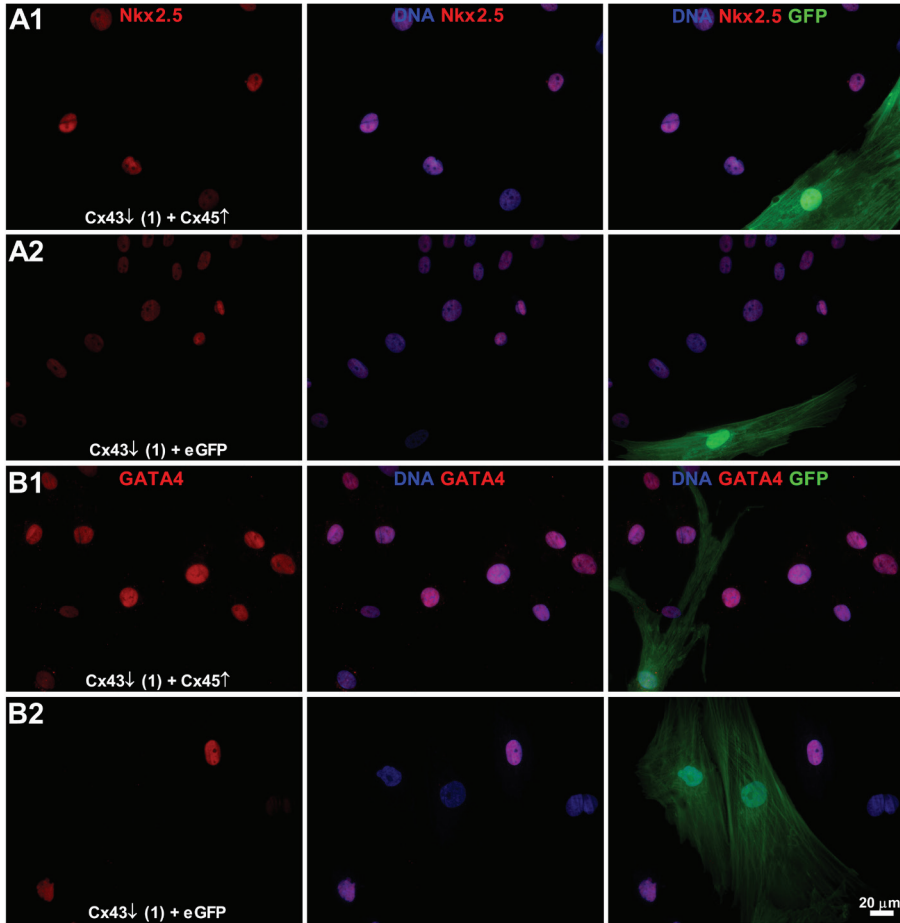
SUPPLEMENTAL FIGURES
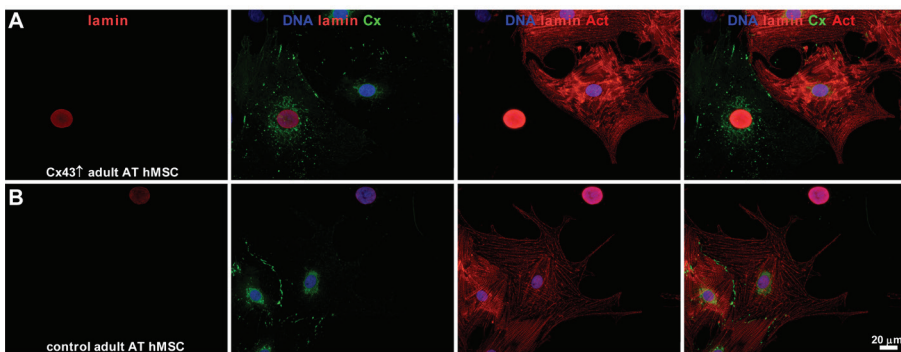
Supplemental Figure 1. Immunocytological assessment of cardiomyogenic differentiation of genetically modified adult AT hMSCs after 10 days of co-culture with nrCMCs. (A-B) Upon co-culture with nrCMCs, Cx43↑ adult AT hMSCs nor control adult AT hMSCs stained positive for α-actinin. Cx43 (indicated as Cx) plaques at the interfaces between Cx43↑ adult AT hMSCs and an adjacent nrCMC are present.
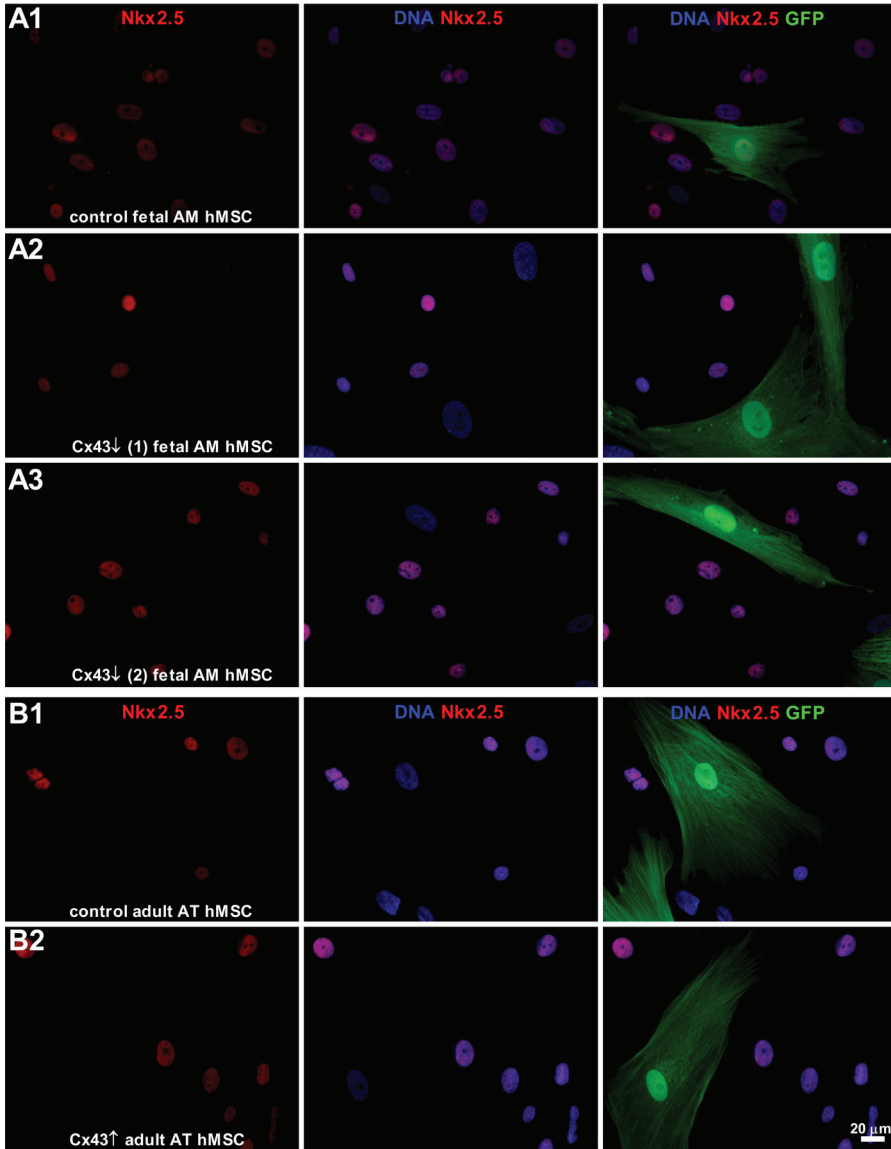
Supplemental figure 2. Immunocytological assessment of cardiomyogenic differentiation of genetically modified adult AT hMSCs and fetal AM hMSCs after 10 days of co-culture with nrCMCs. (A1) Upon co-culture with nrCMCs, a fraction of the GFP-positive control fetal AM hMSCs became positive for the cardiac transcription factor Nkx2.5. (A2-A3, B1-B2) GFP-labeled Cx43↓(1) fetal AM hMSCs, Cx43↓(2) fetal AM hMSCs, Cx43↑ adult AT hMSCs and control adult AT hMSCs in co-culture with nrCMCs did not stain positive for Nkx2.5.

Supplemental figure 3. Immunocytological assessment of cardiomyogenic differentiation of genetically modified adult AT hMSCs and fetal AM hMSCs after 10 days of co-culture with nrCMCs. (A1) Upon co-culture with nrCMCs, a fraction of the GFP-positive control fetal AM hMSCs became positive for the cardiac transcription factor GATA4. (A2-A3, B1-B2) GFP-labeled Cx43↓ (1) fetal AM hMSCs, Cx43↓(2) fetal AM hMSCs, Cx43↑ adult AT hMSCs and control adult AT hMSCs in co-culture with nrCMCs did not stain positive for GATA4.

Supplemental figure 4. Investigation by immunocytology of cardiomyogenic differentiation of fetal AM hMSCs in co-culture with nrCMCs after rescue of Cx43 knockdown by Cx45 overexpression. In the presence of nrCMCs, a fraction of the GFP-positive Cx43↓(1)+Cx45↑ fetal AM hMSCs (A1 and B1) expressed Nkx2.5 and GATA4, while Cx43↓(1)+eGFP fetal AM hMSCs (A2 and B2) did not.

CHAPTER V

ANTIPROLIFERATIVE TREATMENT OF MYOFIBROBLASTS PREVENTS ARRHYTHMIAS IN VITRO BY LIMITING MYOFIBROBLAST-INDUCED DEPOLARIZATION

Saïd F.A. Askar, MSc; Arti A. Ramkisoensing, MD, MSc; Martin J. Schalij, MD, PhD; Brian O. Bingen, MSc; Jim Swildens, MSc; Arnoud van der Laarse, PhD; Douwe E. Atsma, MD, PhD; Antoine A.F. de Vries, PhD; Dirk L. Ypey, PhD; Daniël A. Pijnappels, PhD.

Department of Cardiology, Leiden University Medical Center, Leiden, The Netherlands.

ABSTRACT

Aims: Cardiac fibrosis is associated with increased incidence of cardiac arrhythmias, but the underlying proarrhythmic mechanisms remain incompletely understood and antiarrhythmic therapies are still suboptimal. This study tests the hypothesis that myofibroblast (MFB) proliferation leads to tachyarrhythmias by altering the excitability of cardiomyocytes (CMCs), and that inhibition of MFB proliferation would thus lower the incidence of such arrhythmias.

Methods&Results: Endogenous MFBs in neonatal rat CMC cultures proliferated freely, or under control of different dosages of antiproliferative agents (mitomycin-C and paclitaxel). At day 4 and 9, arrhythmogeneity of these cultures was studied by optical and multi-electrode mapping. Cultures were also studied for protein expression and electrophysiological properties.

MFB proliferation slowed conduction from 15.3±3.5 cm/s (day 4) to 8.8±0.3 cm/s (day 9) (n=75,p<0.01), while MFB numbers increased to 37.4±1.7% and 62.0±2%. At day 9, 81.3% of these cultures showed sustained spontaneous reentrant arrhythmias. However, only 2.6% of mitomycin-C treated cultures (n=76,p<0.0001) showed tachyarrhythmias, and ectopic activity was decreased. Arrhythmia incidence was drug-dose dependent and strongly related to MFB proliferation. Paclitaxel-treatment yielded similar results. CMCs were functionally coupled to MFBs, and more depolarized in cultures with ongoing MFB proliferation, in which only L-type Ca^{2+} channel-blockade terminated 100% of reentrant arrhythmias, in contrast to Na^+-blockade (36%,n=12).

Conclusion: Proliferation of MFBs in myocardial cultures gives rise to spontaneous, sustained reentrant tachyarrhythmias. Antiproliferative treatment of such cultures prevents the occurrence of arrhythmias by limiting MFB-induced depolarization, conduction slowing and ectopic activity. This study could provide a rationale for a new treatment option for cardiac arrhythmias.

INTRODUCTION

Cardiac arrhythmias remain a leading cause of mortality in the Western world, despite a variety of treatment options.[1] Particularly, implantable cardioverter defibrillators have shown to be effective in improving survival of patients at risk. However, the underlying arrhythmogenic substrate is left untreated and therefore the occurrence of arrhythmias is not prevented.[2] Catheter ablation therapy may serve as an alternative and potentially curative treatment modality. However, its long-term benefits and effects on survival are yet unknown.[3] Furthermore, anti-arrhythmic drug therapy appears to have no significant effect on the survival in larger groups of patients suffering from cardiac arrhythmias and is associated with significant and potentially lethal side effects.[4] The limited therapeutic efficacy and adverse effects associated with these therapies is partly explained by our insufficient understanding of the tissue substrate and proarrhythmic mechanisms that are responsible for the occurrence of lethal ventricular tachyarrhythmias.

Taken together, current treatment of cardiac arrhythmias, including means to prevent arrhythmias, is still suboptimal. It is therefore essential to better comprehend the underlying proarrhythmic tissue substrate and to provide new rationales for the development of more effective treatment options aimed at preventing arrhythmias from occurring.

Cardiac fibrosis, for example as a result of ischemic heart disease and aging, deteriorates the well organized nature of the working myocardium due to a dramatic increase in fibroblastic cells, called myofibroblasts (MFBs).[5,6] This may increase electrical heterogeneity and the risk for lethal arrhythmias.[7,8] However, the functional role of MFBs in cardiac arrhythmias is still incompletely understood, especially the impact of their proliferative capacity on myocardial tissue. We hypothesized that MFB proliferation is a key factor in the incidence of spontaneous arrhythmias by altering the excitability of cardiomyocytes (CMCs), resulting in slow conduction and increased ectopic activity, and that inhibition of MFB proliferation may lower, or even prevent, the incidence of cardiac arrhythmias. To test this hypothesis, we studied the role of MFB proliferation in the occurrence of spontaneous reentrant arrhythmias in cardiac cultures using several antiproliferative agents, with cytochemical and extra- and intracellular electrophysiological techniques.

METHODS

All animal experiments were approved by the Animal Experiments Committee of the Leiden University Medical Center and conform to the Guide for the Care and Use of Laboratory Animals as stated by the US National Institutes of Health.

CELL ISOLATION, CELL CULTURE AND ANTIPROLIFERATIVE TREATMENT
Neonatal rat ventricular CMCs were isolated and cultured as described previously.[9]
Cells were plated on fibronectin-coated, round coverslips (15 mm) at a density of
$4-8 \times 10^5$ cells/well in 24-well plates. Endogenous MFBs, present in these cultures,
were allowed to proliferate freely, or under control of antiproliferative agents (mito-
mycin-C (0.05-10 µg/ml) and paclitaxel (0.085 mg/ml), which were added at day 1
of culture and incubated for 2h, resulting in partial or full inhibition of MFB prolif-
eration. In addition, defined ratios of MFBs and CMCs (10/90%, 25/75%, 50/50%)
were mixed and co-cultured in 24-well plates and treated with mitomycin-C as
described above, to maintain initial ratio and cell density.

IMMUNOCYTOLOGICAL ANALYSES
Cultures were fixed in 1% paraformaldehyde, permeabilized with 0.1% Triton X-100
and stained with 1:50-1:200 diluted primary antibodies (see Online Supplement for
details on antibodies). Corresponding Alexa fluor-conjugated secondary (Invitro-
gen, Carlsbad, CA, USA) antibodies were used at a dilution of 1:400. Subsequently,
nuclei were counterstained with Hoechst 33342. Cultures were photographed and
quantified with dedicated software (Image-Pro Plus, version 4.1.0.0, Media Cyber-
netics, Silver Spring, MD, USA).

WESTERN BLOT ANALYSES
Homogenates were made from either 3 different purified CMC cultures, 50/50%
CMC/MFB co-cultures or purified MFB cultures. Next, proteins were separated by
SDS-page and transferred to Hybond PVDF membranes. Blots were blocked in
5% bovine serum albumin in TBS-T. Primary and corresponding HRP-conjugated
secondary antibodies were incubated for 1 h, after which chemiluminescence was
induced by ECL advance detection reagents.

PROLIFERATION ASSAYS
Proliferation assays consisted of quantification of Ki67 expression as judged by Ki67
staining. Furthermore, MFB numbers in cardiac cultures were quantified at day 1, 4
and 9, based on collagen-I staining.

APOPTOSIS ASSAY
Possible pro-apoptotic effects of the antiproliferative treatments were investigated
by active caspase 3 staining, using aforementioned protocol.

OPTICAL AND MULTI-ELECTRODE MAPPING
At day 4 and 9, cardiac cultures were loaded with 16 µmol/L di-4-ANEPPS, given
fresh DMEM/Ham's F12 (37°C) and immediately mapped using the Ultima-L

optical mapping setup (SciMedia, Costa Mesa, CA, USA). Throughout mapping experiments, cultures were kept at 37°C. Optical signal recordings were analyzed using Brain Vision Analyze 0909 (Brainvision Inc, Tokyo, Japan) in order to assess conduction velocity (CV). Spontaneous ectopic activity was assessed in all groups for 24 s after unipolar electrical stimulation, so that if present, reentrant arrhythmias were eliminated, which allowed for ectopic or other spontaneous activity to resume.

For multi-electrode array (MEA) mapping, cells were cultured in glow-discharged, fibronectin-coated MEA culture dishes (Multi Channel Systems, Reutlingen, Germany) and measurements were performed in the associated data acquisition system, typically within 10 seconds after optical mapping. Electrograms were analyzed off-line using MC-Rack software (version 3.5.6, Multi Channel Systems).

WHOLE-CELL PATCH CLAMP AND DYE TRANSFER

Measurements were performed in co-cultures of CMCs and MFBs treated with or without mitomycin-C at day 9 of culture, or co-cultures of CMCs and eGFP-labeled MFBs. After identification of CMCs by phase contrast or fluorescence microscopy, maximal diastolic potentials in CMCs were recorded in current-clamp. For data acquisition and analysis, pClamp/Clampex8 software (Axon Instruments, Molecular Devices, Sunnyvale, CA, USA) was used.

To further study functional cell-cell coupling, co-cultures of calcein AM-loaded CMCs (green) and Katushka-expressing MFBs (red) were investigated for gap junction-mediated calcein transfer into MFBs by fluorescence microscopy.

PHARMACOLOGICAL INTERVENTIONS

The role of ion channel blockade in the maintenance of reentrant arrhythmias was investigated using the selective $Na_V1.5$ blocker Tetrodotoxin (TTX, 5-10 mmol/L; TTX, Sigma-Aldrich) or verapamil (100 mmol/L; Centrafarm, Etten-Leur, the Netherlands) as $Ca_V1.2$ blocker. These blockers were added to the mapping medium, after which the cultures were studied by optical mapping.

STATISTICAL ANALYSES

Statistical analyses were performed using SPSS11.0 for Windows (SPSS Inc., Chicago, IL, USA). Differences were considered statistically significant if $p < 0.05$.

A more detailed description of the Materials and Methods can be found in the Online Supplement.

RESULTS

CHARACTERIZATION OF CARDIAC CELL CULTURES

Cultures from neonatal rat ventricles (25 isolations) were studied for expression of cell type-specific and gap junction proteins at day 9 of culture. All cultured fibroblasts had the MFB phenotype as judged by α-smooth muscle actin (α-SMA) and vimentin expression (Figure 1). Connexin43 (Cx43) was present between adjacent CMCs, MFBs and at heterocellular junctions (Figure 1A).Dye transfer experiments demonstrated functional gap junctional MFB-CMC coupling (supplemental Figure 1). Western blot analyses revealed an inverse linear relationship between MFB percentage and Cx43 levels. In contrast, α-SMA levels showed a positive linear relationship with MFB numbers (Figure 1B-C). Of all α-SMA positive MFBs, 98.5±1.6% also expressed cytoplasmic collagen-I, centered around the nucleus (R^2=0.9921) (Figure 1D, G). CMCs did not express collagen-I, but stained positive for α-actinin (Figure 1E). Of the vimentin-positive MFBs, 98.4±1.3% also co-expressed collagen-I (R^2=0.9960) (Figure 1F, H). Immunocytochemical staining for collagen-I as MFB marker and cardiac α-actinin as CMC-specific marker therefore allowed us to quantify endogenous MFBs in a reliable and standardized manner.

UNINHIBITED MFB PROLIFERATION AND SPONTANEOUS REENTRANT ARRHYTHMIAS

MFB percentage in primary cardiac cultures was 15.6±3.2% at day 1 and progressively increased to 37.4±1.7% at day 4 (p<0.0001) (Figure 2A). At day 2, a spontaneously beating confluent monolayer had formed. At day 4, 24.2% of these cultures showed sustained, spontaneous reentrant tachyarrhythmias (n=33) (Figure 2F), with an average cycle-length of 267±22 ms and conduction velocity (CV) of 15.3±3.5 cm/s. Sustained reentry was defined as repetitive circular activation lasting ≥30 s. MFB proliferation resulted in an MFB percentage of 62.2±2.0% at day 9 (p<0.0001 vs day 1 and 4) (Figure 2B), and a decrease in CV to 8.8±0.3 cm/s (p<0.0001) (Figure 2C). At day 9, 81.3% of all spontaneously active cultures showed reentrant activity (n=75) (Figure 2D). The cycle-lengths of these arrhythmias had increased to 365±57 ms (p<0.001 vs day 4) (Figure 2E).

INHIBITION OF MFB-PROLIFERATION PRESERVES HIGH CV, DECREASES ECTOPIC ACTIVITY AND PREVENTS REENTRANT ARRHYTHMIAS

Assessment of proliferative activity of MFBs was performed by Ki67 staining (Figure 3A). Quantification showed a significant decrease in proliferating MFBs following mitomycin-C treatment (Figure 3B). In such cultures, MFB quantities remained constant throughout follow-up (Figure 3C), with no significant increase in apoptosis compared to control (Figure 3D and Supplemental Figure 2).
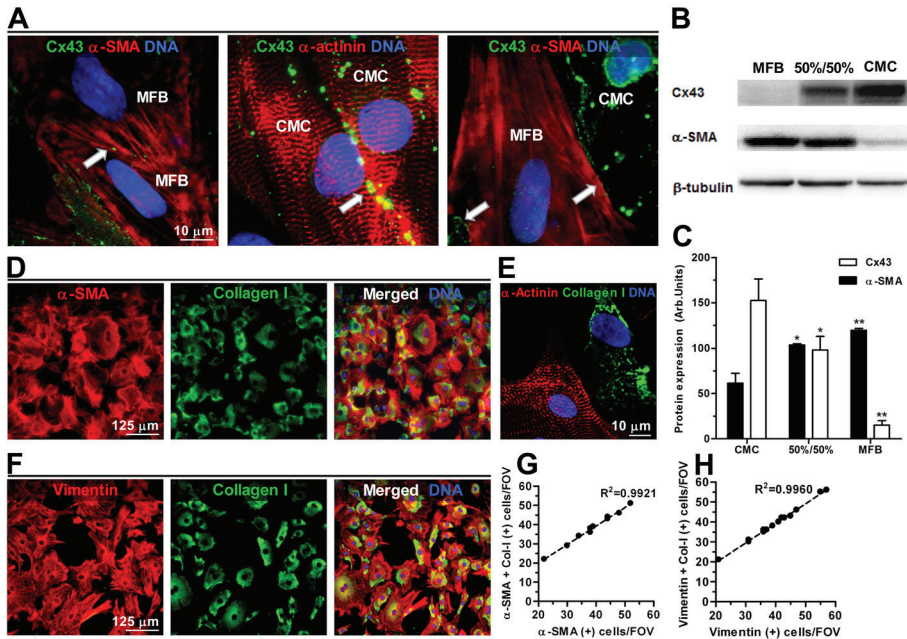
Figure 1. Characterization of cardiac cell cultures at day 9. (A) Immunocytochemical double-staining for Cx43, α-SMA (MFB) or α-actinin (CMC). White arrows mark intercellular expression. (B) Western blot of primary CMC cultures, 50%/50% co-cultures of MFBs/CMCs, and purified MFB cultures. (C) Quantification of Western blots normalized for β-tubulin shows opposing trends of Cx43 and α-SMA expression related to MFB quantity. *:p<0.05 vs CMC; **:p<0.05 vs CMC and 50%/50%. (D) a-SMA and collagen-I double-staining in MFBs. (E) Collagen-I and α-actinin double-staining showing highly specificity for MFBs and CMCs, respectively. (F) Collagen-I and vimentin double-staining in MFBs. (G) Relationship between co-expression of a-SMA and collagen-I in MFBs, and (H) co-expression of vimentin and collagen-I in MFBs. FOV=Field of View.

Under mapping conditions, ≥60% of both treated and untreated cultures were spontaneously active at day 4 and 9. At day 4, CV of mitomycin-C treated cultures was 23±1.9 cm/s, which was significantly higher than in control cultures (~15 cm/s, p<0.0001) (Figure 4E). Furthermore, no arrhythmias were observed (n=17) in mitomycin-C treated cultures (Figure 4C, H). At day 9, CV in mitomycin-C treated cultures remained unaltered. Interestingly, at day 9, only 2.6% of spontaneously active mitomycin-C treated cultures showed sustained reentrant tachyarrhythmias (n=76), which is a dramatic decrease compared to proliferating control cultures (~81% arrhythmias (n=75) at day 9, Figure 4B, F-G). For further evaluation
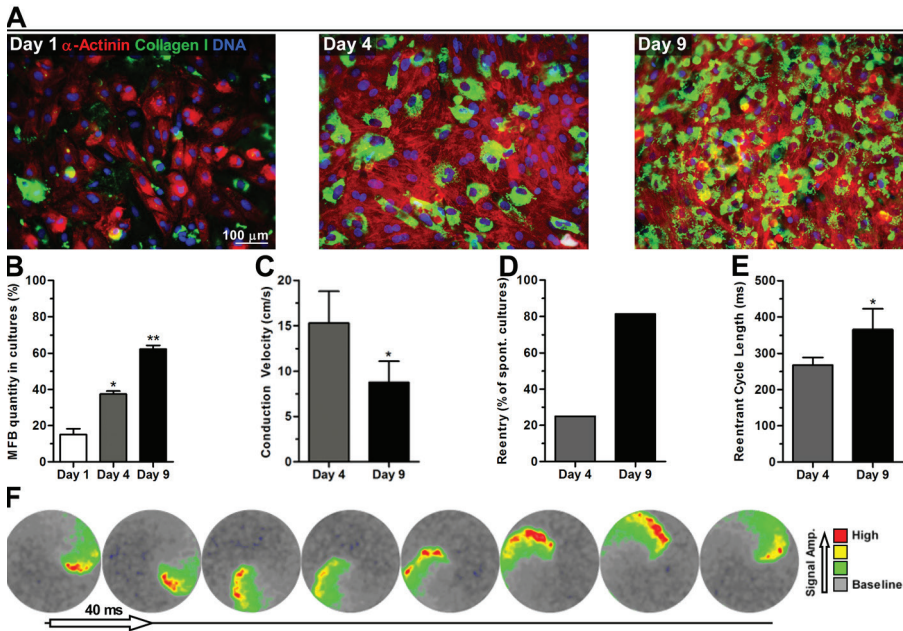
Figure 2. Proliferation of MFBs in cardiac cultures causes conduction abnormalities. (A) Immunocytochemical staining for α-actinin (CMC;red) and collagen-I (MFB;green) in cardiac cultures at day 1, 4, and 9. (B) Quantification of collagen-I positive MFBs at day 1, 4 and 9. Quantities are expressed as a percentage of total number of nuclei. *:p<0.0001 vs day 1. **:p<0.0001 vs day 1 and 4. (C) Progressive increase in MFBs is associated with a lower CV. *:p<0.0001 vs day 4, and (D) is also associated with an increase in the occurrence of spontaneous reentrant tachyarrhythmias and (E) an increase in cycle-length of the reentrant circuits between day 4 and 9. *:p<0.0001 vs day 4. (F) Time-lapse (spacing: 40ms) of a typical high-pass-filtered, spatially averaged optical signal of reentrant activation. Colours represent signal intensities related to changes in membrane potential.

of arrhythmogeneity, the incidence of ectopic activity was studied in treated and untreated cultures. Ectopic activity, e.g. multiple simultaneous or alternating pacemaker sites in one culture, was observed less frequently in mitomycin-treated cultures than in untreated cultures at day 4 (25% (n=24) versus 43% (n=23)) and day 9 (8% (n=37) versus 71% (n=35), respectively (Figure 4A, D).

Analyses of extracellular electrograms from MEA mapping experiments showed distinct differences between control cultures (n=12) and mitomycin-C treated cultures (n=11) (Figure 4I-J). Peak-to-peak electrogram amplitude was higher in mitomycin-C treated cultures (702±304 mV vs 96±23 mV, p<0.0001) (Figure 4K).
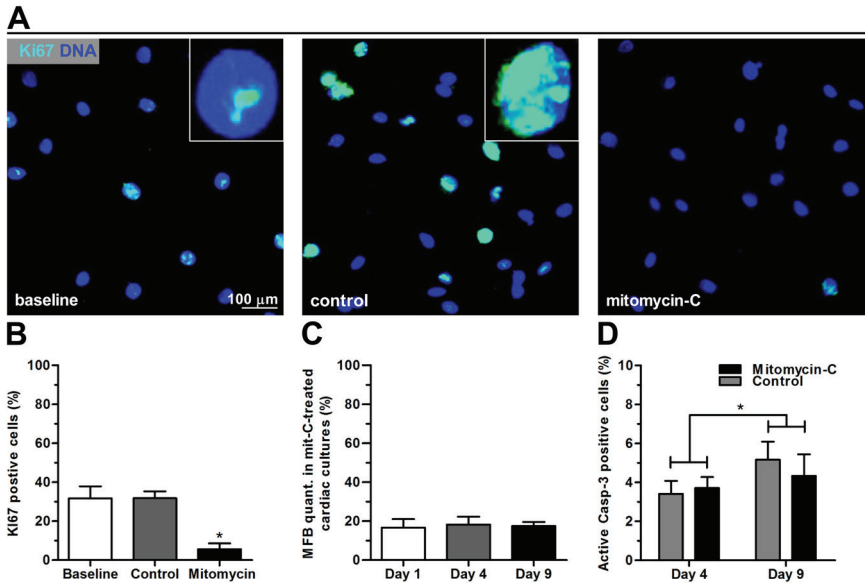
Figure 3. Mitomycin-C is a potent inhibitor of MFB proliferation (A) Typical examples of Ki67 staining in MFBs, indicating proliferation at baseline (day 1) and 3 days later for control and mitomycin-C treated cultures. Insets show magnified nucleus positive for Ki67 staining. (B) Effect of mitomycin-C treatment on Ki67 positive staining in MFBs. *:p<0.001 vs baseline and control. (C) MFB quantification in mitomycin-C treated cardiac cultures shows a stable MFB quantity throughout time (p=ns). (D) Quantification of active caspase-3 staining shows no significant differences in apoptosis between mitomycin-C treated and control cultures, although small but significant increases were found over time (*:p<0.05).

Spontaneous electrical activation frequency was lowered by mitomycin-C treatment compared to control (0.28±0.22HZ vs 3.22±0.22Hz, p<0.0001) (Figure 4L).

DOSE-DEPENDENT EFFECTS OF MITOMYCIN-C TREATMENT ON PRESERVATION OF ELECTROPHYSIOLOGICAL PARAMETERS

As mitomycin-C treatment had such a profound impact on conduction properties of myocardial cultures, dose-dependency was studied next. Dosages administrated at day 1 of culture were 10, 5, 2.5, 0.5 and 0.05 mg/ml. At day 9, cultures were studied and subsequently stained for collagen-I (Figure 5A). Mitomycin-C decreased the amount of MFBs in a dose-dependent manner (Figure 5B). Furthermore, mitomycin-C had a strong dose-dependent effect on cell density (p<0.001). In addition, cardiomyocyte count, calculated by subtracting collagen-I positive cells from total cell count, did not change significantly (Figure 5C).
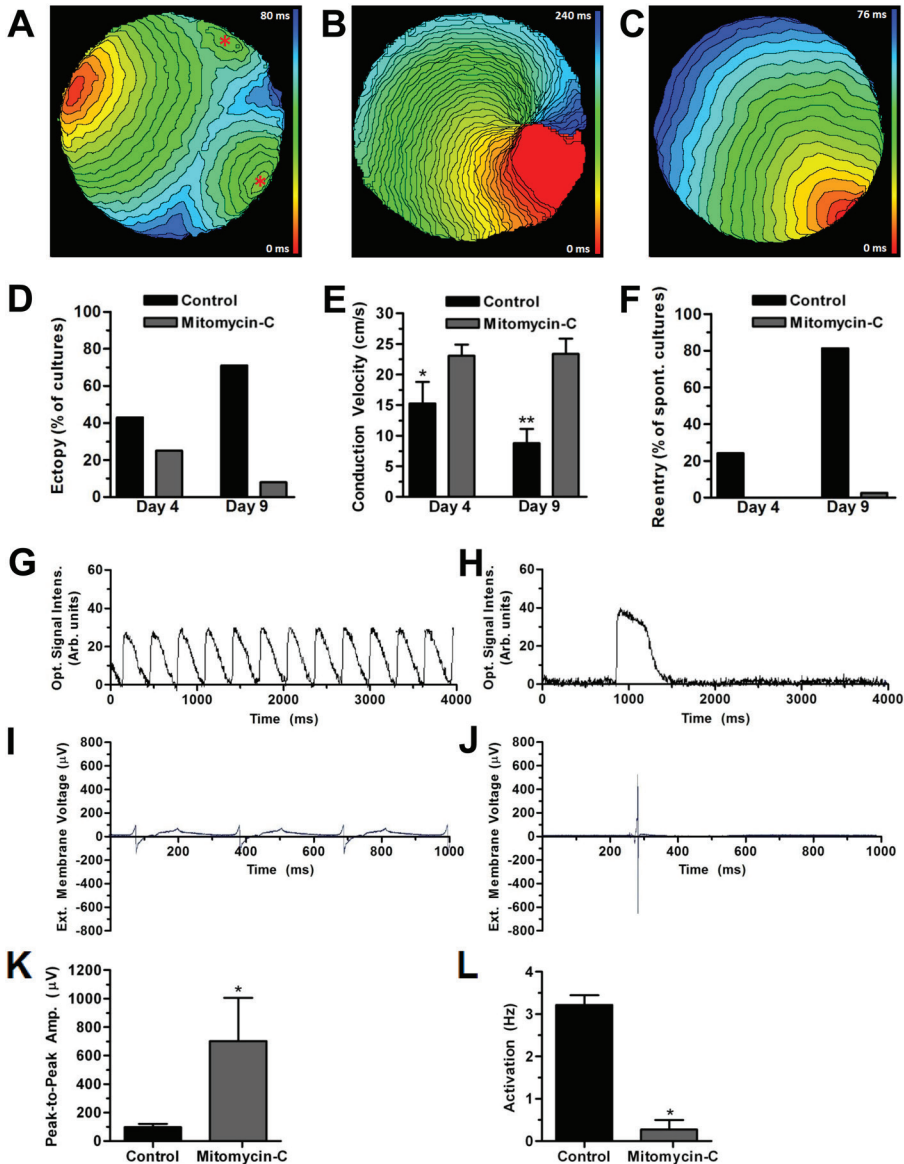
Figure 4. Effects of mitomycin-C treatment on ectopic activity, CV and reentrant tachyar-
rhythmias in cardiac cultures. (A) Activation map of ectopic activity in an untreated culture
at day 4 (4 ms isochrone spacing). Red asterisks mark ectopic foci. (B) Activation map
of a reentrant tachyarrhythmia in an untreated cardiac culture (spacing: 4ms). (C) Typi-
cal activation map of uniform conduction across a mitomycin-C treated culture (spacing:
4ms). (D) Quantification of incidence of ectopic activity at day 4 and 9 reveals a substantial

reduction by mitomycin-C treatment. (E) CV measured by optical mapping. *:p<0.001 vs mitomycin-C day 4-9 and control day 9. **:p<0.001 vs day 4-9 mitomycin-C. (F) Spontaneous reentry occurrence in mitomycin-C treated and control cultures at day 4 and 9. (G) Typical example of a non-high-pass-filtered, spatially filtered optical signal of repetitive activation in a non-treated, fibrotic culture showing reentrant tachyarrhythmias. (H) Typical example of a non-high-pass-filtered, spatially filtered optical signal of uniform conduction across a mito mycin-C treated culture. (I) Local extracellular multi-electrode array recording of a reentrant tachyarrhythmia. (J) Multi-electrode array recording of a mitomycin-C treated culture. (K) Quantification of electrical signal amplitude from multi-electrode array recordings at day 9 (p<0.0001 vs control). (L) Beating frequency of cultures measured by such arrays at day 9. *: p<0.0001 vs control.

These dose-dependent changes in MFB quantities and cell density were related to significant electrophysiological changes in the cultures. At day 9, CV was 7.3±2.4 cm/s at 0.05 µg/ml mitomycin-C and significantly rose with increasing dosages (Figure 5D). MFB percentages at various mitomycin-C dosages directly correlated with CV (R^2=0.94) (Figure 5E). Furthermore, the incidence of sustained reentrant arrhythmias showed a negative mitomycin-C dose-dependent relationship, with no occurrence of arrhythmias at 10 mg/ml (n=25) and 5 mg/ml (n=20), 10% at 2.5 mg/ml (n=31), 29% at 0.5 mg/ml (n=17), 92% at 0.05 mg/ml (n=13), and 93% for control (n=27) (Figure 5F).

CMC-MFB CO-CULTURES AT PREDETERMINED CELL DENSITY AND MFB-DEPENDENT CONDUCTION ABNORMALITIES

Cell density is an important determinant of conduction patterns, as this directly influences cell-to-cell contacts essential for action potential propagation. To further study the quantitative effects of MFBs on conduction and arrhythmias, fixed ratios of MFBs and CMCs were plated out, while inhibiting proliferation with 10 mg/ml mitomycin-C. As a result, average cell density between the co-culture groups did not differ significantly at day 9. MFB quantities were 15.7±2.0% (0% added MFBs), 26.8±2.5% (10% added), 38.0±3 (25% added) and 59.0±1.6% (50% added) at day 9. CV did not differ significantly between 0% (n=18) and 10% (n=20) added MFBs (23.1±2.2 cm/s vs 22.1±1.8 cm/s, p=0.51) at day 9. However, 25% and 50% added MFBs slowed conduction to 14.2±3.5 cm/s and 10.9±2.4 cm/s, respectively (p<0.05 vs all) (Supplemental Figure 3A). Furthermore, no arrhythmias were found in cultures containing 0% and 10% added MFBs, but at 25% and 50% added MFBs, occurrence was 27.8% (n=36) and 35.7% (n=28), respectively (Supplemental Figure 3C).

Unfortunately, cultures with added MFB percentages higher than 50% developed structural inhomogeneities from day 6 onwards and could therefore not be
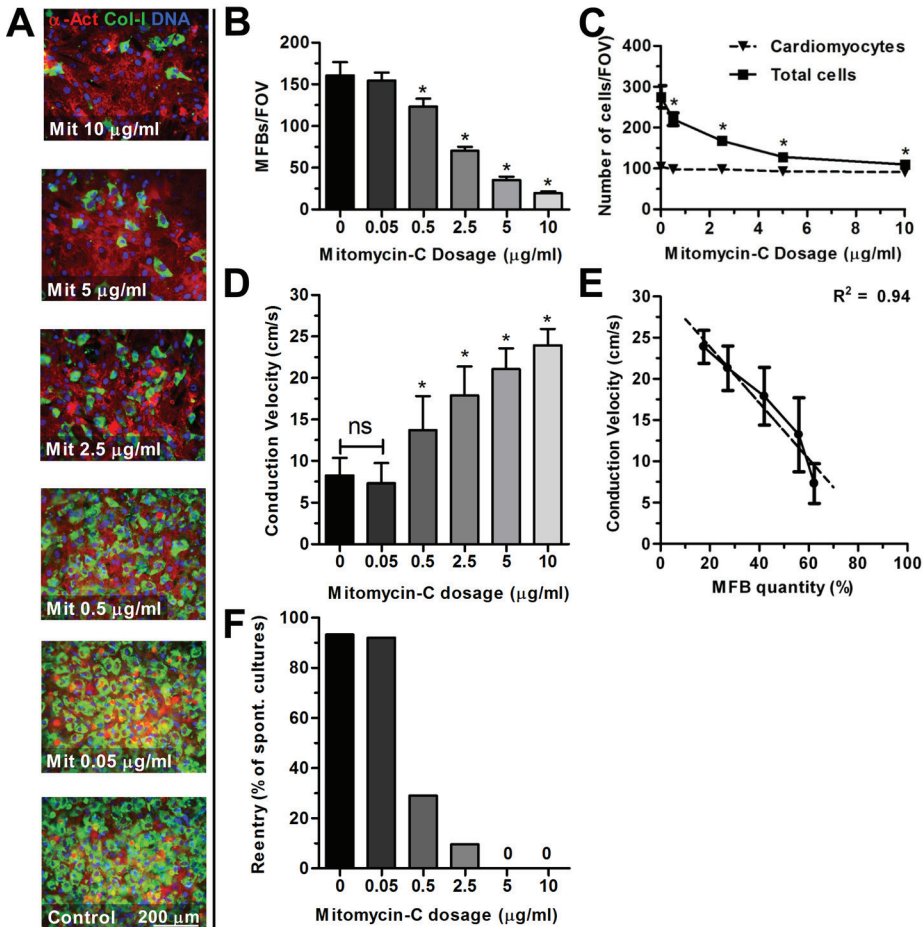
Figure 5. Dose-dependent effect of mitomycin-C treatment on arrhythmias at day 9 of culture. (A) Immunocytochemical double-staining for α-actinin (CMC;red) and collagen-I (MFB;green) in cardiac cultures treated with different dosages of mitomycin-C. (B) Dose-dependent effect of mitomycin-C on MFB quantities in cardiac cultures as determined by collagen-I staining. *:$p<0.001$ vs all including control (0 μg/ml). (C) Quantification of collagen-I staining shows a dose-dependent effect of mitomycin-C on total cell count without affecting CMC count. CMC count was calculated by subtract the number of MFBs from the total number of nuclei. *:$p<0.01$ vs all including control. (D) Dose-dependent effect of mitomycin-C on CV (*:$p<0.05$ vs all). (E) Plot of average MFB percentage found for different dosages against CV found in these groups shows a negative linear association between MFB percentage and CV. FOV: Field of View. (F) Dose-dependent effect of mitomycin-C on reentry occurrence.

studied at day 9. Nevertheless, linear regression analysis revealed a strong inverse relationship between plated MFB percentages and CV at day 4 (Supplemental Figure 3B).

A potentially secondary preventive effect of mitomycin-C on the occurrence of spontaneous arrhythmias was studied in 50%/50% CMC/MFB co-cultures either treated with mitomycin-C or allowed to proliferate freely. At day 4, CV in mitomycin-C treated cultures was 10.9±3.3 cm/s with 60.2±3.8% MFBs. In contrast, in control cultures with an equally high initial number of MFBs, CV decreased to 4.9±1.1 cm/s, while MFB percentages increased to 78.8±4.7% (p<0.0001 vs treated cultures) (Supplemental Figure 3D). Furthermore, arrhythmia occurrence was 3.1-fold higher in the non-treated cultures (26% (n=17) vs 82% (n=23)) (Supplemental Figure 3E).

CHARACTERISTICS OF REENTRANT TACHYARRHYTHMIAS

In untreated, arrhythmic cultures, cycle-length of the reentrant circuits was strongly related to CV (R^2=0.83, Figure 6A). Reentry was typically associated with a decrease in CV of 5.0±1.2 cm/s as compared to non-reentrant conduction in cultures from the same experimental group. Furthermore, administration of tetrodotoxin (TTX) to 12 untreated, arrhythmic cultures at concentrations of 5 mM and 20 mM at day 9 of culture, resulted in a significantly lower CV (Figure 6B, D-E), but had only a mild to moderate effect on terminating reentrant arrhythmias (Figure 6C). Next, 100 mM verapamil was administered to block L-type Ca^{2+}-channels, which terminated 100% of the remaining arrhythmias (Figure 6C). Internal PBS control did not affect arrhythmia persistence. Additionally, 12 untreated, arrhythmic cultures were immediately treated with verapamil without prior TTX administration, which also terminated all arrhythmias. In mitomycin-C treated cultures, 20 µM TTX completely blocked propagation for ≥30 seconds, after which propagation resumed at a significantly lower CV of 11.5±2.0 cm/s (n=10, previously 24.2±2.0 cm/s, p<0.0001).

To further study the role of MFB proliferation in arrhythmogeneity, CMCs were investigated for their electrophysiological properties by patch-clamp experiments in active cultures treated with or without mitomycin-C. Cultures had comparable beating frequencies (0.5-1 Hz). After 9 days of ongoing MFB proliferation, the maximal negative diastolic potential of CMCs was significantly reduced (-44±9mV, n=11) as compared to those of CMCs in mitomycin-C treated cultures (-68±7mV, n=12, p<0.001) (Figure 6F).

In co-cultures of eGFP-labeled MFBs with CMCs, at equal density and ratio as day 9 of free proliferation, diastolic membrane potentials of CMCs (-48±6mV, n=8) were comparable to those derived at day 9 of free proliferation. This is in agreement with the low CV and increased ectopic activity found in such cultures and their tolerance to TTX treatment.
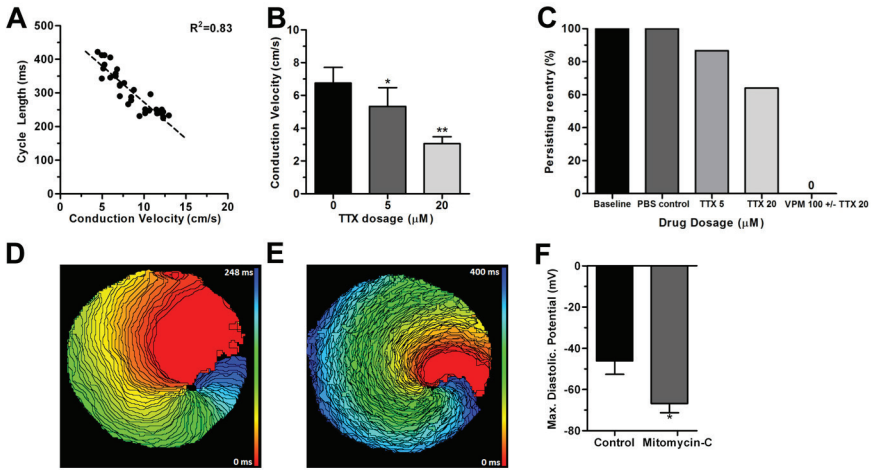
Figure 6. Characteristics of reentrant tachyarrhythmias at day 9. (A) Linear association between cycle-length and CV (R^2=0.83, n=35). (B) TTX significantly decreased CV in a dose dependent manner (*:$p<0.05$ vs baseline, **:$p<0.0001$ vs 0 and 5 µM). (C) Persistence of reentrant circuits after administration of TTX and/or verapamil. (D) Activation map of a reentrant tachyarrhythmia in an untreated cardiac culture (spacing: 4ms). (E) Activation map of the same reentrant tachyarrhythmia shown in panel E after 5 min of incubation with 20 µM TTX. Of note is the increased number of isochronal lines (4 ms), indicating conduction slowing. (F) Maximal diastolic potential measured in CMCs from control and mitomycin-C treated cultures at day 9.

PREVENTION OF ARRHYTHMIAS BY PACLITAXEL, ANOTHER ANTIPROLIFERATIVE AGENT

Cultures were treated with 0.085 mg/ml paclitaxel and studied identically to mitomycin-C treated cultures. In paclitaxel-treated MFB cultures, less Ki67 positive cells were found (Supplemental Figure 4B-C) and apoptosis was not significantly increased compared to vehicle-control (0.9% DMSO) treated cultures (Supplemental Figure 4D, 5). Interestingly, vehicle treatment alone also inhibited proliferation. Spontaneous activity under optical mapping conditions was >60% for both treated and untreated groups. CV at day 4 was 17.3±1.6 (vs 11.1±3.6 cm/s in control), without reentry (n=27) in the paclitaxel-treated group, whereas 61.5% (n=11) of controls showed reentry (Supplemental Figure 4E-F). At day 9, paclitaxel-treated cultures contained 33.3±2.9% MFBs (Supplemental Figure 4A), and CV was 15.0±1.5 cm/s ($p<0.01$ vs day 4 and control), while arrhythmias were observed in 5% of spontaneously active cultures (n=23). In control cultures at day 9, CV was 6.5±1.4 cm/s, with a reentry incidence of 93% (n=15) (Supplemental Figure 4E-F).

DISCUSSION

Key findings of this study are (1) proliferation of myofibroblasts in myocardial cultures results in a highly pro-arrhythmogenic substrate, in which CMCs are depolarized, conduction is slow and mainly Ca^{2+}-driven, and ectopic activity is increased, thereby giving rise to spontaneous, sustained reentrant tachyarrhythmias, and (2) antiproliferative treatment of these cultures prevents or substantially reduces the occurrence of arrhythmias by limiting myofibroblasts-induced depolarization and preserving uniform, rapid, Na^+-driven impulse propagation in CMCs, with less ectopic activity, but without noticeable adverse effects on electrophysiological properties and without increased apoptosis in the treated cultures.

MYOFIBROBLASTS AND CARDIAC ARRHYTHMOGENEITY

In vitro studies indicate that MFBs could play a role in modulating electrophysiological properties in remodeled hearts, and thereby contribute to arrhythmogenesis. Rook *et al.* showed that cardiac fibroblasts and CMCs are able to form functional heterocellular gap junctions.[10] Gaudesius *et al.*,[11] and previous studies by our group,[12,13] demonstrate that fibroblasts coupled to CMCs are able to slowly conduct electrical impulses through electrotonic interaction. Paracrine activity of cardiac fibroblasts may also contribute to a reduction in CV.[14] Besides their effects on CV, MFBs may also induce ectopic activity in cardiac cultures as demonstrated by Miragoli *et al.*[15] Recently, a study by Zlochiver *et al.* showed that MFBs are able to contribute to rhythm disturbances in cardiac cultures,[16] which was further investigated in a number of *in silico* studies.[17,18] Novel in the present study is the finding that ongoing proliferation of endogenous MFBs in neonatal rat CMC cultures results in the creation of a highly arrhythmogenic substrate, and that antiproliferative treatment of cardiac cultures prevents spontaneous reentrant tachyarrhythmias.

REENTRANT TACHYARRHYTHMIAS IN CARDIAC CULTURES WITH ONGOING MFB PROLIFERATION

In previous studies, functional reentry was induced by rapid electrical pacing of the cultures.[16,19,20] In the present study the focus was on the ability of myocardial cultures to spontaneously generate such reentrant arrhythmias. MFBs are known to contribute to both automaticity and slow conduction,[11,15,21] therefore reentry may occur in the absence of externally applied electrical impulses. We confirmed this by showing that ~81% of all cultures with ongoing MFB proliferation and without apparent anatomical obstacles, showed spontaneous, sustained reentrant tachyarrhythmias at day 9 of culture.

By allowing MFBs to proliferate freely in CMC cultures, CMCs became increasingly depolarized due to increasing MFB-CMC interactions. The present study

shows that this eventually leads towards a depolarized resting membrane potential at which voltage-gated fast Na^+-channels are largely inactivated and propagation becomes mainly dependent on activation of Ca^{2+}-channels. It is known that Ca^{2+}-driven propagation contributes to slow conduction.[7] In line with this observation, all arrhythmias in the present study were terminated when L-type Ca^{2+}-channels were blocked. In contrast, most arrhythmias sustained after Na^+-channel blockade, indicating that electrical propagation in such conditions appears to be mainly Ca^{2+}-driven. Recently, Chang *et al.* showed similar results in another *in vitro* model of reentry, using non-fibroblastic cells.[20] Moreover, as these CMCs become depolarized by increasing numbers of MFB, they could become active as local pacemaker site through depolarized-induced automaticity,[22] and thereby add to the proarrhythmogenic nature of fibrotic cultures. The present study shows that around 50% of all fibrotic cultures, which did not show reentrant arrhythmias at the time of mapping, showed multiple simultaneous or alternating pacemaker sites.

Ongoing MFB proliferation also had an effect on the cycle-length of the tachyarrhythmias. At day 4, average cycle-length was 267 ± 22 ms at a CV of 15.3 ± 3.5 cm/s, whereas at day 9, the cycle-length increased to 365 ± 57 ms at a CV of only 8.8 ± 3 cm/s. These data may explain how different degrees of fibrosis during various stages of cardiac remodeling could both determine the vulnerability to arrhythmias and the rate of atrial or ventricular arrhythmias. Therefore, future *in vivo* studies are required to better understand the role of MFBs in the arrhythmic heart.

ANTIPROLIFERATIVE TREATMENT OF ENDOGENOUS MYOFIBROBLASTS

In the present study, two different antiproliferative agents were used to study the role of MFB proliferation in arrhythmogeneity. One of these agents is mitomycin-C, a potent DNA-crosslinking agent. After proliferation inhibition by mitomycin-C, CV remained stable from day 4 to day 9, and spontaneous reentry occurrence decreased from 81.3% to 2.6%. Concerning the underlying mechanisms, in cultures treated with mitomycin-C the resting membrane potential of CMCs remained more negative. Therefore propagation remained fast and mainly Na^+-driven, as was shown by addition of TTX to these cultures, in contrast to cultures with ongoing MFB proliferation. In addition, less ectopic activity was observed in cultures treated with mitomycin-C, which most likely resulted from limited MFB-induced depolarization and a subsequent reduction of the occurrence of depolarization-induced automaticity. As a consequence of fast propagation and less ectopic activity the occurrence of reentrant arrhythmias is expected to decrease, which was confirmed in the present study.

By inhibition of MFB proliferation, not only MFB-induced depolarization of CMCs is minimized, but also disruption of low-resistant gap junctional coupling between CMCs by infiltrating MFBs may be prevented, thereby preserving rapid

propagation. Calculations on cell densities indicated that antiproliferative treatment does coincide with a lower total cell density while maintaining the same number of CMCs as the non-treated cultures. In addition, any negative, paracrine effect of MFBs on CV in cardiac cultures will be stabilized after inhibition of proliferation, as such an effect is expected to be cell number-dependent.

To exclude a mitomycin-C specific effect and to establish that proliferation is the key factor in this study, another antiproliferative agent was studied. Paclitaxel, a member of the taxanes drug category, interferes with breakdown of microtubules during cell division. Park *et al.* used the antiproliferative potential of paclitaxel to inhibit coronary restenosis and neointimal hyperplasia in the myocardium.[23] We show that paclitaxel is also suited as agent to reduce the incidence of reentrant tachyarrhythmias in myocardial cultures. Control experiments for paclitaxel included incubation with DMSO (0.9%). DMSO is known to have several effects on cells,[24] and therefore may explain the high incidence of reentry at day 4 in these cultures.The lower CV found in paclitaxel-treated cultures may also be explained by its mechanism of action.[25] Nevertheless, no reentry was observed in paclitaxel-treated cultures with DMSO as vehicle. Importantly, both agents did not result in increased apoptosis, which is in agreement with earlier studies.[26,27]

IN VIVO TRANSLATION

The present study provides new insights in the way cardiac fibrosis may result in arrhythmias, and how this may provide a rationale for a preventive strategy, which currently does not exist. In the clinical setting, myocardial fibrosis increases arrhythmia vulnerability in diseased and aged hearts, and finds its basis in proliferation of MFBs and matrix deposition by these cells. Although functional MFB-CMC coupling remains to be proven *in vivo*, the key role of MFBs in cardiac fibrosis suggests a high significance for *in vivo* arrhythmogeneity of these cells. Measures to control MFB proliferation may therefore counteract different pro-arrhythmic aspects at once. Naturally, *in vivo* studies are necessary to determine whether progressive fibrosis (e.g. in post myocardial infarction or aging) and its pro-arrhythmic consequences can be limited by reducing MFB proliferation. Considering the role of cell proliferation in different physiological processes in the heart,[5,28,29] and possible cardiotoxic effects of antiproliferative agents,[30] careful consideration of the time-frame, location and strength of intervention seems of importance. Still, the strong *in vitro* evidence from this study suggests that approaches to limit MFB proliferation in hearts vulnerable to fibrosis-related conduction disturbances may have profound effects on arrhythmia vulnerability.

STUDY LIMITATIONS

The use of adult human CMCs and MFBs may have been more clinically relevant, but these CMCs cannot be kept in culture for longer periods and the proliferation rate of such MFBs *in vitro* does not allow a study like this within a reasonable time-frame. Furthermore, cardiac MFBs are also involved in secretion of extracellular matrix components, which could contribute to deleterious effects on conduction in fibrotic cardiac tissue. These aspects were not studied in detail and need more dedicated studies in the future. However, it may be expected that with inhibition of MFB proliferation, the secretion of such components is indirectly lowered.

CONCLUSIONS

Proliferation of MFBs in myocardial cultures gives rise to spontaneous, sustained reentrant tachyarrhythmias. However, antiproliferative treatment of such cultures prevents the occurrence of arrhythmias significantly by preserving a physiological membrane potential and rapid, Na^+-driven propagation in CMCs. Hence, our study indicates that MFB proliferation may be a novel target for future anti-arrhythmic strategies.

FUNDING

ACKNOWLEDGEMENTS

CONFLICT OF INTEREST

None.

REFERENCES

1.   Huikuri HV, Castellanos A, Myerburg RJ. Sudden death due to cardiac arrhythmias. *N Engl J Med* 2001;**345**:1473-1482.

2.   Borleffs CJ, van Erven L, Schotman M, Boersma E, Kies P, van der Burg AE *et al*. Recurrence of ventricular arrhythmias in ischaemic secondary prevention implantable cardioverter defibrillator recipients: long-term follow-up of the Leiden out-of-hospital cardiac arrest study (LOHCAT). *Eur Heart J* 2009;**30**:1621-1626.

3.   Zeppenfeld K, Stevenson WG. Ablation of ventricular tachycardia in patients with structural heart disease. *Pacing Clin Electrophysiol* 2008;**31**:358-374.

4.   Arshad A, Mandava A, Kamath G, Musat D. Sudden cardiac death and the role of medical therapy. *Prog Cardiovasc Dis* 2008;**50**:420-438.

5.   Frangogiannis NG. The mechanistic basis of infarct healing. *Antioxid Redox Signal* 2006;**8**:1907-1939.

6.   Porter KE, Turner NA. Cardiac fibroblasts: at the heart of myocardial remodeling. *Pharmacol Ther* 2009;**123**:255-278.

7.   Kleber AG, Rudy Y. Basic mechanisms of cardiac impulse propagation and associated arrhythmias. *Physiol Rev* 2004;**84**:431-488.

8.   van der Burg AE, Bax JJ, Boersma E, Pauwels EK, van der Wall EE, Schalij MJ. Impact of viability, ischemia, scar tissue, and revascularization on outcome after aborted sudden death. *Circulation* 2003;**108**:1954-1959.

9.   Pijnappels DA, Schalij MJ, Ramkisoensing AA, van Tuyn J, de Vries AA, van der Laarse A *et al*. Forced alignment of mesenchymal stem cells undergoing cardiomyogenic differentiation affects functional integration with cardiomyocyte cultures. *Circ Res* 2008;**103**:167-176.

10.   Rook MB, Jongsma HJ, de Jonge B. Single channel currents of homo- and heterologous gap junctions between cardiac fibroblasts and myocytes. *Pflugers Arch* 1989;**414**:95-98.

11.   Gaudesius G, Miragoli M, Thomas SP, Rohr S. Coupling of cardiac electrical activity over extended distances by fibroblasts of cardiac origin. *Circ Res* 2003;**93**:421-428.

12.   Pijnappels DA, van Tuyn J, de Vries AA, Grauss RW, van der Laarse A, Ypey DL *et al*. Resynchronization of separated rat cardiomyocyte fields with genetically modified human ventricular scar fibroblasts. *Circulation* 2007;**116**:2018-2028.

13.   van Tuyn J, Pijnappels DA, de Vries AA, de Vries I, van der Velde-van Dijke I, Knaan-Shanzer S *et al*. Fibroblasts from human postmyocardial infarction scars acquire properties of cardiomyocytes after transduction with a recombinant myocardin gene. *FASEB J* 2007;**21**:3369-3379.

14.   Pedrotty DM, Klinger RY, Kirkton RD, Bursac N. Cardiac fibroblast paracrine factors alter impulse conduction and ion channel expression of neonatal rat cardiomyocytes. *Cardiovasc Res* 2009;**83**:688-697.

15.   Miragoli M, Salvarani N, Rohr S. Myofibroblasts induce ectopic activity in cardiac tissue. *Circ Res* 2007;**101**:755-758.

16.   Zlochiver S, Munoz V, Vikstrom KL, Taffet SM, Berenfeld O, Jalife J. Electrotonic myofibroblast-to-myocyte coupling increases propensity to reentrant arrhythmias in two-dimensional cardiac monolayers. *Biophys J* 2008;**95**:4469-4480.

17.   Jacquemet V, Henriquez CS. Loading effect of fibroblast-myocyte coupling on resting potential, impulse propagation, and repolarization: insights from a microstructure model. *Am J Physiol Heart Circ Physiol* 2008;**294**:H2040-H2052.

18.   Xie Y, Garfinkel A, Camelliti P, Kohl P, Weiss JN, Qu Z. Effects of fibroblast-myocyte coupling on cardiac conduction and vulnerability to reentry: A computational study. *Heart Rhythm* 2009;**6**:1641-1649.

19.   Bian W, Tung L. Structure-related initiation of reentry by rapid pacing in monolayers of cardiac cells. *Circ Res* 2006;**98**:e29-e38.

20.   Chang MG, Zhang Y, Chang CY, Xu L, Emokpae R, Tung L *et al*. Spiral waves and reentry dynamics in an in vitro model of the healed infarct border zone. *Circ Res* 2009;**105**:1062-1071.

21.   Miragoli M, Gaudesius G, Rohr S. Electrotonic modulation of cardiac impulse conduction by myofibroblasts. *Circ Res* 2006;**98**:801-810.

22.   Rosenthal JE, Ferrier GR. Contribution of variable entrance and exit block in protected foci to arrhythmogenesis in isolated ventricular tissues. *Circulation* 1983;**67**:1-8.

23.   Park SJ, Shim WH, Ho DS, Raizner AE, Park SW, Hong MK *et al*. A paclitaxel-eluting stent for the prevention of coronary restenosis. *N Engl J Med* 2003;**348**:1537-1545.

24.   Berliner DL, Ruhmann AG. The influence of dimethyl sulfoxide on fibroblastic proliferation. *Ann N Y Acad Sci* 1967;**141**:159-164.

25.   Casini S, Tan HL, Demirayak I, Remme CA, Amin AS, Scicluna BP *et al*. Tubulin polymerization modifies cardiac sodium channel expression and gating. *Cardiovasc Res* 2010;**85**:691-700.

26.   Axel DI, Kunert W, Goggelmann C, Oberhoff M, Herdeg C, Kuttner A *et al*. Paclitaxel inhibits arterial smooth muscle cell proliferation and migration in vitro and in vivo using local drug delivery. *Circulation* 1997;**96**:636-645.

27.   Nieto A, Cabrera CM, Catalina P, Cobo F, Barnie A, Cortes JL *et al*. Effect of mitomycin-C on human foreskin fibroblasts used as feeders in human embryonic stem cells: immunocyto-chemistry MIB1 score and DNA ploidy and apoptosis evaluated by flow cytometry. *Cell Biol Int* 2007;**31**:269-278.

28.   Souders CA, Bowers SL, Baudino TA. Cardiac fibroblast: the renaissance cell. *Circ Res* 2009;**105**:1164-1176.

29.   Bergmann O, Bhardwaj RD, Bernard S, Zdunek S, Barnabe-Heider F, Walsh S *et al*. Evidence for cardiomyocyte renewal in humans. *Science* 2009;**324**:98-102.

30.   Yeh ET, Tong AT, Lenihan DJ, Yusuf SW, Swafford J, Champion C *et al*. Cardiovascular complications of cancer therapy: diagnosis, pathogenesis, and management. *Circulation* 2004;**109**:3122-3131.

METHODS

All animal experiments were approved by the Animal Experiments Committee of the Leiden University Medical Center and conform to the Guide for the Care and Use of Laboratory Animals as stated by the US National Institutes of Health.

CELL ISOLATION AND CULTURE

Primary neonatal rat cardiomyocytes (CMCs) and cardiac fibroblasts were isolated and cultured as described previously[1,2]. Immediately following isolation, cell suspensions were spinned down, resuspended and filtered through a 20 mm cell-strainer to remove cell-aggregates. Subsequently, cells were counted and plated out on fibronectin-coated round coverslips (15 mm) at a cell density of $4\text{-}8\text{x}10^5$ cells/well in 24-well plates (Corning Life Sciences, Amsterdam, the Netherlands), depending on the experiment.

For co-culture experiments with fixed myofibroblast (MFB) quantities (0%, 10%, 25%, 50%, 75%, and 90%), primary CMCs, and MFBs obtained from an earlier isolation (passage 3-4), were counted and mixed in specific, pre-determined ratios before plating. Co-cultures were treated with mitomycin-C (Sigma-Aldrich, St. Louis, MO, USA) to maintain original CMC-fibroblast ratios. All cultures were refreshed daily and cultured in a humidified incubator at 37°C and 5% CO_2.

ANTIPROLIFERATIVE TREATMENT

Antiproliferative treatment of cultures was performed at day 1 of culture. The choice of different types of antiproliferative agents was based on their specific mechanisms of action, thereby allowing a more accurate study of the role of proliferation in arrhythmogeneity, rather than an agent-specific effect.

Different dosages of the antiproliferative agent of interest (mitomycin-C dissolved in PBS; ranging from 10 µg/ml to 0.05 µg/ml or paclitaxel dissolved in DMSO; 0.085 mg/ml, both from Sigma-Aldrich) were diluted in growth medium (Ham's-F10 supplemented with 10% fetal bovine serum (FBS, Invitrogen, Carlsbad, CA, USA), 10% horse serum (HS, Invitrogen), and penicillin (100 U/ml) and streptomycin (100 mg/ml, P/S; Bio-Whittaker, Carlsbad, CA, USA)) and incubated for 2 hours. Cultures were then rinsed twice in PBS and once in a 1:1 mixture of Dulbecco's modified Eagle's medium (DMEM, Invitrogen) and Ham's F10 medium (ICN Biomedicals, Irvine, CA, USA) supplemented with 5% HS and P/S, before being kept on this medium throughout the experiment. Non-treated controls were rinsed identically.

CHARACTERIZATION OF CULTURES

Immunocytochemical analyses
Following mapping experiments, cultures were stained for proteins of interest, or cultures were stained parallel to mapping experiments, as described in earlier studies[1]. Cultures were stained for α-smooth muscle actin (α-SMA) and vimentin expression to study fibroblasts phenotype (Sigma-Aldrich), collagen-I expression to quantify myofibroblast (MFB) numbers (Abcam, Cambridge, MA, USA), Ki67 expression to identify actively proliferating cells (Abcam) and α-actinin as cardiomyocyte-specific marker (Sigma-Aldrich). Furthermore, cultures were also stained for connexin 43 (Cx43) (Sigma-Aldrich) to study gap junction formation between CMCs and MFBs. Alexa donkey-anti-mouse IgG 568 and Alexa donkey-anti-rabbit IgG 488 secondary (Invitrogen) antibodies were used at a dilution of 1:400. For all staining, nuclei were counterstained using Hoechst 3342 (Invitrogen). A fluorescent microscope equipped with a digital camera (Nikon Eclipse, Nikon Europe, Badhoevedorp, the Netherlands) and dedicated software (Image-Pro Plus, version 4.1.0.0, Media Cybernetics, Silver Spring, MD, USA) was used to analyze the cultures. All proteins of interest were studied in at least 6 different cultures from a specific group, from which at least 20 representative images were taken at different magnifications (10, 40, 100x). All cultures were stained using the same solutions and captured using equal exposure times for the protein of interest.

Western-blot analyses
Cx43 expression was studied in a MFB-density dependent manner and correlated with α-SMA expression. Homogenates were made from 3 different purified CMC cultures, 50%/50% CMC/MFB co-cultures and purified MFB cultures, size-fractionated on NuPage 12% Tris-Acetate NuPage gels (Invitrogen) and transferred to Hybond PVDF membranes (GE Healthcare, Waukesha, WI, USA). These membranes were incubated with antibodies against Cx43 or α-SMA (both from Sigma-Aldrich) for 1 h followed by incubation with corresponding HRP-conjugated secondary antibodies (Santa Cruz Biotechnologies,Santa Cruz, CA, USA). β-tubulin (Millipore, Billerica, MA, USA) expression was determined to check for equal protein loading. Chemiluminescence was induced by ECL advance detection reagents (GE Healthcare) and caught on Hyperfilm ECL (GE Healthcare), after which the intensity of Cx43 and α-SMA bands were quantified by Scion Image analysis software (Scion Corporation, Frederick, MD, USA).

Proliferation assays
To assess the effect of antiproliferative treatments on MFB proliferation, MFB cultures were seeded at $5x10^4$ cells/well in a 24-wells plate and stained for Ki67

(Abcam). Ki67 is a cellular marker for cell proliferation, and was quantified for positive staining in MFBs, before and 3 days after treatment. Quantification was performed on 6 cultures from which 8 images were taken per culture at 40x magnification. These cultures were kept on DMEM/Ham's F10 + 5% HS and refreshed daily. Furthermore, collagen-I staining was performed after optical mapping experiments on at least 6 cardiac cultures to determine the number of MFBs in cultures treated with different antiproliferative agents and dosages (mitomycin-C 10 µg/ml, 5 µg/ml, 2.5 µg/ml, 0.5 µg/ml, 0.05 µg/ml) at day 1, 4 and 9. Quantification of total nuclei count, and cells expressing collagen-I was performed on at least 6 images and averaged per culture per timepoint per dosage.

Apoptosis assay
Antiproliferative treatment may lead to increased apoptosis. Therefore, we investigated the expression of active caspase-3 (Abcam), an established marker for apoptosis, in cultures treated with antiproliferative agents and appropriate controls. These cardiac cultures were seeded at $4x10^5$ cells/well in a 24-wells format. The same protocol was used as described earlier for immunocytochemical staining. Total nuclei number and cells expressing active caspase-3 were quantified within the same image and averaged for 6 images per culture for 6 different cultures at 40x magnification.

OPTICAL AND MULTI-ELECTRODE MAPPING
To investigate action potential propagation patterns on a whole-culture scale, cultures ($8x10^5$ cells/well in a 24-wells format), treated with or without antiproliferative agents, were optically mapped with the voltage-sensitive dye di-4-ANEPPS (Invitrogen), on day 4 and 9. For reasons of standardization and reproducibility, only spontaneously active cultures with high degrees of structural and functional homogeneity (determined by light-microscopy and electrophysiological mapping) were included for further analyses. As a result, 95 out of every 100 cultures (wells) were included. On days of mapping experiments, cells were incubated with culture medium (DMEM/Ham's F10 + 5% horse serum) containing 16 µmol/L di-4-ANEPPS for 15±5 minutes. Following incubation, cells were refreshed with DMEM/Ham's F12 (37°C) and immediately mapped. Mapping experiments in a 24-well plate typically did not exceed 30 min. Excitation light (λ_{ex}=525±25nm) was delivered by a halogen arc-lamp (MHAB-150W, Moritex Corporation, San Jose, CA, USA). Fluorescent emission light (λ_{em}>590 nm) was passed through a camera lens (1x Plan-Apo, WD=15 mm; Leica, Wetzlar, Germany) and focused onto a 100 by 100 pixels (100 mm²) CMOS camera (Ultima-L, SciMedia, Costa Mesa, CA, USA) by a 1.6x converging lens, resulting in a total field of view of 256 mm² and a spatial resolution of 160 µm/pixel. During measurements, cultures were kept at 37°C. Electrical

activation was recorded for at least 4 seconds at a rate of 500 frames/s, high-pass filtered and analyzed using Brain Vision Analyze 0909 (Brainvision Inc, Tokyo, Japan). The same culture was never exposed for longer than 40 s to minimize phototoxic effects. Importantly, mapping of the same culture at both day 4 and 9 appeared to be well tolerated as no structural inhomogeneities were observed and CV did not change significantly over time in mitomyocin-C treated cultures.

Each pixels' signal was averaged in a fixed grid of 3x3 pixels. Activation time points were determined at dF/dt_{max}, which corresponds to the timepoint of maximum upstroke velocity. Conduction velocity (CV) in cultures with a uniform activation pattern was calculated between two 3 by 3 pixel grids, typically spaced 2-8 mm apart, and perpendicular to the activation wavefront. For cultures showing reentrant conduction wavefronts, CV was determined similarly at half the maximal distance from the core perpendicular to the wavefront over a length of 2-4 mm. Per culture, CV was determined in 6-fold and averaged for further comparisons. Reentrant cycle length was calculated from 3 separate cycles per culture and averaged. As this study focuses on reentry occurrence and prevention of such arrhythmias, all CV values for reentry and non reentry cultures were pooled within each different group, as this inclusion makes CV a valuable parameter in determining therapeutic effects *in vitro*.

For multi-electrode array (MEA) mapping, cells were cultured in glow-discharged, fibronectin-coated MEA culture dishes (Multi Channel Systems, Reutlingen, Germany) and measurements were performed as described previously (2), typically within 10 seconds after optical mapping.

ASSESSMENT OF ECTOPIC ACTIVITY

Spontaneous ectopic activity was defined as multiple simultaneous or alternating pacemaker sites. In our cultures, 53% of fibrotic cultures (n=47) versus 23% (n=44) in mitomycin-C treated cultures showed ectopic activity spontaneously at day 4. However, at day 9 a high percentage of non-treated cultures showed spontaneous reentry, which continuously excites the cardiac tissue and thereby greatly decreases the possibility of ectopic activity. Therefore, to be able to quantify ectopic activity at day 9, reentry needed to be eliminated in a non-pharmacological manner. For this purpose, we used a custom-made epoxy-coated platinum electrode and performed unipolar stimulation with 6 V for 4 seconds using an electrical stimulus module with corresponding software (Multichannel Systems), which successfully eliminated re-entry in >90% of the cultures. This allowed for spontaneous ectopic activity to resume, which was detected by mapping of the cultures for 24 seconds directly after applying the stimulus. This allowed for quantification of ectopic activity at day 9. To provide a balanced comparative view, these experiments were performed identically at day 4 and 9 in mitomycin-C treated and control cultures.

WHOLE-CELL PATCH-CLAMP

Whole-cell patch-clamp measurements were performed in co-cultures of CMCs and MFBs treated with or without mitomycin-C at day 9 of culture. In addition, MFBs were labeled with eGFP using lenti-viral vectors (LV.CMV.eGFP.HBVPRE; MOI 10), refreshed daily and passaged twice before these cells were co-cultured with CMCs at equal density and ratio at day 9 of free MFB proliferation. After identification of CMCs by phase contrast or fluorescence microscopy, maximal diastolic potentials in CMCs were recorded in current-clamp. Whole-cell recordings were performed at 25°C using a L/M-PC patch-clamp amplifier (3kHz filtering) (List-Medical, Darmstadt, Germany). The pipette solution contained (in mmol/L) 10 Na_2ATP, 115 KCl, 1 $MgCl_2$, 5 EGTA, 10 HEPES/KOH (pH 7.4). Tip and seal resistance were 2.0-2.5 MW and >1 GW, respectively. The bath solution contained (in mmol/L) 137 NaCl, 4 KCl, 1.8 $CaCl_2$, 1 $MgCl_2$, and 10 HEPES (pH 7.4). For data acquisition and analysis, pClamp/Clampex8 software (Axon Instruments, Molecular Devices, Sunnyvale, CA, USA) was used.

DYE TRANSFER

To establish functional coupling between MFBs and CMCs, MFBs were labeled with a lenti-viral vector encoding kathuska (MOI 20). MFBs were kept in culture for 2 weeks and were at least passaged twice before usage in experiments. CMC cultures with a density of 1.0×10^5 cells/well were treated with 10 µg/ml mitomycin-C to prevent endogenous MFB overgrowth. At day 4, these cultures (n=12) were loaded for 30 minutes with calcein-AM (Invitrogen) diluted in HBSS (Gibco), which once internalized is converted to the green fluorescent dye calcein. Cells were rinsed twice with PBS and kept on culture medium containing 2.5 mmol/L probenecid (Invitrogen) to block extracellular leakage. Kathuska labeled MFBs were subsequently plated out in a 1:1 ratio with the calcein-loaded CMCs. Brightfield and fluorescent images (at least 10 per culture) were captured after 24 hours.

PHARMACOLOGICAL INTERVENTIONS

To study the role of Nav1.5 and Cav1.2 channels in the maintenance of reentrant arrhythmias in cultures with high numbers of MFBs, increasing doses of Tetrodotoxin (TTX) (5 and 20 mmol/L; Sigma-Aldrich) were added to the cultures followed by administration of verapamil (100 mmol/L; Centrafarm, Etten-leur, the Netherlands) during optical mapping experiments. As internal control, PBS was administered to the mapping medium prior to pharmacological interventions.

To study the role of Cav1.2 blockade exclusively, arrhythmic cultures were immediately treated with verapamil without prior TTX administration. Both 20 mM TTX and 100 mM verapamil are expected to fully block the targeted ion channels in neonatal rat CMCs[3,4]. The electrophysiological effects of these drugs were evaluated by

optical mapping, directly, 1 min and 5 min after administration. In identical fashion, TTX was administered to mitomyocin-C treated cultures at day 9, showing uniform, rapid activation, and evaluated for persistence of electrical activation.

STATISTICAL ANALYSIS

Statistical analyses were performed using SPSS11.0 for Windows (SPSS Inc., Chicago, IL, USA). Data were compared with one-way or two-factor mixed ANOVA test with Bonferroni post-hoc correction if appropriate, and expressed as mean±SD. Linear correlation analysis was performed by calculating Pearson's correlation coefficient. Comparison between two groups was performed using the student-t test. Differences were considered statistically significant if $p < 0.05$.

REFERENCE LIST

1. Pijnappels DA, Schalij MJ, van Tuyn J, Ypey DL, De Vries AA, van der Wall EE *et al*. Progressive increase in conduction velocity across human mesenchymal stem cells is mediated by enhanced electrical coupling. *Cardiovasc Res* 2006;**72**:282-291.

2. Pijnappels DA, Schalij MJ, Ramkisoensing AA, van Tuyn J, de Vries AA, van der Laarse A *et al*. Forced alignment of mesenchymal stem cells undergoing cardiomyogenic differentiation affects functional integration with cardiomyocyte cultures. *Circ Res* 2008;**103**:167-176.

3. Motlagh D, Alden KJ, Russell B, Garcia J. Sodium current modulation by a tubulin/GTP coupled process in rat neonatal cardiac myocytes. *J Physiol* 2002;**540**:93-103.

4. Verhoeven FA, Moerings EP, Lamers JM, Hennemann G, Visser TJ, Everts ME. Inhibitory effects of calcium channel blockers on thyroid hormone uptake in neonatal rat cardiomyocytes. *Am J Physiol Heart Circ Physiol* 2001;**281**:H1985-H1991.
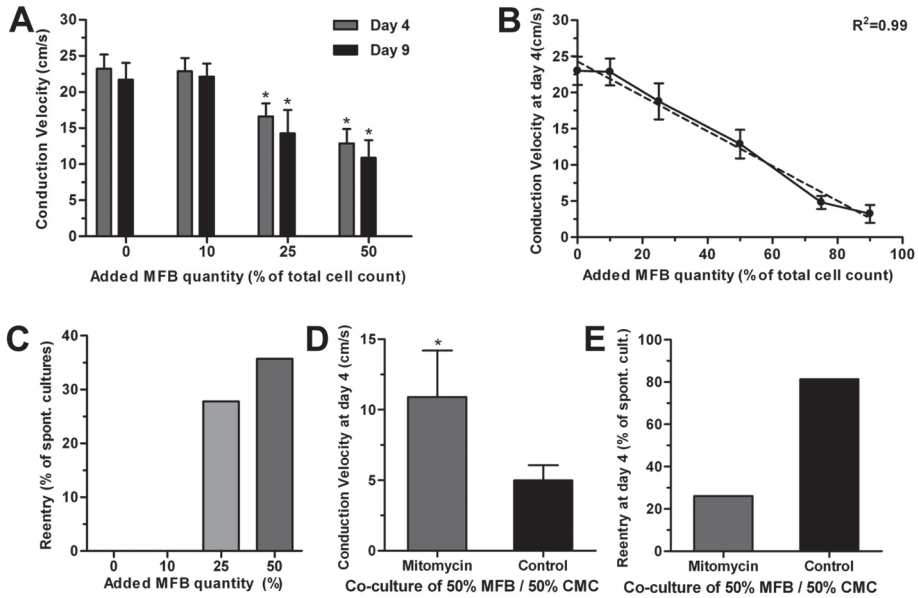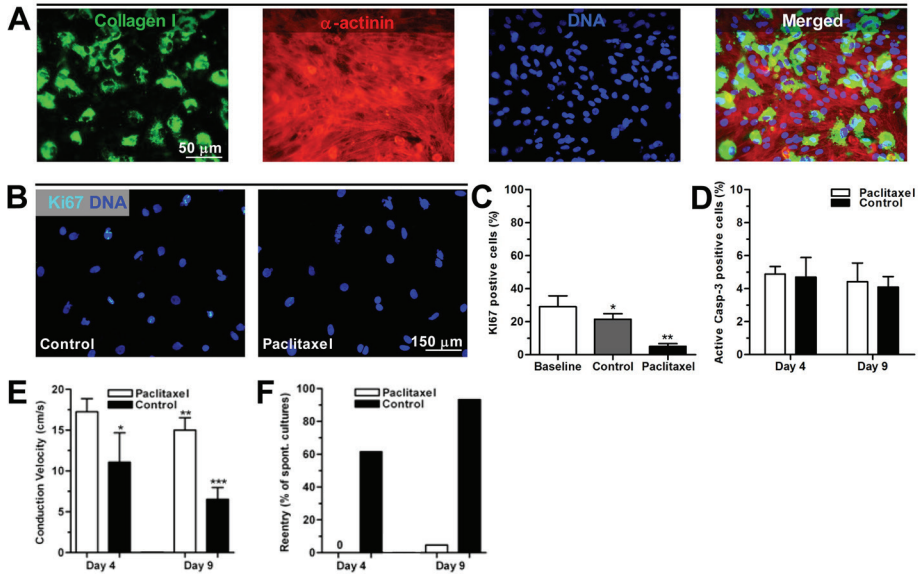
SUPPLEMENTAL FIGURES
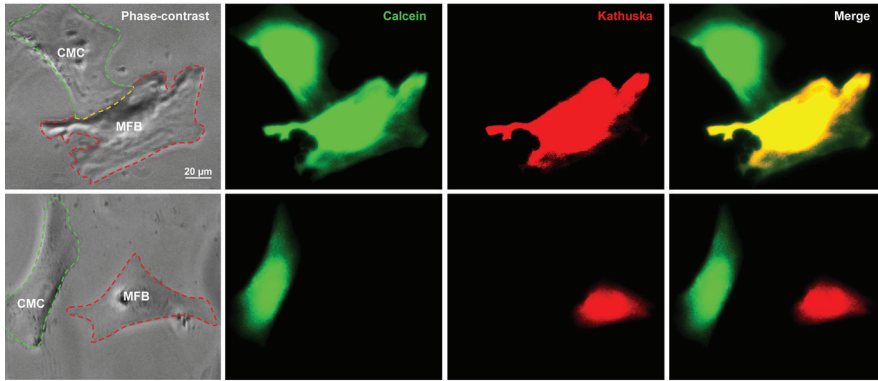
Supplemental figure 1. Dye transfer experiments of CMCs loaded with calcein (green) and MFBs labeled with Kathushka (red). MFBs in direct contact with calcein-loaded CMCs (top) were positive for the gap-junctional permeable green fluorescent dye calcein. In contrast, MFBs that remained separate (bottom) from CMCs were negative for this dye. These results indicate that CMCs and MFBs are functionally coupled.
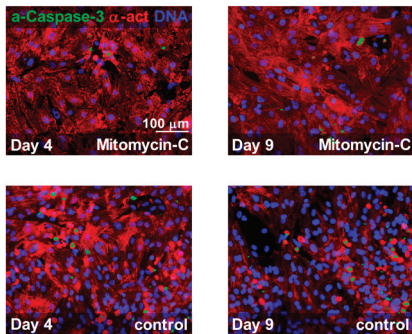
Supplemental figure 2. Mitomycin-C does not increase apoptosis in myocardial cultures. Representative images of immunocytochemical staining for caspase-3 in mitomycin-C treated cultures and control cultures at day 4 and 9. Nuclei were counterstained with Hoechst and caspase-3 positive nuclei were quantified and expressed as a percentage of total cell count, which was not significantly affected by mitomycin-C treatment. Total cell count was defined as the total number of viable nuclei added to the amount of caspase-3 positive cells.

Supplemental figure 3. MFB-CMC co-cultures at predetermined cell density and the effects on conduction abnormalities. (A) CV slows according to plated MFB percentage, except for 10% MFBs. *:p<0.05 vs all. (B) CV at day 4 shows a strong linear association with added MFB percentage. Dotted line represents regression line. (C) Occurrence of spontaneous arrhythmias at day 9 is MFB quantity-dependent and rises with increasing added MFB percentages. (D) Mitomycin-C administration to 50%/50% MFB-CMC co-cultures results in a higher CV at day 4 compared to control. *:p<0.0001 vs control. (E) Uninhibited proliferation of MFBs in a 50%/50% CMC/MFB co-culture results in a 3.1-fold increase in reentry occurrence (n=23) compared to mitomycin-C treated cultures (n=17) of initially identical cellular composition.

Supplemental figure 4. Paclitaxel exhibits anti-arrhythmic effects through MFB prolife-ration inhibition at day 4 and 9 of culture. (A) Immunocytochemical staining for collagen-I (MFB, green) and α-actinin (CMC, red) at day 9 in a paclitaxel-treated cardiac culture. (B) Ki67 staining shows a substantial reduction in positive cells by paclitaxel administration. (C) Quantification of Ki67-positive MFBs before and after paclitaxel treatment. *:p<0.05 vs baseline, **:p<0.05 vs baseline and control. (D) Quantification of apoptotic cells by active caspase-3 staining shows no significant increase in apoptosis by 10 μmol/L paclitaxel. (E) Paclitaxel-treated cultures maintain a higher CV compared to control cultures. *:p<0.05 vs paclitaxel at day 4. **:p<0.05 vs paclitaxel at day 4 and control at day 9. ***:p<0.05 vs control at day 4 and paclitaxel at day 9. (F) Paclitaxel treatment dramatically decreased reentry occurrence compared to control at both day 4 and 9 of culture.
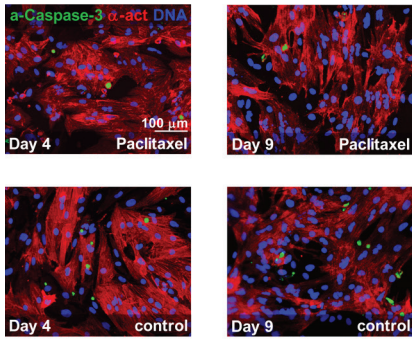
Supplemental figure 5. Paclitaxel does not increase apoptosis in myocardial cultures. Representative images of active caspase-3 immunocytochemical staining in paclitaxel-treated cultures and control cultures at day 4 and 9. Nuclei were counterstained with Hoechst and active caspase-3 positive nuclei were quantified and expressed as a percentage of total cell count, which was not significantly affected by paclitaxel treatment. Total cell count was defined as the total number of viable nuclei added to the amount of caspase-3 positive cells.

CHAPTER VI

MISINTERPRETATION OF COCULTURE DIFFERENTIATION EXPERIMENTS BY UNINTENDED LABELING OF CARDIOMYOCYTES THROUGH SECONDARY TRANSDUCTION: DELUSIONS AND SOLUTIONS

Arti A. Ramkisoensing, MSc, MD; Antoine A.F. de Vries, PhD; Martin J. Schalij, MD, PhD; Douwe E. Atsma, MD, PhD; Daniël A. Pijnappels, PhD.

Laboratory of Experimental Cardiology, Department of Cardiology, Heart Center Leiden, Leiden University Medical Center, Leiden, The Netherlands.

ABSTRACT

Cardiomyogenic differentiation of stem cells can be accomplished by coculture with cardiomyocytes (CMCs). To facilitate their identification, stem cells are often labeled through viral transduction with a fluorescent protein. A second marker to distinguish stem cell-derived CMCs from native CMCs is rarely used. This study aimed to investigate the occurrence of secondary transduction of unlabeled neo-natal rat (nr) CMCs after coculture with human cells that had been transduced 0, 7 or 14 days earlier with a vesicular stomatitis virus (VSV) G protein-pseudo-typed lentiviral vector (LV) encoding enhanced green fluorescent protein (GFP). To reduce secondary LV transfer, GFP-labeled cells were incubated with non-heat-inactivated human serum (NHI) or with VSV-neutralizing rabbit serum (αVSV). Heat-inactivated human serum (HI) and normal rabbit serum were used as controls. Immunostaining showed substantial *GFP* gene transfer to nrCMCs in cocultures started at the day of transduction indicated by the presence of GFP-positive/human lamin A/C-negative nrCMCs. The extent of secondary transduction was significantly reduced in cocultures initiated 7 days after *GFP* transduction, while it was completely abolished when human cells were added to nrCMCs 14 days post-transduction. Both NHI and αVSV significantly reduced the occurrence of secondary transduction compared to their controls. However, under all circumstances, GFP-labeled human cells had to be passaged for 14 days prior to coculture initiation to prevent any horizontal *GFP* gene transfer to the nrCMCs. This study emphasizes that differentiation experiments involving the use of viral vector-marked donor cells should be interpreted with caution and describes measures to reduce/prevent secondary transduction.

INTRODUCTION

Whether somatic stem cells (SSCs) can undergo cardiomyogenic differentiation without genetic intervention is a topic of much debate.[1,2] At least part of the confusion may relate to application of different criteria and methods to identify SSC-derived cardiomyocytes (CMCs) and to the use of SSCs from different sources and differently aged donors.[2-4] Intramyocardial transplantation and coculture with CMCs are commonly used to investigate cardiomyogenic differentiation potential of SSCs. However, these studies often do not include the use of species-, strain- or gender-specific markers to unambiguously demonstrate derivation of a CMC from a stem cell. Instead, stem cells are transduced with a viral vector encoding a fluorescent protein and the appearance of cells coexpressing the fluorescent protein and one or more CMC markers is taken as proof for their cardiomyogenic differentiation.[5-11] An often neglected pitfall of these studies is secondary transduction of CMCs by viral vector-marked stem cells. Pan *et al.* previously showed that hematopoietic target cell-associated vesicular stomatitis virus (VSV) G protein-pseudotyped lentiviral vector (LV) particles can transduce neighboring cells.[12] In this study, secondary transduction of neonatal rat (nr) CMCs by adult human cells that had previously been transduced with an enhanced green fluorescent protein (GFP)-encoding LV was studied. Also, options to abolish secondary transduction were investigated including incubation of LV-GFP-treated cells with VSV-specific antiserum or with normal human serum, which contains natural antibodies that can neutralize VSV in a complement-dependent manner.[13]

MATERIALS AND METHODS

Human tissues were obtained with donors' written informed consent and with approval of the Medical Ethics Committee of Leiden University Medical Center (LUMC). The study conformed to the principles of the Declaration of Helsinki. Animal experiments were approved by LUMC's Animal Experiments Committee and conformed to the Guide for Care and Use of Laboratory Animals (10236).[14]

Adult bone marrow (BM)- or adipose tissue (AT)-derived human mesenchymal stem cells (hMSCs) and human skin fibroblasts (hSFs) were transduced with *GFP* (multiplicity of infection 18 HeLa cell-transducing units/cell) using the VSV G protein-pseudotyped human immunodeficiency virus type 1 vector CMVPRES (hereinafter referred to as LV-GFP).[15,16] This specific vector dose resulted in transduction efficiencies of nearly 100% without causing overt cytotoxicity. The aforementioned cell types and nrCMCs were isolated and cultured as previously described.[17-19] nrCMC cultures typically contained ± 10% cardiac fibroblasts and were mitomycin C-treated to prevent proliferation of the latter cell type.[19] For a schematic overview
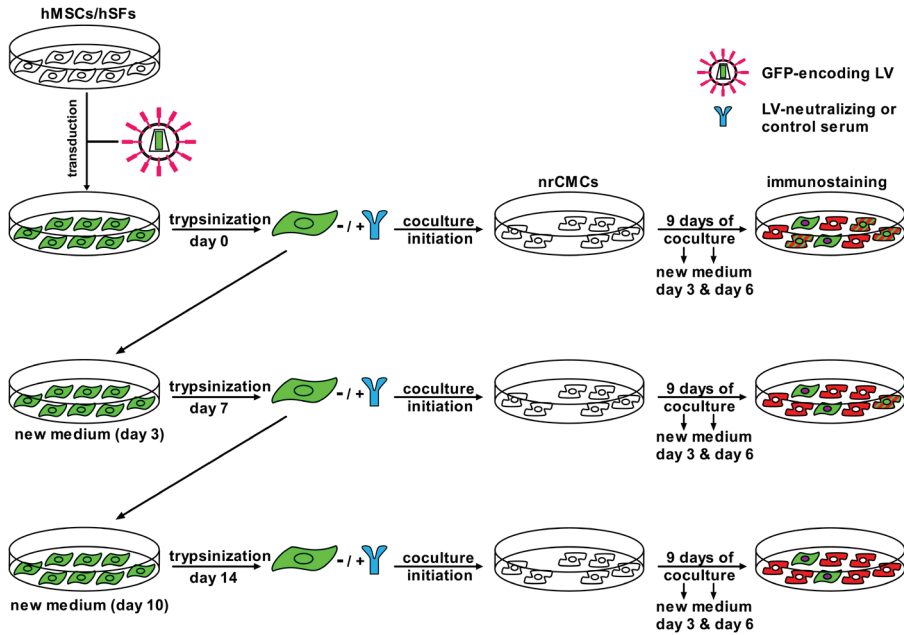
Figure 1. Schematic overview of the experimental setup. After incubation with LV-GFP for 4 hours, hMSCs or hSFs were washed three times with phosphate-buffered saline, detached using buffered 0.05% trypsin-0.02% EDTA solution and either immediately cocultured with nrCMCs (1:10 ratio) or subjected to an additional culture period of 7 or 14 days with 1 or 2 passages, respectively, prior to use in coculture. Medium was refreshed weekly. To reduce secondary transduction, GFP-labeled cells were incubated in NHI or αVSV for 1 h before start of coculture with nrCMCs. Controls were cells incubated with HI and normal rabbit serum, respectively. Neutralization experiments were conducted with freshly transduced human cells, but also with GFP-labeled cells that had been kept in monoculture for 7 or 14 days. After 9 days of coculture, cells were subjected to immunostaining. Abbreviations: LV-GFP, self-inactivating, vesicular stomatitis virus G-protein pseudotyped lentiviral vector coding for GFP; hMSCs, human mesenchymal stem cells; hSFs, human skin fibroblasts; nrCMCs, neonatal rat cardiomyocytes; GFP, enhanced green fluorescent protein; αVSV, vesicular stomatitis virus-neutralizing rabbit serum; NHI, non-heat-inactivated human serum; HI, heat-inactivated human serum.

of the experimental setup see Figure 1. After 9 days of coculture, cells were subjected to immunostaining as previously described.[17] Primary antibodies specific for human lamin A/C (clone 636, VP-L550, Vector laboratories, Burlingame, CA) α-actinin (clone EA53, A7811) and connexin43 (C6219) (both from Sigma-Aldrich, Zwijndrecht, Netherlands) were used. These were visualized with Alexa Fluor-conjugated secondary antibodies, while nuclei were stained using Hoechst 33342 (all from Invitrogen, Breda, Netherlands). Image J software (Institutes of Health, Bethesda, MD) was used to determine the number of GFP-positive/human lamin A/C-negative nrCMCs in randomly chosen regions (³3,000 cells analyzed/condition). Human-specific quantitative RT-PCR analyses were used to detect possible cardiomyogenic differentiation of the human cells after 9 days of coculture with nrCMCs.[17]

Experimental results were expressed as mean±standard deviation for a given number (n) of observations. Data was analyzed by Student's t-test for direct comparisons. Analysis of variance followed by appropriate post-hoc analysis was performed for multiple comparisons. Statistical analysis was performed using SPSS 16.0 for Windows (SPSS, Chicago, IL). Differences were considered statistically significant at $p<.05$.

RESULTS

Cocultures initiated with freshly transduced adult BM hMSCs, AT hMSCs or hSFs contained 51.2±2.1%, 40.6±3.8% and 8.9±0.6% of GFP-labeled nrCMCs, respectively (Figure 2A&D). *GFP* gene transfer to nrCMCs was strongly reduced in cocultures started with human cells 7 days post-transduction (BM hMSCs: 11.1±0.55%, AT hMSCs: 2.60±0.2%, hSFs: 2.10±0.1%; $p<.01$) (Figure 2B&D) and completely abolished using human cells that had been transduced 14 days earlier (Figure 2C&D). In none of the cocultures, expression of human *ACTN2*, *TNNT2*, *NPPA*, *MYL2*, *MYL7*, *GATA4* or *NKX2-5* was observed by quantitative RT-PCR confirming previous findings that hSFs and adult hMSCs do not undergo cardiomyogenesis when coincubated with nrCMCs (Figure 2E).[17]

Secondary transduction was inhibited by treatment of GFP-labeled adult BM hMSCs with non-heat-inactivated human serum (NHI) or VSV-neutralizing rabbit serum (αVSV) prior to coculture initiation. Compared to controls (heat-inactivated human serum and normal rabbit serum, respectively), incubation of the hMSCs with NHI or αVSV significantly reduced *GFP* gene transfer to nrCMCs in cocultures started at the day of transduction ($p<.01$) (Figures 3&4, A1, B1, C) or 7 days later ($p<.01$) (Figures 3&4, A2, B2, C), while hMSCs that had been transduced 14 days before coculture initiation did not give rise to any secondary transduction of nrC-MCs (Figures 3&4, A3, B3, C).
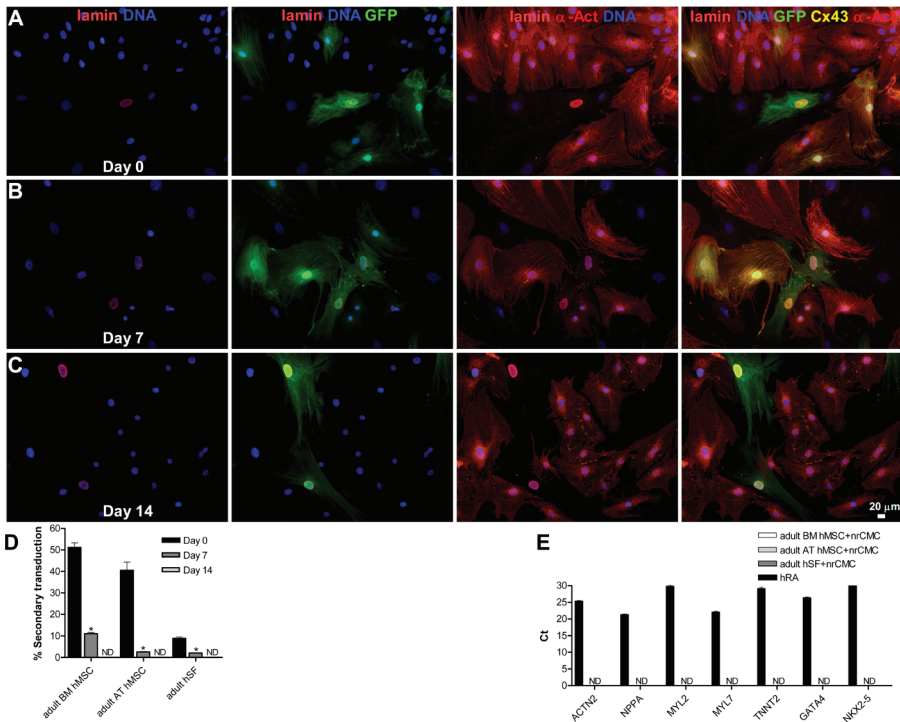
Figure 2. Secondary transduction of nrCMCs after coculture for 9 days with GFP-labeled human cells. (A): Typical fluorescence images of GFP- and human lamin A/C (lamin)-double-positive adult BM hMSCs and of cardiac α-actinin (α-Act)-positive nrCMCs in cocultures initiated at the day of transduction of the human cells with LV-GFP. A considerable number of GFP-positive/human lamin A/C-negative nrCMCs is present after 9 days of coincubation indicating secondary transduction of nrCMCs. Cocultures were also stained for connexin43 (Cx43). Nuclei were stained with the DNA-binding fluorochrome Hoechst 33342. (B): In cocultures that were started 7 days after human cell transduction, adult BM hMSCs showed significant less horizontal *GFP* gene transfer to nrCMCs than those initiated with freshly transduced adult BM hMSCs. (C): Secondary transductions were not observed in mixed cultures of nrCMCs and LV-GFP-transduced adult BM hMSCs that had been passaged twice during a 14-day time period before coculture initiation. (D): Quantitative analysis of secondary transduction of nrCMCs in coculture with LV-GFP-transduced adult BM hMSCs, AT hMSCs or hSFs. The graph is based on a minimum of 3,000 cells analyzed per experimental group and time point. *, $p < .01$. (E): Human-specific qRT-PCR showed that none of the three human cell types expressed the cardiomyocyte marker genes *ACTN2*, *TNNT2*, *NPPA*, *MYL2*, *MYL7*, *GATA4* or *NKX2-5* after 9 days of coculture with nrCMCs. Human right atrium (hRA) samples were used as a positive control. Abbreviations: nrCMCs, neonatal rat cardiomyocytes; GFP, enhanced green fluorescent protein; BM, bone marrow; hMSCs, human mesenchymal stem cells; LV-GFP, self-inactivating, vesicular stomatitis virus G-protein pseudotyped lentiviral vector coding for GFP; AT, adipose tissue; hSFs, human skin fibroblasts; qRT-PCR, quantitative reverse transcription-polymerase chain reaction; ND, not detected.
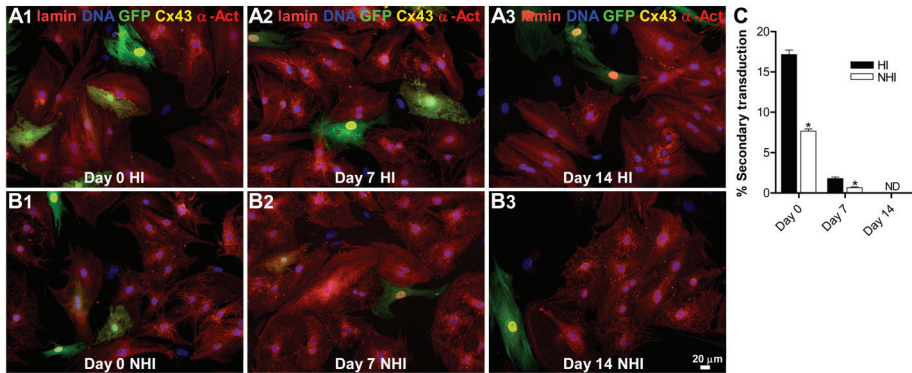
Figure 3. Secondary transduction of nrCMCs is reduced by incubating LV-GFP-transduced adult BM hMSCs with NHI prior to coincubation with nrCMCs. (A1, B1): Typical fluorescence images of 9-day-old cocultures of GFP- and human lamin A/C (lamin)-double-positive cells with cardiac α-actinin (α-Act)-positive nrCMCs initiated at the day of transduction of the human cells with LV-GFP and following their treatment with NHI or HI. Incubation with NHI before coculture initiation leads to a significant reduction of horizontal *GFP* gene transfer to nrCMCs compared to incubation with HI as shown by a lower percentage of GFP-positive/ human lamin A/C-negative nrCMCs (A2, B2): Treatment prior to coculture initiation of adult BM hMSCs that had been transduced 7 days earlier with LV-GFP with NHI resulted in less secondary transduction of nrCMCs than incubation with HI. Also, in cocultures started 7 days after exposure of adult BM hMSCs to LV-GFP the occurrence of secondary transduction was significantly reduced compared to those containing freshly transduced adult BM hMSCs. (A3, B3): Horizontal *GFP* gene transfer to nrCMCs was completely abolished in cocultures initiated 14 days after human cell transduction for both the NHI- and HI-treated adult BM hMSCs. Nuclei were stained with the DNA-binding fluorochrome Hoechst 33342. (C): Quantitative analysis of horizontal *GFP* gene transfer to nrCMCs in coculture with LV-GFP-labeled adult hMSCs that had been treated with NHI or HI before coculture initiation. The graph is based on a minimum of 3,000 cells analyzed per experimental group and time point. *, *p* <.01. Abbreviations: nrCMCs, neonatal rat cardiomyocytes; LV-GFP, self-inactivating, vesicular stomatitis virus G-protein pseudotyped lentivirus vector coding for enhanced green fluorescent protein; BM, bone marrow; hMSCs, human mesenchymal stem cells; GFP, enhanced green fluorescent protein; NHI, non-heat-inactivated human serum; HI, heat-inactivated human serum.
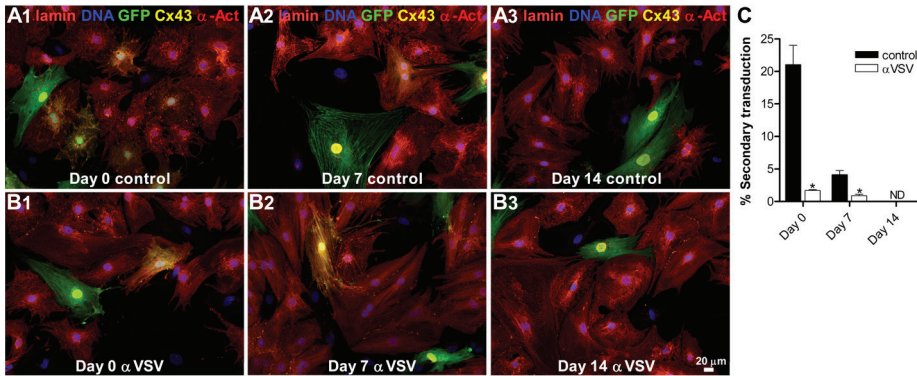
Figure 4. Secondary transduction of nrCMCs is reduced by incubating LV-GFP-transduced adult BM hMSCs with αVSV prior to coincubation with nrCMCs. (A1, B1): Representative micrographs of 9-day-old cocultures of GFP- and human lamin A/C (lamin)-double-positive cells with cardiac α-actinin (α-Act)-positive nrCMCs initiated at the day of transduction of the human cells with LV-GFP and following their treatment with αVSV or normal rabbit serum (control). Incubation with αVSV before coculture initiation leads to a significant reduction of secondary transduction of nrCMCs compared to incubation with normal rabbit serum as shown by a lower percentage of GFP-positive/human lamin A/C-negative nrCMCs (A2, B2): Treatment prior to coculture initiation of adult BM hMSCs that had been transduced 7 days earlier with LV-GFP with αVSV resulted in less secondary transductions of nrCMCs than incubation with control serum. Also, in cocultures started 7 days after exposure of adult BM hMSCs to LV-GFP the occurrence of secondary transduction was significantly reduced compared to those containing freshly transduced adult BM hMSCs. (A3, B3): Horizontal *GFP* gene transfer to nrCMCs was completely abolished in cocultures initiated 14 days after human cell transduction for both the αVSV- and rabbit serum-treated adult BM hMSCs. Nuclei were stained with the DNA-binding fluorochrome Hoechst 33342. (C): Quantitative analysis of secondary transduction of nrCMCs in coculture with GFP-labeled adult BM hMSCs that had been treated with αVSV before coculture initiation. The graph is based on a minimum of 3,000 cells analyzed per experimental group and time point. *, $p < .01$. Abbreviations: nrCMCs, neonatal rat cardiomyocytes; LV-GFP, self-inactivating, vesicular stomatitis virus G-protein pseudotyped lentivirus vector coding for enhanced green fluorescent protein; BM, bone marrow; hMSCs, human mesenchymal stem cells; αVSV, vesicular stomatitis virus-neutralizing rabbit serum; GFP, enhanced green fluorescent protein.

DISCUSSION AND CONCLUSIONS

The key findings of this study are 1) hMSCs, and to a lesser extent, hSFs labeled with GFP by lentiviral gene transfer serve as a reservoir of functional LV particles causing secondary transductions of cocultured nrCMCs. 2) Passaging of the LV-GFP-transduced cells and frequent refreshment of culture medium prior to coculture initiation reduce and ultimately abolish *GFP* gene transfer to nrCMCs over time. 3) Incubation of the LV-GFP-transduced hMSCs with NHI or αVSV before coculture with nrCMCs greatly decreases *GFP* gene transfer to nrCMCs but does not shorten the time needed to completely eliminate secondary transduction. The strong inhibitory effect of NHI and αVSV on the frequency of GFP-labeled nrCMCs indicates that pseudo-transduction or vesicle uptake are not major contributors to the occurrence of GFP-positive nrCMCs in our coculture system.[20] Furthermore, the absence in the cocultures of human lamin A/C-positive cells expressing CMC markers excludes heterocellular fusion as cause for the appearance of GFP-labeled nrCMCs. Our results are in line with those of Pan *et al.*, who showed secondary transduction resulting from release of VSV G protein-pseudotyped LV particles by murine whole BM cells but did not investigate the effects of repeated passaging or treatment with αVSV or NHI of LV-transduced cells on horizontal gene transfer.[12]

CARDIOMYOGENIC DIFFERENTIATION VERSUS SECONDARY TRANSDUCTION

The ability of SSCs to undergo cardiomyogenesis remains a controversial topic. Coincubation with CMCs and intramyocardial transplantation are frequently used to investigate cardiomyogenic differentiation of SSCs.[5-11] In these experiments, the SSCs are often labeled with GFP using viral vectors before coincubation with nrCMCs and their cardiomyogenic differentiation is inferred from the occurrence of GFP-positive cells expressing CMC markers. In our laboratory, an antibody detecting human lamin A/C has been used as a second identifier besides GFP positivity to distinguish human cells from cocultured nrCMCs.[17,18] Also, quantitative RT-PCR with human-specific primer pairs can be used to assess cardiomyogenesis in human cells cocultured with nrCMCs.[17,18] Using this approach, human cardiomyocyte-specific gene expression was not observed even not under conditions that gave rise to high percentages of GFP- and α-actinin-double positive cells. Our finding that coincubation of LV-GFP-treated human cells with untransduced nrCMCs leads to considerable secondary transduction of the latter cells highlights the importance of using an endogenous marker to assess stem cell differentiation in the presence of the differentiated cell type(s) to be generated. This is particularly relevant when the combination of viral vector and target cell does not allow elimination of reidual gene transfer activity by repeated cell passaging/prolonged cell culture as is the case when using episomal viral vectors (e.g. adenoviral vectors) or post-mitotic target cells.

DISCLOSURE

None.

REFERENCES

1. Pijnappels DA, Schalij MJ, Atsma DE. Response to the letter by Rose et al. Circ Res 2009;104:e8.
2. Rose RA, Keating A, Backx PH. Do mesenchymal stromal cells transdifferentiate into functional cardiomyocytes? Circ Res 2008;103:e120.
3. Koninckx R, Hensen K, Daniels A et al. Human bone marrow stem cells co-cultured with neonatal rat cardiomyocytes display limited cardiomyogenic plasticity. Cytotherapy 2009;11:778-792.
4. Rose RA, Jiang H, Wang X et al. Bone marrow-derived mesenchymal stromal cells express cardiac-specific markers, retain the stromal phenotype, and do not become functional cardiomyocytes in vitro. Stem Cells 2008;26:2884-2892.
5. Kodama H, Inoue T, Watanabe R et al. Cardiomyogenic potential of mesenchymal progenitors derived from human circulating CD14+ monocytes. Stem Cells Dev 2005;14:676-686.
6. Nishiyama N, Miyoshi S, Hida N et al. The significant cardiomyogenic potential of human umbilical cord blood-derived mesenchymal stem cells in vitro. Stem Cells 2007;25:2017-2024.
7. Numasawa Y, Kimura T, Miyoshi S et al. Treatment of human mesenchymal stem cells with angiotensin receptor blocker improved efficiency of cardiomyogenic transdifferentiation and improved cardiac function via angiogenesis. Stem Cells 2011;29:1405-1414.
8. Orlandi A, Pagani F, Avitabile D et al. Functional properties of cells obtained from human cord blood CD34+ stem cells and mouse cardiac myocytes in coculture. Am J Physiol Heart Circ Physiol 2008;294:H1541-H1549.
9. Pijnappels DA, Schalij MJ, Ramkisoensing AA et al. Forced alignment of mesenchymal stem cells undergoing cardiomyogenic differentiation affects functional integration with cardiomyocyte cultures. Circ Res 2008;103:167-176.
10. Shinmura D, Togashi I, Miyoshi S et al. Pretreatment of human mesenchymal stem cells with pioglitazone improved efficiency of cardiomyogenic transdifferentiation and cardiac function. Stem Cells 2011;29:357-366.
11. Tsuji H, Miyoshi S, Ikegami Y et al. Xenografted human amniotic membrane-derived mesenchymal stem cells are immunologically tolerated and transdifferentiated into cardiomyocytes. Circ Res 2010;106:1613-1623.
12. Pan YW, Scarlett JM, Luoh TT et al. Prolonged adherence of human immunodeficiency virus-derived vector particles to hematopoietic target cells leads to secondary transduction in vitro and in vivo. J Virol 2007;81:639-649.
13. Beebe DP, Cooper NR. Neutralization of vesicular stomatitis virus (VSV) by human complement requires a natural IgM antibody present in human serum. J Immunol 1981;126:1562-1568.
14. National Institutes of Health. Guide for the Care and Use of Laboratory Animals. 1-1-2002.
15. Seppen J, Rijnberg M, Cooreman MP et al. Lentiviral vectors for efficient transduction of isolated primary quiescent hepatocytes. J Hepatol 2002;36:459-465.
16. van Tuyn J, Pijnappels DA, de Vries AA et al. Fibroblasts from human postmyocardial infarction scars acquire properties of cardiomyocytes after transduction with a recombinant myocardin gene. FASEB J 2007;21:3369-3379.
17. Ramkisoensing AA, Pijnappels DA, Askar SF et al. Human embryonic and fetal mesenchymal stem cells differentiate toward three different cardiac lineages in contrast to their adult counterparts. PLoS One 2011;6:e24164.

18. Ramkisoensing AA, Pijnappels DA, Swildens J et al. Gap Junctional Coupling with Cardiomyo-cytes is Necessary but Not Sufficient for Cardiomyogenic Differentiation of Cocultured Human Mesenchymal Stem Cells. Stem Cells 2012;30:1236-1245.

19. Askar SF, Bingen BO, Swildens J et al. Connexin43 silencing in myofibroblasts prevents arrhyth-mias in myocardial cultures: role of maximal diastolic potential. Cardiovasc Res 2012;93:434-444.

20. Burghoff S, Ding Z, Godecke S et al. Horizontal gene transfer from human endothelial cells to rat cardiomyocytes after intracoronary transplantation. Cardiovasc Res 2008;77:534-543.

CHAPTER VII

ENGRAFTMENT PATTERNS OF HUMAN ADULT MESENCHYMAL STEM CELLS EXPOSE ELECTROTONIC AND PARACRINE PRO-ARRHYTHMIC MECHANISMS IN MYOCARDIAL CELL CULTURES

Arti A. Ramkisoensing, MSc, MD*; Saïd F.A. Askar, MSc*, Douwe E. Atsma, MD, PhD; Martin J. Schalij, MD, PhD; Antoine A.F. de Vries, PhD*; Daniël A. Pijnappels, PhD*.

*Equal Contribution

160 **ABSTRACT**

Background: After intramyocardial injection, mesenchymal stem cells (MSCs) may engraft and influence host myocardium. However, engraftment rate and pattern of distribution are difficult to control *in vivo*, hampering assessment of potential adverse effects. In this study, the role of MSCs engraftment patterns on arrhythmicity in controllable *in vitro* models is investigated.

Methods&Results: Co-cultures of 4×10^5 neonatal rat cardiomyocytes (nrCMCs) and 7% or 28% adult human (h) MSCs in diffuse or clustered distribution patterns were prepared. Electrophysiological effects were studied by optical mapping and patch-clamping. In diffuse co-cultures, hMSCs dose-dependently decreased nrCMC excitability, slowed conduction and prolonged APD_{90}. Triggered activity (14% vs. 0% in controls) and increased inducibility of reentry (53% vs. 6% in controls) were observed in 28% hMSC co-cultures. MSC clusters increased APD_{90}, slowed conduction locally, and increased reentry inducibility (23%), without increasing triggered activity. Pharmacological heterocellular electrical uncoupling increased excitability and conduction velocity to 133% in 28% hMSC co-cultures, but did not alter APD_{90}. Transwell experiments showed that hMSCs dose-dependently increased APD_{90}, APD dispersion, inducibility of reentry and affected specific ion channel protein levels, while excitability was unaltered. Incubation with hMSC-derived exosomes did not increase APD in nrCMC cultures.

Conclusions: Adult hMSCs affect arrhythmicity of nrCMC cultures by heterocellular coupling leading to depolarization-induced conduction slowing and by direct release of paracrine factors that negatively affect repolarization rate. The extent of these detrimental effects depends on the number and distribution pattern of hMSCs. These results suggest that caution should be urged against potential adverse effects of myocardial hMSC engraftment.

INTRODUCTION

Over the past decade, stem cell therapy has been subject of studies aiming to improve function of damaged hearts. Particularly mesenchymal stem cells (MSCs) have been of interest in these efforts.[1,2] In spite of the fact that only low percentages of injected MSCs survive and integrate in damaged myocardium, therapeutic effects have been found in pre-clinical studies.[3,4] Moreover, genetically modified MSCs have also been investigated as vehicles of biological functions such as biological pacemakers.[5] Also, intramyocardial transplantation of bone marrow-derived cells, including human (h) MSCs, into diseased human myocardium has been shown to improve cardiac function.[6] These positive effects on cardiac function are believed to be mainly mediated by paracrine factors released from the transplanted cells.[7] Therefore, increasing engraftment rate to improve the therapeutic effects of transplanted cells seems a logical step and is indeed the focus of current stem cell research.[8,9] However, the risk of adverse effects with higher engraftment rates in largely uncontrolled engraftment patterns is unknown. The number of transplanted cells that actually engrafts and their distribution patterns are difficult to regulate. Only few studies have focused on these aspects. Fukushima *et al.* showed that engraftment patterns of transplanted bone marrow cells may depend on administration route, *i.e.* direct intramyocardial injection resulted in a more clustered distribution than intracoronary infusion.[10] Such clustering may lead to formation of local conduction blocks, potentially facilitating reentrant tachyarrhythmias. Additionally, *in vitro* studies by Chang *et al.* have indicated that administration of hMSCs to myocardial cell cultures may indeed increase pro-arrhythmic risk.[11] However, besides indirect implications that electrotonic coupling of MSCs with host cardiomyocytes may be responsible for their pro-arrhythmic effects, the mechanisms underlying MSC-dependent arrhythmogeneity remain unknown. Also, insights concerning differences between pro-arrhythmic effects of distinct engraftment profiles of MSCs are still limited. As a result, further investigation of potentially pro-arrhythmic actions of hMSCs is required. Such studies are especially important to improve therapeutic efficacy and to contain the hazardous potential of MSC therapy in the heart. Therefore, this study aimed to investigate the effects of engraftment characteristics of MSCs (*i.e.* different numbers and distribution patterns) on arrhythmicity using controllable *in vitro* models. We found that hMSCs can indeed be pro-arrhythmic depending on their number and distribution pattern and that direct contact between neonatal rat ventricular cardiomyocytes (nrCMCs) and hMSCs as well as paracrine effects of hMSCs on nrCMCs are important contributors to the pro-arrhythmic effects of hMSCs. The results of this study suggest that caution is warranted against potential pro-arrhythmic effects of MSC transplantation in cardiac tissue. The acquired knowledge about the mechanisms by which hMSCs can

cause arrhythmias may help to develop strategies how to increase the safety and efficacy of intramyocardial hMSC administration.

MATERIALS AND METHODS

A more detailed description of the materials and methods can be found in the Supplemental Material, which also includes methods of immunocytological stainings, western blot, dye-transfer and patch-clamp experiments.

ISOLATION, CULTURE AND CHARACTERIZATION OF HMSCS

Human tissue samples were collected after having obtained written informed consent of the donors and with the approval of the medical ethics committee of Leiden University Medical Center (LUMC). The procedures used in this investigation conformed to the Declaration of Helsinki. Human MSCs were purified from leftover bone marrow samples derived from adult ischemic heart disease patients (n=4 donors). hMSCs were characterized by immunophenotyping and by their adipogenic and osteogenic differentiation potential as described in the online supplement.

ISOLATION AND CULTURE OF NRCMCS

All animal experiments were approved by LUMC's animal experiments committee and conform to the Guide for the Care and Use of Laboratory Animals, as stated by the US National Institutes of Health (10236).[12] Briefly, hearts were rapidly excised from isoflurane-anesthetized animals, the ventricles were minced into pieces and dissociated by treatment with collagenase type I (450 units/mL; Worthington Biochemical, Lakewood, NJ). The myocardial cells were pre-plated to minimize contamination of the nrCMC cultures with non-cardiomyocytes. Purified myocardial cells were plated on fibronectin (Sigma-Aldrich Chemie, Zwijndrecht, the Netherlands)-coated coverslips in 24-wells plates (Corning Life Sciences, Amsterdam, the Netherlands) at a density of $1\text{-}4\times10^5$ cells/well depending on the experiment. All cultures were treated with 10 µg/mL mitomycin-C (Sigma-Aldrich Chemie) to halt proliferation of endogenous fibroblasts.

CO-CULTURE OF NRCMCS AND CLUSTERED OR DIFFUSELY SPREAD HMSCS

To investigate the effects on arrhythmicity of myocardial engraftment of hMSCs in different patterns and doses, co-cultures of nrCMCs and hMSCs were prepared. To mimic a diffuse engraftment pattern, 4.0×10^5 nrCMCs were mixed with 2.8×10^4 (7%) or 1.12×10^5 (28%) hMSCs and added onto coverslips in wells of a 24-well cell culture plate. To mimic a clustered engraftment pattern, rings with an outer

diameter of 15 mm and a central inner diameter of 3 or 6 mm were lasered in Parafilm M (Bemis Company, Neenah, WI, USA) and attached to the coverslips. Next, hMSCs were applied in these circles (3 mm: 2.8×10^4 cells or 6 mm: 1.12×10^5 cells). After attachment, the Parafilm was removed and the attached hMSCs were overlaid with 4.0×10^5 nrCMCs.

OPTICAL MAPPING

Electrophysiological parameters were determined by optical mapping as described previously.[13] Cultures were loaded with di-4-ANEPPS (Invitrogen, Breda, the Netherlands) for 10 min at 37°C. Cultures were then given fresh DMEM/F12 (Invitrogen) and optically mapped using the Micam Ultima-L optical mapping system (Scimedia USA, Costa Mesa, CA).

ANALYSIS OF THE INFLUENCE OF PARACRINE FACTORS ON ELECTROPHYSIOLOGICAL PARAMETERS OF NRCMC CULTURES

Mitomycin-C-treated adult hMSCs were seeded in 24-well plate transwell inserts (Corning Life Sciences). To mimic as much as possible the conditions of the non-transwell experiments, the inserts contained 2.8×10^4 or 1.12×10^5 hMSCs and were placed above 4.0×10^5 mitomycin-C-treated nrCMCs seeded on fibronectin-coated coverslips. Control cultures consisted of nrCMC cultures with no, empty or nrCMC (1.12×10^5 cells)-filled transwell inserts. In addition, exosomes were derived from hMSCs[14,15] and incubated with nrCMCs cultures for 9 days.

STATISTICS

Experimental data was analyzed by the Mann-Whitney-U test for direct comparisons, or the Wilcoxon signed-rank test for paired observations. For multiple comparisons, the Kruskal-Wallis test with Dunn's *post-hoc* correction was used. Experimental results were expressed as mean±standard deviation (SD) for a given number (n) of observations. Statistical analysis was performed using SPSS 16.0 for Windows (SPSS, Chicago, IL). Differences were considered statistically significant at $P < 0.05$.
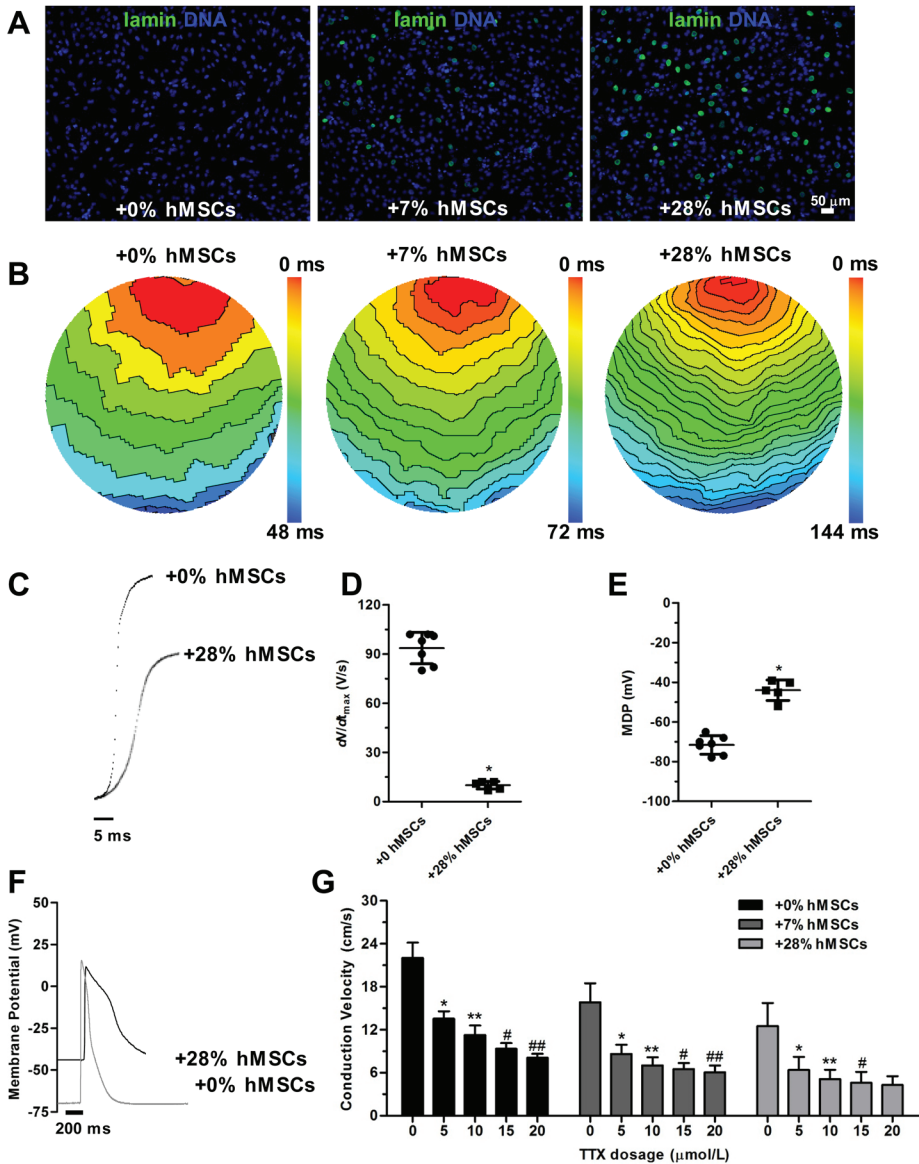
Figure 1. Conduction slowing and decreased excitability in myocardial cell cultures containing diffusely spread hMSCs. (A) Fluorescent microscopy images of myocardial cell cultures containing 0%, 7% or 28% hMSCs stained for human-specific lamin A/C (green). (B) Activation maps of myocardial cell cultures with 0%, 7% or 28% added hMSCs. Isochrones: 6 ms. (C) Typical action potential upstroke traces recorded with current-clamp in nrCMCs in a control culture or in culture with 28% hMSCs. (D) Quantification of maximum depolarization rate (dV/dt$_{max}$). *$P<$0.05 vs. 0% hMSCs. (E) Quantification of MDP recorded in

nrCMCs. *P<0.05 vs. 0% hMSCs. (F) Typical voltage traces from nrCMCs in myocardial cell cultures containing 0% or 28% hMSCs. (G) Quantification of the effect of stepwise increasing TTX dose. *P<0.05 vs. 0 μmol/L TTX, **P<0.05 vs. 5 μmol/L TTX, #P<0.05 vs. 10 μmol/L TTX, ##P<0.05 vs. 15 μmol/L TTX.

RESULTS

DIFFUSELY SPREAD HMSCS DOSE-DEPENDENTLY DECREASE CONDUCTION VELOCITY (CV) AND EXCITABILITY IN MYOCARDIAL CELL CULTURES

Adult hMSCs used in this study fulfilled established identity criteria, as shown in the Online Supplement (Supplemental Figure 1). The pro-arrhythmic effects of hMSCs were first investigated in co-cultures of hMSCs and nrCMCs in which the hMSCs were evenly distributed throughout the monolayer (Figure 1A). Addition of 7% or 28% hMSCs to nrCMCs dose-dependently slowed conduction from 21.6±1.8 cm/s (0% hMSCs, n=15) to 17.1±3.1 (7% hMSCs, n=20) and 12.6±3.2 cm/s (28% hMSCs, n=64, P<0.05 between experimental groups, Figure 1B). Current-clamping of parallel cultures revealed a decrease in upstroke velocity in 28% hMSC-containing myocardial cell cultures (10±2 [n=5] vs. 94±10 V/s [n=7] in control cultures, P<0.05, Figure 1C-D). Moreover, maximal diastolic potentials (MDPs) were less negative for nrCMCs in co-culture with 28% hMSCs (-44±5 [n=5] vs. -72±5 mV [n=7] in control cultures, P<0.05, Figure 1E-F). To study the effects of diffusely spread hMSCs on excitability of nrCMC cultures, CV after administration of the voltage-gated sodium channel blocker tetrodotoxin (TTX) in increments of 5 μmol/L to 20 μmol/L was measured. In co-cultures containing 0% or 7% hMSCs, a TTX concentration-dependent decrease in CV was observed for the entire dose range (Figure 1G). However, in cultures with 28% added hMSCs, the conduction-slowing effect of TTX was saturated between 15 and 20 μmol/L (P>0.05). Moreover, the magnitude of the drop in CV by increasing TTX doses declined with increasing hMSC numbers, indicating diminished availability of Nav1.5 and thereby confirming the ability of hMSCs to decrease excitability.

HMSCS EXERT PRO-ARRHYTHMIC EFFECTS THROUGH ELECTRICAL COUPLING WITH NEIGHBORING NRCMCS

The mechanisms through which hMSCs negatively affect the excitability of nrC-MCs were studied by investigating co-cultures for the expression of N-cadherin, α smooth muscle actinin (αSMA) and connexin-43 (Cx43). Adult hMSCs co-cultured with nrCMCs (n=3,000 hMSCs analyzed) stained negative for αSMA (Supplemental Figure 2A). Also, no N-cadherin was present at hMSC-nrCMC junctions (Supplemental Figure 2B). Cx43 was detected at interfaces between hMSCs and nrCMCs (Figure 2A1), but in lower quantities (20.2±2.2%, $P<0.0001$) than at nrCMC-nrCMC junctions (Figure 2A2). Functional electrical heterocellular coupling between hMSCs and nrCMCs was investigated by dye-transfer experiments. The enhanced green fluorescent protein (GFP)-labeled hMSCs showed a significantly lower dye intensity (18.7±3.0%, $P<0.001$) than adjacent, calcein-loaded nrCMCs (Figure 2B1-B2). Also, although a large fraction of GFP-positive cells had taken up the dye (84.5±4.5%), not all hMSCs were positive for calcein. The lower Cx43 levels at hMSC-nrCMC borders than at nrCMC-nrCMC interfaces were utilized to investigate the effect of heterocellular uncoupling by a low dose of the gap-junctional uncoupler 2-aminoethoxydiphenylborate (2-APB) on conduction in hMSC-nrCMC co-cultures. After administration of 2 μmol/L 2-APB, CV in 19 co-cultures of nrC-MCs and 28% hMSCs rose to 133±16% of the values measured before 2-APB addition (Figure 2C-D), whereas vehicle-treated (0.01% DMSO, n=5) cultures showed no significant change (*i.e.* CV post 0.01% DMSO was 104±8% of CV before 0.01% DMSO). 2-APB increased action potential upstroke velocity from 10±3 to 29±7 V/s (n=4, $P<0.05$). Furthermore, negativity of MDP of nrCMCs increased by 33% to -59±4 mV ($P<0.05$ vs. without 2-APB) while action potential duration until 90% repolarization (APD_{90}) remained unaltered by the 2-APB treatment of the co-cultures (Figure 2E). Importantly, treatment with 2 μmol/L 2-APB did not significantly affect any of these parameters in myocardial cell cultures lacking hMSCs (data not shown).
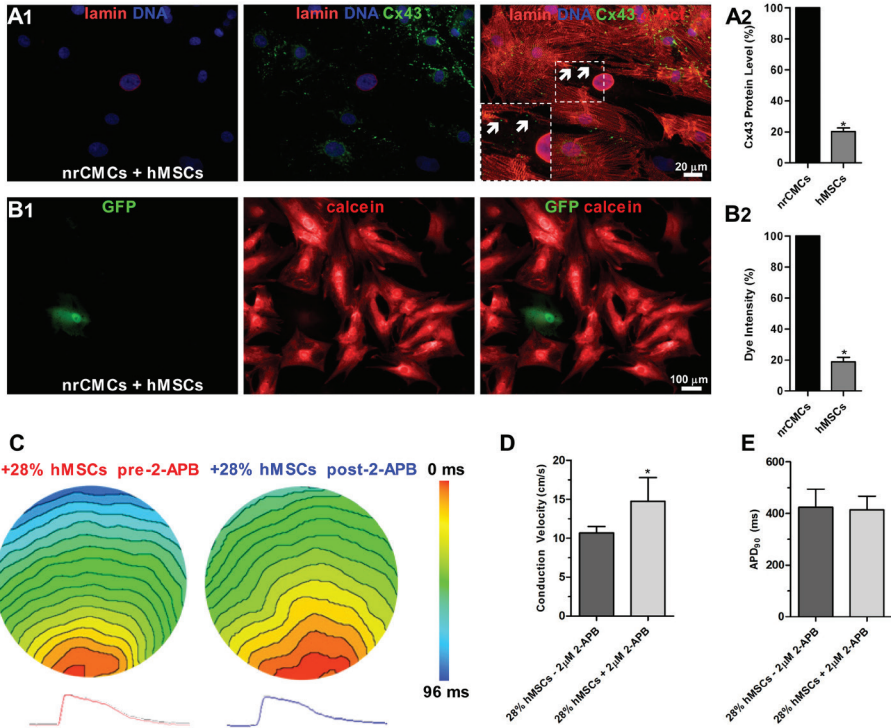
Figure 2. Diffusively spread hMSCs slow conduction through electrotonic coupling. (A1) Immunocytological analyses reveals lower Cx43 (green) levels at heterocellular interfaces between human lamin A/C-positive hMSCs (red) and α-actinin-positive nrCMCs (red/orange) than at homocellular junctions between nrCMCs. (A2) Quantification of junctional Cx43 levels at hMSC-nrCMC and at nrCMC-nrCMC interfaces. *$P<0.001$ vs. nrCMCs. (B1) Dye transfer from nrCMCs to GFP-positive hMSCs. (B2) Quantification of dye intensity in GFP-positive hMSCs. *$P<0.001$ vs. nrCMCs. (C) Activation maps before and after 2-APB administration to a myocardial cell culture containing 28% diffusely spread hMSCs. (D) 2-APB treatment increases CV in myocardial cell cultures with hMSCs. *$P<0.05$ vs. pre-2-APB. (E) Partial uncoupling by 2-APB does not affect repolarization in myocardial cell cultures containing evenly spread hMSCs.
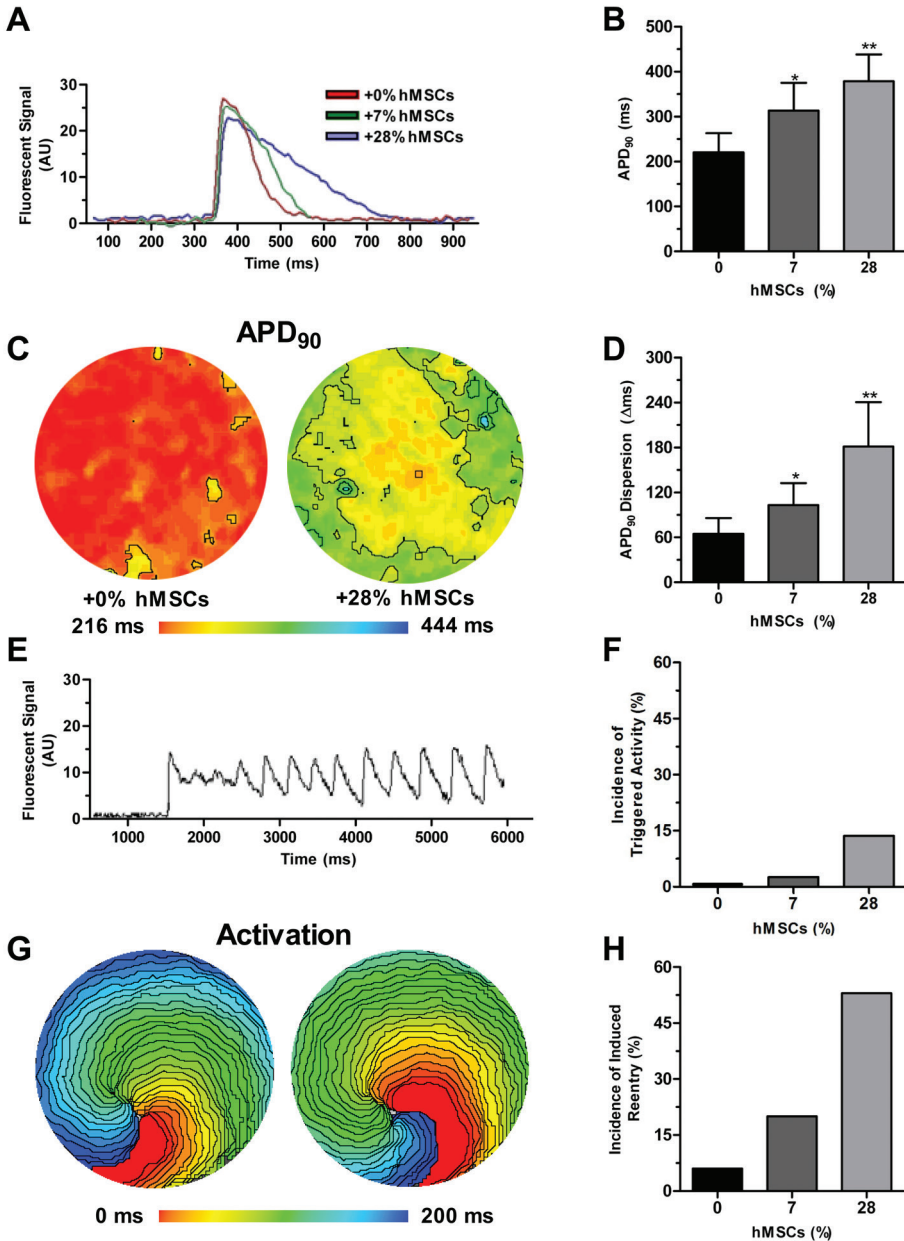
Figure 3. Slowing and dispersion of repolarization in myocardial cell cultures containing diffusely spread hMSCs. (A) Optical traces of myocardial cell cultures containing 0%, 7% or 28% hMSCs show (B) prolongation of repolarization in an hMSC dose-dependent manner. *$P<0.05$ vs. 0 and 28% hMSCs, **$P<0.05$ vs. 0% and 7% hMSCs. (C) APD_{90} maps of myo-

cardial cell cultures reveal (D) an hMSC dose-dependent increase in dispersion of repolarization throughout the entire culture. *$P<0.05$ vs. 0 and 28% hMSCs, **$P<0.05$ vs. 0% and 7% hMSCs. (E) Optical trace of triggered activity in a myocardial cell culture containing 28% hMSCs. (F) Incidence of triggered activity positively correlates with the number of hMSCs in myocardial cell cultures. (G) Activation map of 2 consecutive reentrant activations during a reentrant tachyarrhythmia in a myocardial cell culture containing 28% hMSCs. (H) Inducibility of reentry increases with the number of hMSCs in myocardial cell cultures.

DIFFUSELY SPREAD HMSCS DECREASE REPOLARIZATION RESERVE AND INCREASE ARRHYTHMICITY IN MYOCARDIAL CELL CULTURES

APD_{90} was 314 ± 61 and 379 ± 60 ms in myocardial cell cultures containing 7% (n=24) and 28% hMSCs (n=86), respectively, compared to 221 ± 43 ms in control cultures (n=16) (Figure 3A-B). This corresponds to an hMSC dose-dependent prolongation of repolarization time of 142% and 171%, respectively ($P<0.05$ between all groups). These findings were confirmed with patch-clamp experiments (APD_{60} of 186 ± 10 ms for nrCMCs in control cultures and of 300 ± 21 ms in cultures with 28% added hMSCs [n=5, $P<0.05$]). Optical mapping showed that addition of hMSCs to myocardial cell cultures caused an increase in spatial heterogeneity of repolarization (Figure 3C). In control cultures, the maximal spatial difference between APD_{90} values within the same culture was 65 ± 21 ms (n=18). In cultures with 7% or 28% added hMSCs, APD_{90} dispersion was 103 ± 29 (n=13) and 181 ± 59 ms (n=17), respectively ($P<0.05$, Figure 3D).

Pro-arrhythmic consequences of these findings were revealed by 1 Hz stimulation, which evoked triggered activity in 14% of cultures with 28% added hMSCs (n=66, Figure 3E). Cultures containing 7% hMSCs showed a lower incidence of triggered activity (2.6%, n=39) and triggered activity was absent in control cultures (n=39, Figure 3F). Next, inducibility of reentrant arrhythmias was investigated by applying a burst stimulation protocol (Figure 3G). Reentry was induced in 6% (n=16), 20% (n=10) and 53% (n=15) of cultures containing 0%, 7% and 28% hMSCs, respectively (Figure 3H).

After confirming reproducibility of triggered activity in the same culture, the ATP-sensitive K^+-channel opener P1075 was administered, which abolished all episodes of triggered activity (n=6, Figure 4A, B). As P1075 strongly shortened APD_{90} (Figure 4C) and reduced APD dispersion (Figure 4D) without affecting CV (Figure 4E), reduced repolarization reserve and steeper spatial APD gradients caused by hMSCs seem to be crucial for inducing triggered activity.

Clustered hMSCs provide a substrate for reentry in myocardial cell cultures.
Optical mapping of myocardial cell cultures containing a central cluster of hMSCs revealed local slowing of conduction to 4.7 ± 1.6 and 5.4 ± 1.3 cm/s in hMSC clusters
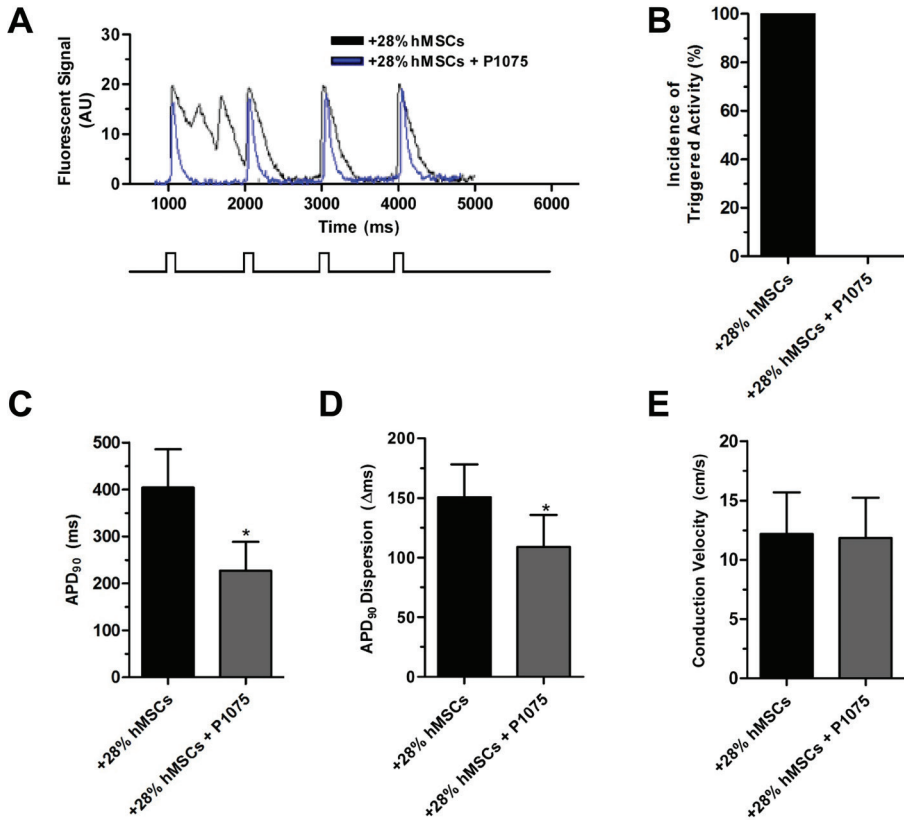
Figure 4. Increasing repolarization reserve lowers the incidence of triggered activity in nrCMC cultures containing diffusely spread hMSCs. (A) Optical traces of a myocardial cell culture with 28% hMSCs before and after P1075 administration, and corresponding (B) incidences of triggered activity. (C) Quantification of APD$_{90}$, (D) APD$_{90}$ dispersion and (E) CV before and after P1075 treatment in myocardial cell cultures with 28% hMSCs. *$P<0.05$ vs. 28% hMSCs.

with a diameter of 3 mm (n=21) and of 6 mm (n=20), respectively (P=NS), whereas CV outside these clusters remained as high as in control cultures (22.2±1.7 and 22.4±1.8 vs. 22.4±2.3 cm/s, P=NS, Figure 5A-C). APD$_{90}$ was prolonged inside the 3-mm hMSC clusters (333±30 vs. 254±58 ms outside, $P<0.05$) and inside the 6-mm hMSC clusters (343±48ms vs 310±40 ms outside, $P<0.05$, Figure 5D-G). Due to these local effects, APD$_{90}$ dispersion was also increased in cultures with a 3- or 6 mm cluster of hMSCs (Figure 5D). Interestingly, APD$_{90}$ in the ring of nrC-MCs around 6-mm hMSC clusters was significantly prolonged (310±40 ms) compared to that in control cultures (245±61 ms) or in the ring of nrCMCs around
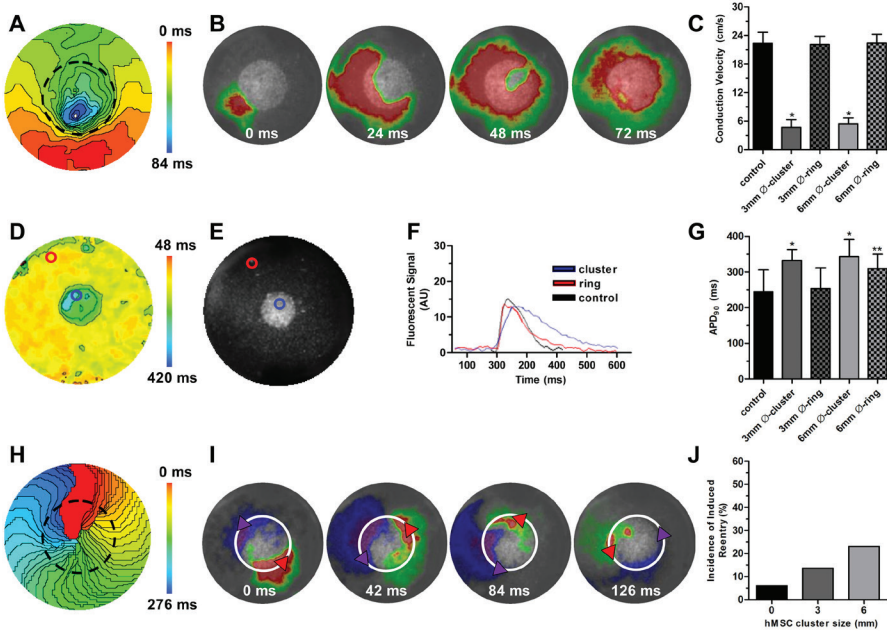
Figure 5. Myocardial cell cultures containing clustered hMSCs are substrates for reentry. (A) Typical activation map of a myocardial cell culture containing 28% hMSCs in a centrally located cluster with a diameter of 6 mm (black dotted line). (B) Pseudo-voltage map sequence projected over a picture of the same culture containing a 6-mm hMSC cluster shows (C) local conduction slowing inside the cluster. *$P<0.05$ vs. outer ring. (D) APD$_{90}$ map of a culture with a 3-mm cluster of hMSCs. (E) Micrograph of a myocardial cell culture with a 3-mm hMSC cluster and (F) traces of action potentials inside (blue) and outside (red) of the hMSC cluster. (G) APD$_{90}$ in myocardial cell cultures containing different-sized hMSC clusters. *$P<0.05$ vs. outer ring, **$P<0.05$ vs. control and outer, 3-mm ring. (H) Activation map and (I) pseudo-voltage map sequence of a reentrant tachyarrhythmia anchored at a 6-mm hMSC cluster (demarcated by black dotted and white line, respectively). (J) The incidence of induced reentry in myocardial cell cultures increases with the size of the centrally located hMSC cluster.

3-mm hMSC clusters (254±58 ms, $P<0.05$ vs. all, Figure 5F-G). No triggered activity was observed in any of these cultures. However, burst stimulation induced reentry in 6% of the control cultures (n=16) and in 14% (n=22) and 23% (n=30) of the cultures with 3- and 6-mm central clusters of hMSCs, respectively (Figure 5H-J). Induced reentrant arrhythmias anchored to the hMSC clusters.

HMSCS RELEASE FREE PARACRINE FACTORS THAT PROLONG REPOLARIZATION BUT DO NOT AFFECT CONDUCTION

To study a possible paracrine contribution[16] to hMSC-induced APD prolongation, transwell experiments were conducted. Transwells with inserts containing 0%, 7% or 28% hMSCs had almost identical CVs of 21.9±0.9, 22.3±1.3 and 22.9±0.7 cm/s (*P*=NS). Additionally, the conduction-slowing effect of TTX was very similar for transwell cultures containing different numbers of hMSCs (*P*>0.05, Figure 6A). However, APD_{90} was dose-dependently affected by hMSCs, as APD_{90} was 227±35 ms for controls (n=38) as compared to 300±91 and 362±88 ms for transwells with inserts containing 7% hMSCs (n=46) and 28% hMSCs (n=45), respectively (*P*<0.05, Figure 6B). Dispersion of repolarization showed a similar positive relation with hMSC numbers, with APD_{90} dispersion values of 78±23, 105±50 and 148±72 ms for transwells whose inserts contained 0%, 7% and 28% hMSCs (Figure 6C). None of the transwell cultures displayed triggered activity. However, inducibility of reentry was slightly increased from 14% (n=29) in controls to 16% (n=44) and 24% (n=38) for transwells with 7% and 28% of hMSCs, respectively (Figure 6D). Patch-clamp experiments also showed a prolonged APD in nrCMCs exposed to the secretome of 28% hMSCs (335±6 ms, n=4) compared to unexposed CMCs (193±7 ms, n=4, *P*<0.05, Figure 7A-B). However, dV/dt_{max} (104±7 V/s vs. 107±9 V/s in controls, *P*=0.72, Figure 7C) and resting membrane potential (-68±4 mV vs. -67±3 mV in controls, *P*=0.72) were unaffected by the hMSC secretome. Western blot analysis of ion channel protein levels in nrCMCs exposed to the hMSC secretome of 28% hMSCs revealed lower levels of Cav1.2 (0.43±0.01 vs. 0.22±0.04 arbitrary units, *P*<0.05) and Kv4.3 (0.26±0.04 vs. 0.22±0.04 arbitrary units, *P*<0.05), while the Kir2.1 level was not significantly altered (0.30±0.03 vs. 0.27±0.05, *P*>0.05, Figure 7D).

To investigate whether exosomes (*i.e.* microvesicles secreted by mammalian cells containing instructive molecules including cytokines, mRNAs and miRNAs) were responsible for these effects, exosomes from the hMSC secretome (representing 28% hMSCs) were added to pure nrCMC cultures and refreshed every 2 days (Figure 8A). At day 9, optical mapping did not reveal any changes in APD_{90} (Figure 8B) or CV (Figure 8C) by adding hMSC-derived exosomes to nrCMC cultures, suggesting that the effect of the hMSC secretome on APD prolongation is primarily mediated by directly secreted factors, rather than by secreted microvesicle-associated factors.
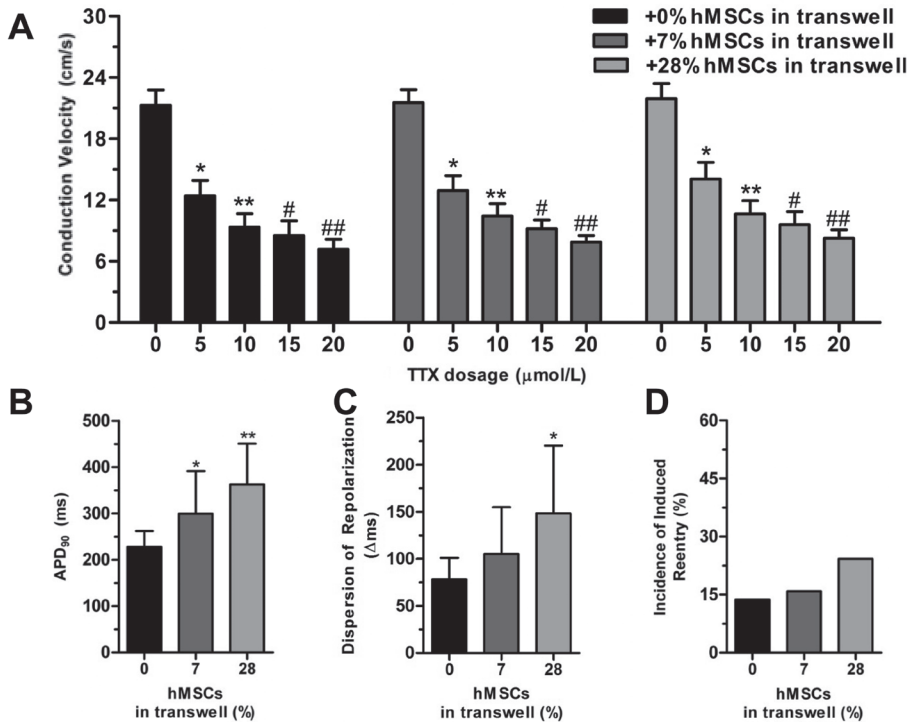
Figure 6. Paracrine mechanisms are responsible for hMSC-dependent prolongation of repolarization in myocardial cell cultures. (A) Dose-dependent effects of Nav1.5 blockade by TTX do not differ between control cultures and myocardial cell cultures exposed to the secretomes of different numbers of hMSCs. *$P<0.05$ vs. 0 μmol/L TTX, **$P<0.05$ vs. 5 μmol/L TTX, #$P<0.05$ vs. 10 μmol/L TTX, ##$P<0.05$ vs. 15 μmol/L TTX. (B) Quantification of APD_{90}. *$P<0.05$ vs. 0% and 28% hMSCs, **$P<0.05$ vs. 0% and 7%. (C) Quantification of dispersion of repolarization. *$P<0.05$ vs. 0%. (D) Incidences of induced reentry in myocardial cell cultures exposed to transwells containing 0%, 7% or 28% of added hMSCs.
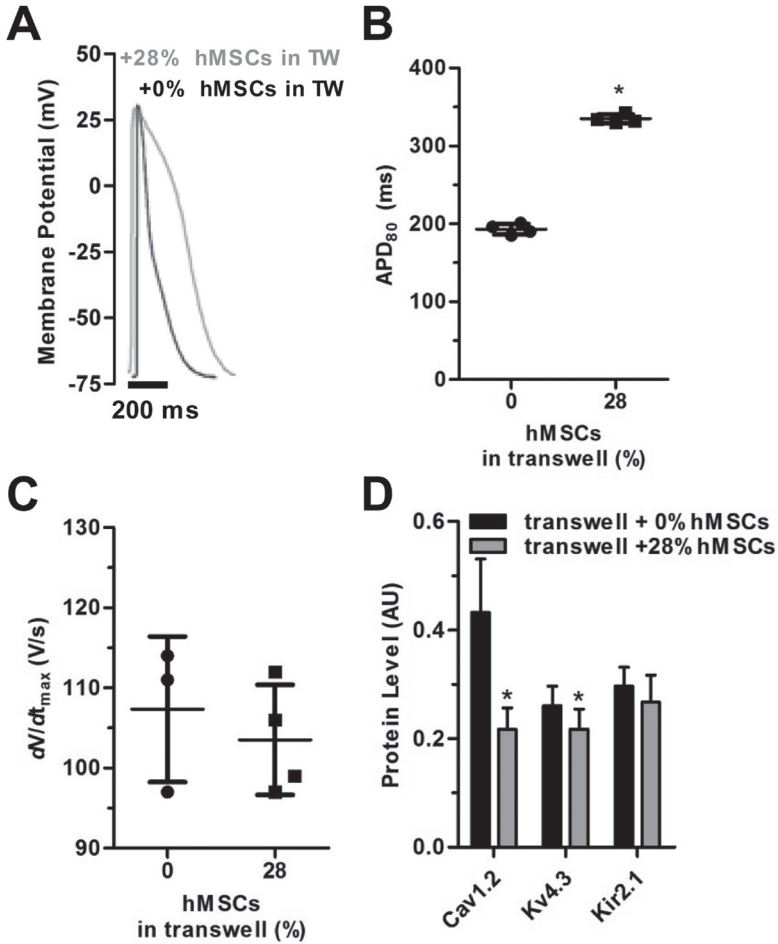
Figure 7. The hMSC secretome also affects nrCMCs at the cellular level. (A) Typical voltage traces of action potentials recorded in current-clamp experiments on nrCMCs subjected to the hMSC secretome and on control nrCMCs show (B) prolonged APD but (C) normal dV/dt_{max}.*$P<0.05$ vs. 0% hMSCs in transwells. (D) Quantification of western blot analyses of Cav1.2, Kv4.3 and Kir2.1 levels. Values are corrected for glyceraldehyde 3-phosphate dehydrogenase (GAPDH) levels. *$P<0.05$ versus transwell + 0% hMSCs. TW: transwell.
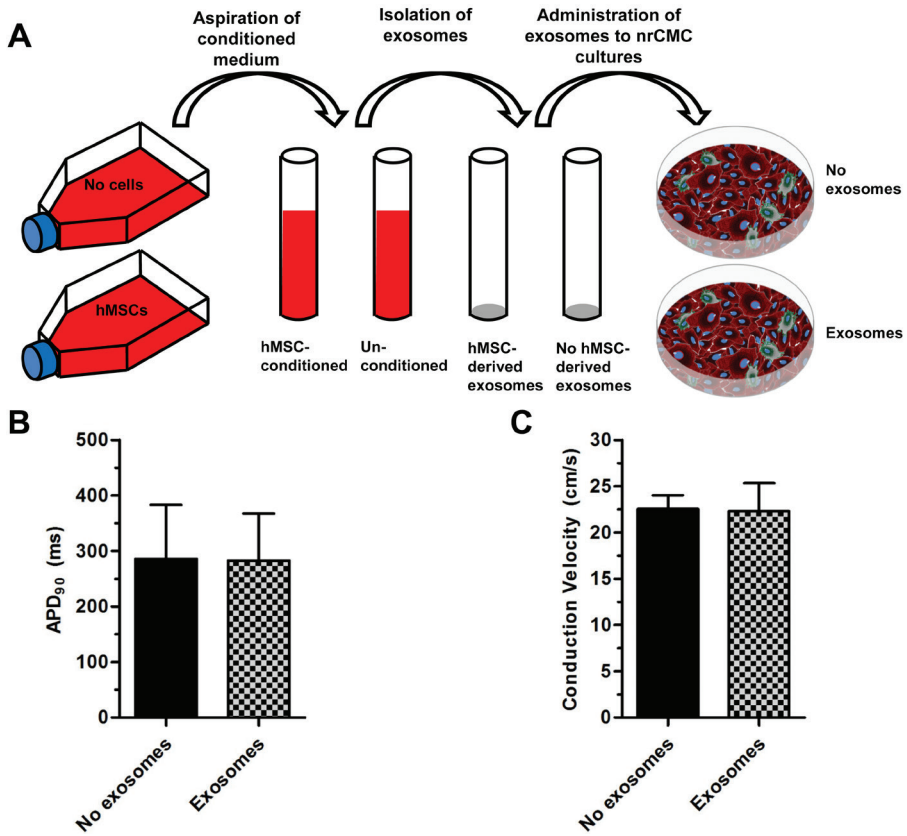
Figure 8. Human MSC-derived exosomes do not appear to exert pro-arrhythmic effects on nrCMCs. (A) Schematic overview of experiments investigating the pro-arrhythmic effects of hMSC-derived exosomes. (B) Adding exosomes to nrCMC cultures does not affect CV or (C) APD_{90} under optical mapping conditions.

DISCUSSION

This study has shown that (i) adult bone marrow-derived hMSCs contribute to APD dispersion, triggered activity and reentrant tachyarrhythmias in neonatal rat myocardial cell cultures; (ii) the pro-arrhythmic effects of hMSCs are mediated by two separate mechanisms, *i.e.* functional coupling of hMSCs with adjacent nrCMCs resulting in partial nrCMC depolarization and conduction slowing, and paracrine signaling of hMSCs to neighboring nrCMCs that slows nrCMC repolarization; and (iii) the number and distribution pattern of the MSCs in the myocardial cell cultures determine the type and severity of the arrhythmias.

EFFECT OF HMSC TRANSPLANTATION ON CARDIAC ELECTROPHYSIOLOGY

Whether and how cardiac cell therapy may increase the risk of ventricular arrhythmias remain topics of debate.[17-20] Gap-junctional coupling between transplanted cells and host cardiomyocytes appears to be essential for functional electrical integration, thereby preventing an increase in electrical heterogeneity, leading to arrhythmias.[21] Other studies have emphasized the role of cell alignment in electrical integration of transplanted cells in recipient myocardium and the potential pro-arrhythmic consequences of malalignment.[22] The number and distribution of donor cells in the host myocardium may also affect their arrhythmogenic potential.[11] However, very little is known about cell therapy-associated pro-arrhythmic mechanisms.

The current study demonstrates that both evenly spread and clustered hMSCs can exert pro-arrhythmic effects in myocardial cell cultures in a dose-dependent manner. However, the types of evoked arrhythmias depended on hMSC distribution pattern. By applying the hMSCs in a diffuse pattern, interactions with surrounding nrCMCs are maximized leading to increases in triggered activity and induced reentry incidence, while in myocardial cell cultures containing central clusters of hMSCs only the propensity towards reentry was increased. Triggered activity in diffuse co-cultures was associated with decreased repolarization reserve as APD shortening by opening of ATP-sensitive K^+-channels abolished such episodes, which together with pseudo-electrogram morphology, points to early afterdepolarizations as likely cause of triggered activity. As the P1075-treated cultures did not show any triggered activity, the concomitant APD shortening by P1075 did not lead to increased reentry incidence.[23]

The mechanism of early afterdepolarizations is considered to be reactivation of L-type calcium channels that linger within the window current due to a decreased repolarizing force.[23] As this mechanism is based on a highly complex and delicate balance between depolarizing and repolarizing forces that depends on activation and (de-)inactivation mechanics of ion channels, the absence of triggered activ-

ity in myocardial cell cultures containing clustered hMSCs can be explained by hMSC density-dependent skewing of action potential dynamics beyond the window current. The notion of density-dependent pro-arrhythmic effects of hMSCs is supported by findings of differences in CV and APD inside the 6-mm hMSC clusters in comparison to equal amounts of more diffusely integrated hMSCs. As hMSC clusters formed local zones of conduction delay and refractoriness, the cluster size-dependent increase in inducibility of reentry is most likely attributable to the increased possibility of spiral wave anchoring with increasing obstacle sizes.[24] Higher inducibility of reentry in cultures with diffusely spread hMSCs than in those containing clustered hMSCs indicates stronger pro-arrhythmic effects of widespread than of locally concentrated hMSC-nrCMC interactions.

ROLE OF HETEROCELLULAR COUPLING IN CONDUCTION SLOWING BY HMSCS

Conduction slowing is widely recognized as a pro-arrhythmic feature that increases the probability of wave front collision, partial conduction block and spiral wave formation.[23] In an earlier study, Chang *et al.* revealed that hMSCs slow conduction in myocardial cell cultures, presumably by electrotonic heterocellular interactions.[11] Two other studies showed the ability of hMSCs to overcome local conduction blocks by functional coupling to nrCMCs and passively and slowly conducting action potentials.[25,26] In the present study, we confirmed slowed conduction by hMSCs in myocardial cell cultures without anatomical conduction block. Importantly, hMSCs were shown to reduce nrCMC excitability as dV/dt_{max} and TTX sensitivity were decreased. Treatment of diffuse co-cultures with low doses of the gap-junctional uncoupler 2-ABP indicated that heterocellular coupling was the dominant mechanism responsible for the conduction-slowing effect of hMSCs. Although 2-APB, as most pharmacological agents, has other known effects, [27,28] these effects occur at higher dosages and cannot account for the increase in CV observed in Figure 2D. Partial heterocellular uncoupling increased CV in co-cultures and nrCMCs showed a more negative MDP and a higher action potential upstroke velocity, which are all indicative of partially restored excitability.[29] Heterocellular mechanical coupling was also investigated in the current study. Myofibroblasts were recently shown to exert pro-arrhythmic effects by providing a non-compliant mechanical resistance through their rigid cytoskeleton, which contains large amounts of αSMA and may thereby activate stretch-activated ion channels in nrCMCs.[30,31] However, the adult hMSCs used in this study did not express αSMA or N-cadherin in co-cultures with nrCMCs, which makes it unlikely that mechanical coupling plays a major role in hMSC-associated conduction slowing and arrhythmicity.

ROLE OF PARACRINE SIGNALING IN REPOLARIZATION SLOWING AND DISPERSION BY HMSCS

In cardiac arrhythmogenesis, prolonged repolarization times and dispersion of repolarization are considered crucial pro-arrhythmic factors for triggered activity and reentrant tachyarrhythmias.[23] Interestingly, while experiments with commercially obtained hMSCs reported no effect of these cells on repolarization or the incidence of triggered activity,[11] the present study provides evidence that clinically used hMSCs from ischemic heart disease patients in co-culture with nrCMCs can prolong repolarization time, increase repolarization dispersion and promote triggered activity, which is likely to be caused by spatial repolarization gradient steepening.[23] The mechanism of decreased repolarization reserve was elusive at first. In contrast to the effects of heterocellular uncoupling between nrCMCs and myofibroblasts,[32] decreasing heterocellular coupling between hMSCs and nrCMCs did not affect APD. However, it is becoming increasingly evident that the hMSC is a cell type with high paracrine activity that secretes a wide variety of directly secreted and exosome/microvesicle-associated factors associated with reverse remodeling and anti-inflammatory and pro-angiogenic activity.[33-35] These findings combined with the APD prolongation at the periphery of co-cultures containing clustered hMSCs, where there is no physical contact between hMSCs and nrCMCs raised the possibility that paracrine rather than electrotonic mechanisms are responsible for the decreased repolarization reserve. Indeed, experiments with hMSCs in transwell inserts to allow passage of the hMSC secretome without physical contact between hMSCs and nrCMCs, revealed hMSC dose-dependent increases in APD, dispersion of repolarization and inducibility of reentry in the nrCMCs seeded on the bottom of the transwell. As hMSC-derived exosomes did not significantly affect nrCMC APD, it is likely that APD prolongation in our model was based on directly secreted paracrine factors. Loss of biological activity of exosomes is unlikely, since they were purified using established procedures.[14,15] The current study has not provided any indication of pro-arrhythmic effects of exosomes purified from hMSC cultures. As exosomes may have a significant contribution to the therapeutic effects caused by the paracrine activity of MSCs, they might therefore represent a safer alternative to cell therapy for improving heart function.[16,36]

Paracrine activity of hMSCs has been associated with beneficial effects in *in vivo* models of cardiac remodeling.[33] A common feature of these models was the low engraftment rate of the hMSCs. As suggested in this study, higher hMSC engraftment rates might lead to increased production of paracrine factors tipping the balance from beneficial to adverse effects. Interestingly, paracrine signaling did not alter conduction or excitability, as the sensitivity of CV to Nav1.5 blockade by TTX remained the same between myocardial cell cultures exposed to the secretome of 0%, 7% or 28% hMSCs. It did, however, change the ion channel levels as revealed

by western blot analyses. In particular, Cav1.2 and Kv4.3 levels were significantly lowered by exposure to the hMSC secretome. While decreased Cav1.2 expression would theoretically shorten APD, lowered Kv4.3 expression prolongs APD by decreasing I_{to}.[37] Since APD prolongation was found both in optical mapping and patch-clamp experiments, the effect of lowered Kv4.3 expression appeared to be dominant in our cultures. The Kir2.1 level was not significantly altered in nrCMCs cultured below hMSC-containing transwell inserts, which is consistent with findings of intact excitability of nrCMCs exposed to the hMSC secretome. Although functional effects of altered ion channel expression are likely, more research is needed to be certain, since paracrine factors may also modulate the activity of proteins involved in cardiac impulse propagation by direct binding to these proteins or by inducing their post-translational modification. For example, a recent study by Desantiago showed that MSCs are able to increase I_{CaL} through the PI3K/Akt pathway.[38] Pinpointing the paracrine factors that are responsible for the pro-arrhythmic effects observed in our study and unraveling their mechanisms of action are subjects of future studies. The findings of the current study may raise cautionary concerns regarding the use of genetically-modified MSCs as biological pacemakers. [5] Such an approach relies on the premise that MSCs are electrically inert, other than their ability to couple to surrounding cells and achieve automaticity by electrotonic interactions. If MSCs modulate electrical behavior via secreted factors, using MSCs as pacemakers may have unintended APD prolonging effects and may increase the pro-arrhythmic risk.

Study Limitations

Due to ethical and technical limitations, cardiomyocytes of human adults could not be not investigated in this study. As an alternative, nrCMCs were used as these cells are available in large amounts and can be maintained in culture as contractile monolayers for the time period needed for mechanistic studies on stem cell engraftment. However, their ion channel expression profile and distribution of gap junctions differs from those of human adult CMCs. Therefore, the comparability of neonatal rat CMCs to adult and clinical situations may be limited. Nevertheless, 2-dimensional *in vitro* models of rat myocardial tissue have shown to be relevant for studying cardiac electrophysiology, by mimicking key electrophysiological processes in the intact heart.[39]

As the current model utilized healthy nrCMCs, the implications of current findings for disease models for stem cell therapy need to be investigated in future studies. To assess the consequences of this study for hMSC transplantation in the heart, our findings should be considered in the context of 3-dimensional, anisotropic myocardium.

CONCLUSION

In myocardial cell cultures, adult hMSCs slow conduction, prolong repolarization, increase spatial dispersion of repolarization and cause triggered activity and reentrant arrhythmias by different mechanisms. Electrotonic coupling of hMSCs to nrCMCs reduces excitability and thereby CV, while the paracrine factors that are directly secreted by hMSCs slows nrCMC repolarization. Thus, caution is warranted against potential pro-arrhythmic effects of MSC transplantation in cardiac tissue. The observation that the pro-arrhythmic activity of hMSCs in co-cultures with nrCMCs is strongly influenced by their number and distribution suggests that by controlling MSC engraftment rate and patterns the critical balance between therapeutic potential and hazardous risk of MSC therapy for cardiac diseases may be tipped in the right direction.

DISCLOSURE

None.

REFERENCES

1. Gerson SL. Mesenchymal stem cells: no longer second class marrow citizens. *Nat Med.* 1999;5:262-264.

2. Prockop DJ. Marrow stromal cells as stem cells for nonhematopoietic tissues. *Science.* 1997;276:71-74.

3. Grauss RW, Winter EM, van TJ, Pijnappels DA, Steijn RV, Hogers B, van der Geest RJ, de Vries AA, Steendijk P, van der Laarse A, Gittenberger-de Groot AC, Schalij MJ, Atsma DE. Mesenchymal stem cells from ischemic heart disease patients improve left ventricular function after acute myocardial infarction. *Am J Physiol Heart Circ Physiol.* 2007;293:H2438-H2447.

4. Pijnappels DA, Gregoire S, Wu SM. The integrative aspects of cardiac physiology and their implications for cell-based therapy. *Ann N Y Acad Sci.* 2010;1188:7-14.

5. Plotnikov AN, Shlapakova I, Szabolcs MJ, Danilo P, Jr., Lorell BH, Potapova IA, Lu Z, Rosen AB, Mathias RT, Brink PR, Robinson RB, Cohen IS, Rosen MR. Xenografted adult human mesenchymal stem cells provide a platform for sustained biological pacemaker function in canine heart. *Circulation.* 2007;116:706-713.

6. van Ramshorst J, Bax JJ, Beeres SL, Dibbets-Schneider P, Roes SD, Stokkel MP, de Roos A, Fibbe WE, Zwaginga JJ, Boersma E, Schalij MJ, Atsma DE. Intramyocardial bone marrow cell injection for chronic myocardial ischemia: a randomized controlled trial. *JAMA.* 2009;301:1997-2004.

7. Segers VF and Lee RT. Stem-cell therapy for cardiac disease. *Nature.* 2008;451:937-942.

8. Cheng K, Li TS, Malliaras K, Davis DR, Zhang Y, Marban E. Magnetic targeting enhances engraftment and functional benefit of iron-labeled cardiosphere-derived cells in myocardial infarction. *Circ Res.* 2010;106:1570-1581.

9. Segers VF and Lee RT. Biomaterials to enhance stem cell function in the heart. *Circ Res.* 2011;109:910-922.

10. Fukushima S, Varela-Carver A, Coppen SR, Yamahara K, Felkin LE, Lee J, Barton PJ, Terracciano CM, Yacoub MH, Suzuki K. Direct intramyocardial but not intracoronary injection of bone marrow cells induces ventricular arrhythmias in a rat chronic ischemic heart failure model. *Circulation.* 2007;115:2254-2261.

11. Chang MG, Tung L, Sekar RB, Chang CY, Cysyk J, Dong P, Marban E, Abraham MR. Proarrhythmic potential of mesenchymal stem cell transplantation revealed in an in vitro coculture model. *Circulation.* 2006;113:1832-1841.

12. National Institutes of Health. Guide for the Care and Use of Laboratory Animals. 1-1-2002. Ref Type: Statute

13. Askar SF, Ramkisoensing AA, Schalij MJ, Bingen BO, Swildens J, van der Laarse A, Atsma DE, de Vries AA, Ypey DL, Pijnappels DA. Antiproliferative treatment of myofibroblasts prevents arrhythmias in vitro by limiting myofibroblast-induced depolarization. *Cardiovasc Res.* 2011;90:295-304.

14. Lasser C, Eldh M, Lotvall J. Isolation and characterization of RNA-containing exosomes. *J Vis Exp.* 2012;e3037.

15. Thery C, Amigorena S, Raposo G, Clayton A. Isolation and characterization of exosomes from cell culture supernatants and biological fluids. *Curr Protoc Cell Biol.* 2006;Chapter 3:Unit.

16. Ranganath SH, Levy O, Inamdar MS, Karp JM. Harnessing the mesenchymal stem cell secretome for the treatment of cardiovascular disease. *Cell Stem Cell.* 2012;10:244-258.

17. Gepstein L. Electrophysiologic implications of myocardial stem cell therapies. *Heart Rhythm.* 2008;5:S48-S52.

18. Ly HQ and Nattel S. Stem cells are not proarrhythmic: letting the genie out of the bottle. *Circulation.* 2009;119:1824-1831.

19. Macia E and Boyden PA. Stem cell therapy is proarrhythmic. *Circulation.* 2009;119:1814-1823.

20. Smith RR, Barile L, Messina E, Marban E. Stem cells in the heart: what's the buzz all about? Part 2: Arrhythmic risks and clinical studies. *Heart Rhythm*. 2008;5:880-887.

21. Abraham MR, Henrikson CA, Tung L, Chang MG, Aon M, Xue T, Li RA, O' Rourke B, Marban E. Antiarrhythmic engineering of skeletal myoblasts for cardiac transplantation. *Circ Res*. 2005;97:159-167.

22. Pijnappels DA, Schalij MJ, Ramkisoensing AA, van TJ, de Vries AA, van der Laarse A, Ypey DL, Atsma DE. Forced alignment of mesenchymal stem cells undergoing cardiomyogenic differentiation affects functional integration with cardiomyocyte cultures. *Circ Res*. 2008;103:167-176.

23. Kleber AG and Rudy Y. Basic mechanisms of cardiac impulse propagation and associated arrhythmias. *Physiol Rev*. 2004;84:431-488.

24. Lim ZY, Maskara B, Aguel F, Emokpae R, Jr., Tung L. Spiral wave attachment to millimeter-sized obstacles. *Circulation*. 2006;114:2113-2121.

25. Beeres SL, Atsma DE, van der Laarse A, Pijnappels DA, van TJ, Fibbe WE, de Vries AA, Ypey DL, van der Wall EE, Schalij MJ. Human adult bone marrow mesenchymal stem cells repair experimental conduction block in rat cardiomyocyte cultures. *J Am Coll Cardiol*. 2005;46:1943-1952.

26. Pijnappels DA, Schalij MJ, van TJ, Ypey DL, de Vries AA, van der Wall EE, van der Laarse A, Atsma DE. Progressive increase in conduction velocity across human mesenchymal stem cells is mediated by enhanced electrical coupling. *Cardiovasc Res*. 2006;72:282-291.

27. Maruyama T, Kanaji T, Nakade S, Kanno T, Mikoshiba K. 2APB, 2-aminoethoxydiphenyl borate, a membrane-penetrable modulator of Ins(1,4,5)P3-induced Ca^{2+} release. *J Biochem*. 1997;122:498-505.

28. Harks EG, Camina JP, Peters PH, Ypey DL, Scheenen WJ, van Zoelen EJ, Theuvenet AP. Besides affecting intracellular calcium signaling, 2-APB reversibly blocks gap junctional coupling in confluent monolayers, thereby allowing measurement of single-cell membrane currents in undissociated cells. *FASEB J*. 2003;17:941-943.

29. Kizana E, Chang CY, Cingolani E, Ramirez-Correa GA, Sekar RB, Abraham MR, Ginn SL, Tung L, Alexander IE, Marban E. Gene transfer of connexin43 mutants attenuates coupling in cardiomyocytes: novel basis for modulation of cardiac conduction by gene therapy. *Circ Res*. 2007;100:1597-1604.

30. Rosker C, Salvarani N, Schmutz S, Grand T, Rohr S. Abolishing myofibroblast arrhythmogenicity by pharmacological ablation of alpha-smooth muscle actin containing stress fibers. *Circ Res*. 2011;109:1120-1131.

31. Thompson SA, Copeland CR, Reich DH, Tung L. Mechanical coupling between myofibroblasts and cardiomyocytes slows electric conduction in fibrotic cell monolayers. *Circulation*. 2011;123:2083-2093.

32. Askar SF, Bingen BO, Swildens J, Ypey DL, van der Laarse A, Atsma DE, Zeppenfeld K, Schalij MJ, de Vries AA, Pijnappels DA. Connexin43 silencing in myofibroblasts prevents arrhythmias in myocardial cultures: role of maximal diastolic potential. *Cardiovasc Res*. 2012;93:434-444.

33. Timmers L, Lim SK, Arslan F, Armstrong JS, Hoefer IE, Doevendans PA, Piek JJ, El Oakley RM, Choo A, Lee CN, Pasterkamp G, de Kleijn DP. Reduction of myocardial infarct size by human mesenchymal stem cell conditioned medium. *Stem Cell Res*. 2007;1:129-137.

34. Williams AR and Hare JM. Mesenchymal stem cells: biology, pathophysiology, translational findings, and therapeutic implications for cardiac disease. *Circ Res*. 2011;109:923-940.

35. Lai RC, Chen TS, Lim SK. Mesenchymal stem cell exosome: a novel stem cell-based therapy for cardiovascular disease. *Regen Med*. 2011;6:481-492.

36. Lai RC, Arslan F, Lee MM, Sze NS, Choo A, Chen TS, Salto-Tellez M, Timmers L, Lee CN, El Oakley RM, Pasterkamp G, de Kleijn DP, Lim SK. Exosome secreted by MSC reduces myocardial ischemia/reperfusion injury. *Stem Cell Res*. 2010;4:214-222.

37.   Hoppe UC, Marban E, Johns DC. Molecular dissection of cardiac repolarization by in vivo Kv4.3 gene transfer. *J Clin Invest*. 2000;105:1077-1084.

38.   Desantiago J, Bare DJ, Semenov I, Minshall RD, Geenen DL, Wolska BM, Banach K. Excitation-contraction coupling in ventricular myocytes is enhanced by paracrine signaling from mesenchymal stem cells. *J Mol Cell Cardiol*. 2012;52:1249-1256.

39.   Tung L and Zhang Y. Optical imaging of arrhythmias in tissue culture. *J Electrocardiol*. 2006;39:S2-S6.

SUPPLEMENTAL MATERIAL

ISOLATION, CULTURE AND CHARACTERIZATION OF HUMAN MESENCHYMAL STEM CELLS (HMSCS)

Human tissue samples were collected after having obtained written informed consent of the donors and with the approval of the medical ethics committee of Leiden University Medical Center (LUMC), where all investigations were performed. Investigations with human tissues conformed to the Declaration of Helsinki. Adult hMSCs were purified from leftover bone marrow (BM) samples derived from ischemic heart disease patients (n=4 donors). Briefly, the mononuclear cell fraction of the BM was isolated by Ficoll density gradient centrifugation, transferred to a 75-cm^2 cell culture flask (Becton Dickinson, Franklin Lakes, NJ) in standard hMSC culture medium (*i.e.* Dulbecco's modified Eagle's medium [DMEM; Invitrogen, Breda, the Netherlands] containing 10% fetal bovine serum [FBS; Invitrogen and incubated at 37°C in humidified 95% air/5%CO$_2$. Twenty-four h after seeding, the non-adherent cells were removed and the remaining hMSCs were expanded by serial passage using standard methods.[1] The hMSCs were characterized according to generally accepted criteria using flow cytometry for the detection of surface antigens and adipogenic and osteogenic differentiation assays to establish multipotency. Surface marker expression was examined after culturing the cells for at least 3 passages. Thereafter, the hMSCs were detached using a buffered 0.05% trypsin-0.02% EDTA solution (TE; Lonza, Vervier, Belgium), suspended in phosphate-buffered saline (PBS) containing 1% bovine serum albumin fraction V (BSA; Sigma-Aldrich Chemie, Zwijndrecht, the Netherlands) and divided in aliquots of 10^5 cells. Cells were then incubated for 30 min at 4°C with fluorescein isothiocyanate- or phycoerythrin-conjugated monoclonal antibodies (MAbs) directed against human CD105 (Ancell, Bayport, MN), CD90, CD73, CD45, CD34 or CD31 (all from Becton Dickinson). Labeled cells were washed three times with PBS containing 1% BSA and analyzed using a BD LSR II flow cytometer (Becton Dickinson). Isotype-matched control MAbs (Becton Dickinson) were used to determine background fluorescence. At least 10^4 cells per sample were acquired and data were processed using FACSDiva software (Becton Dickinson). Established differentiation assays were used to determine the adipogenic and osteogenic differentiation ability of the cells. Briefly, 5×10^4 hMSCs per well were plated in a 12-well cell culture plate (Corning Life Sciences, Amsterdam, the Netherlands) and exposed to adipogenic or osteogenic differentiation medium. Adipogenic differentiation medium consisted of MEM-plus (*i.e.* α-minimum essential medium [Invitrogen] containing 10% FBS, supplemented with insulin, dexamethason, indomethacin and 3-isobutyl-1-methylxanthine (all from Sigma-Aldrich Chemie) to final concentrations of 5 μg/mL, 1 μmol/L, 50 μmol/L and 0.5 μmol/L, respectively, and was refreshed every

3-4 days for a period of 3 weeks. Lipid accumulation was assessed by Oil Red O (Sigma-Aldrich Chemie) staining of the cultures (15 mg of Oil Red O per mL of 60% 2-propanol). Osteogenic differentiation medium consisted of MEM-plus containing 10 mmol/L β-glycerophosphate, 50 µg/mL ascorbic acid and 10 nmol/L dexamethason (all from Sigma-Aldrich Chemie) and was refreshed every 3-4 days for a period of 3 weeks. Osteogenic differentiation was evaluated by histochemical detection of alkaline phosphatase activity and calcium deposition. To measure alkaline phosphatase activity, cells were washed with PBS and subsequently incubated for 5 min with substrate solution (0.2 mg/mL a-naphthyl-1-phosphate [Sigma-Aldrich Chemie] 0.1 mol/L Tris-HCl [pH 8.9], 0.1 mg/mL magnesium sulfate and 0.6 mg/mL Fast Blue RR [Sigma-Aldrich Chemie]). Thereafter, calcium deposits were visualized by staining of the cells for 5 min with 2% Alizarin Red S (Sigma-Aldrich Chemie) in 0.5% NH_4OH (pH 5.5).

NEONATAL RAT VENTRICULAR CARDIOMYOCYTE (NRCMC) ISOLATION AND CULTURE

All animal experiments were approved by LUMC's animal experiments committee and conformed to the Guide for the Care and Use of Laboratory Animals, as stated by the US National Institutes of Health[2] (permit number: 10236). Isolation of nrCMCs from two-day-old neonatal Wistar rats was done essentially as described previously.[3] In brief, hearts were rapidly excised from isoflurane-anesthetized animals and minced into small pieces. After two sequential digestion steps with collagenase type I (450 units/mL; Worthington, Lakewood, NJ), a 75-min pre-plating step was performed to minimize the number of non-cardiomyocytes in the myocardial cell suspension. Next, the resulting cell suspension was passed through a nylon cell strainer with a mesh pore size of 70 µm (Becton Dickinson) to remove cell aggregates and, after counting, the cells were plated on fibronectin (Sigma-Aldrich Chemie)-coated round glass coverslips in 24-well cell culture plates (Corning Life Sciences, Amsterdam, the Netherlands) at a density of $1-4\times10^5$ cells/well depending on the experiment. To stop cell proliferation and to maintain the initial established ratios between cell types, cultures were incubated for 2 h with 10 µg/mL mitomycin-C (Sigma-Aldrich Chemie) at day 1 of culture. Culture medium was refreshed daily, except in experiments investigating paracrine effects. In these experiments, cells received fresh medium every 2 days to allow for sufficient exposure to paracrine factors. Cultures were refreshed with DMEM/Ham's F10 culture medium (1:1, v/v; both from Invitrogen) supplemented with 5% horse serum (HS; Invitrogen) and cultured in a humidified incubator at 37°C and 5% CO_2.

PREPARATION OF CO-CULTURES BETWEEN NRCMCS AND CLUSTERED OR DIFFUSELY SPREAD HMSCS

To investigate in an *ex vivo* model system the effects of myocardial engraftment of hMSCs in different patterns and doses on arrhythmogeneity, co-cultures of nrC-MCs and hMSCs were prepared. To mimic a diffuse engraftment pattern, 4.0×10^5 nrCMCs with mixed with 2.8×10^4 (7%) or 1.12×10^5 (28%) hMSCs and added onto a fibronectin-coated glass coverslip in a well of a 24-well cell culture plate. To mimic a clustered engraftment pattern, the hMSCs were applied to the center of a glass coverslip in a circle with a diameter of 3 mm (2.8×10^4 cells) or of 6 mm (1.12×10^5 cells). To keep the hMSCs centered, rings with an outer diameter of 15 mm and an inner diameter of 3 or 6 mm were lasered in Parafilm M (Bemis Flexible Packaging, Neenah, WI, USA) using a PLS3.60 laser (Universal Lasersystems. Scottsdale, AZ). Next, these rings were sterilized with 70% ethanol and attached to fibronectin-coated coverslips. A drop of hMSC suspension was then applied to the center of each ring and the cells were allowed to adhere for at least 2 h. Finally, the rings of Parafilm M were removed and 4.0×10^5 nrCMCs were plated out on top of the hMSC cluster.

ELECTROPHYSIOLOGICAL MEASUREMENTS IN CO-CULTURES OF NRCMCS AND HMSCS

To facilitate the identification of hMSCs in co-cultures with nrCMCs, these cells were labeled with enhanced green fluorescent protein (GFP) using the vesicular stomatitis virus G protein-pseudotyped, self-inactivating human immunodeficiency virus type 1 vector CMVPRES,[4] essentially as described by van Tuyn *et al*.[5] At day 9 of culture, co-cultures of nrCMCs and GFP-labeled hMSCs in a diffuse or clustered pattern were subjected to whole-cell patch-clamp experiments in parallel to optical mapping experiments. Whole-cell current-clamp recordings were performed at 25ºC using an L/M-PC patch-clamp amplifier (List Medical, Darmstadt, Germany) with 3 kHz filtering. Pipette solution contained (in mmol/L) 10 Na_2ATP, 115 KCl, 1 $MgCl_2$, 5 EGTA, 10 HEPES/KOH (pH 7.4). Tip resistance was 2.0 – 2.5 MΩ, and seal resistance >1 GΩ. The bath solution contained (in mmol/L) 137 NaCl, 4 KCl, 1.8 $CaCl_2$, 1 $MgCl_2$, 10 HEPES/KOH (pH 7.4). For data acquisition and analysis pClamp/Clampex8 software (Axon Instruments, Molecular Devices, Sunnyvale, CA) was used. Current-clamp recordings were performed in unlabeled nrCMCs adjacent to GFP-labeled hMSCs. For partial uncoupling experiments, nrCMCs were studied after 20 min of incubation with 2-aminoethoxydiphenyl borate (2-APB; Tocris, Ballwin, MO).

OPTICAL MAPPING

Electrophysiological parameters were determined by optical mapping as described previously.[6] In brief, nrCMC-hMSC co-cultures were loaded with 6 µmol/L of the

voltage-sensitive dye di-4-ANEPPS (Invitrogen) diluted in DMEM/Ham's F12 culture medium (Invitrogen) for 10 min at 37°C in humidified 95% air/5%CO_2. Subsequently, the culture medium was replaced by fresh DMEM/Ham's F12 and the cultures were optically mapped using the Micam Ultima-L optical mapping system (SciMedia USA, Costa Mesa, CA). Optical signals were recorded and analyzed using Brainvision Analyze 1108 (Brainvision, Tokyo, Japan). Cultures were electrically stimulated with a 10 ms pulse at ≥1.5× diastolic threshold and paced at 1 Hz (Multichannel systems, Reutlingen, Germany) to determine conduction velocity (CV) and action potential duration at 90% of full repolarization (APD_{90}), as well as dispersion of repolarization. Dispersion of repolarization was calculated as the maximal spatial difference in APD_{90} within the same culture. Areas of dispersion analysis were at least 4×4 pixels. Inducibility of reentry was tested by applying a bipolar, 14-Hz burst stimulation protocol. Reentry was defined as >2 consecutive circular activations. For partial uncoupling experiments, cultures were mapped before and after 20 min of incubation with 2-APB. The principle of partial uncoupling was based on the low connexin 43 (Cx43) plaque density at heterocellular hMSC-nrCMC junctions as compared to that at homocellular nrCMC-nrCMC junctions. This renders the gap junctional communication between nrCMCs and hMSCs more sensitive to uncoupling by 2 µmol/L of 2-APB than that between nrCMCs and nrCMCs. Thus, treatment of the co-cultures with 2-APB could effectively uncouple hMSCs from nrCMCs while preserving nrCMC reserves of Cx43 necessary for conduction. Although 2-APB may have other known effects, these are not expected to be active at the used dosages[7,8] and are not expected to increase conduction velocity.

To study the effects of fast sodium channel blockade, cultures were successively exposed to 5, 10, 15 and 20 µmol/L tetrodotoxin (TTX; Alomone Labs, Jerusalem, Israel) by stepwise increasing the drug concentration. The influence of APD on arrhythmicity was studied using the ATP-sensitive potassium channel opener P1075 (10 µmol/L; Tocris).

ANALYSIS OF MARKERS INVOLVED IN MECHANICAL AND ELECTRICAL COUPLING
Alpha smooth muscle actin (αSMA) and N-cadherin, proteins involved in mechanical coupling, were visualized by immunostaining as described previously.[1] In short, on day 9 after culture initiation, the co-cultures of nrCMCs and adult BM hMSCs were fixed on ice with 4% formaldehyde in PBS for 30 min, washed with PBS, permeabilized with 0.1% Triton X-100 in PBS for 5 min at 4°C and rinsed again with PBS. To decrease non-specific antibody binding, the cells were next incubated at room temperature with 0.1% donkey serum (Sigma-Aldrich Chemie) in PBS for 30 min. Thereafter, the co-cultures were incubated overnight at 4°C with an αSMA-specific mouse MAb (clone 1A4; A2547; Sigma-Aldrich Chemie) or with an N-cadherin-specific mouse MAb (clone ID-7.2.3; C3825; Sigma-Aldrich Chemie) diluted

1:400 and 1:100, respectively, in PBS containing 0.1% donkey serum. To distinguish nrCMCs from hMSCs, co-cultures were stained with a rabbit polyclonal antibody (PAb) recognizing the striated muscle-specific protein troponin I (H-170; Santa Cruz Biotechnology, Santa Cruz, CA; dilution 1:100). Binding of the primary antibodies to their target antigen was visualized using Alexa Fluor 568-conjugated donkey anti-mouse IgG and Alexa Fluor 488-conjugated donkey anti-rabbit IgG (both from Invitrogen) at dilutions of 1:200. hMSCs in the co-cultures were identified by labeling with a human lamin A/C-specific murine MAb (clone 636; Vector Laboratories, Burlingame, CA; dilution 1:200). Lamin A/C staining was visualized with Qdot 655-streptavidin conjugates (Invitrogen; dilution 1:200) after incubation of the cells with biotinylated goat anti-mouse IgG2b secondary antibodies (Santa Cruz Biotechnology; dilution 1:200). Nuclei were stained by incubating the cells for 10 min at room temperature with 10 µg/mL Hoechst 33342 (Invitrogen) in PBS.

The expression of the gap junctional protein Cx43, which plays an important role in the electrical coupling of nrCMCs, was also studied by immunocytological stainings. Co-cultures of nrCMCs and hMSCs were stained with a Cx43-specific rabbit PAb (C6219; Sigma-Aldrich Chemie) and with a mouse MAb recognizing sarcomeric α-actinin (clone EA53; Sigma-Aldrich Chemie; dilution 1:200). The primary antibodies were visualized using Alexa Fluor 568-coupled donkey anti-mouse IgG and Alexa Fluor 488-linked donkey anti-rabbit IgG secondary antibodies at dilutions of 1:200 (both Invitrogen). Again, the hMSCs in the co-cultures were identified by labeling with a human lamin A/C-specific murine MAb as described above. Nuclei were stained using a 10 µg/mL solution of Hoechst 33342 in PBS. Cells that went through the entire staining procedure but were not exposed to primary antibodies served as negative controls. A fluorescence microscope equipped with a digital color camera (Nikon Eclipse 80i; Nikon Instruments Europe, Amstelveen, the Netherlands) and dedicated software (NIS Elements [Nikon Instruments Europe] together with ImageJ [version 1.43; National Institutes of Health, Bethesda, MD]) were used for data analysis. ImageJ was used to determine the intensity of the Cx43-associated fluorescence in several randomly chosen, equally-sized border regions between hMSCs and nrCMCs and between adjoining nrCMCs. Fluorescent images of cells stained with the same antibody were always recorded with the same exposure time.

ANALYSIS OF FUNCTIONAL COUPLING

Dye transfer assays were used to directly determine functional heterocellular coupling between nrCMCs and GFP-positive hMSCs. Four days after cell isolation, nrCMC cultures with a density of 2×10^5 cells per well in a 12-well cell culture plate (Corning Life Sciences) were loaded with dye by incubation for 15 min with 4 mmol/L calcein red-orange AM (calcein; Invitrogen) in Hank's balanced

salt solution (Invitrogen). Thereafter, the cells were rinsed three times with PBS and were kept in the incubator in nrCMC culture medium supplemented with 2.5 mmol/L Probenecid (Invitrogen) for ³30 min before 2×10^4 GFP-positive hMSCs (n=3 cultures for each of the 4 hMSC isolates) were added. Probenecid blocks organic anion transporters located in the plasma membrane thus preventing calcein efflux from the dye-loaded nrCMCs. Fluorescent images (³30 per group) were captured after 8 h and evaluated in a blinded manner. In all experimental groups, GFP-positive hMSCs surrounded by the same number of nrCMCs were analyzed. ImageJ was used to determine the intensity of the calcein-associated fluorescence in several randomly chosen, equally-sized subcellular regions for both the GFP-positive hMSCs and the adjoining nrCMCs. To correct for possible variations in calcein loading efficiency, the dye intensity in the GFP-positive hMSCs was expressed as a percentage of that in the surrounding nrCMCs. The percentage of calcein-positive cells among the GFP-labeled hMSCs was also determined by counting these cells in ³60 fields of view per experimental group.

ANALYSIS OF THE INFLUENCE OF PARACRINE FACTORS ON NRCMC CULTURES

To investigate the influence of hMSC paracrine factors on the electrophysiological properties of nrCMC cultures, transwell experiments were conducted. Mitomycin-C-treated adult hMSCs were seeded in 24-well plate transwell inserts (membrane diameter: 6.5 mm, surface area: 0.33 cm², membrane pore size: 0.4 μm; Corning Life Sciences). To allow direct comparison with the previously described co-culture experiments, the transwell inserts contained 2.8×10^4 or 1.12×10^5 hMSCs, which were placed above 4.0×10^5 mitomycin-C-treated nrCMCs seeded on fibronectin-coated coverslips. Control cultures consisted of nrCMC cultures with empty transwells, nrCMC cultures without transwells and nrCMC cultures with transwells containing 1.12×10^5 nrCMCs. All cultures included in these experiments were refreshed with standard nrCMC culture medium every 2 days. To confirm optical mapping results, patch-clamp experiments were also performed on nrCMCs exposed to the hMSC secretome using the transwell cell culture system and on nrCMCs of control cultures.

WESTERN BLOT ANALYSES

To investigate Cav1.2, Kir2.1 and Kv4.3 levels, western blot analyses were performed on whole-cell protein extracts obtained from nrCMC layers cultured under transwell inserts containing hMSCs or no cells. Proteins were extracted by homogenization using RIPA buffer (150 mM NaCl, 1% Nonidet P-40, 0.5% sodium deoxycholate, 0.1% SDS, 50 mM Tris-HCl [pH 8.0] supplemented with protease inhibitors [cOmplete, Mini Protease Inhibitor Cocktail Tablets from Roche Diagnostics Nederland, Almere, the Netherlands]). At least 5 samples comprised of ≥2 cultures per

group were used. Total protein (10 µg/lane) was loaded onto NuPage 10% Bis-Tris gels (Invitrogen) and electrophoresis was performed for 2 h at 150 V, after which proteins were transferred to Hybond-P polyvinylidene difluoride membranes (GE healthcare, Diegem, Belgium) overnight using a wet blotting system. After blocking for 1 h at room temperature with 10 mmol/L Tris-HCl (pH7.6), 0.05% Tween-20 and 150 mmol/L NaCl (TBST) containing 5% BSA, the membranes were incubated for 1 h at room temperature with primary antibodies diluted in TBST-5% BSA. The primary antibodies were affinity-purified rabbit anti-mouse Cav1.2 (ACC-003; Alomone labs; dilution: 1/500), rabbit anti-human Kir2.1 (APC-026; Alomone labs; dilution: 1/1,000) and rabbit anti-rat Kv4.3 (P0358; Sigma-Aldrich Chemie; dilution: 1/1,000). For normalization purposes, a mouse MAb recognizing the housekeeping protein glyceraldehyde-3-phosphate dehydrogenase (GAPDH; clone 6C5; MAB374; Merck Millipore, Billerica, MA; dilution 1:50,000) was used. Following three 15-min washing steps with TBST, the membranes were incubated with appropriate horseradish peroxidase (HRP)-conjugated rabbit or mouse IgG-specific goat secondary antibodies (sc-3837 and sc-2005 from Santa Cruz Biotechnology, Santa Cruz, CA) diluted 15,000-fold in TBST-5% BSA. Following additional washing steps, blots were developed using SuperSignal West Femto Maximum Sensitivity Substrate (Thermo Scientific, Rockford, IL). The chemiluminescence signals were captured using a ChemiDoc XRS imaging system (Bio-Rad Laboratories, Veenendaal, the Netherlands).

EXOSOME EXPERIMENTS

To investigate their pro-arrhythmic effects, exosomes from the hMSC secretome were isolated under sterile conditions using previously established procedures.[9,10] Human MSCs were seeded into porcine skin gelatin type A (Sigma-Aldrich Chemie)-coated cell culture flasks with a surface area of 75 cm^2 (1.8 million cells per flask). As control, equal-sized gelatin-coated flasks without cells were used. Every 2 days, culture medium was collected from the flasks and spun for 10 minutes at 303 $\times$ g to remove cellular debris. The supernatant was transferred to clean tubes and stored shortly at 4°C. Subsequently, supernatants were centrifuged for 30 min at 4°C and 10,000 $\times$ g in a precooled Optima L-70K ultracentrifuge (Beckman Coulter Nederland, Woerden, the Netherlands) for another debris removal step. Next, supernatants were filtered through Millex 0.45-µm pore size polyethersulfone syringe filters (Merck Millipore) and spun for 60 min at 4°C and 100,000 $\times$ g to pellet the exosomes. Exosomes were resuspended in ice-cold PBS by gentle agitation for 2 h at 4°C. Exosomes were stored at -80°C until later use.

To study the effects of the hMSC-derived exosomes on the electrical properties of nrCMCs, 4×10^5 of these cells were added to single wells of a 24-well cell culture plate onto a fibronectin-coated glass coverslip. The resulting nrCMC cultures were given fresh medium with or without exosomes every 2 days. Exosomes were added to the medium in a quantity calculated to approximate the amount of exosomes in the hMSC secretome during the transwell experiments (Amount of hMSCs per flask / amount of hMSCs in transwells (*i.e.* 1.12 x10^5 cells) = dilution of exosome stock needed per nrCMC culture). After 9 days of culture, nrCMC cultures were subjected to optical mapping for electrophysiological investigation by a blinded researcher.

REFERENCES

1. Ramkisoensing AA, Pijnappels DA, Askar SF, Passier R, Swildens J, Goumans MJ, Schutte CI, de Vries AA, Scherjon S, Mummery CL, Schalij MJ, Atsma DE. Human embryonic and fetal mesenchymal stem cells differentiate toward three different cardiac lineages in contrast to their adult counterparts. *PLoS One*. 2011;6:e24164.

2. National Institutes of Health. Guide for the Care and Use of Laboratory Animals. 1-1-2002.

3. Pijnappels DA, Schalij MJ, van TJ, Ypey DL, de Vries AA, van der Wall EE, van der Laarse A, Atsma DE. Progressive increase in conduction velocity across human mesenchymal stem cells is mediated by enhanced electrical coupling. *Cardiovasc Res*. 2006;72:282-291.

4. Seppen J, Rijnberg M, Cooreman MP, Oude Elferink RP. Lentiviral vectors for efficient transduction of isolated primary quiescent hepatocytes. *J Hepatol*. 2002;36:459-465.

5. van Tuyn J, Pijnappels DA, de Vries AA, van der Velde-van Dijke I, Knaan-Shanzer S, van der Laarse A, Schalij MJ, Atsma DE. Fibroblasts from human postmyocardial infarction scars acquire properties of cardiomyocytes after transduction with a recombinant myocardin gene. *FASEB J*. 2007;21:3369-3379.

6. Askar SF, Ramkisoensing AA, Schalij MJ, Bingen BO, Swildens J, van der Laarse A, Atsma DE, de Vries AA, Ypey DL, Pijnappels DA. Antiproliferative treatment of myofibroblasts prevents arrhythmias in vitro by limiting myofibroblast-induced depolarization. *Cardiovasc Res*. 2011;90:295-304.

7. Maruyama T, Kanaji T, Nakade S, Kanno T, Mikoshiba K. 2APB, 2-aminoethoxydiphenyl borate, a membrane-penetrable modulator of Ins(1,4,5)P3-induced Ca2+ release. *J Biochem*. 1997;122:498-505.

8. Harks EG, Camina JP, Peters PH, Ypey DL, Scheenen WJ, van Zoelen EJ, Theuvenet AP. Besides affecting intracellular calcium signaling, 2-APB reversibly blocks gap junctional coupling in confluent monolayers, thereby allowing measurement of single-cell membrane currents in undissociated cells. *FASEB J*. 2003;17:941-943.

9. Lasser C, Eldh M, Lotvall J. Isolation and characterization of RNA-containing exosomes. *J Vis Exp*. 2012;e3037.

10. Thery C, Amigorena S, Raposo G, Clayton A. Isolation and characterization of exosomes from cell culture supernatants and biological fluids. *Curr Protoc Cell Biol*. 2006;Chapter 3:Unit.

SUPPLEMENTAL FIGURES
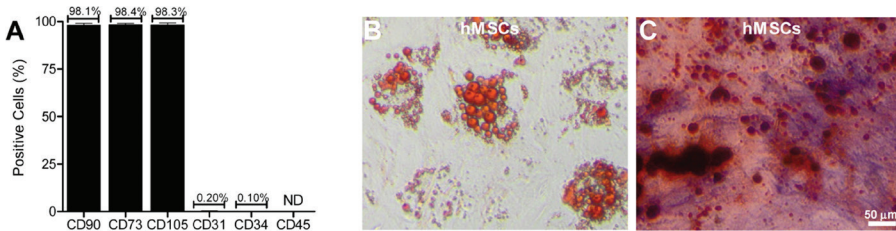
Supplemental figure 1. Characterization of adult BM hMSCs. (A) Flow cytometric analyses showed abundant surface expression of the MSC markers CD90, CD73 and CD105 and hardly any surface expression of the hematopoietic cell markers CD34 and CD45 or the endothelial cell marker CD31. Percentages are means of ≥4 measurements. ND is not detected. (B) Adipogenic differentiation was visualized by the presence of Oil Red O-stained fat vacuoles. (C) Calcium depositions and alkaline phosphatase activity were present after osteogenic differentiation of the hMSCs.
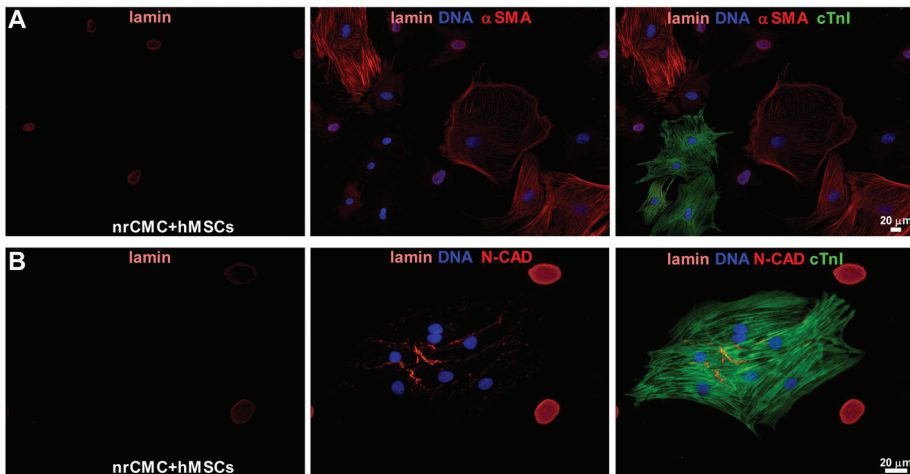
Supplemental figure 2. Analyse of markers involved in mechanical coupling. (A) Immunocytological staining showed no expression of alpha smooth muscle actin (aSMA; orange/red) by adult BM hMSCs in co-culture with nrCMCs. (B) Also, no N-cadherin (indicated as N-CAD; orange/red), was detected at contact areas between hMSCs and nrCMCs. hMSCs were detected using an antibody directed against human-specific lamin A/C (red), while nrCMCs were identified using an antibody directed against cardiac troponin I (cTnI; green). Nuclei were stained with the DNA-binding fluorochrome Hoechst 33342.

CHAPTER VIII

SUMMARY, CONCLUSIONS, DISCUSSIONS, AND FUTURE PERSPECTIVES
SAMENVATTING EN CONCLUSIES

Summary

The general introduction of this thesis, **Chapter I**, describes the origins and typical characteristics of mesenchymal stem cells (MSCs). Next, the capacity of MSCs to undergo cardiac differentiation *in vitro* and *in vivo* is discussed with emphasis on the criteria and the methods used to determine differentiation into cardiac cell types. Finally, an overview is presented of the clinical studies using MSCs to treat cardiac diseases, including outcomes and (potential) hurdles.

The aim of this thesis was to study the integration and cardiac differentiation of MSCs in cardiac tissue using dedicated *in vitro* models and molecular interventions.

In **Chapter II** the cardiac differentiation potential of MSCs derived from human (h) embryonic, fetal and adult tissues in co-cultures with neonatal rat ventricular cardiomyocytes (nrCMCs) was evaluated. It was shown that the capacity of hMSCs to differentiate towards cardiomyocytes, smooth muscle cells and endothelial cells declined with the age of the MSC donor. Cardiomyogenic differentiation was most efficient in embryonic hMSCs, occurred at a lower frequency in fetal hMSCs and could not be detected in hMSCs from adults.

In **Chapter III** the effects of alignment of neonatal rat MSCs on electrical integration in nrCMC cultures was studied using multi-electrode arrays. During 9 days of co-culture a portion of these MSCs differentiated towards cardiac muscle cells and depending on the predefined direction of alignment the degree of electrical integration of the MSCs with surrounding cardiomyocytes differed significantly.

The role of gap junctional coupling between cultured cardiomyocytes and hMSCs in inducing cardiac differentiation of the hMSCs was studied in **Chapter IV**. Connexin 43 downregulation and subsequent connexin 45 upregulation in fetal hMSCs co-cultured with nrCMCs decreased and restored, respectively, their ability to differentiate into cardiomyocyte-like cells that could produce action potentials.

In **Chapter V**, co-cultures between lentiviral vector-modified hMSCs and nrCMCs were used to investigate secondary transduction of cardiomyocytes with vector particles originating from primary transduced. Secondary transduction of native cardiomyocytes under these conditions is a frequent event, thereby seriously disturbing the interpretation of experiments in which cardiac differentiation of MSCs is inferred from the co-expression of specific cardiac features together with a virally introduced marker gene. However, with some additional measures the percentage of falsely labeled cells can be reduced to zero.

Chapter VI shows the results of a study focusing on the role of hMSC engraftment patterns on arrhythmicity in nrCMC cultures. Not only the percentage of engrafted cells affected arrhythmia incidence and characteristics but also the pattern in which these cells engrafted (clustered *versus* diffuse distribution). Electrical

coupling between hMSCs and cardiomyocytes as well as secretion of certain freely diffusible paracrine factors contributed to the pro-arrhythmic effects observed in these co-cultures.

Besides the pro-arrhythmic effects of transplanting unexcitable cells in cardiac tissue, also the role of endogenous, unexcitable myofibroblasts in arrhythmogenesis was studied. Accordingly, in **Chapter VII** nrCMC cultures were treated with cytostatic agents (*i.e.* mitomycin-c and paclitaxel) to inhibit the proliferation of the (myo)fibroblasts in these cultures. This strongly reduced the incidence of reentrant arrhythmias by preserving tissue excitability.

In conclusion, the cardiac differentiation potential of hMSCs negatively correlates with donor age, which in its own turn shows a negative relationship with connexin 43 levels in these cells. However, a causal relationship between connexin 43 expression levels and cardiomyogenic differentiation potential only exists for hMSCs from prenatal sources, *i.e.* while knockdown of connexin 43 expression in fetal hMSCs inhibits their ability to differentiate into cardiomyocytes, connexin 43 overexpression in adult hMSCs does not endow them with cardiomyogenic differentiation capacity. In addition, co-culture studies showed that the alignment and distribution of MSCs affect their electrical integration into host myocardium and are major determinants of their pro-arrhythmic risk. The mechanisms underlying the pro-arrhythmic effects of hMSCs are to some extent comparable to those of cardiac myofibroblasts, cells that are found in fibrotic myocardium.

DISCUSSION & FUTURE PERSPECTIVES

Whether and to which extent mesenchymal stem cells (MSCs) are intrinsically able, or can be forced, to undergo cardiac differentiation, especially with regard to formation of functional cardiomyocytes (CMCs), has been subject of intense investigation.[1] The incentive for these studies was probably based on the apparent advantageous properties of MSCs following transplantation in damaged myocardium. Their ease with which MSCs can be isolation from a variety of relatively easily accessible tissues (*e.g.* bone marrow and adipose tissue) and subsequently expanded *in vitro*, their favorable immunological effects and indications that these cells could differentiate towards cardiac cells contributed to a rapid transition from bench to bed.[2] However, the initial enthusiasm for MSC therapy to actually regenerate myocardial tissue after ischemic damage is now replaced with contemplation, while new strategies are being developed to overcome the encountered challenges related to cardiac cell therapy.[3-5]
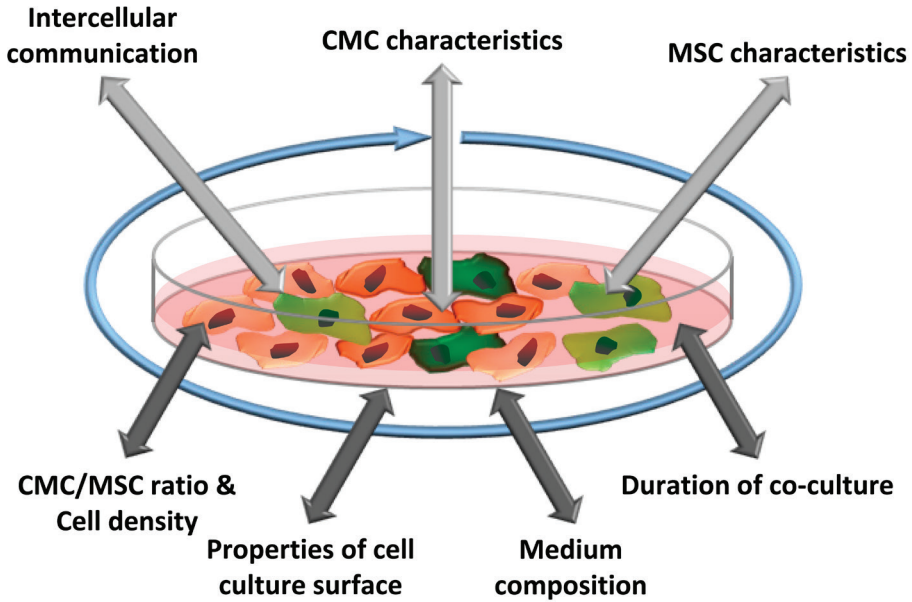
Figure 1. Schematic overview of factors that might affect the outcome of studies on cardio-myogenic differentiation of MSCs using co-culture models. Intrinsic and extrinsic factors are indicated by light and dark grey arrows, respectively. These factors probably also affect each other, thereby creating a highly complex and dynamic setting in which the outcome is determined by the interplay between the various factors.

Before stem cells can undergo cardiomyogenic differentiation specific tran-scriptional pathways need to be activated. A method from which it is believed to deliver the triggers needed to initiate this process involves co-culture with CMCs. However, the exact co-culture conditions needed to induce (complete) cardiomyo-genic differentiation in MSCs, if possible at all, are not fully understood.[6] It is there-fore no surprise that conflicting results have been reported about the potential of MSCs to undergo cardiomyogenesis as most of these studies relied on co-cultures between MSCs and CMCs.[7-9] In fact, there is still little known about the triggers for cardiac differentiation in any stem cell type using any model, especially when it comes to guiding differentiation towards a specific cardiac cell type.[10] In CMC-MSC co-culture models a number of factors and mechanisms have been identified which seem to play a role in inducing cardiomyogenic differentiation. However, the degree to which these factors contribute to the underlying mechanism of car-diomyogenic differentiation is directly influenced by the experimental setup and conditions. Basically these factors can be divided into two groups, intrinsic and extrinsic factors (Figure 1).

Intercellular communication between co-cultured cells could be one of these intrinsic factors. It has been shown that MSCs derived from human or rodent tissue express certain proteins called connexins (Cx).[11] These proteins form hemichannels called connexons which consist of a ring of 6 connexin molecules with a central pore. When connexons in 2 neighboring cells associate with each other, gap junctions are formed. These intercellular channels comprise relatively aselective low-conductance conduits allowing transmission of electrical and chemical signals between MSCs.[12] MSCs can also form functional gap junctions with adjacent CMCs, thereby establishing heterocellular communication.[13] The degree and nature of gap junctional communication is determined by several factors, including the extent of physical contact between cells, the surface levels of Cxs, the spreading of gap junctions across the plasma membrane, the specific Cx isoforms incorporated in the gap junctions and the conductive properties of the connexons, which are regulated by chemical, electrical and mechanical signals as well as by posttranslational modifications (*e.g.* phosphorylation).[14] In this thesis it has been shown that functional gap junctional coupling between neonatal rat ventricular CMCs (nrCMCs) and co-cultured adult human MSCs is important for the induction of cardiomyogenic differentiation in these stem cells (Chapter IV). Therefore the degree of intercellular communication, determined by the factors named above, could directly affect the efficiency and extent to which MSCs differentiate into CMCs.

The *characteristics of CMCs* used in co-culture experiments might also affect the propensity of MSCs to acquire a cardiomyogenic phenotype. For practical reasons nrCMCs are the primary choice for CMC-MSC co-culture experiments. Such CMCs can be kept in culture for many days without losing excitability and contraction.[15] These key properties of CMCs have been linked to induction of cardiomyogenic differentiation.[16,17] However, during the isolation procedure CMCs might become damaged, thereby affecting their characteristics in terms of excitation and contraction. Additionally, CMCs are mostly isolated from 2-day old rats, but at this stage the heart is still under development with changing CMC characteristics,[18] and a seemingly insignificant difference in age (12 h or 1 day difference for example) might therefore affect the outcome of co-culture experiments. Importantly, although breeding of rats can be standardized to some degree, the actual time point of conception and parturition could create a significant variety in age when different nests are put together to create a sufficient supply. Also, intercellular communication between hMSCs and non-human CMCs could be suboptimal, but obtaining hCMCs in large quantities and keeping them in culture long enough to conduct such co-culture experiments does not seem feasible.

Besides culture-related aspects, one also needs to consider that healthy, nrCMCs are very different from those found in the target tissue of cardiac cell therapy, being a diseased human heart.[19] In such a heart, and especially near the border

zone of myocardial infarction, CMCs are often remodeled, exposed to pro-apoptotic/necrotic signals, inflammatory stimuli and changes in pH, redox balance and oxygen tension. Therefore, even if the conditions are fully standardized in CMC-MSC co-culture experiments and cardiac differentiation can indeed be studied in a robust fashion, the data derived from these experiments should always be interpreted and presented with great care.

Logically, also the *characteristics of MSCs* might have an impact on the outcome of cardiac differentiation experiments in co-cultures of MSCs and CMCs. Human adult MSCs are usually derived from tissues like bone marrow or fat, while human MSCs can also be derived from fetal tissues and neonatal sources like amnion, placenta and umbilical cords.[1] Although some studies suggest that the source of MSC could determine their potential to differentiate towards certain cell types,[20] it is now recognized that donor age of MSCs certainly affects their differentiation potential, including their ability to form cardiac cells.[21,22] This phenomenon can be explained by the fact that cellular plasticity in general declines with age.[23] In this thesis it is shown that Cx43 expression levels in hMSCs also decline with age, which is accompanied by a loss of cardiomyogenic differentiation. However, while Cx43 knockdown fully eliminated the cardiomyogenic differentiation potential of fetal human MSCs in co-culture with CMCs, overexpression of Cx43 in adult human MSCs did not cause them to become CMCs when coupled to nrCMCs. This shows that the potential of stem cells to differentiate into various cell types is constrained by other factors and mechanisms besides those related to gap junctions. Importantly, the recent developments in genetic reprogramming of cells, including those involving direct cardiac reprogramming of fibroblasts have further uncovered the requirements for cardiomyogenic differentiation.[24,25]

One of the extrinsic factors in these co-culture experiments that could affect the outcome is the *CMC to MSC ratio and density* at which the cells are plated, as this determines the extent of intercellular communication through gap junctions, ligand-receptor interactions and vesicle release/uptake as well as the cumulative strength of cardiomyogenic cues. Consequently, a relatively high number of adjacent CMCs will probably have a greater influence on a MSC than a lower number of CMCs thereby increasing the likelihood that a suprathreshold stimulus for cardiomyogenic differentiation is achieved. Although this thesis (Chapter 4) does not provide direct evidence for a role of paracrine factors in inducing cardiac differentiation, in other situations and under other conditions such factors could be of importance.[26] Increasing the supply of paracrine factors could result in a higher local concentration of these factors and thereby have a stronger effect. This may, for instance, hold true for hypoxia-induced myocardial angiogenesis, which is often suggested to represent the major beneficial effect in cardiac cell therapy.[27]

It is known that the *characteristics of the cell culture supports and coatings* used in cardiac differentiation experiments can have a strong effect on the induction of differentiation.[28,29] However, the underlying mechanisms of these *in vitro* findings remain poorly understood. Coatings applied in culture dishes interact with their surface and create a substrate on which cells can attach, survive and grow. Such coatings are usually based on extracellular matrix components and act as ligand for transmembrane receptors called integrins, which ensure attachment. Apparently, the degree of attachment, and thereby flattening and spreading of cells, could have an effect on the outcome of cardiac differentiation experiments. In the developing heart, stem and progenitor cells attach to adjacent cells and extracellular structures, however, whether inhibition of this process also leads to suboptimal growth of heart muscle, as a consequence of disturbed cardiac differentiation, is still not fully understood.[30]

The conditions to which cultured cells are exposed largely depend on *the composition of the culture medium* applied onto the cells. Especially serum, which is a key ingredient of most culture media and derived from species like bovine and equine, is known to affect the outcome of cardiac differentiation experiments, especially when using embryonic stem cells.[31,32] Serum is rich in proteins, including various growth factors. How these or other factors in serum modulate the propensity of stem cells to differentiate into cardiac cells is incompletely understood. However, it is known that depending on source, concentration and pretreatment *e.g.* heat treatment to inactivate complement. of serum, the proliferation rate, growth and viability of stem cells is changed.[33] These changes may have a direct or indirect effect on the susceptibility to certain cardiac differentiation-inducing stimuli.

Once stem cells and CMCs are put together in culture and have attached to the underlying surface, the *duration of co-culture* is likely to determine to which extent cardiomyogenic differentiation can take place. Based on other cardiac differentiation protocols, a 10-day incubation time seems sufficient to allow formation of cardiac cells.[34] Apparently, during this period stem cells are exposed to the appropriate stimuli of sufficient duration and (cumulative) strength to activate cardiac transcriptional pathways. However, if other requirements for cardiomyogenic differentiation, which are listed above, are not met, obviously, MSC-derived CMCs will not be obtained.

Parallel to extensive *in vitro* studies, also numerous pre-clinical *in vivo* studies,[1,35,36] as well as clinical studies have been performed to assess the therapeutic potential of cell transplantation in the diseased heart.[4,37-39] Although a significant number of these clinical trials have studied the effect of transplanted bone marrow cells in damaged myocardium, few clinical studies have investigated the effects of MSC transplantation on cardiac function.[40-42] Nevertheless, most of these studies showed a beneficial effect. This effect is often associated with enhanced

myocardial perfusion,[43] although such trials obviously do not allow detailed investigation of the therapeutic mechanisms. As these mechanisms remain poorly understood, there is only a very small basis for the development of strategies to enhance the therapeutic effects. As another result, the therapeutic window of cardiac MSC therapy in general and the possible (dose-dependent) hazardous effects of MSC transplantation are still unknown. While the optimal therapeutic effect could be achieved by trial-and-error, such an approach bears the danger of going beyond the therapeutic window, resulting in detrimental effects on cardiac function,[44] a danger that is typical for any new intervention. In this thesis it was shown that the alignment of transplanted MSCs determines their degree of spatial and functional integration with adjacent CMC fields, which was reflected as changes in conduction velocity. In the intact heart, the extracellular matrix is the main determinant of cell alignment.[45] However, in the damaged heart, particularly after myocardium infarction, this matrix undergoes extensive changes/remodellng and cellular spatial arrangement is disturbed especially in the border zones of the infarcted areas.[46] In most stem cell studies focusing on myocardial infarction, cells have been injected in the border zone and could therefore not be properly guided in their alignment. As a result structural and functional heterogeneity may increase locally leading to different conduction velocities in specific directions and areas, which could increase the pro-arrhythmic risk if the number of misaligned cells is high enough.[47] Additional guidance in the alignment of transplanted cells or tissue engineering techniques might overcome these potential dangers.[48] Furthermore, in chapter 6 it was shown that the number and engraftment patterns of transplanted MSCs affect pro-arrhythmic risk by two different mechanisms. While electrotonic interaction between MSCs and CMCs lead to partial depolarization of the CMCs, secretion of paracrine factors from MSCs results in prolongation of the cardiac action potential duration. Depending on the extent of these effects, which is directly related to the number and engraftment pattern of MSCs, the incidence of arrhythmias was strongly increased in MSC-CMC co-cultures. Although *in vivo* studies are needed to proof the relevance of these mechanisms in the intact organism, *in vitro* studies like the ones described in this thesis could help us in developing strategies to minimize the adverse effects related to MSC therapy for the heart and may also help to guide the development/improvement of cardiac cell therapy involving other (stem) cell types.

Nevertheless, virtually all current interventions in cardiovascular medicine target either symptoms or certain disease pathways, but do not actually heal the damaged heart. Despite the existing deficiencies in our knowledge and understanding of stem cells and their therapeutic potential, there is no denying in the positive impact regenerative medicine could have on patients suffering from cardiovascular diseases in either the near or distant future.

REFERENCES

1. Williams AR and Hare JM. Mesenchymal stem cells: biology, pathophysiology, translational find-ings, and therapeutic implications for cardiac disease. *Circ Res*. 2011;109:923-940.

2. Bieback K, Wuchter P, Besser D, Franke W, Becker M, Ott M, Pacher M, Ma N, Stamm C, Kluter H, Muller A, Ho AD. Mesenchymal stromal cells (MSCs): science and f(r)iction. *J Mol Med (Berl)*. 2012;90:773-782.

3. Anversa P, Kajstura J, Rota M, Leri A. Regenerating new heart with stem cells. *J Clin Invest*. 2013;123:62-70.

4. Suncion VY, Schulman IH, Hare JM. Concise review: the role of clinical trials in deciphering mechanisms of action of cardiac cell-based therapy. *Stem Cells Transl Med*. 2012;1:29-35.

5. Segers VF and Lee RT. Biomaterials to enhance stem cell function in the heart. *Circ Res*. 2011;109:910-922.

6. Pijnappels DA, Schalij MJ, Atsma DE. Response to the letter by Rose et al. *Circ Res*. 2009;104:e8.

7. Ramkisoensing AA, de Vries AA, Schalij MJ, Atsma DE, Pijnappels DA. Brief report: Misinter-pretation of co-culture differentiation experiments by unintended labeling of cardiomyocytes through secondary transduction: delusions and solutions. *Stem Cells*. 2012;30:2830-2834.

8. Rose RA, Jiang H, Wang X, Helke S, Tsoporis JN, Gong N, Keating SC, Parker TG, Backx PH, Keating A. Bone marrow-derived mesenchymal stromal cells express cardiac-specific markers, retain the stromal phenotype, and do not become functional cardiomyocytes in vitro. *Stem Cells*. 2008;26:2884-2892.

9. Siegel G, Krause P, Wohrle S, Nowak P, Ayturan M, Kluba T, Brehm BR, Neumeister B, Kohler D, Rosenberger P, Just L, Northoff H, Schafer R. Bone marrow-derived human mesenchymal stem cells express cardiomyogenic proteins but do not exhibit functional cardiomyogenic differentia-tion potential. *Stem Cells Dev*. 2012;21:2457-2470.

10. Mummery CL and Lee RT. Is heart regeneration on the right track? *Nat Med*. 2013;19:412-413.

11. Valiunas V, Doronin S, Valiuniene L, Potapova I, Zuckerman J, Walcott B, Robinson RB, Rosen MR, Brink PR, Cohen IS. Human mesenchymal stem cells make cardiac connexins and form functional gap junctions. *J Physiol*. 2004;555:617-626.

12. Kleber AG and Rudy Y. Basic mechanisms of cardiac impulse propagation and associated arrhythmias. *Physiol Rev*. 2004;84:431-488.

13. Beeres SL, Atsma DE, van der Laarse A, Pijnappels DA, van TJ, Fibbe WE, de Vries AA, Ypey DL, van der Wall EE, Schalij MJ. Human adult bone marrow mesenchymal stem cells repair experi-mental conduction block in rat cardiomyocyte cultures. *J Am Coll Cardiol*. 2005;46:1943-1952.

14. Jansen JA, van Veen TA, de Bakker JM, van Rijen HV. Cardiac connexins and impulse propaga-tion. *J Mol Cell Cardiol*. 2010;48:76-82.

15. Zhang Y, Sekar RB, McCulloch AD, Tung L. Cell cultures as models of cardiac mechanoelectric feedback. *Prog Biophys Mol Biol*. 2008;97:367-382.

16. Hosoda T, Zheng H, Cabral-da-Silva M, Sanada F, Ide-Iwata N, Ogorek B, Ferreira-Martins J, Arranto C, D'Amario D, del MF, Urbanek K, D'Alessandro DA, Michler RE, Anversa P, Rota M, Kajstura J, Leri A. Human cardiac stem cell differentiation is regulated by a mircrine mechanism. *Circulation*. 2011;123:1287-1296.

17. Iijima Y, Nagai T, Mizukami M, Matsuura K, Ogura T, Wada H, Toko H, Akazawa H, Takano H, Nakaya H, Komuro I. Beating is necessary for transdifferentiation of skeletal muscle-derived cells into cardiomyocytes. *FASEB J*. 2003;17:1361-1363.

18. Vornanen M. Excitation-contraction coupling of the developing rat heart. *Mol Cell Biochem*. 1996;163-164:5-11.

19. Buja LM and Vela D. Cardiomyocyte death and renewal in the normal and diseased heart. *Cardio-vasc Pathol*. 2008;17:349-374.

20. Strioga M, Viswanathan S, Darinskas A, Slaby O, Michalek J. Same or not the same? Comparison of adipose tissue-derived versus bone marrow-derived mesenchymal stem and stromal cells. *Stem Cells Dev.* 2012;21:2724-2752.

21. Sethe S, Scutt A, Stolzing A. Aging of mesenchymal stem cells. *Ageing Res Rev.* 2006;5:91-116.

22. Roobrouck VD, Ulloa-Montoya F, Verfaillie CM. Self-renewal and differentiation capacity of young and aged stem cells. *Exp Cell Res.* 2008;314:1937-1944.

23. Jones DL and Rando TA. Emerging models and paradigms for stem cell ageing. *Nat Cell Biol.* 2011;13:506-512.

24. Ieda M, Fu JD, Delgado-Olguin P, Vedantham V, Hayashi Y, Bruneau BG, Srivastava D. Direct reprogramming of fibroblasts into functional cardiomyocytes by defined factors. *Cell.* 2010;142:375-386.

25. Song K, Nam YJ, Luo X, Qi X, Tan W, Huang GN, Acharya A, Smith CL, Tallquist MD, Neilson EG, Hill JA, Bassel-Duby R, Olson EN. Heart repair by reprogramming non-myocytes with cardiac transcription factors. *Nature.* 2012;485:599-604.

26. Mirotsou M, Jayawardena TM, Schmeckpeper J, Gnecchi M, Dzau VJ. Paracrine mechanisms of stem cell reparative and regenerative actions in the heart. *J Mol Cell Cardiol.* 2011;50:280-289.

27. Gnecchi M, Zhang Z, Ni A, Dzau VJ. Paracrine mechanisms in adult stem cell signaling and therapy. *Circ Res.* 2008;103:1204-1219.

28. Lisi A, Briganti E, Ledda M, Losi P, Grimaldi S, Marchese R, Soldani G. A combined synthetic-fibrin scaffold supports growth and cardiomyogenic commitment of human placental derived stem cells. *PLoS One.* 2012;7:e34284.

29. Zhang J, Klos M, Wilson GF, Herman AM, Lian X, Raval KK, Barron MR, Hou L, Soerens AG, Yu J, Palecek SP, Lyons GE, Thomson JA, Herron TJ, Jalife J, Kamp TJ. Extracellular matrix promotes highly efficient cardiac differentiation of human pluripotent stem cells: the matrix sandwich method. *Circ Res.* 2012;111:1125-1136.

30. Lockhart M, Wirrig E, Phelps A, Wessels A. Extracellular matrix and heart development. *Birth Defects Res A Clin Mol Teratol.* 2011;91:535-550.

31. Ojala M, Rajala K, Pekkanen-Mattila M, Miettinen M, Huhtala H, Aalto-Setala K. Culture conditions affect cardiac differentiation potential of human pluripotent stem cells. *PLoS One.* 2012;7:e48659.

32. Passier R, Oostwaard DW, Snapper J, Kloots J, Hassink RJ, Kuijk E, Roelen B, de la Riviere AB, Mummery C. Increased cardiomyocyte differentiation from human embryonic stem cells in serum-free cultures. *Stem Cells.* 2005;23:772-780.

33. Roobrouck VD, Vanuytsel K, Verfaillie CM. Concise review: culture mediated changes in fate and/or potency of stem cells. *Stem Cells.* 2011;29:583-589.

34. Smits AM, Ramkisoensing AA, Atsma DE, Goumans MJ. Young at heart. An update on cardiac regeneration. *Minerva Med.* 2010;101:255-270.

35. Malliaras K and Marban E. Cardiac cell therapy: where we've been, where we are, and where we should be headed. *Br Med Bull.* 2011;98:161-185.

36. Sturzu AC and Wu SM. Developmental and regenerative biology of multipotent cardiovascular progenitor cells. *Circ Res.* 2011;108:353-364.

37. Makkar RR, Smith RR, Cheng K, Malliaras K, Thomson LE, Berman D, Czer LS, Marban L, Mendizabal A, Johnston PV, Russell SD, Schuleri KH, Lardo AC, Gerstenblith G, Marban E. Intracoronary cardiosphere-derived cells for heart regeneration after myocardial infarction (CADUCEUS): a prospective, randomised phase 1 trial. *Lancet.* 2012;379:895-904.

38. Rodrigo SF, Ramshorst J, Beeres SL, Bax JJ, Schalij MJ, Atsma DE. Cell therapy for the treatment of chronic ischemic heart disease. *Curr Pharm Des.* 2011;17:3308-3327.

39. van Ramshorst J, Bax JJ, Beeres SL, bbets-Schneider P, Roes SD, Stokkel MP, de RA, Fibbe WE, Zwaginga JJ, Boersma E, Schalij MJ, Atsma DE. Intramyocardial bone marrow cell injection for chronic myocardial ischemia: a randomized controlled trial. *JAMA*. 2009;301:1997-2004.

40. Chen SL, Fang WW, Ye F, Liu YH, Qian J, Shan SJ, Zhang JJ, Chunhua RZ, Liao LM, Lin S, Sun JP. Effect on left ventricular function of intracoronary transplantation of autologous bone marrow mesenchymal stem cell in patients with acute myocardial infarction. *Am J Cardiol*. 2004;94:92-95.

41. Hare JM, Traverse JH, Henry TD, Dib N, Strumpf RK, Schulman SP, Gerstenblith G, DeMaria AN, Denktas AE, Gammon RS, Hermiller JB, Jr., Reisman MA, Schaer GL, Sherman W. A randomized, double-blind, placebo-controlled, dose-escalation study of intravenous adult human mesenchymal stem cells (prochymal) after acute myocardial infarction. *J Am Coll Cardiol*. 2009;54:2277-2286.

42. Hare JM, Fishman JE, Gerstenblith G, DiFede Velazquez DL, Zambrano JP, Suncion VY, Tracy M, Ghersin E, Johnston PV, Brinker JA, Breton E, Davis-Sproul J, Schulman IH, Byrnes J, Mendizabal AM, Lowery MH, Rouy D, Altman P, Wong Po FC, Ruiz P, Amador A, Da SJ, McNiece IK, Heldman AW. Comparison of allogeneic vs autologous bone marrow-derived mesenchymal stem cells delivered by transendocardial injection in patients with ischemic cardiomyopathy: the POSEIDON randomized trial. *JAMA*. 2012;308:2369-2379.

43. Lee J and Terracciano CM. Cell therapy for cardiac repair. *Br Med Bull*. 2010;94:65-80.

44. Smith RR, Barile L, Messina E, Marban E. Stem cells in the heart: what's the buzz all about? Part 2: Arrhythmic risks and clinical studies. *Heart Rhythm*. 2008;5:880-887.

45. Hirschy A, Schatzmann F, Ehler E, Perriard JC. Establishment of cardiac cytoarchitecture in the developing mouse heart. *Dev Biol*. 2006;289:430-441.

46. Fomovsky GM, Rouillard AD, Holmes JW. Regional mechanics determine collagen fiber structure in healing myocardial infarcts. *J Mol Cell Cardiol*. 2012;52:1083-1090.

47. Pijnappels DA, Gregoire S, Wu SM. The integrative aspects of cardiac physiology and their implications for cell-based therapy. *Ann N Y Acad Sci*. 2010;1188:7-14.

48. Chien KR, Domian IJ, Parker KK. Cardiogenesis and the complex biology of regenerative cardiovascular medicine. *Science*. 2008;322:1494-1497.

SAMENVATTING

De algemene introductie van dit proefschrift, **Hoofdstuk I**, geeft de eigenschappen en de oorsprong van mesenchymale stamcellen (MSCs) weer. Tevens wordt de *in vitro* en *in vivo* capaciteit van MSCs om te differentiëren naar hartspiercellen beschreven. Hierbij wordt specifiek ingegaan op hoe differentiatie naar hartspiercel gedefiniëerd wordt en op de methoden die gebruikt worden om het proces van differentiatie in stamcellen te onderzoeken. Tenslotte, wordt er een overzicht gegeven van de klinische studies die gebruikmaken van MSCs om hartziekten te behandelen. Hierbij worden tevens de uitkomsten en conclusies van deze studies beschreven.

Het hoofddoel van dit proefschrift was dan ook de integratie van MSCs in hartspierweefsel en de differentiatie van MSCs naar hartspiercellen in deze omgeving kritisch te onderzoeken.

In **Hoofdstuk II** werd het differentiatie vermogen van MSCs die afkomstig waren uit humane (h) embryonale, foetale en volwassen bronnen, met elkaar vergeleken. Specifiek werd het vermogen om te differentiëren naar hartspiercel, gladde spiercel en endotheelcel onderzocht. Aangetoond werd dat de capaciteit van hMSCs om te differentiëren naar deze drie celtypen, direct gerelateerd was aan de leeftijd van de weefseldonor, waarbij het differentiatie vermogen van embryonale MSCs superieur was ten opzichte van de andere MSCs.

Hoofdstuk III evalueerde de effecten van ruimtelijke oriëntatie van getransplanteerde stamcellen op de functionele integratie met gekweekte hartspiercellen waarbij gebruik gemaakt werd van micro-electrode arrays. Gedurende 9 dagen co-cultuur met de hartspiercellen, differentiëerde een deel van de MSCs naar hartspiercel en afhankelijk van de vooraf gedefiniëerde ruimtelijke oriëntatie was de mate van electrische integratie significant verschillend.

De rol van gap junctie koppeling tussen gekweekte hartspiercellen en hMSCs bij het induceren van differentiatie naar hartspiercel van deze hMSCs werd bestudeerd in **Hoofdstuk IV**. Het genetisch blokkeren van de expressie van het gap junctie eiwit connexine 43 in hMSCs resulteerde in het verlies van vermogen om te differentiëren naar hartspiercel. Wanneer vervolgens de expressie van het connexine 45 eiwit in deze hMSCs verhoogd werd, keerde het differentiatie vermogen naar hartspiercel van deze cellen terug.

In **Hoofdstuk V** werd secondaire transductie van neonatale rat hartspiercellen onderzocht door deze te kweken in co-cultuur met humane cellen die getransduceerd werden met een lentivirale vector die codeerde voor een fluorescent eiwit. De resultaten toonden dat secondaire transductie in dit soort modellen frequent voorkomt. Hierdoor wordt de interpretatie van dit soort experimenten, waarbij slechts expressie van een fluorescent eiwit door een stamcel gebruikt wordt ter identificatie

van deze cel, sterk verstoord. In deze studie worden echter meerdere mogelijkheden beschreven om het plaatsvinden van secondaire transductie te voorkomen.

Hoofdstuk VI beschrijft de resultaten van een studie die zich gericht heeft op de rol van integratie patronen van hMSCs op de incidentie en eigenschappen van aritmieën in hartspiercelkweken. Niet alleen het percentage geïntegreerde hMSCs beïnvloedt het pro-aritmisch vermogen van de hartspiercelkweken, maar ook het integratiepatroon (geclusterd versus diffuus). Electrische koppeling tussen hMSCs en hartspiercellen en de secretie van bepaalde paracriene factoren dragen bij aan de pro-aritmische effecten die geobserveerd werden in deze co-culturen.

Naast de pro-aritmische effecten van getransplanteerde niet-exciteerbare cellen in hartspierweefsel werd bestudeerd maar ook de rol van endogene, niet-exciteerbare myofibroblasten. In **Hoofdstuk VII** werd bestudeerd of en op welke manier anti-proliferatieve behandeling van myofibroblasten in hartspiercelkweken het ontstaan van aritmieën kon voorkomen. De incubatie met cytostatica (mitomycine-c en paclitaxel) reduceerde de incidentie van re-entry aritmieën sterk door weefsel exciteerbaarheid in stand te houden.

Concluderend, het vermogen van hMSCs te differentiëren tot een hartspiercel neemt af met de donorleeftijd, dat op zichzelf ook een negatieve relatie heeft met het Cx43 expressie niveau. De expressie van Cx43 is essentieel bij het differentiatie proces van MSCs die afkomstig zijn van jonge donoren, maar het is niet een sturende factor bij cardiale differentiatie van MSCs afkomstig uit volwassen donoren. Naast de bovenstaande factoren, beïnvloeden ruimtelijke oriëntatie en integratie van MSCs de electrische integratie van deze cellen in het myocardiale weefsel. Dit kan leiden tot pro-aritmische effecten na stamcel therapie. De onderliggende pro-aritmische mechanismen zijn deels vergelijkbaar met die van cardiale myofibroblasten, die aanwezig zijn in het fibrotische hartspierweefsel.

LIST OF PUBLICATIONS

FULL PAPERS

Ramkisoensing AA, de Vries AA, Atsma DE, Schalij MJ, Pijnappels DA. Interaction between Myofibroblasts and Stem Cells in the Fibrotic Heart: Balancing between Deterioration and Regeneration. *Cardiovasc Res. 2014 Feb 27*

Ramkisoensing AA*, Askar SFA*, Atsma DE, Schalij MJ, de Vries AAF, Pijnappels DA. Engraftment Patterns of Human Adult Mesenchymal Stem Cells Expose Electrotonic and Paracrine Pro-Arrhythmic Mechanisms in Myocardial Cell Cultures. *Circ Arrhythm Electrophysiol. 2013 Apr;6(2):380-91*

Ramkisoensing AA, de Vries AAF, Schalij MJ, Atsma DE, Pijnappels DA. Misinterpretation of coculture differentiation experiments by unintended labeling of cardiomyocytes through secondary transduction: delusions and solutions. *Stem Cells. 2012 Dec;30(12):2830-4*

Ramkisoensing AA, Pijnappels DA, Swildens J, Schalij MJ, de Vries AAF*, Atsma DE*. Induction of cardiomyogenic differentiation in human mesenchymal stem cells is mediated by gap junctional coupling with cultured rat cardiomyocytes. *Stem Cells. 2012 Jun;30(6):1236-45*

Ramkisoensing AA, Pijnappels DA, Askar SFA, Passier R, Swildens J, Goumans MJ, Schutte CI, de Vries AAF, Scherjon S, Mummery CL, Schalij MJ, Atsma DE. Human Embryonic and Fetal Mesenchymal Stem Cells Differentiate toward Three Cardiac Lineages in contrast to Their Adult Counterparts. *PLoS ONE 6(9): e24164*

Askar SAF, Ramkisoensing AA, Schalij MJ, Bingen BO, Swildens J, van der Laarse A, Atsma DE, de Vries AAF, Ypey DL, Pijnappels DA. Antiproliferative Treatment of Myofibroblasts Prevents Arrhythmias In Vitro by Limiting Myofibroblast-Induced Depolarization. *Cardiovasc Res. May 1;90(2):295-304*

Smits AM, Ramkisoensing AA, Atsma DE, Goumans MJ. Young at heart. An update on cardiac regeneration. *Minerva Med. 2010 Aug, 101 (4). 255-70*

Pijnappels DA, Schalij MJ, Ramkisoensing AA, van Tuyn J, de Vries AAF, van der Laarse A, Ypey DL, Atsma DE. Forced Alignment of Mesenchymal Stem Cells

Undergoing Cardiomyogenic Differentiation Affects Functional Integration with Cardiomyocyte Cultures. *Circ Res. 2008 Jul 18;103(2):167-76*

*Equal contribution

SELECTED PEER-REVIEWED ABSTRACTS

Ramkisoensing AA, Pijnappels DA, Swildens J, Schalij MJ, de Vries AAF, Atsma DE. Induction of cardiomyogenic differentiation in human mesenchymal stem cells is mediated by gap junctional coupling with cultured rat cardiomyocytes. *Journal of the American College of Cardiology. 2012;59(13s1):E855-E855*

Ramkisoensing AA, Pijnappels DA, Swildens J, Schalij MJ, de Vries AAF, Atsma DE. Induction of cardiomyogenic differentiation in human mesenchymal stem cells is mediated by gap junctional coupling with cultured rat cardiomyocytes. *Circulation. 2011; 124: A10462*

Ramkisoensing DA, Pijnappels DA, Passier R, de Vries AAF, Scherjon S, Mummery CL, Schalij MJ, Atsma DE. Embryonic and Fetal Mesenchymal Stem Cells do undergo Cardiac Differentiation in contrast to their Adult Counterparts: the Younger the Better. *Keystone Symposia 2010, Cardiovascular Development and Repair*

Ramkisoensing AA, Pijnappels DA, de Vries AA, van der Laarse A, Schalij, Atsma DE. Hypoxia accelerates and enhances cardiomyogenesis in mesenchymal stem cells: an environmental cue for a cardiac challenge. *European Heart Journal, 2009 Vol. 30, 505-505*

Ramkisoensing AA, Pijnappels DA, van Tuyn J, Farias HA, Gomez CL, de Vries AAF, Ypey DL, van der Laarse A, Schalij MJ, Atsma DE. Cardiomyogenic differentiation potential of mesenchymal stem cells declines with increase in age: Rebuilding the heart with old or new bricks? *Journal of the American College of Cardiology. 2009; 53: A147*

Ramkisoensing AA, Pijnappels DA, van Tuyn J, de Vries AAF, van der Wall EE, Schalij MJ, Atsma DE, van der Laarse A. Mechanical Stretch Boosts Cardiomyogenic Differentiation of Normal and Genetically Modified Human and Murine Bone Marrow-Derived Mesenchymal Stem Cells. *Journal of the American College of Cardiology. 2007; 49: 233A*

ACKNOWLEDGEMENTS

Als eerste wil ik graag de mensen bedanken die mijn promotie mogelijk gemaakt hebben. Professor Schalij, ik kan oprecht zeggen dat mijn promotietijd mijn leven verrijkt heeft. Bedankt voor de mogelijkheid om deze in het laboratorium Experimentele Cardiologie door te brengen. Professor Atsma, Douwe, bedankt voor de begeleiding maar vooral bedankt voor alle wijze levenslessen. Die komen nog dagelijks van pas. Twan, jouw enthousiasme werkt aanstekelijk en jouw kennis is onuitputtelijk. Onze samenwerking heeft mijn promotieonderzoek naar een hoger niveau gebracht.

Het secretariaat van het Hart Long Centrum, met name Talitha, wil ik graag bedanken voor de hulp bij een tal van zaken.

Het laboratorium Experimentele Cardiologie is gedurende 6 jaar mijn thuis geweest. Eerst als student daarna als arts-onderzoeker. Ik ben wetenschappelijk opgegroeid voor de ogen van onze analisten. Margreet en Minka bedankt voor de gezelligheid. Lieve Cindy, bedankt voor alles, voor de ondersteuning, voor de speurtocht naar alle aanwezige LightCycler qPCR apparaten in het LUMC en natuurlijk ook voor alle leuke verhalen over je dochters.

Saïd, Seitje, je bent en blijft altijd mijn maatje. We hebben letterlijk 4 jaar dag in en dag uit frustraties maar ook overwinningen met elkaar gedeeld. Ik ben blij dat jij mijn paranimf wil zijn. Marc, we kennen elkaar eigenlijk al heel lang. Ik kan mij onze ontmoeting in de overdrachtsruimte van de Reumatologie nog goed herinneren. Bedankt voor de begeleiding en gezellige tijd in Boston. Ik vind het jammer dat we in Nederland nooit hebben kunnen samenwerken. Zeinab and Jolanda, good luck with (finishing) your PhD training. I am sure it will turn out just great. Melina en Vanessa, we hebben helaas niet veel samengewerkt, maar de congressen waren altijd erg leuk samen. Cheryl, thank you for all the antibodies I was allowed to test. All the best with finishing your thesis. Jim, zonder onze samenwerking had ik dit proefschrift in deze vorm nooit kunnen afronden. Dank hiervoor.

Ik heb maar korte tijd in het laboratorium van dr. Wu in Boston kunnen rondkijken, desalniettemin heeft het grote indruk op mij gemaakt. Dear dr. Wu, thank you for giving me the opportunity to visit your laboratory.

De afdelingen Anatomie en Embryologie, Moleculaire Celbiologie, Nierziekten, Klinische Genetica en IHB wil ik bedanken voor de succesvolle samenwerking.

Beste collega's in het Rijnland ziekenhuis van de Interne Geneeskunde, Maagdarmleverziekten, Longziekten en de Intensive Care, dit proefschrift maakt waarschijnlijk duidelijk hoe groot de stap naar de kliniek voor mij was. De afgelopen twee jaar ben ik mij steeds meer thuis gaan voelen in de kliniek. Bedankt voor het geduld, voor de begeleiding en de gezelligheid. Binnenkort zal ik beginnen op de

CURRICULUM VITAE

Arti A. Ramkisoensing was born on February 1st, 1980 in The Hague and in this city she obtained her Gymnasium diploma from the Dalton College. She received her Medical and Biomedical Sciences degree, both *cum laude*, in 2008 and 2009, respectively. During her studies she performed internships at the laboraties of Experimental Hematology (prof. dr. W.E. Fibbe) and Cardiology (prof. dr. A. van der Laarse, prof. dr. M.J. Schalij and prof. dr. D.E. Atsma). In 2008, she started her PhD training in the latter laboratory under supervision of prof. dr. M.J. Schalij, prof. dr. D.E. Atsma and dr. A.A.F. de Vries. During her training she focused on how cardiac differentiation is regulated in multipotent stem cells of different species and origins. During, but also after this PhD training, she was an invited reviewer for various journals, especially Stem Cells, on a frequent basis.

In 2012 she became a LUMC Cardiology resident under supervision of prof. dr. M.J. Schalij and started her pre-cardiology phase in Internal Medicine at the Rijnland hospital in Leiderdorp (supervisor dr. M.J.F.M. Jansen). She will return to the LUMC to finish her Cardiology training in 2016.

SELECTED GRANTS, AWARDS, AND FELLOWSHIPS

- 2011 American Heart Association International Travel Grant, American Heart Association, Orlando, Florida, USA
- 2011 Keystone Symposia (National Heart, Lung and Blood Institute) Scholarship, Keystone, Colorado, USA
- 2011 First Contact Initiative Grant, Council of Basic Science, European Society of Cardiology
- 2010 Travel grant, Leiden University Foundation, Leiden, The Netherlands
- 2009 Travel grant, Council of Basic Science, European Society of Cardiology, Barcelona, Spain
- 2009 Scholarship from the Harvard Medical School to attend the "Days of Molecular Medicine" symposium; Harvard Medical School, Boston, Massachusetts, USA
- 2008 Abstract Award, Netherlands Society of Cardiology, Amsterdam, The Netherlands
- 2006 Student Research Award Biomedical Sciences, Leiden University Medical Center, Leiden, The Netherlands
- 2005 Honours Class "Medical Humanities: illness and health in science and art", Honours Programme Leiden University, Leiden, The Netherlands
- 2004 Excellent Student Programme, Leiden University Medical Center, Leiden, The Netherlands